Going with the flow: the distribution, biomass and grazing rate of *Potamocorbula* and *Corbicula* with varying freshwater flow (May and October 2009-2011).

J. Thompson[1], K. Gehrts[2], F. Parchaso[1], H. Fuller[2]

[1] U.S. Geological Survey, Menlo Park, CA; [2] Division of Environmental Services, Department of Water Resources , West Sacramento, CA

Summary of findings:

Spatially intensive benthic samples from >200 stations were analyzed for bivalve biomass, filtration rate, grazing rate, and water column turnover rate for three Octobers (2009-2011) to determine if the increased freshwater flow in fall 2011 would decrease the bivalve grazing in the low salinity zone in fall. Relative to the previous two dry years, the biomass of bivalves was decreased in the shallow portions of Grizzly and Honker Bays and in Western Suisun Marsh (including Montezuma and Suisun Slough) in 2011. The reduction in biomass was sufficient to limit the potential for bivalves to control phytoplankton biomass accumulation in fall. It is likely they could decrease the phytoplankton biomass by their feeding, but they did not have a sufficient grazing rate to exceed the phytoplankton growth rate during fall 2011, if the phytoplankton growth rate is assumed to be similar to that observed by Kimmerer et al. (2012) in 2006-2007.

Introduction

The POD conceptual model recognizes that food limitation may be contributing to the decline of Delta Smelt (Baxter et al. 2008). The questions of how food has changed during the POD years and the factors responsible for those changes have not been resolved. We know that the variability in salinity decreased in late summer and fall during the POD and that Delta Smelt are mostly in the low salinity zone (LSZ) during this period. There are several components of the LSZ food web that might be affected by this change in salinity. We discuss here the response of the benthic bivalves and how their change in biomass in space and time might reduce phytoplankton, copepods, bacteria, and possibly microzooplankton.

The distributions of *Potamocorbula amurensis* (*Potamocorbula* hereafter) and *Corbicula fluminea* (*Corbicula* hereafter) are dependent on the salinity distribution at the time their larvae are available for settlement, the number of adults present in the area of settlement, and the environmental stresses on the population after settlement. Field data shows that these bivalves overlap within the LSZ region which is consistent with laboratory studies on the juvenile/larval salinity tolerances for both species (Nicolini and Penry 2000, McMahon 1999). Based on data collected for the Environmental Monitoring Program Benthic Program we know that *Potamocorbula* is more persistent and is a larger presence in the LSZ than is *Corbicula*. We have also observed that the pattern is reversed upriver of the LSZ where the freshwater clam, *Corbicula*, becomes the dominant form. It is important to understand the dynamics of both clams as previous field (Thompson et al 2008, Lopez et al. 2006) and modeling (Lucas et al 2002, Lucas et al 2009) work has shown that both bivalves can limit phytoplankton biomass in the bay and delta. In addition, experimental work has shown zooplankton nauplii and ciliates can be filtered out of the water column by *Potamocorbula* in the bay (Kimmerer et al 1994, Greene et al 2011). *Corbicula* can filter

fast-moving ciliates (Scherwass et al 2001) and glochidia (Scherwass et al 2005) but there have been no experiments on their ability to filter copepod nauplii. Thus, *Potamocorbula* may limit food supplies in the LSZ and both *Potamocorbula* and *Corbicula* may consume phytoplankton and zooplankton as it is transported towards the LSZ although *Corbicula* are likely to dominate in this upstream habitat in most years.

Because Delta Smelt feed on zooplankton (mostly calanoid copepods, Nobriga 2002) throughout their lives, any direct reduction in zooplankton through filtration by bivalves or indirect reduction in zooplankton due to food limitation needs to be examined. Thus, this project concentrated on the magnitude of bivalve grazing within the LSZ, within the tidal dispersion zone of the LSZ, and upstream of the LSZ during the fall periods.

Bivalve conceptual models

The distribution and dynamics of *Potamocorbula* and *Corbicula* are based on their physiological salinity limits and their life history characteristics. As explained below, *Potamocorbula* is the dominant grazer within the LSZ and *Corbicula* is the dominant grazer upstream of X2. As X2 and the LSZ moves up- and down-bay, the overlapping region of *Corbicula* and *Potamocorbula* moves with it so we will always have to consider both species when we examine foodweb dynamics in the LSZ. In addition, declines in phytoplankton biomass can not be assumed to be due to local grazing due to the tidal dispersion of pelagic particles and thus grazing must be assessed in regions within the tidal dispersion sphere of influence. The major difference in *Potamocorbula* and *Corbicula* other than their salinity tolerance is their method and season of reproduction that determines their distribution within their salinity range and their response to the fall increase in salinity intrusion.

Potamocorbula

Potamocorbula is a dioecious (sexes are separate), fecund (45,000-220,000 oocytes), broadcast spawning bivalve with external fertilization, a short lived non swimming trochophore larvae and a motile suspension feeding veliger larvae. Both larval stages have a broad salinity tolerance (2-30). The larvae settle at day 17-19 and thus can be moved by the currents for substantial distances before settling.

Potamocorbula recruitment usually occurs in the western Delta in fall and in the northern estuary in early spring through fall (Parchaso and Thompson 2002). Thus larvae have been available to respond to the recent fall periods of increasing salinity. We observed an increase in the biomass and abundance of *Potamocorbula* at Chipps Island in late 1999 and early 2000 (USGS unpublished data). We hypothesize that the increasing salinity in fall that began in 1999 allows fall larvae to settle further upstream. The high salinity may also allow *Potamocorbula* that settles in previously marginal salinity zones to persist, because individuals have grown sufficiently large in fall to become more tolerant of environmental stresses during the following winter.

The antidote to this fall incursion of bivalves is a large outflow event such as was seen in spring 2006. The mass mortality in spring 2006, observed as a drop in abundance and biomass of *Potamocorbula* to near zero at a Chipps Island station (USGS unpublished data), was short lived. The recruitment and subsequent biomass was very high in the fall of 2006 at that location because there were no adults to interfere with the larvae, and the salinity was high enough for a long enough period to allow the recruits to grow and persist. The elevated fall 2006 biomass then carried into the spring of the following year when Delta outflow was again low. We hypothesize that the effect of the recent increases in fall salinity

was an increase in recruitment of *Potamocorbula* in traditionally lower salinity areas. The corollary to this hypothesis is that if these animals are given sufficient time to grow they become more resistant to osmotic and physical stresses during the winter peaks in Delta outflow which results in higher grazing rates in the following spring than we might expect with normal fall salinity distributions.

Corbicula

Corbicula is a simultaneous hermaphrodite (Kraemer and Galloway 1986) thereby making it possible for one individual to establish a population. Adults hold unfertilized eggs until there is sufficient food at which time they produce sperm and the eggs are fertilized. The larvae (pediveligers) develop in 3-5 days, are brooded in the gills of the adult before release, cannot swim but are found in the plankton for their first 48 hours, and are limited to salinities ≤2. They depend on their small size (200 µm) and mass (0.1 mg dry weight) to allow currents to re-suspend and transport them after settling (Aldridge and McMahon 1978). As a freshwater bivalve, this strategy is good for moving larvae downstream with the currents but may be less effective at widening their distribution throughout the system. It is not surprising that *Corbicula*, as a freshwater bivalve, would have an opposite reproductive seasonality to that of *Potamocorbula*. Eng (1979) and Heinsohn (1958) found a large spawning peak in the spring followed by a smaller fall peak in the Delta. If this reproductive seasonality persists today then *Corbicula* is most likely to expand down river and down-bay in the spring but its expansion into new down bay areas is likely to be limited in fall by the increasing salinity.

Methods

The DWR EMP program sampled 175 benthic stations (single sample at each location with a 0.05m^2 bottom grab) throughout the Delta and northern bay in one week in May and October from 2007-2011 (Figure 1). The sampling design (generalized random tessellated stratified design) allows for a random selection of stations in various strata which DWR defined as habitat type (lake, large river, river, slough, bay, large bay). The station locations changed each year for all but 50 stations (the annual panal) which were sampled throughout the program. Twenty two additional stations were added beginning in October 2009 to establish channel-shoal pairings at some locations to determine if shallow locations had significantly different bivalve populations than their adjacent channel stations. In order to focus on the low salinity zone and it's nearby habitat, we further parsed the strata into the following regions (Figure 2): Grizzly/Honker Bays (≤4m), Shallow Suisun Bay (not in channel and <7m), Channel Suisun Bay, Lake (Big Break and Sherman Lake with adjoining sloughs), Western Suisun Marsh (Suisun Slough, Montezuma Slough west of Nurse Slough), Eastern Suisun Marsh (Montezuma Slough east of Nurse Slough), and Confluence (Sacramento River up to Browns Island, San Joaquin River to False River out of Franks Tract).

Samples were sieved through 0.5mm screens, preserved in 10% formalin in the field, and changed to 70% alcohol at 1-2 weeks. Samples of live bivalves were collected at annual panel stations to estimate weight as a function of length; clams were measured, dried, weighed, ashed, and reweighed to determine ash-free dry weight (AFDW). Samples were sorted by a contractor (Hydrozoology) and returned to DWR. Bivalves from all samples were measured using an image analyzer or hand calipers and length of each animal in each sample was converted to AFDW using the live animal length to weight conversions calculated at the annual panel stations. Biomass at a station was estimated by summing these values.

Consumption rate was estimated two ways. The first rate, the filtration rate, is the highest consumption rate that we would expect. Filtration rate is the product of bivalve biomass and species specific pumping

rates (PR's) which were adjusted for temperature. *Potamocorbula* pumping rates have been estimated at two temperatures to be ≈400 L $(gAFDW)^{-1}d^{-1}$ at temperatures ≥15°C and 270 L $(gAFDW)^{-1}d^{-1}$ at temperatures <15°C (Cole et al. 1992). *Corbicula* pumping rate was determined at four temperatures by Foe and Knight 1986) and data were fitted to an exponential model which was then used to determine temperature specific pumping rates. Filtration rates assume no depletion boundary layer (the local reduction in food concentration when vertical mixing rate is too low to compensate for the loss due to consumption at the bed) and that animals filter all of the time. The second rate, the grazing rate, incorporates a concentration boundary layer and is smaller than the filtration rate when there are large populations. Filtration rates were converted to grazing rates by reducing the pumping rates to adjust for the presence of a concentration boundary layer. This adjustment was based on O'Riordan's (1995, Figure 7b) refiltration relationship, $n_{max} = F_c/(s/d_o)$, where n_{max} is the maximum refiltration proportion (ie the proportion of water previously filtered), F_c is a species specific refiltration factor determined in the laboratory for *Potamocorbula* (2.5) and *Venerupis* (3.0, similar to *Corbicula* in size and habit), s is the distance between siphon pairs, and d_0 is the diameter of the excurrent siphon. The diameter of the excurrent siphon was changed throughout each year to reflect the change in average size of animals as the year progressed, and the distance between siphon pairs was based on density of animals observed in our benthic sampling assuming equidistant spacing within the 0.05 m^2 grab. The use of maximum refiltration proportion maximizes the effect of the concentration boundary layer resulting in a conservative grazing rate estimate. The combined use of filtration rate and grazing rate should give a reasonable range of possible consumption rates. We assumed all bivalves grazed continuously.

Data and Approach

Biomass, filtration rate, grazing rate and grazing rate water column turnover rate have been calculated for each region and are summarized in Tables 1-4. Water column turnover rate is a method of normalizing grazing and filtration rates by depth of the water column. The resulting number is more intuitive of the bivalves effect on pelagic particles (biologic and refractory) than grazing rate because it reflects the number of times in a day that a population could filter the overlying water column if the water was stationary. With this value, the importance of water depth becomes apparent; if it is assumed that the same population lived on the bottom of a 1m vs a 10m water column, the bivalves would filter the 1 m water column ten times the rate at which they filter the deeper water column.

The data are not normally distributed and regions have unequal number of samples so non-parametric measures of statistical significance (Kruskal-Wallis) have been used to compare regions and time periods. As with most benthic data, the median value is shown in plots because it is the best way to eliminate the influence of one very high or very low value in a region.

Findings

General Distribution Patterns

When the entire sampling domain with the data from all three years is combined, there are several observations that can be made about persistent patterns that don't seem to be affected by water year type (Figures 3 and 4a). First *Potamocorbula* has a larger presence, and thus larger filtration rate in fall than spring, and the opposite is true of *Corbicula*. Second, *Potamocorbula* have very low filtration rates in the spring in the shallows of Grizzly and Honker Bays for all three years. Third, filtration rates for both

bivalves in the lower reaches of Sacramento and San Joaquin Rivers (just upstream of confluence) are consistently lower than the surrounding areas and there appears to be less seasonality in this region than in the rest of the system.

These persistent distribution patterns become even more apparent when we narrow the focus to the LSZ (Figure 4b). We can also see that the area where the two bivalve species overlaps can be described as within and just upstream of the confluence and on the eastern end of Montezuma Slough (east of Nurse Slough). When the distributions are plotted separately for each year (Figure 5a) and compared for May and October we see that the zone of overlap in May is within the range of X2 over the previous 6 months with a few exceptions in 2009-2010. In 2011 *Potamocorbula* were consistently upstream of the maximum X2 in the previous 6 months. This pattern persists into fall 2011 with *Potamocorbula* being observed upstream of the X2 maximum in all years (Figure 5b). Unlike May 2011, the October 2011 distribution showed some *Corbicula* within the X2 range.

Differences between years in regions (Fall 2009-2011)

When the filtration rates, grazing rates, and water column turnover rates are compared between years within the regions, only the values in the Grizzly/Honker Bay shallows and the Western Suisun Marsh showed a statistically significant difference between years (Kruskal-Wallis, $p<0.05$). Grizzly/Honker bay biomass, filtration, grazing, and turnover rates were all similar in 2009 and 2010 but were significantly less in 2011 than in 2010 (Figure 6a, 6b). The western Suisun Slough rates were similar in 2009 and 2010 but the 2011 rates were different from both the 2009 and 2010 rates (Figure 7a, 7b). The location of these decreased grazing rates is important as we might expect pelagic primary producers to do best in the shallows of Grizzly and Honker Bays and we might expect that marsh production would have a better chance of reaching other consumers when the bivalve grazers were greatly reduced as seen in 2011.

Differences between areas in years (Fall 2009-2011)

Because we are most interested in the effect that the bivalve grazers have on the system, we will show grazing turnover rates in this section (data for other parameters are in tables 1-4). The pattern and values for grazing turnover rate were similar in 2009 and 2010 with the shallow regions, Grizzly/Honker Bay, Suisun Bay Shallow, and West Suisun Marsh, having much higher values than the remaining areas that are mostly upstream or deeper than these stations (Figures 8 and 9). The bimodal distribution of values highlights the significant differences in these groups. The Confluence region had significantly lower turnover rates than those observed in Grizzly/Honker Bay and in the West Suisun Marsh in both 2009 and 2010. The West Suisun Marsh also had significantly higher rates than were observed in Suisun Channel in 2009 and 2010. In addition the Confluence rates were significantly lower than the Grizzly/Honker Bay rates and the West Suisun Marsh rates were significantly higher than the rates in the Lakes region in 2010 Figure 9).

Grazing turnover rates in 2011were lower and the bimodal distribution of values was less pronounced. There were no significant differences between the regions with the median values fell between 0.1 and 0.5 d^{-1} (Figure 10).

Time Series in Grizzly/Honker Bay Shallows

Figures 11 and 12 show the full time series (May 2009-October 2011) for all parameters for the Grizzly/Honker Bay region. Because the shallow areas are the presumed source of locally grown phytoplankton, grazing in this region is the most likely to have an effect on net phytoplankton growth.

Biomass, filtration rate, grazing rate, and grazing rate turnover rate all show the same strong seasonal pattern which is expected since all values are derived from biomass. In this region, where the bivalves are almost all *Potamocorbula*, filtration rate is derived from biomass with one conversion factor. It should be noted that in other regions, where *Corbicula* and *Potamocorbula* occur together the conversions are less linearly related to biomass.

Spring filtration rates (medians of 0.2-0.3 m d^{-1}) are about an order of magnitude less than fall filtration rates (2, 4, and 1 m d^{-1}). Grazing rates showed a similar pattern with spring rates (0.2, 0.3, and 0.1 m d^{-1}) an order of magnitude less than fall rates (2, 3, 1 m d^{-1}). Grazing water column turnover rate was very low with populations needing 10-20 days to totally turnover the water column in spring (0.1, 0.1, 0.05 d^{-1}). Fall grazing turnover rates were much higher with populations turning over the water column every 1-2 days (0.6, 1, 0.4 d^{-1}). If we assume a spring phytoplankton growth rate of 0.5-0.6 d^{-1} (Kimmerer et al in press) we can state that the bivalves were unlikely to be a controlling factor on spring phytoplankton biomass accumulation in any year. Fall phytoplankton growth rates have not been recently measured but summer rates (0.7-1.0 d^{-1}) would be about equivalent to the loss rates by bivalves in 2009-2010 but not in 2011 when bivalve turnover rates (0.4 d^{-1}) were unlikely to limit a bloom from developing in the shallow water.

Significance of Findings

We saw a decline in bivalve biomass and therefore grazing rate during and following the increased freshwater flow in spring and fall 2011. In examining the shallow Grizzly and Honker Bay data we found that bivalve grazing was unlikely to have an impact on net phytoplankton growth in spring during any of the years examined (2009-2011). We also found that the fall grazing rates were sufficient to potentially limit phytoplankton biomass accumulation in 2009-2010 but not in 2011.

The reduction in bivalve biomass and therefore grazing in 2011 could be due to recruitment losses in spring or fall and our ongoing work with the monitoring station samples should help delineate the cause. We were surprised by the persistence of *Potamocorbula* in the confluence area in 2011 despite the down bay position of X2. Our present working hypothesis is that it is the salinity gradient and therefore change in salinity over short periods of time that is important in determining the distribution of both species rather than the absolute salinity at a location. If true, this hypothesis would support the presence of *Potamocorbula* upstream of X2 in spring 2011.

Next Steps

Fall Study: We will measure bivalves and calculate biomass, filtration rate and grazing rate of the bivalves in the May and October 2012 GRTS samples when the samples have been sorted. We are presently measuring bivalves in the monitoring stations to better determine the seasonality of recruitment of both species and to determine if there are interannual and spatial differences in recruitment. Recruitment patterns are a critical component in our understanding of why bivalves have limited success in some areas and during some periods. We are submitting abstracts for two posters for the Bay-Delta conference that will highlight what we learn about recruitment for each species.

HSG Study: We are finishing the analyses of the May 2011 data and when that is complete we will repeat the analysis done here on the samples from throughout the study domain. The values reported will include biomass, grazing and filtration rates, and recruit abundance and the analysis will include the effect of depth on these rates for each species.

The combination of analyses in both studies will give us an opportunity to examine if and when populations that settle in the fall are still present in spring and if these "carry-over" populations are adding a new dimension to the bivalve community seasonal patterns.

Literature Cited

Aldridge DW, and McMahon RF 1978. Growth, fecundity, and bioenergetics in a natural population of the freshwater clam, *C. fluminea malinensis* Philippi, from north central Texas. Journal of Molluscan Studies 44: 49-70.

Baxter R, Breuer R, Brown L, Chotkowski M, Feyrer F, Gingras M, Herbold B, Mueller-Solger A, Nobriga M, Sommer T, Souza K (2008) Pelagic Organism Decline Progress Report: 2007 Synthesis of Results, Sacramento

Cole BE, Cloern JE (1984) Significance of biomass and light availability to phytoplankton productivity in San Francisco Bay. Mar Ecol Prog Ser 17:15-24.

Eng LL. 1979. Population dynamics of the Asiatic clam, *C. fluminea fluminea* (Muller) in the concrete-lined Delta-Mendota Canal of central California. p. 39–168 in J. C. Britton (ed.), First International *C. fluminea* Symposium, Fort Worth, TX, Texas Christian University Research Foundation

Foe, C. and A. Knight. 1986. A thermal energy budget for juvenile Corbicula fluminea American Malacological Bulletin, Special Edition No. 2:143-150.

Greene VE, Sullivan LJ, Thompson JK, Kimmerer W. 2011. Grazing impact of the invasive clam *Corbula amurensis* on the microplankton assemblage of the northern San Francisco Estuary. Marine Ecology Progress Series, 431:183-193.

Heinsohn GE. 1958. Life history and ecology of the freshwater clam, *C. fluminea fluminea*. Santa Barbara, CA, University of California: 64.

Kimmerer WJ, Gartside E, Orsi JJ. 1994. Predation by an introduced clam as the likely cause of substantial declines in zooplankton of San Francisco Bay. Mar Eco Prog Ser 324:207-218

Kimmerer WJ, Parker AE, Lidstrom UE, Carpenter EJ. 2012. Short-term and interannual variability in primary production in the low-salinity zone of San Francisco Estuary. Estuaries and Coasts. In press.

Kraemer L R and Galloway ML. 1986. Larval development of *C. fluminea fluminea* (Muller) (Bivalvia: C. flumineacea): an appraisal of its heterochrony. American Malacological Bulletin 4: 61-79.

Lopez CB, Cloern JE, Schraga TS, Little AJ, Lucas LV, Thompson JK, and Burau JR, 2006,

Ecological values of shallow-water habitats: implications for restoration of disturbed ecosystems , Ecosystems 9: 422-440

Lucas LV, Cloern JE, Thompson JK, and Monsen NE, 2002, Functional variability of habitats in the Sacramento-San Joaquin Delta: restoration implications: Ecological Applications, v.12, no. 5, p. 1528-1547

Lucas LV, Thompson JK, Brown LR. 2009. Why are diverse relationships observed between phytoplankton biomass and transport time?. Limnol. Oceanog. 54(1):381-390

McMahon RF. 1999. Invasive characteristics of the freshwater bivalve *C. fluminea fluminea*. Nonindigenous Freshwater Organisms: Vectors, Biology, and Impacts. R. Claudi and J. H. Leach. New York, Lewis Publishers: 315-346.

McManus GB, York JK, Kimmerer WJ 2008. Microzooplankton dynamics in the low salinity zone of the San Francisco Estuary. Verh Internat Verein Limnol 30:196-202

Nicolini MH, Penry DL, 2000. Spawning, fertilization, and larval development of *Potamocorbula amurensis* (Mollusca: Bivalvia) from San Francisco Bay, California. Pacific Science, 54:377-388.

Nobriga ML 2002. Larval delta smelt diet composition and feeding incidence: environmental and ontogenetic influences. Calif Fish Game 88:149-164

O'Riordan, C.A., Monismith, S.G., Koseff, J.R., 1995. The effect of bivalve excurrent jet dynamics on mass transfer in a benthic boundary layer. Limnology and Oceanography 40 (2), 330-344.

Parchaso F, Thompson JK. 2002. The influence of hydrologic processes on reproduction of the introduced bivalve *Potamocorbula amurensis* in northern San Francisco Bay, California. Pacific Science, 56(3):329-345.

Scherwass A, Eimer A, and Arndt, H. 2001. Selective influence of filter-feeding benthic bivalves (*C. fluminea* sp., *Mytilus* sp.) on planktonic ciliates. Verh. Int. Verein. theor. angew. Limnol.: 27, 3315-3318.

Scherwass, A., Arndt, H. 2005. Structure, dynamics and control of the ciliate fauna in the potamoplankton of the river Rhine. Archiv für Hydrobiologie: 164(3), 287-307

Schlekat DW, Lee BG, Luoma SN, 2002. Assimilation of selenium from phytoplankton by three benthic invertebrates: effect of phytoplankton species. Mar Eco Prog Ser 237:79-85

Thompson JK, Koseff JR, Monismith SG, Lucas LV, 2008. Shallow water processes govern system-wide phytoplankton bloom dynamics: A field study. J Mar Syst 74:153-166

Werner I, Hollibaugh, JT, 1993. *Potamocorbula amurensis*: comparison of clearance rates and assimilation efficiencies for phytoplankton and bacterioplankton. Limnol Oceanogr 38:949-964.

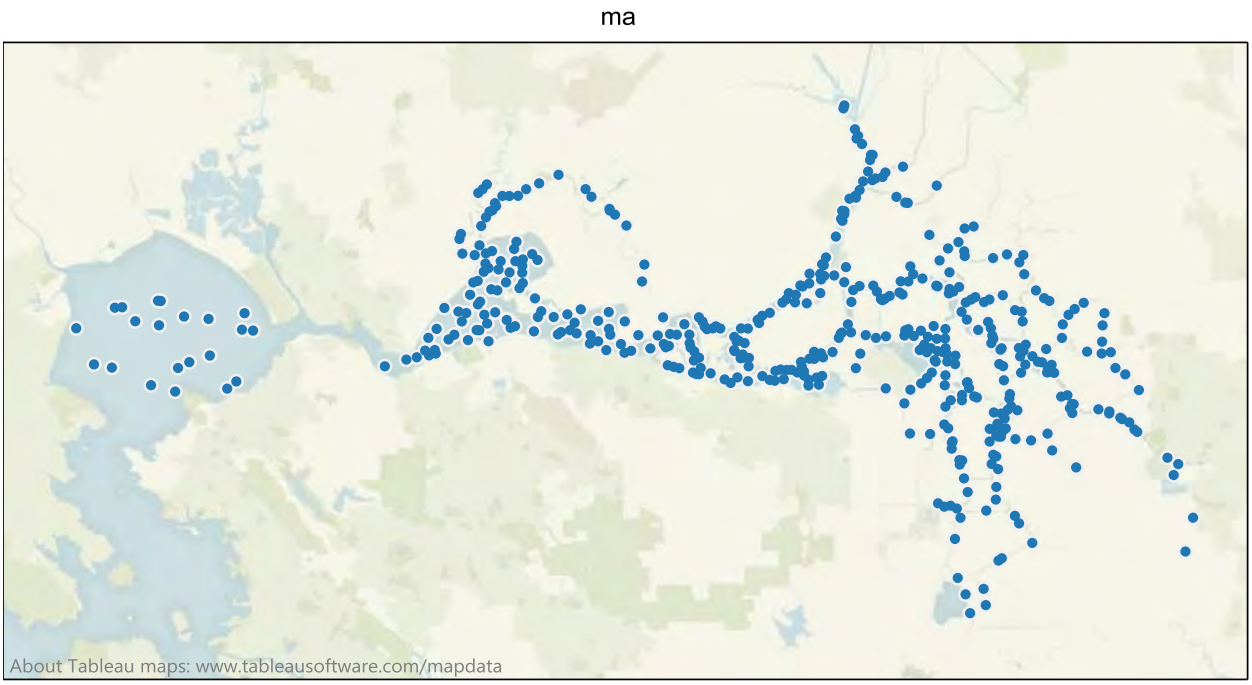

Map based on average of long and lat. The data is filtered on year, Panel and Strata. The year filter has multiple members selected. The Panel filte has multiple members selected. The Strata filter has multiple members selected

Figure 1. Composite (2007-2011) of all stations sampled by DWR in the GRTS benthic study.

Grizzly/Honker Bay

West Suisun

Sheet 3

Map based on long and lat. Color shows details about year. The data is filtered on Strata, Location and Sub habitat. The Strata filter keeps Bay and Slough. The Locatio
of Nurse Sl.. The view is filtered on year and Exclusions (lat,long,year). The year filter has multiple members selected. The Exclusions (lat,long,year) filter specifies a set

year

- 2009
- 2010
- 2011

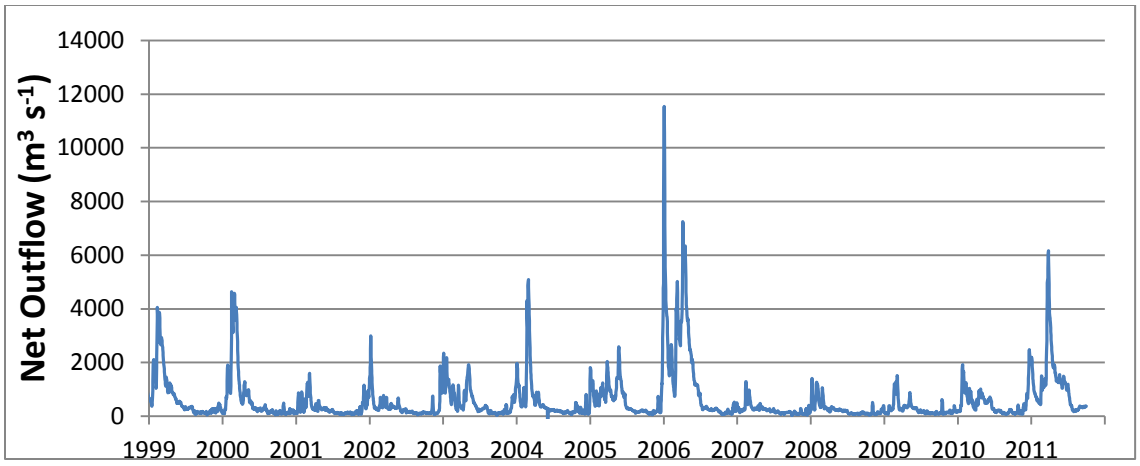

Figure 3. Net Delta Outflow for pelagic organism decline (1999- present). Note the years of the benthic study encompass a dry-below normal year (2009), a dry-above normal year (2010), and a wet year(2011).

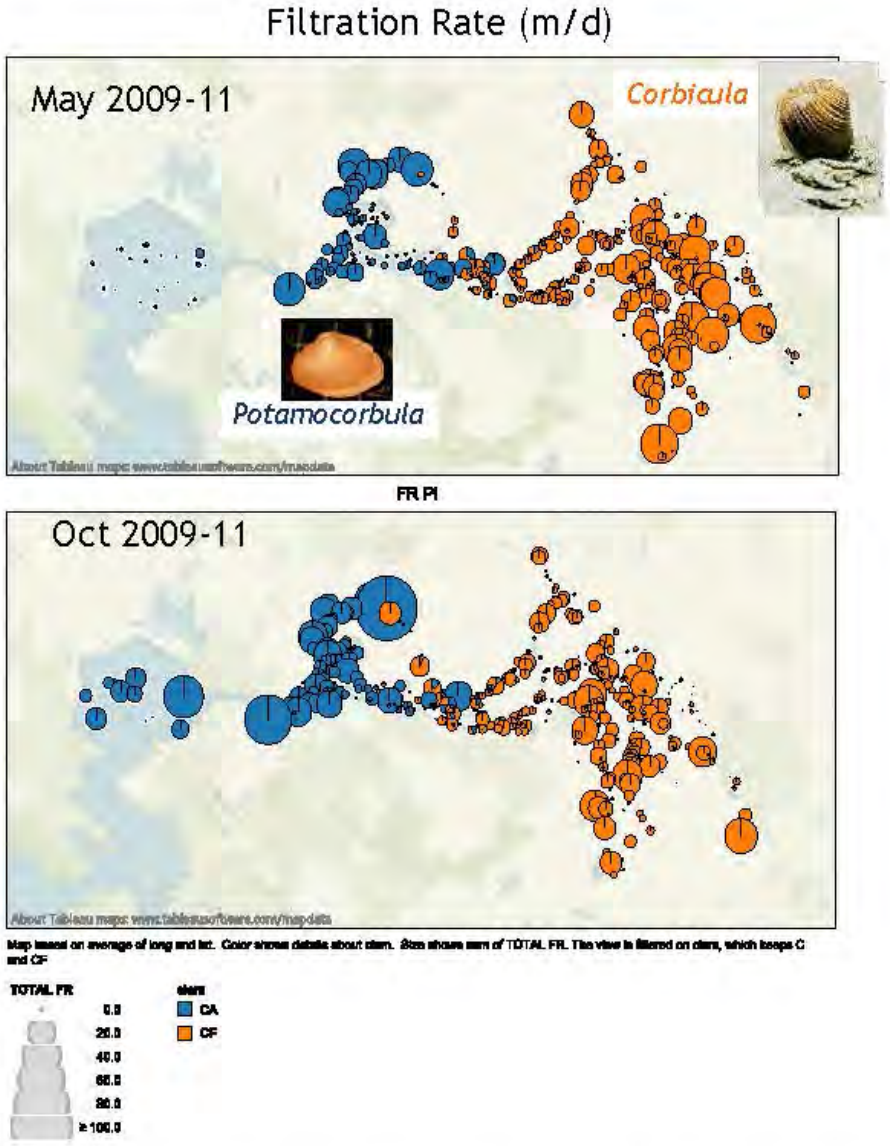

Figure 4a. Filtration rate for *Potamocorbula* (blue) and *Corbicula* for May and October of 2009-2011. The combination of data sets allows us to see persistent patterns that were not influenced by freshwater inflow during these three years.

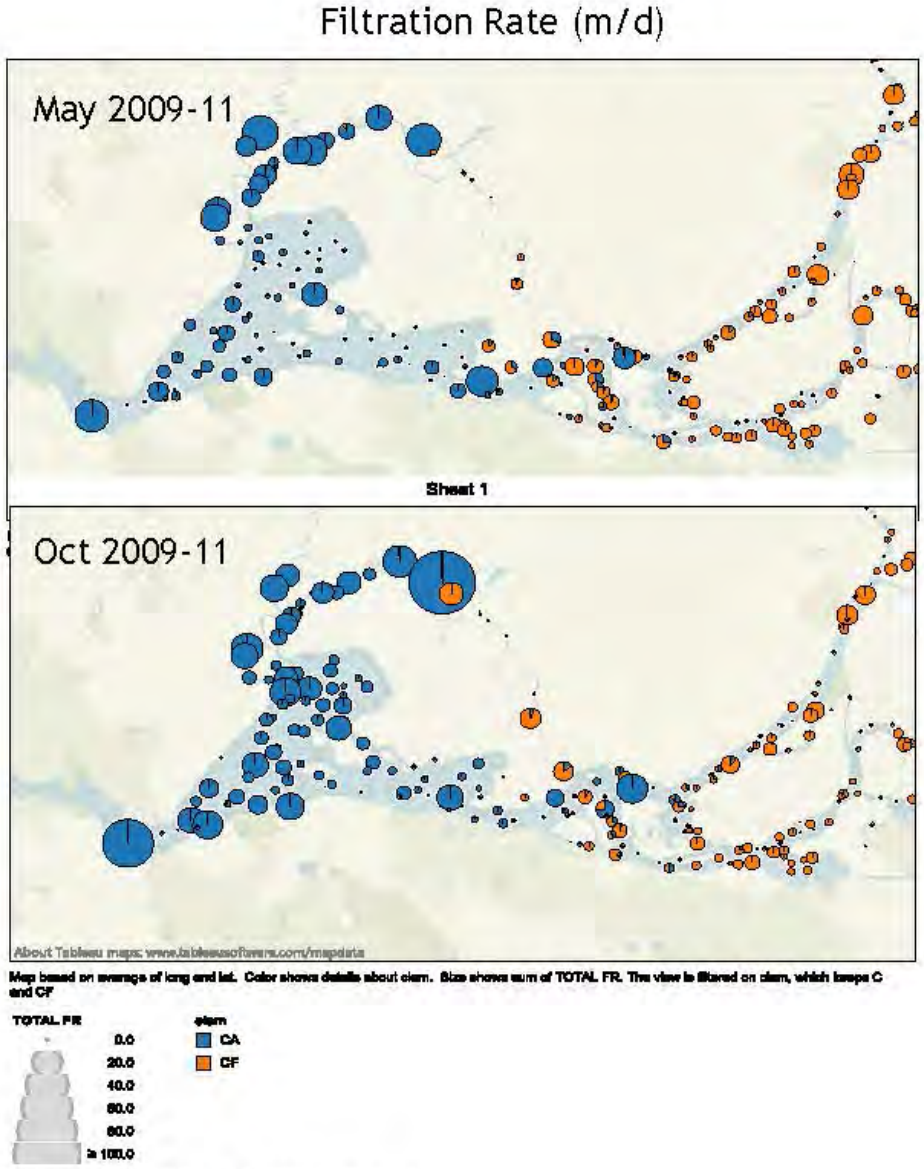

Figure 4b A close-up of the LSZ region in Figure 4a

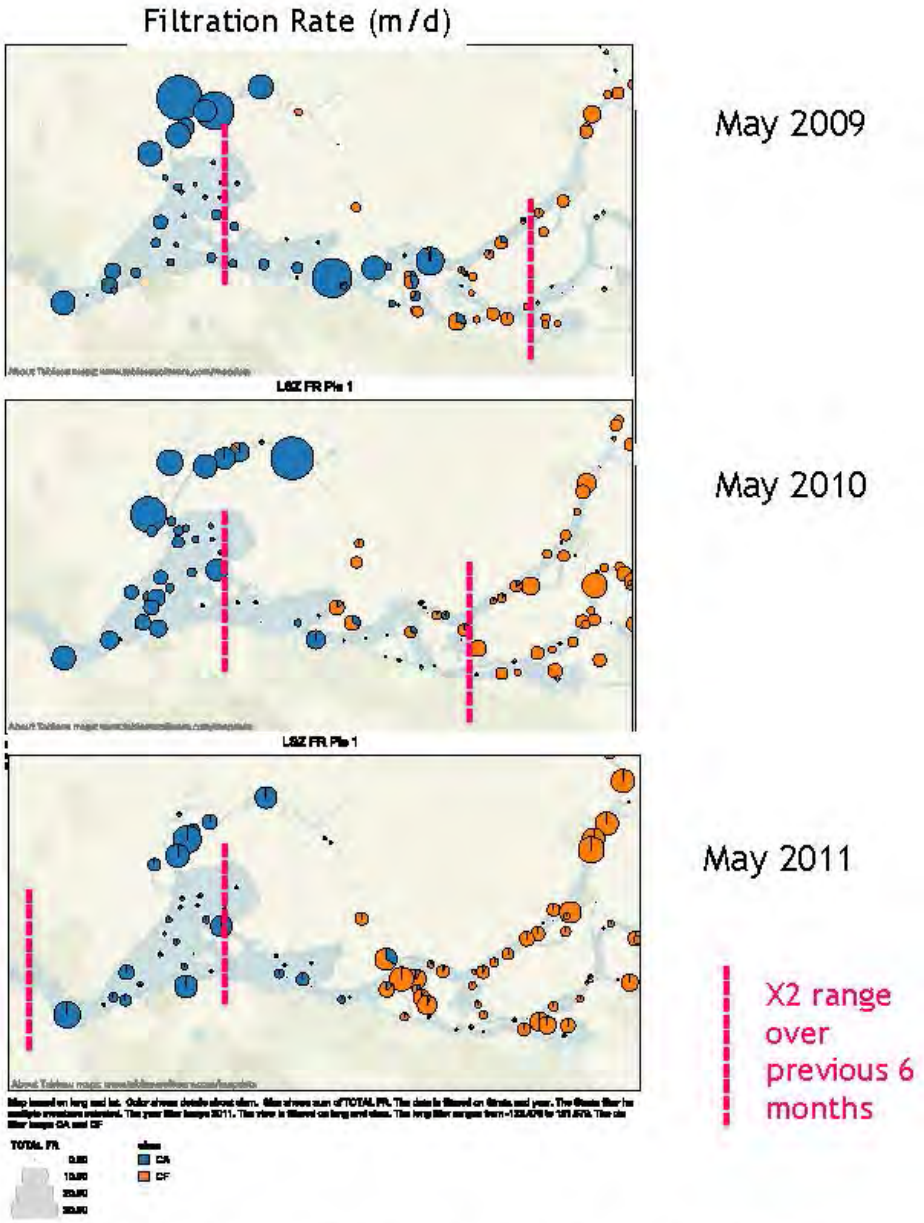

Figure 5a. Filtration rate for both bivalves in May 2009, 2010, and 2011. Range of X2 over previous 6 months shown on map as range where bivalves were expected to overlap.

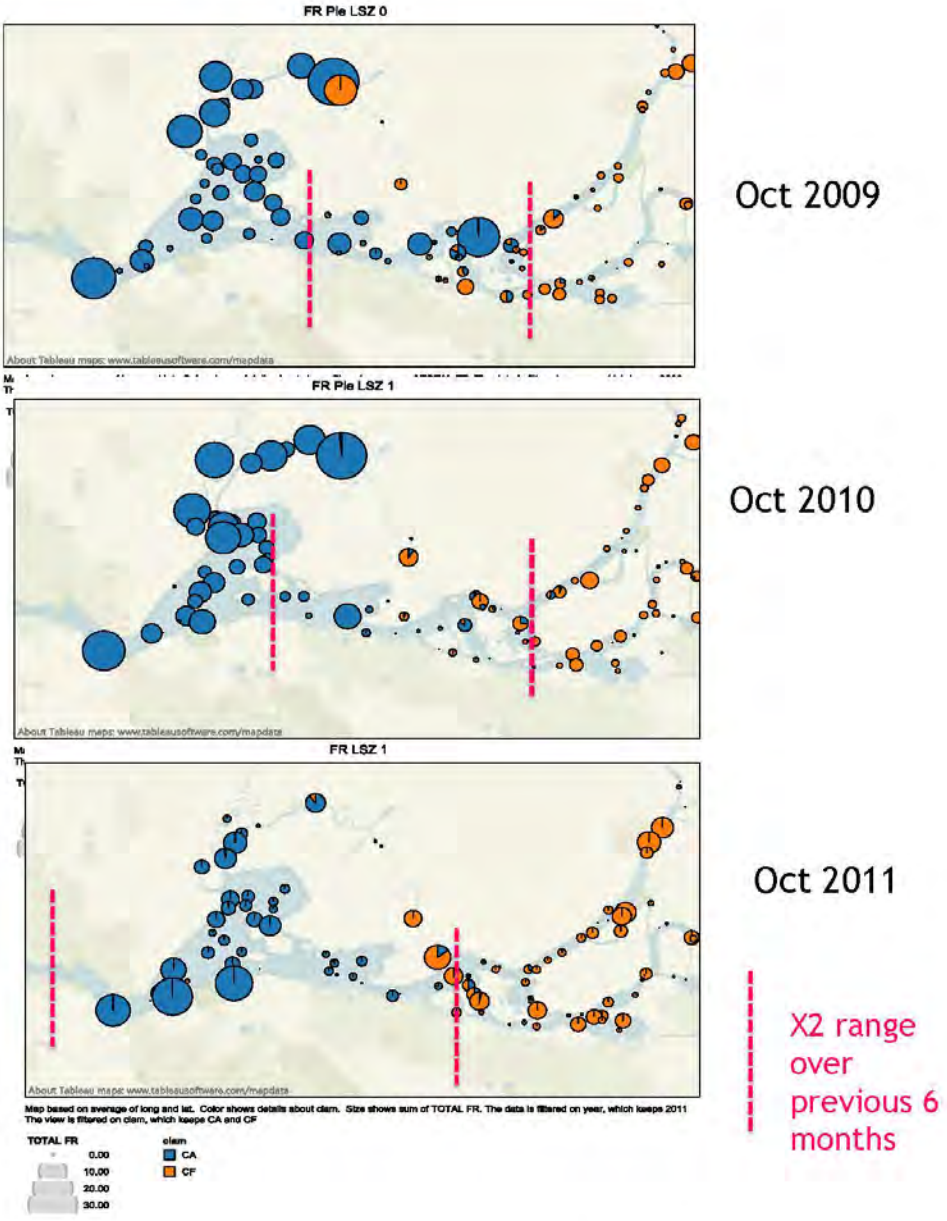

Figure 5b. Filtrattion rate for both bivalves in October 2009,2010, and 2011. Range of X2 over previous 6 months shown on map as range where bivalves were expected to overlap.

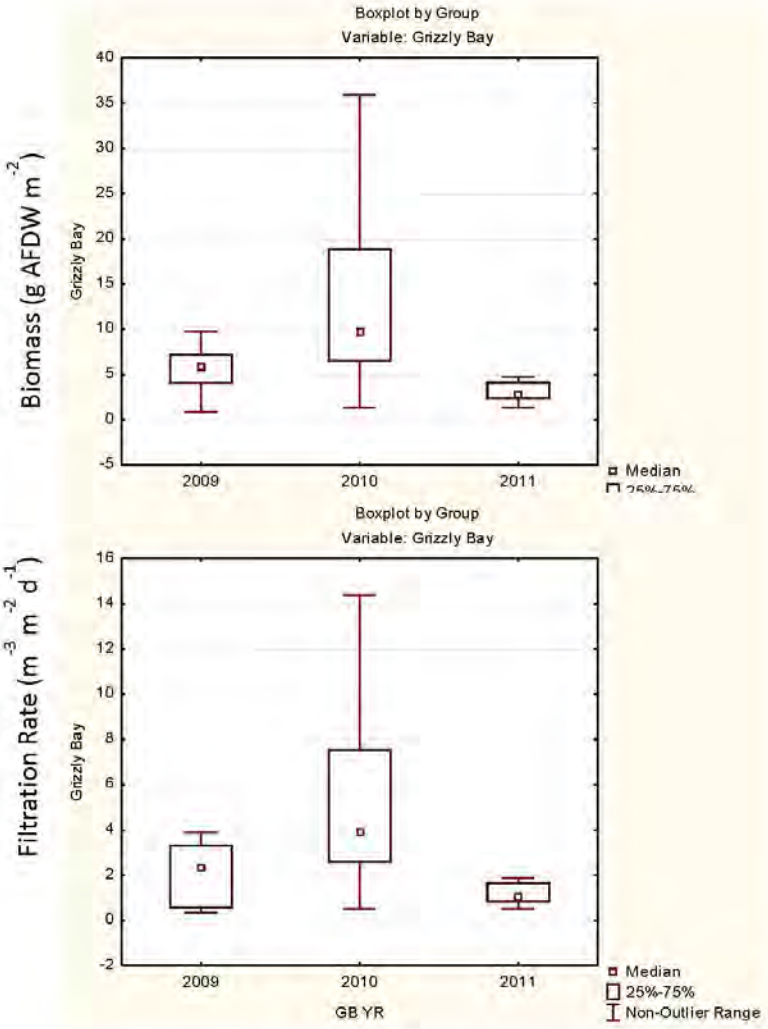

Figure 6a. Biomass and filtration rate during the October sampling periods in Grizzly/Honker Bay shallows. All values (biomass, filtration rate, grazing rate, and turnover rate) for Grizzly/Honker Bay clams were not significantly different between 2009 and 2010 but were significantly different for 2010 and 2011.

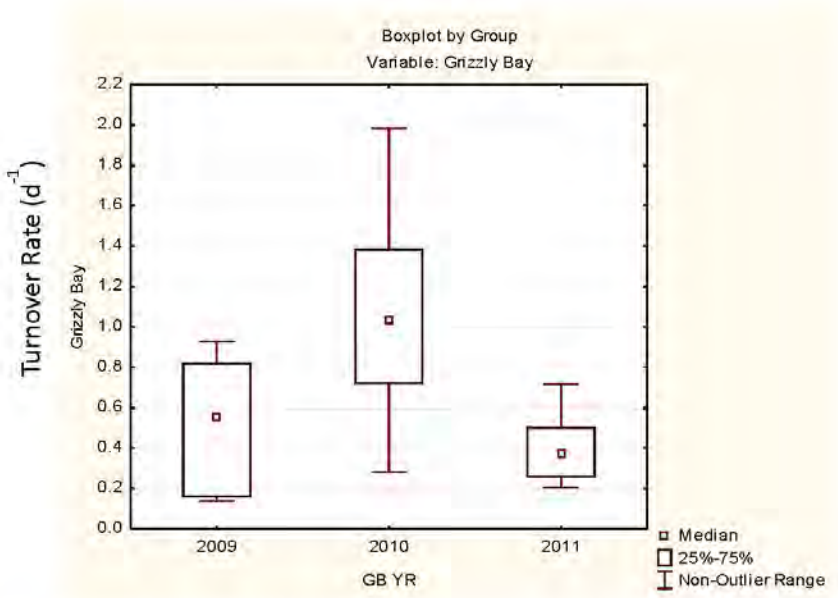

Figure 6b. Grazing rate normalized by water depth in Grizzly/Honker Bay shallows estimates water column turnover rate, the more conservative of the two calculated turnover rates.

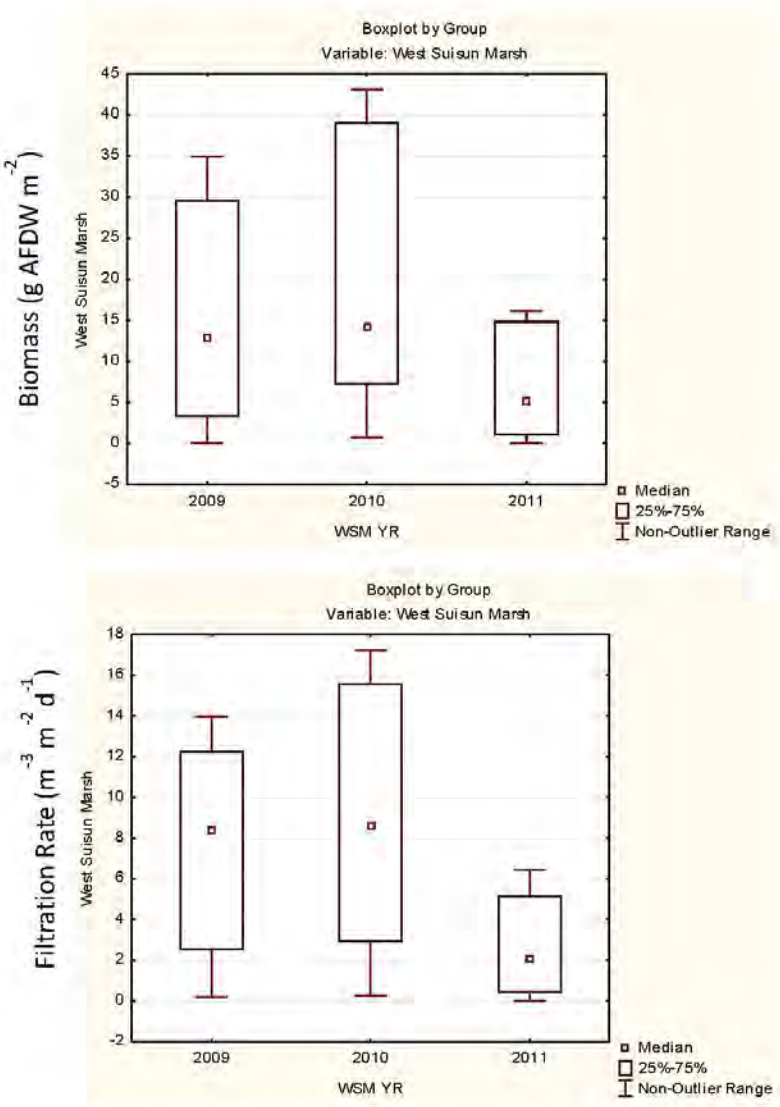

Figure 7a. Biomass and filtration rate during the October sampling periods in West Suisun Marsh region. All values (biomass, filtration rate, grazing rate, and turnover rate) for West Suisun Marsh clams were not significantly different between 2009 and 2010 but were significantly different for 2010 and 2011.

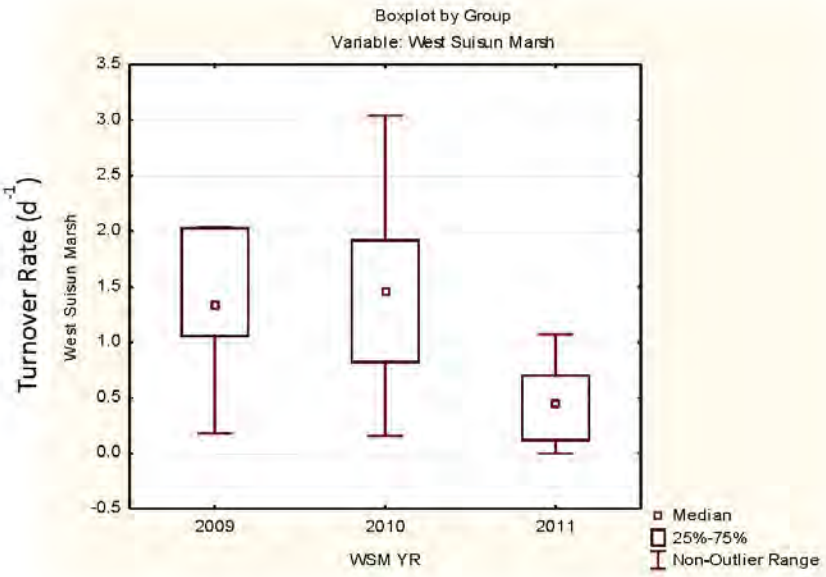

Figure 7b. Grazing rate normalized by water depth in West Suisun Marsh estimates water column turnover rate, the more conservative of the two calculated turnover rates.

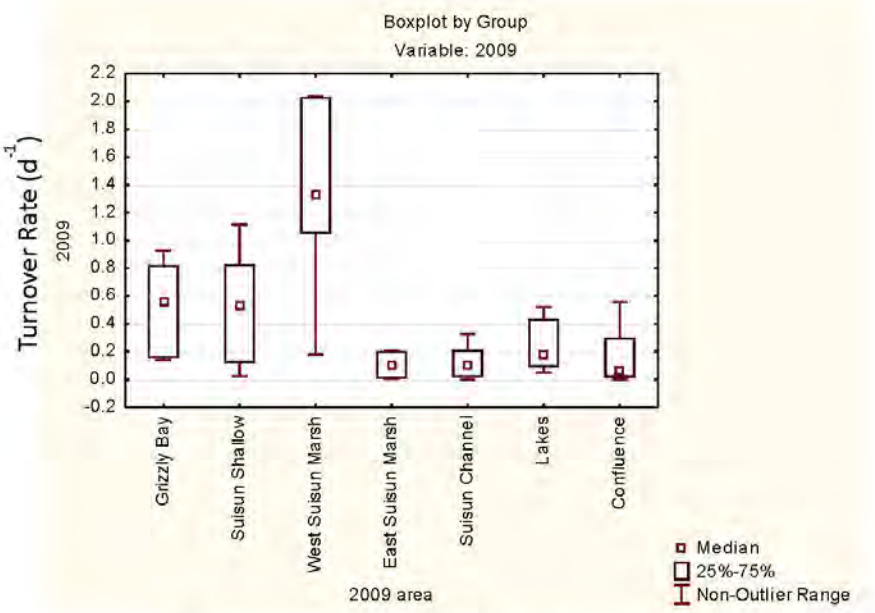

2009	Grizzly/ Honker Bay	Suisun Shallow	West Suisun Marsh	East Suisun Marsh	Suisun Channel	Lakes	Confluence
Grizzly/Honker Bay							0.049
Suisun Shallow							
West Suisun Marsh					0.00006		0.000004
East Suisun Marsh							
Suisun Channel			0.00006				
Lakes							
Confluence	0.0492		0.000004				

Figure 8. Grazing turnover rates for all regions in 2009. Table shows regions that had similar values (line) and those significantly different at $p \leq 0.05$ (Kruskal-Wallis test).

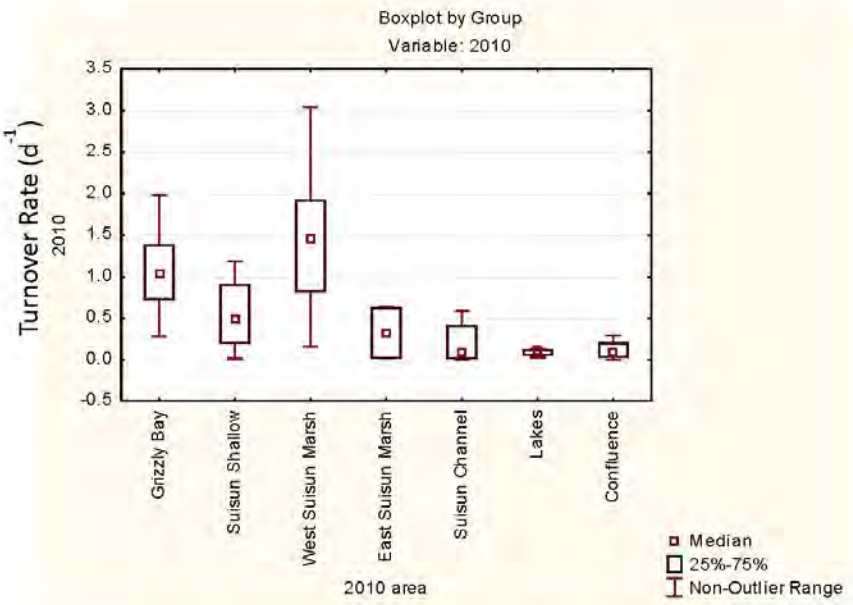

2010	Grizzly/ Honker Bay	Suisun Shallow	West Suisun Marsh	East Suisun Marsh	Suisun Channel	Lakes	Confluence
Grizzly/Honker Bay					0.006		0.0004
Suisun							
West Suisun Marsh					0.0006	0.025	0.00002
East Suisun Marsh							
Suisun Channel	0.006		0.0006				
Lakes			0.025				
Confluence	0.0004		0.00002				

Figure 9. Grazing turnover rates for all regions in 2010. Table shows regions that had similar values (line) and those significantly different at $p \leq 0.05$ (Kruskal-Wallis test).

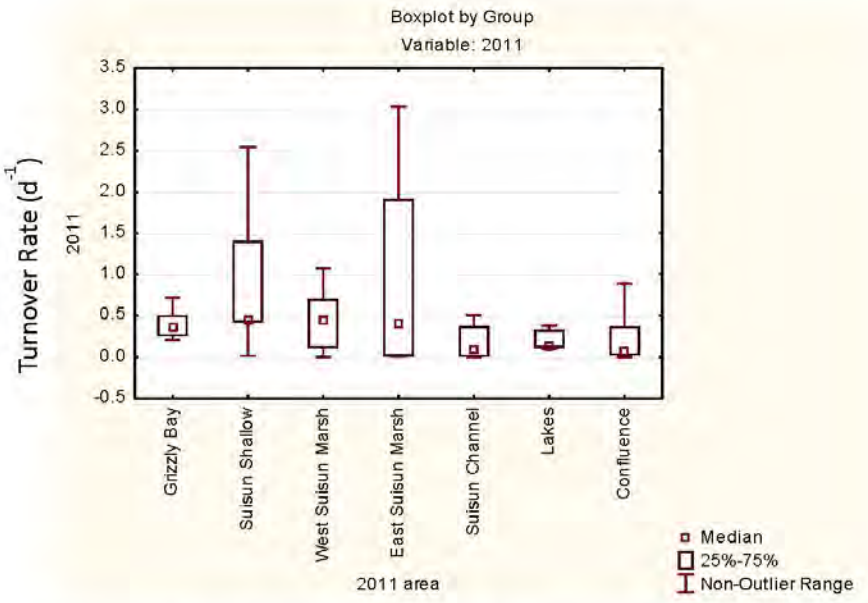

2011	Grizzly/ Honker Bay	Suisun Shallow	West Suisun Marsh	East Suisun Marsh	Suisun Channel	Lakes	Confluence
Grizzly/Honker Bay							
Suisun Shallow							
West Suisun Marsh							
East Suisun Marsh							
Suisun Channel							
Lakes							
Confluence							

Figure 10. Grazing turnover rates for all regions in 2011. Table shows all regions had statistically similar values (line) at $p \leq 0.05$ (Kruskal-Wallis test).

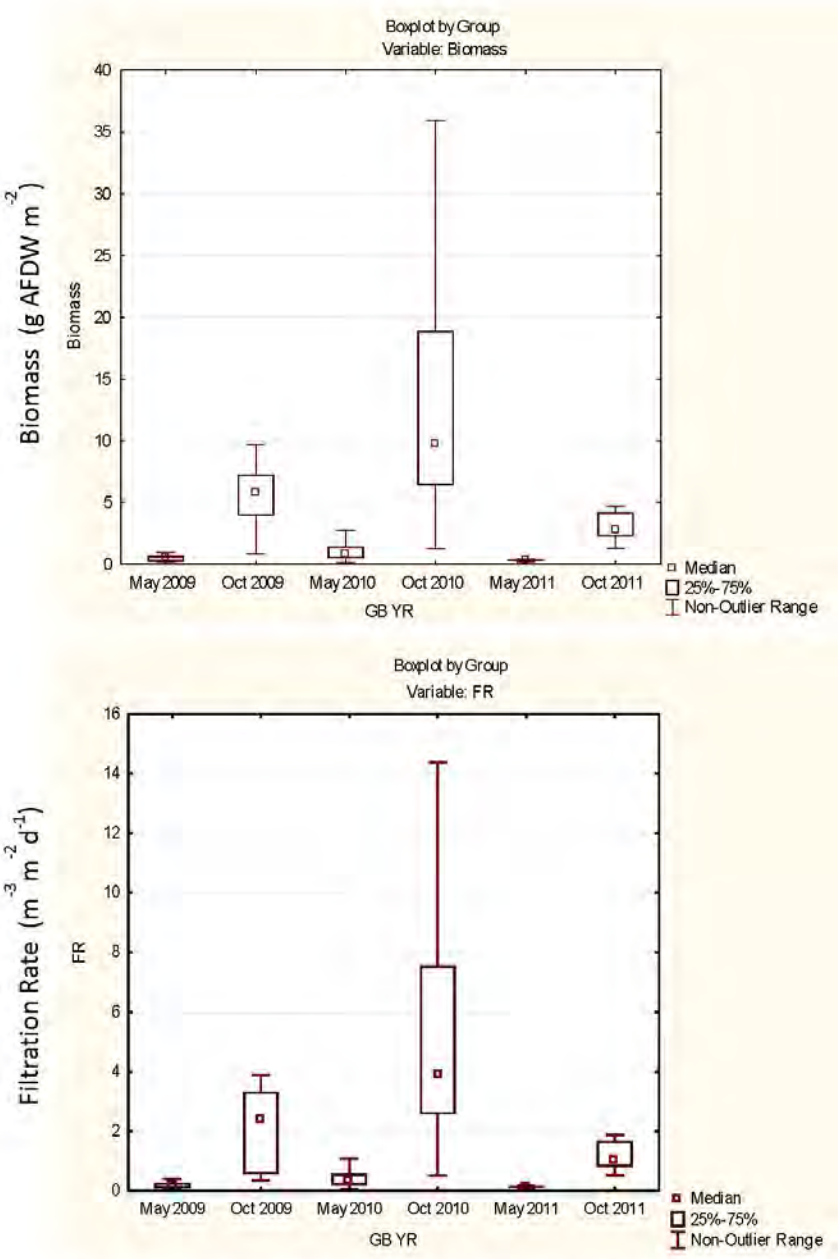

Figure 11. Biomass and filtration rate of bivalves in the shallow habitat of Grizzly and Honker Bays in May 2009-October 2011.

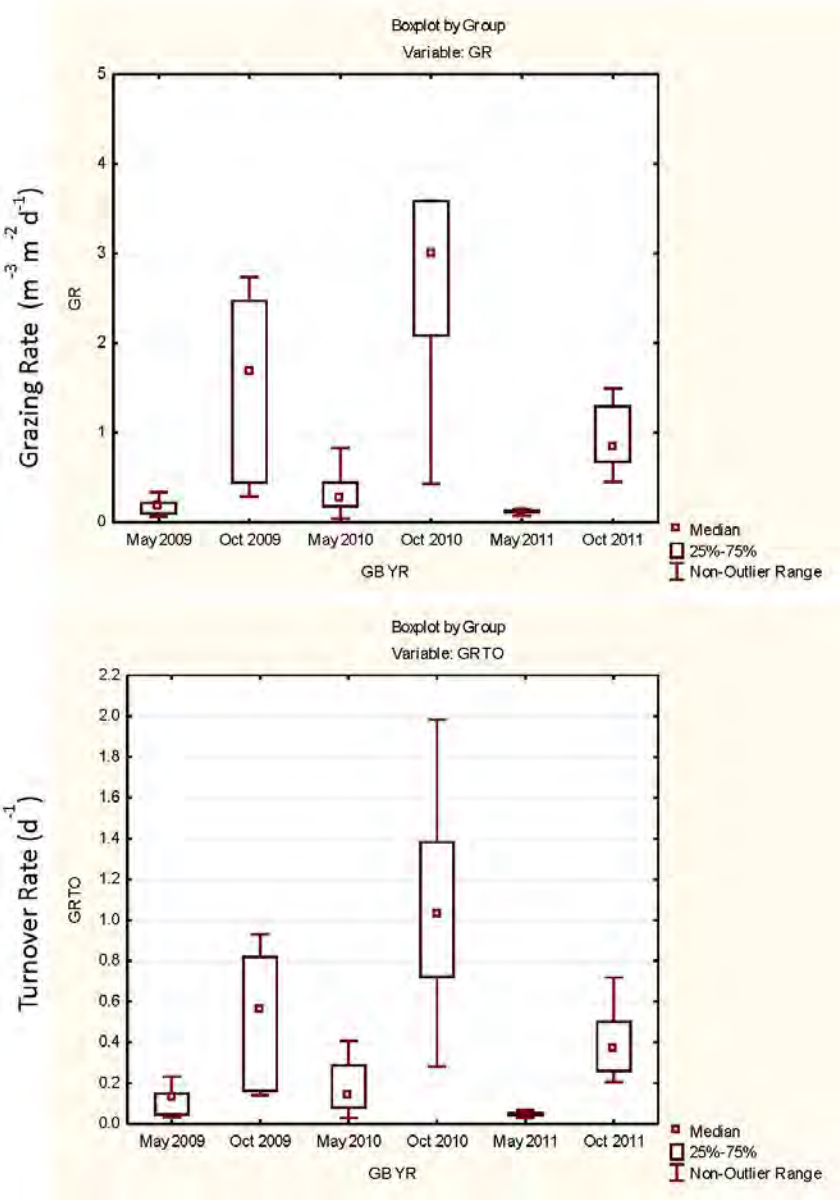

Figure 12. Grazing rate and water column turnover rate of bivalves in the shallow habitat of Grizzly and Honker Bays in May 2009-October 2011.

Table 1. Biomass (g AFDW m^{-2}) (N: sample number, CL: confidence limit)

Region	N	Mean	-95% CL	+95%CL	Median	Min	Max
2009							
Grizzly/Honker Bay	11	5.3	3.5	7.1	5.8	0.9	9.7
Suisun Shallows	10	8.4	3.6	13.2	8.4	0.3	17.2
Suisun Channel	16	7.3	0.1	14.6	3.3	0.0	56.4
East Suisun Marsh	2	11.7	-135.8	159.2	11.7	0.1	23.3
West Suisun Marsh	11	16.0	7.3	24.6	12.9	0.0	34.9
Confluence	28	11.9	5.8	17.9	5.9	0.0	57.4
Lakes	7	8.1	4.2	12.0	7.9	2.0	12.8
2010							
Grizzly/Honker Bay	9	13.6	4.8	22.4	9.8	1.3	35.9
Suisun Shallows	11	7.2	2.0	12.4	4.2	0.0	21.1
Suisun Channel	12	9.0	-0.5	18.5	3.3	0.0	53.5
East Suisun Marsh	2	27.5	-310.2	365.3	27.5	0.9	54.1
West Suisun Marsh	11	25.6	8.2	42.9	14.3	0.7	90.6
Confluence	25	10.4	5.4	15.3	5.5	0.0	43.9
Lakes	6	7.2	-4.5	19.0	3.3	0.9	30.0
2011							
Grizzly/Honker Bay	9	3.6	1.8	5.3	2.8	1.3	9.1
Suisun Shallows	9	13.3	-0.7	27.3	4.0	1.7	49.2
Suisun Channel	16	9.0	2.0	16.0	3.4	0.0	42.6
East Suisun Marsh	4	28.9	-29.1	87.0	19.3	0.4	76.7
West Suisun Marsh	8	7.3	1.5	13.1	5.2	0.0	16.1
Confluence	30	12.1	6.9	17.2	7.7	0.0	50.7
Lakes	5	4.9	1.6	8.3	3.1	3.0	8.7

Table 2. Filtration Rate ($m^{-3}m^{-2}d^{-1}$)

Region	N	Mean	-95% CL	+95%CL	Median	Min	Max
2009							
Grizzly/Honker Bay	11	2.2	1.3	3.0	2.4	0.4	3.9
Suisun Shallows	10	3.4	1.4	5.3	3.4	0.1	6.9
Suisun Channel	16	3.1	0.2	6.1	1.3	0.0	22.5
East Suisun Marsh	2	0.8			0.8	0.0	1.6
West Suisun Marsh	11	11.6	0.9	22.2	8.4	0.2	57.2
Confluence	28	1.6	0.1	3.2	0.4	0.0	20.7
Lakes	7	0.6	0.3	0.8	0.5	0.2	0.9
2010							
Grizzly/Honker Bay	9	5.4	1.9	9.0	3.9	0.5	14.4
Suisun Shallows	11	2.9	0.8	5.0	1.7	0.0	8.4
Suisun Channel	14	3.2	-0.1	6.4	0.8	0.0	21.4
East Suisun Marsh	2	2.1			2.1	0.1	4.0
West Suisun Marsh	10	13.0	1.0	25.1	8.6	0.3	58.0
Confluence	25	0.9	0.5	1.2	0.6	0.0	3.0
Lakes	6	0.6	-0.4	1.6	0.2	0.1	2.6
2011							
Grizzly/Honker Bay	9	1.4	0.6	2.1	1.0	0.5	3.6
Suisun Shallows	9	3.9	-0.8	8.6	1.6	0.6	19.7
Suisun Channel	16	3.6	0.8	6.4	1.4	0.0	17.0
East Suisun Marsh	4	3.0	-3.2	9.2	1.9	0.0	8.3
West Suisun Marsh	8	2.7	0.6	4.9	2.1	0.0	6.4
Confluence	30	1.1	0.6	1.6	0.6	0.0	4.5
Lakes	5	0.4	0.1	0.7	0.3	0.2	0.7

Table 3. Grazing Rate ($m^{-3}m^{-2}d^{-1}$)

Region	N	Mean	-95% CL	+95%CL	Median	Min	Max
2009							
Grizzly/Honker Bay	11	1.6	0.9	2.2	1.7	0.3	2.7
Suisun Shallows	10	2.4	1.1	3.8	2.4	0.1	4.8
Suisun Channel	16	2.1	0.5	3.6	1.1	0.0	11.7
East Suisun Marsh	2	0.6			0.6	0.0	1.3
West Suisun Marsh	11	8.0	1.2	14.7	6.5	0.2	36.5
Confluence	28	1.2	0.2	2.3	0.4	0.0	13.8
Lakes	7	0.5	0.3	0.7	0.5	0.1	0.7
2010							
Grizzly/Honker Bay	9	3.6	1.5	5.6	3.0	0.4	8.7
Suisun Shallows	11	2.1	0.7	3.6	1.4	0.0	6.4
Suisun Channel	14	2.1	0.2	3.9	0.7	0.0	11.9
East Suisun Marsh	2	1.7			1.7	0.1	3.3
West Suisun Marsh	11	8.4	1.5	15.4	4.3	0.2	37.1
Confluence	26	0.7	0.4	0.9	0.5	0.0	2.1
Lakes	6	0.4	-0.1	0.9	0.2	0.1	1.3
2011							
Grizzly/Honker Bay	9	1.1	0.6	1.6	0.8	0.4	2.7
Suisun Shallows	8	3.1	-0.4	6.6	1.6	0.6	13.2
Suisun Channel	16	2.6	0.7	4.6	1.1	0. 0	11.8
East Suisun Marsh	4	2.1	-2.1	6.4	1.5	0.0	5.6
West Suisun Marsh	9	1.9	0.5	3.3	1.3	0.0	4.9
Confluence	30	0.9	0.5	1.2	0.6	0.0	3.3
Lakes	5	0.4	0.1	0.6	0.3	0.2	0.6

Table 4. Grazing Turnover Rate (d^{-1})

Region	N	Mean	-95% CL	+95%CL	Median	Min	Max
2009							
Grizzly/Honker Bay	11	0.5	0.3	0.7	0.6	0.1	0.9
Suisun Shallows	10	0.5	0.2	0.8	0.5	0.0	1.1
Suisun Channel	16	0.2	0.1	0.3	0.1	0.0	0.6
East Suisun Marsh	2	0.1			0.1	0.0	0.2
West Suisun Marsh	11	2.1	0.6	3.6	1.3	0.2	8.2
Confluence	28	0.3	0.0	0.5	0.1	0.0	2.7
Lakes	7	0.3	0.1	0.4	0.2	0.0	0.5
2010							
Grizzly/Honker Bay	9	1.1	0.6	1.5	1.0	0.3	2.0
Suisun Shallows	11	0.5	0.2	0.8	0.5	0.0	1.2
Suisun Channel	14	0.2	0.1	0.3	0.1	0.0	0.6
East Suisun Marsh	2	0.3			0.3	0.0	0.6
West Suisun Marsh	11	1.5	0.9	2.1	1.5	0.2	3.0
Confluence	25	0.1	0.1	0.2	0.1	0.0	0.6
Lakes	6	0.1	0.0	0.3	0.1	0.0	0.4
2011							
Grizzly/Honker Bay	9	0.4	0.3	0.6	0.4	0.2	0.7
Suisun Shallows	9	0.9	0.2	1.6	0.5	0.0	2.6
Suisun Channel	16	0.2	0.1	0.4	0.1	0.0	1.0
East Suisun Marsh	4	1.0	0	3.2	0.4	0.0	3.0
West Suisun Marsh	8	0.4	0.1	0.8	0.4	0.0	1.1
Confluence	30	0.3	0.1	0.5	0.1	0.0	1.9
Lakes	5	0.2	0.0	0.4	0.1	0.1	0.4

Delta Chinook Final Report

Curry Cunningham, Noble Hendrix, Eva Dusek-Jennings, Robert Lessard and Ray Hilborn

EXECUTIVE SUMMARY

This project developed a stage-structured life history model of summer, spring and winter run Chinook salmon, fitted this model to available data on salmon stock abundance and environmental conditions, and estimated the impact of the environmental conditions on survival of the different stocks of Chinook salmon. This model was then used to forecast how differences in future climate change, marine conditions or productivity, and water exports would affect the survival of the different stocks of Chinook salmon.

We used several statistical techniques to evaluate the relative importance of environmental variables on the survival including both information theoretic approaches and Bayesian approaches. Due to the large number of potential explanatory covariates (59) and the inability to fit all combinations of these covariates, we used Akaike Information Criterion for small sample size (AICc) and a novel method for exploring the model space. The approach used a forward stepwise model building with AICc as the selection criteria. The steps were: 1) fit a null model without any covariate effects to the available data; 2) construct a proposal model by selecting a covariate at random from amongst the set of 59 possible covariates; 3) fit the proposed model to the data; 4) compare the proposal model to the null model; 5) keep proposal model if reduction in AICc value is greater than 2 units; 6) repeat sampling covariates without replacement, fitting the model to data, and evaluating AICc i.e. until all covariates have been tested.

Using the information theoretic approaches we found support for environmental impacts of 14 variables including flow, temperature, sediment concentration, export inflow ratios, exports, ocean upwelling, curl and PDO. The top three environmental drivers affecting fall run were export to inflow ratio, spring upwelling south of the Farallon Islands, and the delta gross channel depletion. The top three drivers affecting spring run were size at Chipps Island, export levels, and sediment concentration at Freemont. The three main factors affecting winter-run were minimum flow during fry rearing, temperatures during egg incubation, and spring upwelling south of the Farallon Islands. We then conducted a Bayesian analysis using these 14 variables to calculate the posterior distribution of the impact of these variables on survival.

We conducted forward simulations under four different export regimes to understand how management of exports would affect each of the races. Furthermore, we evaluated export management under two different climate scenarios and two ocean productivity scenarios to understand how climate variability and ocean productivity may act in concert with management of exports to affect the three Chinook runs. We developed a harvest model that reflected current management of the Central Valley Chinook stocks in which low levels of winter run escapement can reduce fall run harvest.

We found that both climate and exports affected projected survival and the potential recruits per spawner for wild populations. Under current export levels all stocks of spring run would increase across all climate scenarios tested. Winter run would increase except under the most pessimistic of the four climate conditions we evaluated. Mainstem Fall run would have recruits per spawner greater than 1 under the two optimistic climate scenarios and less than 1 under the two pessimistic climate scenarios although the future trend in mainstem fall chinook could be heavily influenced by straying from hatcheries and thus hard to predict. A 30% increase in exports decreased spring and fall stock survival to the point where they would all decline regardless of the climate scenario. A 30% decrease in exports improved survival and recruits per spawner for all stocks.

We found spring Chinook stocks to be most sensitive to exports and less sensitive to climate conditions, whereas winter Chinook were more sensitive to climate conditions than exports.

We did not evaluate alternative ocean harvest scenarios, although reduction or elimination of ocean harvest would increase survival to spawning and thus contribute to rebuilding in the same way as better climate or reduced exports.

INTRODUCTION

Salmon populations in the Sacramento River are far below historical numbers. Fisheries closures have been implemented to protect spring-run Chinook (SRC), winter-run Chinook (WRC), and even fall-run Chinook (FRC), which until 2005, had been considered a healthy stock. The FRC was the staple of the California salmon fishery, has been closed in several years. The FRC have been the most heavily subsidized with hatchery fish. The impact on commercial and recreational fisheries has been dramatic. A variety of reasons in both freshwater and marine environments have been cited as causes of the decline, but it appears that salmon have been subjected to something of a “perfect storm” of deleterious effects, both natural and anthropogenic in origin.

Historically both WRC and SRC used the upstream, higher altitude tributaries of the Sacramento River, but the current extent of accessible freshwater habitat differs greatly and their lower abundances have led to concern and listing by both state and federal agencies (Yoshiyama et al. 1998, 2000, Lindley et al. 2004). WRC and SRC were separated both temporally and geographically in their spawning habitat. Winter-run historically used the headwater springs, spawned in the early summer, emerged from the gravel in late summer, emigrated over the winter, and entered the ocean the following spring (Lindley et al. 2004). Development of eggs was dependent on relatively constant flow and cool temperatures of the spring fed streams. Currently, WRC are confined to spawning in the Sacramento River. SRC used the high spring flows to reach the upper tributaries of the Sacramento in summer and waited out the summer in high elevation pools. Spawning commenced in the fall and juveniles emerged the following spring. Stream residency varied and could last over a year. Out-migration occurred in both spring and fall depending upon time of residency. There are currently several extant subpopulations of SRC. Lindley et al. (2004) suggest that there are four principle groupings that might form the basis of a meta-population structure: 1. Winter-run, 2. Butte Creek spring-run, 3.

Deer and Mill Creek spring-run, 4. Fall-run, late fall-run and Feather/Yuba spring-run. Since several of these runs overlap in their usage of stream and mainstem habitat, it is reasonable to consider that they may compete for resources and therefore a modeling approach that accounts for these overlaps could improve the precision of population predictions. Additionally, variation in survival of one population can provide additional statistical ability to the estimation of environmental effects that influence both populations.

Over the past several decades, substantial resources have been devoted to the management of water resources, fisheries, and habitat in the San Francisco Bay-Sacramento River Delta (Bay-Delta) ecosystem in general, with particular attention being given to resident Chinook salmon runs. There has been increasing concern for species in decline, with the listing of WRC and SRC in the Central Valley (CV) under both federal (Endangered Species Act, ESA) and state laws. The exceedingly low return of FRC in 2008 led to a complete closure of salmon fisheries. Many studies have been conducted in an attempt to explain sources of mortality in freshwater and in the ocean. Tagging studies have shown extremely low survival in freshwater. Wells et al. (2007) showed strong associations between survival and ocean climate indices, providing evidence for a linkage between survival and primary productivity during the marine portion of the life cycle.

Fish interact with natural and anthropogenic aspects of their environment and there can be significant variation in such externalities. Decisions regarding fisheries management, water management and research direction should account for all significant and predictable sources of variation in those externalities where they have a measurable effect on survival. What is lacking is an integrative model that can provide a level of detail in water resource management and fishery management that accounts for interactions between salmon populations, both in the wild as well implicitly captured in the mechanics of fisheries policy.

Although mathematical models of salmon species have been developed both at the individual (e.g., Kimmerer 2001, Jager and Rose 2003) and the population (e.g., Botsford and Brittnacher 1998) level, management and research direction have been based primarily on qualitative compilations of what is known about individual salmon runs. Management would benefit from models that more closely link environmental conditions to biological response. Lessard et al. (*submitted manuscript*) built upon the general principle that survival could be broken down into life history stages so that the relevant environmental factors in each stage could be factored into the estimation of the productivity and capacity parameters that predict density dependence in survival rates. A series of competing models were compared using a statistical modeling and population dynamics platform (OBAN), each reconstructing population dynamics and estimating the relative effects of environmental conditions in freshwater and ocean stages. The study found that temperature, flow and exports explained most of the variation in freshwater. Historically, gate positions of bypasses and cross channels have explained some of the variation in survival, however, water management agencies have responded to biological needs and have in recent years adjusted the timing and magnitude of water redirection activities to mitigate negative effects on salmon. Wind stress curl, a primary productivity surrogate (Wells et al. 2008), was the leading factor explaining variation in ocean survival, although indices such as the Pacific Decadal Oscillation (Mantua et al. 1997) and sea surface temperature also explained variation in ocean survival, although not throughout enough of the timeframe of the study to be statistically competitive in model selection.

For the population dynamics portion of the project, we developed a multi-stock model of the three Central Valley Chinook salmon species-at-risk (WRC, SRC and FRC) that incorporates mortality in all phases of salmon life history, and includes the effects of uncertainty in assessing population status. The approach involves several categories of models: (1) the population dynamics models, (2) the parameter estimation model, (3) the growth model, and (4) the fisheries management model that calibrates fishing effort to the predicted runs of the individual populations.

PART I FITTING A STATISTICAL MODEL

METHODS; MODEL DESCRIPTION

The goal of this project was evaluate the environmental drivers of survival for Chinook salmon populations spawning in the Sacramento River, CA watershed, in a statistically rigorous manner. More generally, our purpose was to test a range of hypotheses describing the putative factors facilitating or limiting survival, factors both natural and anthropogenic in origin and describing both biotic and abiotic processes. To achieve this goal we have created a stage-structured population dynamics model, which estimates the direction and magnitude of influence that a range of these factors, or environmental covariates, have on survival through specific portions of the Chinook life cycle, when fit to available juvenile and adult spawning abundance data. The population dynamics model is currently used to explore the environmental drivers of survival for four fall-run populations including: 1) Mainstem Sacramento wild-spawning Chinook, 2) Battle Creek Coleman National Fish Hatchery produced Chinook, 3) Feather River Hatchery produced Chinook, and 4) American River Nimbus Hatchery produced Chinook, as well as three spring-run populations including: 1) Deer Creek, 2) Mill Creek, and 3) Butte Creek, wild-spawning Chinook.

The stage-structured population dynamics model described in this document compliments and expands upon previous analyses of interactions between environmental factors and survival of Chinook salmon populations of the Sacramento River watershed in several ways. First, while many previous analyses have modeled the survival or productivity of single components of the Sacramento River Chinook stock complex (i.e. (Newman and Rice 2002, Lindley and Mohr 2003, Newman and Brandes 2010, Zeug et al. 2012), fall-run (Newman and Rice 2002), late-fall-run (Newman and Brandes 2010), winter-run (Lindley and Mohr 2003, Zeug et al. 2012)) in isolation, the current population dynamics model is applied to multiple populations of both spring-run and fall-run Chinook and evaluates interactions between these populations at points in the life cycle where co-rearing and co-migration occurs. Second, the current population dynamics model approximates both wild and hatchery type life histories, utilizing historical records of hatchery releases from the Coleman National Fish Hatchery on Battle Creek, the Feather River Hatchery, and the Nimbus Fish Hatchery on the American River compiled by Huber and Carlson (in review). Third, we have utilized estimates of stray rates between hatcheries and wild populations of fall-run Chinook available from the proportional coded wire tagging program (Kormos et al. 2012, Palmer-Zwahlen and Kormos 2013), to reconstruct spawning abundance data in the presence of straying, prior to fitting the estimation model. Fourth, while previous analyses have primarily evaluated survival variation in either the

freshwater or marine portions of the Chinook life cycle, we have created a population dynamics model with both marine and freshwater stages, permitting the testing of competing hypotheses for putative survival influences in all habitats utilized by Sacramento River Chinook. Fifth, while previous stage-structured population dynamics models used to evaluate the interaction between environmental factors and the survival of Sacramento Chinook including Zeug et al. (2012) have defined these interactions based upon a priori information or findings from other systems or laboratory experimentation, the population dynamics model we have created is statistical in nature, estimating the effect of the hypothesized environmental drivers of survival based upon historical variation observed in adult and juvenile abundance. The result is a flexible multi-stock, stage-structured, statistical, population dynamics model that estimates the influence of natural and anthropogenic environmental factors on survival of Chinook salmon throughout their life cycle, using both Bayesian and Maximum Likelihood methods.

The Data

In order to estimate the effect of various environmental covariates as well as basal productivity and capacity for the seven populations in specific life stages, the estimation model is conditioned on different types of data available for the Sacramento River system. The first type of data that are required by the estimation model are time-series of explanatory environmental covariates. For each environmental covariate being evaluated for its influence on Chinook survival, it is necessary to provide, a historical record of its value over time as a model input. Covariate data are z-standardized (Zar 2010) based upon the mean and standard deviation of the time-series (Eq. I.1).

$$X_{t,i} = \frac{x_{t,i} - \sum_{t=1}^{Nt} x_{t,i} / Nt}{\sigma_i} \quad \text{(I.1)}$$

In this way, the ith covariate at time t ($x_{t,i}$) is transformed into units of standard deviations from the time-series mean, rather than untransformed values that span many orders of magnitude among covariates. By transforming covariate data into the same units, the magnitude of subsequently estimated coefficients describing the influence of individual covariates are more readily comparable and estimable.

Potential covariates were chosen for evaluation within the estimation model based upon first principals and a valid biological rationale for why each might be expected to influence either survival rate or stage-specific capacity. Covariates were developed came from a wide range of sources, including a review of the pertinent literature and expert opinion, and were created using data from the period of time throughout the year over which they were expected to exhibit the greatest influence (Table I.1).

TABLE I.1. Environmental covariates

Hypothesis Number	Covariate	Covariate Description	Location	Populations
1	fall.sac.mainstem - sacAirTemp.summer	Sacramento air temperature during summer (July - September) of the brood year	Sacramento, CA	Fall Sacramento Mainstem Wild
2	fall.sac.mainstem - sacAirTemp.spring	Sacramento air temperature during spring (January - March) emergence year	Sacramento, CA	Fall Sacramento Mainstem Wild
3	fall.sac.mainstem - keswick.discharge	Average January - March water discharge (cfs) at Keswick Dam	Keswick Dam	Fall Sacramento Mainstem Wild
4	.1.2.3.4-verona.peak.streamflow	Peak (maximum) streamflow on the Sacramento River mainstem at Verona, CA (January - May)	Verona, Sacramento River	Fall Sacramento Mainstem Wild Fall Battle Creek (CNFH) Hatchery Fall Feather River Hatchery Fall American River (Nimbus) Hatchery
5	.1.2.3.4-yolo.wood.peak.streamflow	Peak (maximum) streamflow into Yolo Bypass at Woodland, CA (January - May)	Into Yolo Bypass at Woodland, CA	Fall Sacramento Mainstem Wild Fall Battle Creek (CNFH) Hatchery Fall Feather River Hatchery Fall American River (Nimbus) Hatchery
6	.1.2.3.4-freeport.sed.conc	Average February - April monthly sediment concentration (mg/L)	Freeport, Sacramento River	Fall Sacramento Mainstem Wild Fall Battle Creek (CNFH) Hatchery Fall Feather River Hatchery Fall American River (Nimbus) Hatchery
7	.1.2.3.4-bass.cpue	Index of Striped Bass abundance as number of striped bass kept	Sacramento - San Joaquin Delta	Fall Sacramento Mainstem Wild Fall Battle Creek (CNFH) Hatchery Fall Feather River Hatchery Fall American River (Nimbus) Hatchery
8	.1.2.3.4-fall.dayflow.geo	Dayflow: Delta Cross Channel and Georgiana Slough Flow Estimate (QXGEO). February - March average	Sacramento - San Joaquin Delta at the Delta Cross Channel and Georgiana Slough	Fall Sacramento Mainstem Wild Fall Battle Creek (CNFH) Hatchery Fall Feather River Hatchery Fall American River (Nimbus) Hatchery
9	.1.2.3.4-fall.dayflow.export	Dayflow: Total Delta Exports and Diversions/Transfers (QEXPORTS). March - May average	Sacramento - San Joaquin Delta	Fall Sacramento Mainstem Wild Fall Battle Creek (CNFH) Hatchery Fall Feather River Hatchery Fall American River (Nimbus) Hatchery
10	.1.2.3.4-fall.dayflow.expin	Dayflow: Export/Inflow Ratio (EXPIN). March - May average	Sacramento - San Joaquin Delta	Fall Sacramento Mainstem Wild Fall Battle Creek (CNFH) Hatchery Fall Feather River Hatchery Fall American River (Nimbus) Hatchery
11	.1.2.3.4-fall.dayflow.cd	Dayflow: Net Channel Depletion (QCD). March - May average	Sacramento - San Joaquin Delta	Fall Sacramento Mainstem Wild Fall Battle Creek (CNFH) Hatchery Fall Feather River Hatchery Fall American River (Nimbus) Hatchery
12	.1.2.3.4-fall.size.chipps	Average size of fall-run Chinook at ocean entry from Chipps Island Trawl	Chipps Island Trawl	Fall Sacramento Mainstem Wild Fall Battle Creek (CNFH) Hatchery Fall Feather River Hatchery Fall American River (Nimbus) Hatchery
13	.1.2.3.4-fall.farallon.temp.early	Average temperature at the Farallon Islands, CA (37° 41.8' N, 122° 59.9' W) during the SPRING months (February - April) BEFORE Chinook ocean entry	Nearshore Region, Farallon Islands, CA	Fall Sacramento Mainstem Wild Fall Battle Creek (CNFH) Hatchery Fall Feather River Hatchery Fall American River (Nimbus) Hatchery
14	.1.2.3.4-fall.farallon.temp.late	Average temperature at the Farallon Islands, CA (37° 41.8' N, 122° 59.9' W) during the SUMMER months (May - July) AFTER Chinook ocean entry	Nearshore Region, Farallon Islands, CA	Fall Sacramento Mainstem Wild Fall Battle Creek (CNFH) Hatchery Fall Feather River Hatchery Fall American River (Nimbus) Hatchery
15	.1.2.3.4-upwelling.north.early	NOAA Index for upwelling at Northern Location (39 N, 125 W), average of SPRING months (April - June)	Nearshore Region	Fall Sacramento Mainstem Wild Fall Battle Creek (CNFH) Hatchery Fall Feather River Hatchery Fall American River (Nimbus) Hatchery
16	.1.2.3.4-upwelling.north.late	NOAA Index for upwelling at Northern Location (39 N, 125 W), average of FALL months (July - December)	Nearshore Region	Fall Sacramento Mainstem Wild Fall Battle Creek (CNFH) Hatchery Fall Feather River Hatchery Fall American River (Nimbus) Hatchery
17	.1.2.3.4-upwelling.south.early	NOAA Index for upwelling at Southern Location (36 N, 122 W), average of SPRING months (April - June)	Nearshore Region	Fall Sacramento Mainstem Wild Fall Battle Creek (CNFH) Hatchery Fall Feather River Hatchery Fall American River (Nimbus) Hatchery
18	.1.2.3.4-upwelling.south.late	NOAA Index for upwelling at Southern Location (36 N, 122 W), average of FALL months (July - December)	Nearshore Region	Fall Sacramento Mainstem Wild Fall Battle Creek (CNFH) Hatchery Fall Feather River Hatchery Fall American River (Nimbus) Hatchery
19	.1.2.3.4.5.6.7-curl.early	NOAA Wind Stress Curl Index for upwelling at Northern Location (39 N, 125 W), average of SUMMER months (April -June)	Nearshore Region	Fall Sacramento Mainstem Wild Fall Battle Creek (CNFH) Hatchery Fall Feather River Hatchery Fall American River (Nimbus) Hatchery Spring Deer Creek Spring Mill Creek Spring Butte Creek
20	.1.2.3.4.5.6.7-curl.late	NOAA Wind Stress Curl for upwelling at Northern Location (39 N, 125 W), average of FALL months (July - December)	Nearshore Region	Fall Sacramento Mainstem Wild Fall Battle Creek (CNFH) Hatchery Fall Feather River Hatchery Fall American River (Nimbus) Hatchery Spring Deer Creek Spring Mill Creek Spring Butte Creek
21	.1.2.3.4.5.6.7-pdo.early	Pacific Decadal Oscillation (PDO), average of January - May monthly indices during first year of mearine residence	Ocean	Fall Sacramento Mainstem Wild Fall Battle Creek (CNFH) Hatchery Fall Feather River Hatchery Fall American River (Nimbus) Hatchery Spring Deer Creek Spring Mill Creek Spring Butte Creek
22	.1.2.3.4.5.6.7-pdo.late	Pacific Decadal Oscillation (PDO), average of October - December monthly indices during first year of mearine residence	Ocean	Fall Sacramento Mainstem Wild Fall Battle Creek (CNFH) Hatchery Fall Feather River Hatchery Fall American River (Nimbus) Hatchery Spring Deer Creek Spring Mill Creek Spring Butte Creek

Hypothesis Number	Covariate	Covariate Description	Location	Populations
23	fall.battle.creek - sacAirTemp.summer	Sacramento air temperature during summer (July - September) of the brood year	Sacramento, CA	Fall Battle Creek (CNFH) Hatchery
24	fall.battle.creek - sacAirTemp.spring	Sacramento air temperature during spring (January - March) emergence year	Sacramento, CA	Fall Battle Creek (CNFH) Hatchery
25	fall.battle.creek - keswick.discharge	Average January - March water discharge (cfs) at Keswick Dam	Keswick Dam	Fall Battle Creek (CNFH) Hatchery
26	fall.battle.creek - battle.discharge	Average January - March water discharge (cfs) on Battle Creek	Cottonwood, Battle Creek	Fall Battle Creek (CNFH) Hatchery
27	fall.battle.creek - battle.peak.gage.ht	Battle Creek peak guage height November - December of brood year	Cottonwood, Battle Creek	Fall Battle Creek (CNFH) Hatchery
28	fall.feather - sacAirTemp.summer	Sacramento air temperature during summer (July - September) of the brood year	Sacramento, CA	Fall Feather River Hatchery
29	fall.feather - sacAirTemp.spring	Sacramento air temperature during spring (January - March) emergence year	Sacramento, CA	Fall Feather River Hatchery
30	fall.feather - keswick.discharge	Average January - March water discharge (cfs) at Keswick Dam	Keswick Dam	Fall Feather River Hatchery
31	fall.feather - feather.oronville.discharge	Average January - March water discharge (cfs) on the Feather River	Oronville, Feather River	Fall Feather River Hatchery
32	fall.american - sacAirTemp.summer	Sacramento air temperature during summer (July - September) of the brood year	Sacramento, CA	Fall American River (Nimbus) Hatchery
33	fall.american - sacAirTemp.spring	Sacramento air temperature during spring (January - March) emergence year	Sacramento, CA	Fall American River (Nimbus) Hatchery
34	fall.american - keswick.discharge	Average January - March water discharge (cfs) at Keswick Dam	Keswick Dam	Fall American River (Nimbus) Hatchery
35	fall.american - american.discharge	Average January - March water discharge (cfs) on the American River	Fair Oaks, American River	Fall American River (Nimbus) Hatchery
36	spring.deer - sacAirTemp.summer	Sacramento air temperature during summer (July - September) of the brood year	Sacramento, CA	Spring Deer Creek
37	spring.deer - sacAirTemp.spring	Sacramento air temperature during spring (January - March) emergence year	Sacramento, CA	Spring Deer Creek
38	.5.6.7-verona.peak.streamflow	Peak (maximum) streamflow on the Sacramento River mainstem at Verona, CA (January - May)	Verona, Sacramento River	Spring Deer Creek Spring Mill Creek Spring Butte Creek
39	.5.6.7-yolo.wood.peak.streamflow	Peak (maximum) streamflow into Yolo Bypass at Woodland, CA (January - May)	Into Yolo Bypass at Woodland, CA	Spring Deer Creek Spring Mill Creek Spring Butte Creek
40	.5.6.7-freeport.sed.conc	Average February - April monthly sediment concentration (mg/L)	Freeport, Sacramento River	Spring Deer Creek Spring Mill Creek Spring Butte Creek
41	.5.6.7-bass.cpue	Index of Striped Bass abundance as number of striped bass kept	Sacramento - San Joaquin Delta	Spring Deer Creek Spring Mill Creek Spring Butte Creek
42	.5.6.7-upwelling.north.early	NOAA Index for upwelling at Northern Location (39 N, 125 W), average of SPRING months (April - June)	Nearshore Region	Spring Deer Creek Spring Mill Creek Spring Butte Creek
43	.5.6.7-upwelling.north.late	NOAA Index for upwelling at Northern Location (39 N, 125 W), average of FALL months (July - December)	Nearshore Region	Spring Deer Creek Spring Mill Creek Spring Butte Creek
44	.5.6.7-upwelling.south.early	NOAA Index for upwelling at Southern Location (36 N, 122 W), average of SPRING months (April - June)	Nearshore Region	Spring Deer Creek Spring Mill Creek Spring Butte Creek
45	.5.6.7-upwelling.south.late	NOAA Index for upwelling at Southern Location (36 N, 122 W), average of FALL months (July - December)	Nearshore Region	Spring Deer Creek Spring Mill Creek Spring Butte Creek
46	spring.deer - deer.discharge	Average October - December water discharge (cfs) at Deer Creek	Vinna, Deer Creek	SpringDeer Creek
47	.5.6.7-spring.dayflow.geo	Dayflow: Delta Cross Channel and Georgiana Slough Flow Estimate (QXGEO). January - March average	Sacramento - San Joaquin Delta at the Delta Cross Channel and Georgiana Slough	Spring Deer Creek Spring Mill Creek Spring Butte Creek
48	.5.6.7-spring.dayflow.export	Dayflow: Total Delta Exports and Diversions/Transfers (QEXPORTS). February - April average	Sacramento - San Joaquin Delta	Spring Deer Creek Spring Mill Creek Spring Butte Creek
49	.5.6.7-spring.dayflow.expin	Dayflow: Export/Inflow Ratio (EXPIN). February - April average	Sacramento - San Joaquin Delta	Spring Deer Creek Spring Mill Creek Spring Butte Creek
50	.5.6.7-spring.dayflow.cd	Dayflow: Net Channel Depletion (QCD). February - April average	Sacramento - San Joaquin Delta	Spring Deer Creek Spring Mill Creek Spring Butte Creek
51	.5.6.7-spring.size.chipps	Average size of spring-run Chinook at ocean entry from Chipps Island Trawl	Chipps Island Trawl	Spring Deer Creek Spring Mill Creek Spring Butte Creek
52	.5.6.7-spring.farallon.temp.early	Temperature at the Farallon Islands, CA (37° 41.8' N, 122° 59.9' W) during the SPRING months (January - March) BEFORE Chinook ocean entry	Nearshore Region	Spring Deer Creek Spring Mill Creek Spring Butte Creek
53	.5.6.7-spring.farallon.temp.late	Temperature at the Farallon Islands, CA (37° 41.8' N, 122° 59.9' W) during the SUMMER months (April - June) AFTER Chinook ocean entry	Nearshore Region, Farallon Islands, CA	Spring Deer Creek Spring Mill Creek Spring Butte Creek
54	spring.mill - sacAirTemp.summer	Sacramento air temperature during summer (July - September) of the brood year	Sacramento, CA	Spring Mill Creek
55	spring.mill - sacAirTemp.spring	Sacramento air temperature during spring (January - March) emergence year	Sacramento, CA	Spring Mill Creek
56	spring.mill - mill.discharge	Average October - December water discharge (cfs) on Mill Creek	Molinos, Mill Creek	Spring Mill Creek
57	spring.butte - sacAirTemp.summer	Sacramento air temperature during summer (July - September) of the brood year	Sacramento, CA	Spring Butte Creek
58	spring.butte - sacAirTemp.spring	Sacramento air temperature during spring (January - March) emergence year	Sacramento, CA	Spring Butte Creek
59	spring.butte - butte.discharge	Average October - December water discharge (cfs) on Butte Creek	Chico, Butte Creek	Spring Butte Creek

The second type of data required are time-series of abundance data for the populations included in the multi-stock population dynamics model. Estimates of the number of adult Chinook returning to natural spawning grounds and hatcheries are available from the GrandTab database (CDF&W 2014) for all seven populations evaluated as part of this study. However, since the Central Valley Constant Fractional Marking Program (CFM) was initiated in 2007, it has been possible to estimate the contribution of hatchery-origin Chinook to the spawning abundance observed on wild spawning grounds and the contribution of wild-origin Chinook

production to observed returns to regional hatcheries (Kormos et al. 2012). Historical abundances for the seven Chinook populations were reconstructed to account for straying between hatcheries and natural spawning grounds, using the average of the estimated proportion of observed adult Chinook straying in 2010 (Kormos et al. 2012) and 2011 (Palmer-Zwahlen and Kormos 2013). Average (2010-2011) proportions of observed adult abundance that were comprised of hatchery and wild individuals in each population (Table I.2), were used to reconstruct historical abundances for the fall-run spawning populations.

Location	Origin	Recovery	2010	2011	Average
Upper Sacramento	Hatchery	Wild	20%	27%	**24%**
Battle Creek	Hatchery	Wild			
	Wild	Hatchery	11%	11%	**11%**
Feather River	Hatchery	Wild	78%	90%	**84%**
	Wild	Hatchery	5%	4%	**5%**
American River	Hatchery	Wild	32%	66%	**49%**
	Wild	Hatchery	21%	23%	**22%**

Table I.2. Proportion of observed adult abundance by location estimated from CWT recoveries to be of wild or hatchery origin in 2010 and 2011, and the average used to reconstruct historical abundances.

For example, in order to reconstruct the fall-run wild Sacramento mainstem population spawning abundance, each year 24% of the observed spawning abundance was remove and reallocated to the Coleman National Fish Hatchery (Battle Creek) adult abundance, while 11% of the observed Battle Creek hatchery (CNFH) abundance was removed as wild migrants into the hatchery (Fig. I.1).

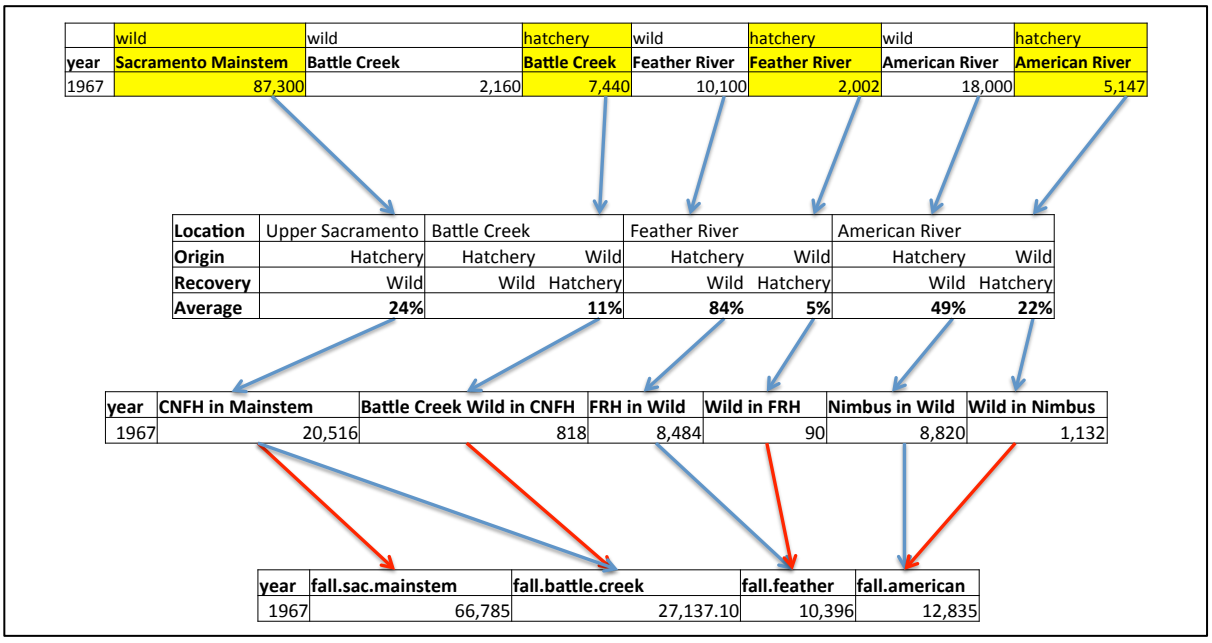

Figure I.1. Empirical schematic showing how the historical abundance of the 1967 population for the four fall-run Chinook populations were reconstructed through additional or removal of the abundance of other stocks.

Adult abundances for the four fall-run Chinook populations were reconstructed using the methods detailed above for years 1967 – 2010 (Fig. I.2). Existing adult abundance estimates reported by CDF&W (2014) for the spring-run populations included in our analyses (i.e. Deer, Mill, and Butte Creeks) were assumed to be minimally impacted by hatchery straying and therefore unaltered (Fig. I.2).

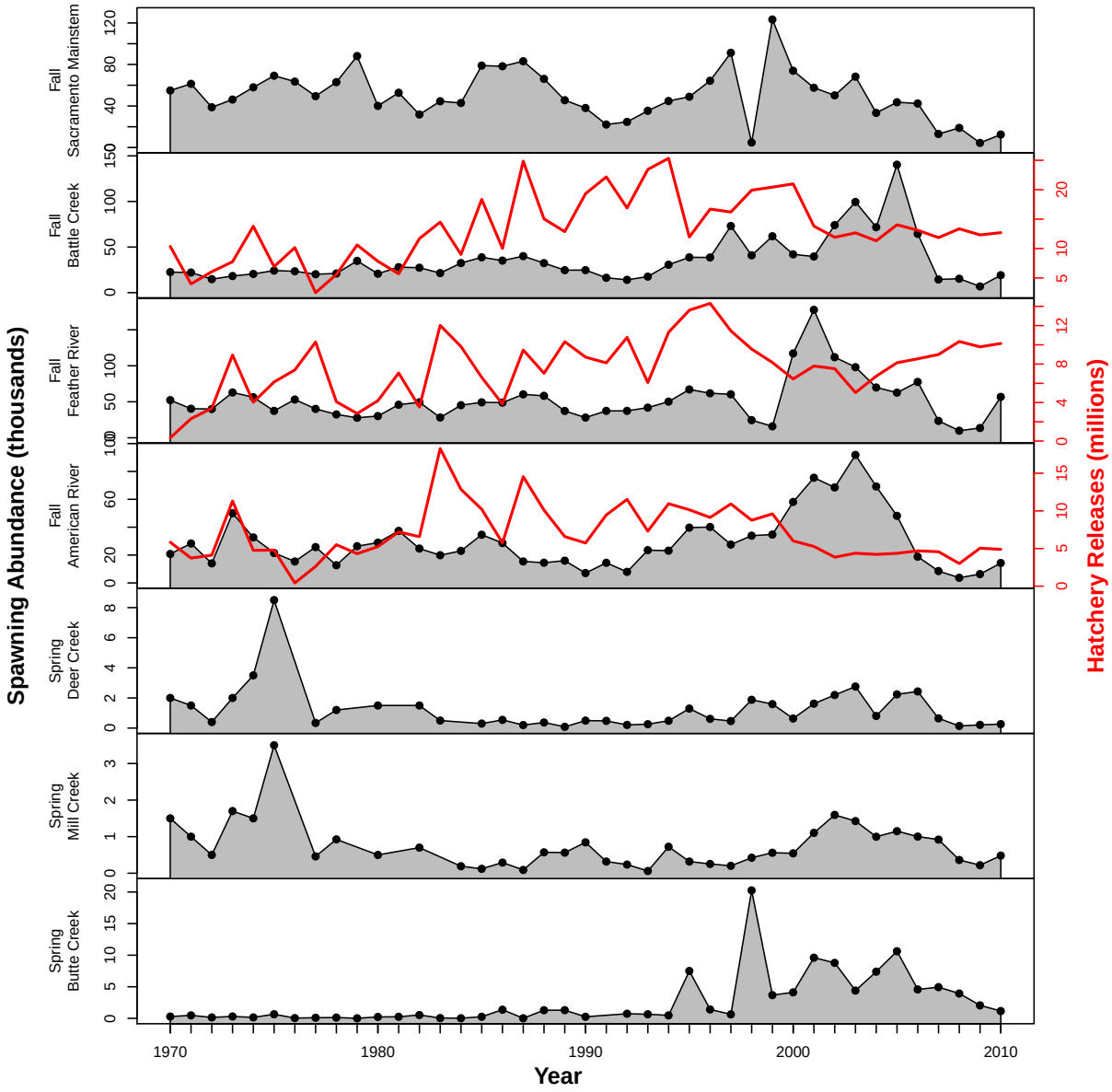

Figure I.2. Adult abundance (grey area plot) and hatchery release (red line) data for Sacramento River Chinook. Fall-run abundances are reconstructed based upon hatchery-wild stray rate estimates, while spring-run abundances are as reported in GrandTab 2014.

Estimates of juvenile Chinook abundance in Sacramento River system were also used to inform estimates of model parameters. The inclusion of additional abundance indices to which

the estimation model is fit, confers a greater ability to partition mortality between life stages and more precise estimation of the strength and magnitude of influence from environmental covariates. Poytress et al. (2014) have used available trap efficiency information to calculate absolute abundance indices for juvenile Chinook passing Red Bluff Diversion Dam, partitioned by race. Fall-run juvenile Chinook abundance estimates from 2002 forward were assumed to be comprised predominantly of two populations, the wild Sacramento Mainstem population and the Battle Creek (CNFH) Hatchery population. Therefore, model estimates of the combined abundance of these two populations were compared to the estimates provided by Poytress et al. (2014) in likelihood calculations.

The third type of data required by the estimation model are historical hatchery releases. As constructed, the estimation model allows for specification of the wild or hatchery life-history type for each population. Three of the seven populations currently in included in our analysis are of hatchery origin, therefore annual hatchery release numbers were required for the Battle Creek (CNFH) Hatchery, Feather River Hatchery, and American River (Nimbus) Hatchery populations. Huber and Carlson (in review) have expended significant time and effort to digitize and render historical hatchery reports in an easily accessible and usable format. For the three hatchery population included in our analysis, we have used these hatchery release data to in place of the functional relationship between spawning abundance and fecundity assumed for the wild spawning populations. Figure I.2 shows hatchery release numbers from Huber and Carlson (in review) for each of the three fall-run hatchery populations.

Hatchery release practices have historically differed amongst facilities and over time, with on-sight releases, releases in the Sacramento-San Joaquin delta, releases in San Francisco Bay, and many locations in between (Huber and Carlson in review). At this time, hatchery release location was not specifically considered. However, for populations whose release strategies allow fish to bypass the mortality incurred in the upriver stage, this should manifest as a reduction in the estimated influence of covariates linked to the upriver stage. In this way, although we do not specifically adjust the model stage pathway depending on hatchery release location in each year, this should not be expected to introduce any significant bias in our estimates of coefficients describing the influence of environmental covariates.

The fourth type of data required for these analyses were annual estimates of harvest rate by population. Harvest rate estimates are available from the U.S. Fish and Wildlife Chinookprod database. For each population of interest, this database uses both the abundance estimates from the Grandtab (CDF&W 2014) database and ocean harvest numbers from the Pacific Fishery Management Council (PFMC) to calculate harvest rates in the marine and in-river regions. For our purposes, we have calculated the total harvest rate by stock and year as the sum of ocean ($C_{t,p}^{ocean}$) and in-river catch ($C_{t,p}^{in-river}$), divided by the total abundance including observed escapement ($E_{t,p}$) and catches for that population (p) in that year (t) (Eq. I.2).

$$hr_{t,p} = \frac{C_{t,p}^{ocean} + C_{t,p}^{in-river}}{E_{t,p} + C_{t,p}^{ocean} + C_{t,p}^{in-river}} \quad \text{(I.2)}$$

Estimation model structure

The purpose of our analysis is to test the various hypotheses regarding what natural and anthropogenic factors have influenced Sacramento River Chinook salmon survival historically, during both the freshwater and marine portions of the Chinook life cycle. Furthermore, we wish to use estimates of the drivers of Chinook survival to generate robust predictions for future abundance under a range of alternative climate change, oceanographic, and water management scenarios. In order to achieve this objective we have created a population dynamics model that estimates the influence of environmental covariates as well as population-specific basal productivity (maximum survival) rates and rearing capacities for different stages in the life cycle.

The statistical population dynamics model is stage-structured, simulating the entire Chinook life cycle from egg to spawning adult, and partitioning mortality events between those separate spatio-temporal stages. For the freshwater portion of the life cycle, these stages are defined by the migration pathways exhibited by the various Chinook populations and the availability of two data types. First, freshwater life stages are defined in accordance with the availability of environmental covariate data, so as to accurately reflect the point in time and location within Sacramento River network where the Chinook have the most substantial exposure to the environmental covariates. Second, model stages are structured to correspond with juvenile indices of abundance at Red Bluff, CA (Poytress et al. 2014). The estimation model contains six stages, three associated with juvenile rearing in freshwater and nearshore regions, and three associated with the marine component of the life cycle (Fig. I.3). The first stage represents rearing of juveniles in tributaries and upper reaches of the Sacramento River mainstem. The second model stage represents the area within the Sacramento River watershed including the Sacramento-San Joaquin Delta through Chipps Island. The third stage represents juvenile rearing in the nearshore region from San Francisco Bay and the Gulf of Farallones. Stages 4-6 represent the years spent in the marine environment, with associated probability of maturation and potential for ocean harvest.

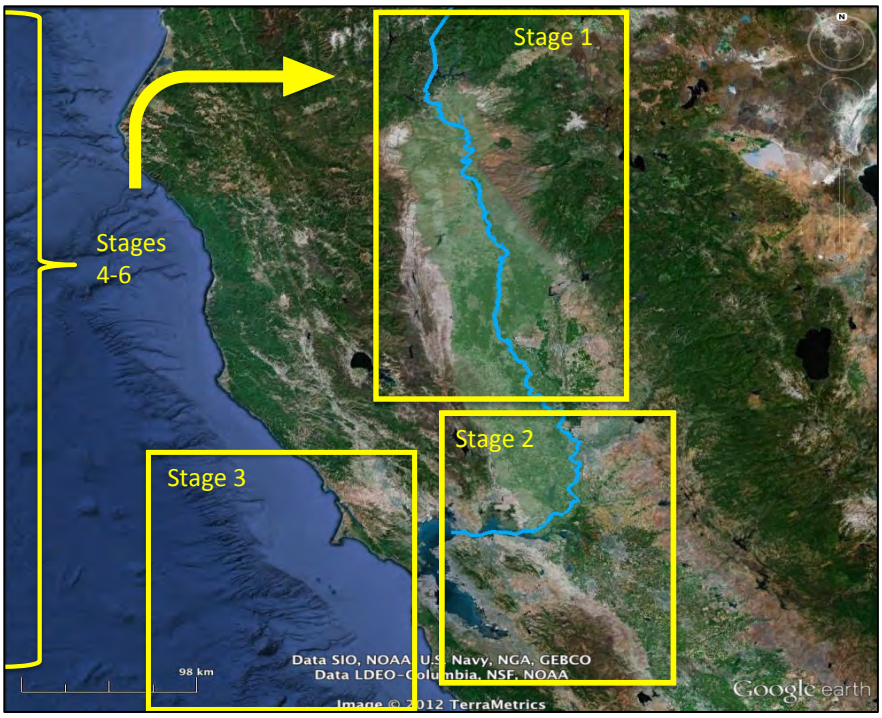

Figure I.3. Map of estimation model stage structure.

The population dynamics model tracks cohorts of Chinook from specific brood years forward in time across sequential model stages. Chinook abundance is represented by $N_{y,s,p}$ or the number of individuals from brood year y, surviving to stage s, of population p. The abundance of Chinook of brood year y and population p, surviving to the end of the current stage (s) is dependent upon the year, stage, and population specific survival rate $SR_{y,s,p}$ in Equation I.3.

(I.3) $$N_{y,s,p} = N_{y,s-1,p} * SR_{y,s,p}$$

Survival though the spatio-temporally explicit life stages is described by a Beverton-Holt transition function (Moussalli and Hilborn 1986). The Beverton-Holt equation, while traditionally used in the evaluation of spawner-recruit data (Beverton and Holt 1957), provides a useful approximation for survival of individuals from one model stage to the next, as influenced by two factors: 1) the productivity rate $p_{y,s,p}$, and 2) the rearing capacity $K_{y,s,p}$ of each stage (Eq. I.4).

(I.4) $$SR_{y,s,p} = \frac{p_{y,s,p}}{1 + \frac{p_{y,s,p} * \sum_{i=1}^{Npop} \alpha_{p,i,s} * N_{y,s-1,i}}{K_{y,s,p}}}$$

In this formulation (Eq. I.4) the year, stage, and population-specific productivity ($p_{y,s,p}$) represents the maximum survival rate in the absence of density-dependent compensation.

Conversely, the year, stage, and population-specific capacity ($K_{y,s,p}$) describes the total number of individuals that can potential survive through the model stage. However, given that we are evaluating multiple co-migrating and co-rearing populations, equation I.4 also includes an interaction effect ($\alpha_{p,i,s}$) which describes how many individuals of the focal population p are displaced with respect to the stage capacity ($K_{y,s,p}$) for each individual of population i. In this way no interaction effect for a stage may be specified with a zero value for all elements of $\alpha_{p,i,s}$ except $\alpha_{p,i=p,s}$. Positive, non-zero values indicate that the abundance of other populations (i) results in a reduction in overall rearing capacity for the focal population (p), and therefore reduced survival at high abundance levels which approach the stage-specific capacity ($K_{y,s,p}$). Specifying $\alpha_{p,i,s}$ elements equal to one create a situation where capacity is shared across populations with symmetric impacts on capacity.

In our current analysis we have identified the Sacramento-San Joaquin Delta stage (2nd) and nearshore stage (3rd) as points of possible competition and therefore capacity interactions within the model. Fall-run and spring-run juvenile Chinook are assumed to compete with members of their own race within these two stages of the life cycle and therefore shared capacities are assumed, with symmetric interactions (i.e. $\alpha_{p,i,s}$ elements equal to 1).

The productivity ($p_{y,s,p}$) capacity ($K_{y,s,p}$) parameters in the population dynamics model are time varying and assumed to change in response to inter-annual variation in the environmental covariates under evaluation. The productivity parameter for population p, of brood year y, in stage s is a function of the basal productivity $\beta_{s,p,0}$, or the average survival for members of that population in the current stage, as well as the sum of environmental covariate c values at time t ($X_{t,c}$) multiplied by their respective coefficients ($\beta_{s,p,c}$) which describe the influence of each covariate on stage and population-specific productivity $p_{y,s,p}$ (Eq. I.5).

$$p_{y,s,p} = \frac{1}{1+\exp\left(-\beta_{s,p,0} - \sum_{c=1}^{Nc_{s,p}} \beta_{s,p,c} * X_{t,c}\right)} \qquad \text{(I.5)}$$

$$t = y + \delta_c$$

δ_c is the covariate-specific temporal reference which is the difference between the brood year y and the year in which the cohort will interact with that covariate, and is used as a pointer to ensure that the covariate value for the correct year is used when tracking each cohort forward in time, and $Nc_{s,p}$ is the number of productivity covariates linked to each population in each stage. The overall productivity parameter value ($p_{y,s,p}$) is a logit transformation of the additive effects of the basal productivity rate and covariate effects, which ensures that its value is smoothly scaled between 0 and 1 (Eq. I.5).

The capacity parameter for each population's brood year specific cohort in each stage ($K_{y,s,p}$) is likewise a function of a basal, or average, stage and population specific capacity across years ($\gamma_{s,p.0}$) and the additive effects of capacity-related covariates ($Y_{t,k}$) and the population-specific coefficients ($\gamma_{s,p.k}$) describing the magnitude and direction of influence each holds (Eq. I.6).

(I.6)
$$K_{y,s,p} = \exp\left(\gamma_{s,p,0} + \sum_{k=1}^{Nk_{s,p}} \gamma_{s,p,k} * Y_{t,k}\right)$$
$$t = y + \delta_k$$

The capacity parameter ($K_{y,s,p}$) is described in natural log space for ease of estimation and to ensure it is bounded within the set of positive values, where k is the covariate reference number and δ_k is the temporal reference for the offset from the brood year for each covariate, indicating when the population interacts with each specific covariate in the life cycle.

However, for populations of Chinook occupying the same habitats and subject to the same environmental covariates, it may be reasonable to assume that a common response in survival to a particular covariate is exhibited. For this reason we have further allowed for a coefficient describing the effect of a particular covariate to be shared across populations. In this way several productivity ($\beta_{s,c}$) capacity ($\gamma_{s.k}$) coefficients may be common across a subset of populations. This reduces model complexity, increases parsimony, and improves the ability to estimate of coefficient values for which a common survival response is biologically defensible.

The basal capacity parameters for a population ($\gamma_{s,p.0}$, see Eq. I.6), or group of interacting populations for which $\alpha_{p,i,s} > 0$ (see Eq. I.4), represent the maximum rearing capacity for that population in that stage over time in the absence of influence from environmental covariates. For populations that are currently well below historical abundance levels, or for populations without subsequent juvenile abundance estimates, it is often difficult to estimate these basal stage capacity values. However, auxiliary information may be used to inform these stage-specific capacities. Recent work by Noble Hendrix, in collaboration with researchers at NOAA, has resulted in monthly juvenile Chinook salmon capacity estimates for the Sacramento River mainstem and the Sacramento-San Joaquin Delta (Hendrix et al. 2014). In place of estimating stage capacities for: 1) Sacramento River mainstem-spawning wild fall-run Chinook in the upstream stage (1st), 2) mainstem-spawning wild, Battle Creek (CNFH) hatchery, Feather River Hatchery, and American River (Nimbus) Hatchery, populations in the Sacramento-San Joaquin Delta stage (2nd), and 3) Deer, Mill, and Butte Creek populations in the Sacramento-San Joaquin Delta stage (2nd), we have used capacity estimates available from NOAA in-stream Chinook capacity modelling (see Appendix A - Delta Submodel). The average of estimated monthly capacities in the Sacramento Mainstem for the period between January and April in each year, was used for as the input capacity for mainstem-spawning wild fall-run population. The average of estimated monthly Sacramento – San Joaquin Delta rearing capacities for the March – May and February – April periods, were used as the input capacities for the fall-run and spring-run populations in that stage, respectively.

Capacity estimates for the Sacramento-San Joaquin Delta from NOAA in-stream Chinook habitat capacity modelling were only available after 1980 (Hendrix et al. 2014). Given that our population dynamics model begins in year 1967, it was necessary to assume a fixed capacity for the period prior to 1980. NOAA Delta capacity estimates correlate most directly with water year type, therefore the average of estimated capacities for the fall-run and spring-run populations by water year type were calculated and used in place of actual capacity estimates

prior to 1980. These average capacities by water year type and Chinook run type were used in years prior to 1980 based on the reported water year.

Survival for cohorts of Chinook is tracked forward in time across spatio-temporal model stages in the same manner (Eq. I.4, I.5, I.6) independent of whether the stage is in the freshwater or marine portion of the life cycle and independent of the ontogenetic status of individuals. However, for the final three model stages representing the 1st, 2nd, and 3rd year in the ocean, it is necessary to account for both the maturation process and marine harvest when tracking the number of individuals entering the next stage. Harvest mortality is assumed to occur after the annual mortality event, but prior to maturation. Catch by year, population, and stage ($C_{t,p,s}$) is the number of surviving individuals multiplied by the population specific harvest rate observed in each year ($hr_{t,p}$), scaled by the stage (i.e. ocean age) specific catchability coefficient (ε_s) (Eq. I.7).

$$C_{t,p,s} = N_{y,s,p} * SR_{y,s,p} * \left(hr_{t,p} / \varepsilon_s\right)$$

(I.7) $$t = y + \rho_s$$

$$\varepsilon_s = \{0, 0, 0, 0, 1.54, 1.0\}$$

In equation I.7, ρ_s is the temporal offset for model stages that indicates the difference between the brood year and the calendar year, so that the proper annual harvest rate may be referenced. Annual harvest rate estimates were obtained from the Pacific Fishery Management Council (PFMC).

For the three ocean life-stages, the number of individuals of a cohort moving to the next stage is governed by the survival rate ($SR_{y,s,p}$), annual catch estimate ($C_{t,p,s}$), and the maturation probability (ϕ_s) (Eq. I.8).

$$N_{y,s+1,p} = \left(N_{y,s,p} * SR_{y,s,p} - C_{t,p,s}\right) * \left(1 - \phi_s\right)$$

(I.8) $$\phi_s = \{0, 0, 0, 0.1, 0.942, 1\}$$

$$t = y + \rho_s$$

While the cohort specific survival rate varies over time, the maturation probability (ϕ_s) is assumed to be temporally invariant. So then, the number of individuals of a cohort advancing to the next ocean stage is the number in the previous stage ($N_{y,s,p}$) that have survived, less the proportion that matures and begins homeward migration (Eq. I.8). The return abundance ($R_{y,s,p}$) is the number of individuals from a cohort that survived marine and harvest mortality, and have initiated the maturation process and return to freshwater to spawn (Eq. I.9).

(I.9) $$R_{y,s,p} = \left(N_{y,s,p} * SR_{y,s,p} - C_{t,p,s}\right) * \phi_s$$

The predicted number of spawning adults of each population in each year ($\hat{A}_{t,p}$) is the sum of returning individuals ($R_{y,s,p}$) across stages or equivalently ocean age classes (Eq. I.10).

(I.10) $$\hat{A}_{t,p} = \sum_{s=1}^{Nstage} R_{y,s,p}$$
$$t = y + \rho_s$$

Depending on whether a wild-type or hatchery-type life history is assumed for each population the next cohort ($N_{y,s=1,p}$) will be created either based on the predicted number of spawning adults and an assumed fecundity value of 2000 eggs/individuals (Eq. I.11) or based upon recorded releases from hatchery facilities (Eq. I.12).

(I.11) $$N_{y,s=1,p} = \hat{A}_{t=y,p} * fec$$

(I.12) $$N_{y,s=1,p} = RH_{t=y,p}$$

In order to estimate the value for model parameters including basal productivities ($\beta_{s,p,0}$) and capacities ($\gamma_{s,p.0}$) for each population in each stage, and coefficients describing the direction and magnitude of influence each environmental covariate has on either productivity ($\beta_{s,p,c}$) or capacity ($\gamma_{s,p.k}$) for individual populations or shared amongst populations ($\beta_{s,c}$ and $\gamma_{s,k}$), the model must be fit to available abundance data. We employ a maximum likelihood approach to compare abundance predictions with available data and estimate model parameter values (Hilborn and Mangel 1997). Predicted adult spawning abundances are calculated (Eq. I.10) as part of the population dynamics model. Absolute abundance estimates for juveniles are available for Chinook passing Red Bluff Diversion Dam (Poytress et al. 2014), and we assume that the mainstem Sacramento wild population and Battle Creek hatchery (CNFH) population comprise the majority of the juvenile fall-run Chinook sampled at this location, so the juvenile abundance estimate is calculated as the sum of these two populations (Eq. I.13)

(I.13) $$\hat{J}_t = \sum_{p=1}^{2} N_{y,s=1,p}$$
$$t = y + \rho_{s=1}$$

Model predicted adult spawning abundances are compared to empirical data, and model parameters are estimated by minimizing the negative log-likelihood of the model given the observed data (Eq. I.14).

(I.14) $$L_A\left(\Theta \mid A_{t,p}\right) = \prod_{t=1}^{n} \frac{1}{\hat{\sigma}_p\sqrt{2\pi}} \exp\left[-\frac{\left(\ln(A_{t,p}) - \ln(\hat{A}_{t,p})\right)^2}{2\hat{\sigma}_p^2}\right]$$

The likelihood of the model parameters, given the spawning abundance data, assume a that observation error in log transformed abundances are normally distributed, with the standard deviation of the observation error distribution ($\hat{\sigma}_p$) equal to the maximum likelihood estimate (Eq. I.15).

(I.15) $$\hat{\sigma}_p = \sqrt{\sum_{t=1}^{n} \frac{\left(\ln(A_{t,p}) - \ln(\hat{A}_{t,p})\right)^2}{n}}$$

Under the same assumptions the observation error likelihood of the model parameters given juvenile abundance data (Eq. I.13) was calculated (Eq. I.16)

(I.16) $$L_J\left(\Theta \mid J_t\right) = \prod_{t=1}^{n} \frac{1}{\hat{\sigma}_J\sqrt{2\pi}} \exp\left[-\frac{\left(\ln(J_t) - \ln(\hat{J}_t)\right)^2}{2\hat{\sigma}_J^2}\right]$$

using the maximum likelihood estimate for the standard deviation of the normal observation error distribution from the juvenile data (Eq. I.17).

(I.17) $$\hat{\sigma}_J = \sqrt{\sum_{t=1}^{n} \frac{\left(\ln(J_t) - \ln(\hat{J}_t)\right)^2}{n}}$$

The total data likelihood (Eq. I.18) is the sum of the negative log of the likelihood from the juvenile and adult abundance data.

(I.18) $$LL_T = -\ln\left(L_A\right) - \ln\left(L_J\right)$$

Model parameter values that minimized the total negative log likelihood (LL_T) were found using AD Model Builder (Fournier et al. 2012). AD Model Builder (ADMB) is a software platform allowing complex non-linear minimizations for models containing a large number of parameters while also permitting profile likelihoods or posterior distributions for parameters of interest to be estimated. ADMB was selected as the software design platform for this project because of its flexibility, computational efficiency and ability to reliably sample a complex multivariate likelihood surface. In addition to its benefits as a fast and stable optimization tool for fitting statistical models to data, ADMB also estimates uncertainty in and correlations between model parameters based on their derivative structure.

When fit to available abundance data the ADMB stage-structured population dynamics model provides estimates of model parameters, uncertainty in those parameter estimates, and the hessian matrix for model parameters from which the parameter covariance matrix may be derived. However, with 37 separate environmental covariates to be tested as competing hypotheses it was necessary to define metrics for model fit and parsimony. We use the Akaike Information Criterion corrected for small sample sizes (AICc) (Burnham and Anderson 2002) as a metric for model parsimony (Eq. I.19).

(I.19) $$AICc = 2LL_T + 2p + \frac{2p\left(p+1\right)}{n-p-1}$$

AICc balances the degree to which a model is able to explain the variability in data (LL_T) against the number of parameters estimated (p) and number of data used in estimation (n), and provides a basis for model selection. The second statistic used to evaluate model fit is the mean absolute percent error in model predictions (Eq. I.20).

$$MAPE_p = \frac{\sum_{t=1}^{n} \left| \frac{\hat{A}_{t,p} - A_{t,p}}{A_{t,p}} \right|}{n} \quad \text{(I.20)}$$

The method we have employed in the Sacramento for modelling the anadromous salmonid life cycle as a series of sequential, spatially-explicit, stage-specific Beverton-Holt transition functions that relate density-dependent survival to habitat covariates is similar to those successfully used to address conservation questions regarding other Chinook salmon populations along the West Coast. The Shiraz model developed by Scheuerell et al. (2006), employed to evaluate anthropogenic and habitat effects on production of Chinook in the Snohomish River basin of Puget Sound, Washington, was one of the first to specify interactions between habitat variables and the productivity and capacity parameters of the Beverton-Holt functions describing survival though life stages. Subsequently, Battin et al. (2007) and Honea et al. (2009) employed stage-structured models governed by linked Beverton-Holt transition functions to evaluate the influence of climate change, hydrologic variability, and habitat restoration on populations of Chinook salmon in the Columbia River basin. All three of these analyses used a Shiraz-type approach by linking habitat and climate covariates to stage-specific survival.

However, the model we have designed for evaluating the environmental drivers of survival for Chinook salmon in the Sacramento River differs from the Shiraz-type models described above (Scheuerell et al. 2006, Battin et al. 2007, Honea et al. 2009) in several fundamental ways. First, the model used in these analyses is statistical in nature. Whereas Scheuerell et al. (2006), Honea et al. (2009), and Battin et al. (2007), all specify the relationships between environmental covariates and the productivity and capacity parameters of the Beverton-Holt function for each stage, based upon *in situ* observations, laboratory experiments, or expert opinion, the estimation framework we have created for the analysis of the drivers of Sacramento River Chinook survival estimates these relationships directly from the abundance data. Second, estimation of the relationships between environmental covariates and the Beverton-Holt productivity and capacity parameters, will not only provide point estimates of the effect of each covariate, but also estimates of uncertainty. By estimating both the value for coefficients describing covariate effects, as well as their uncertainty, we are not only be able to discern which covariates have the largest influence, but also which covariates have had a consistent influence historically. Finally, by estimating the value of coefficients describing the magnitude and direction of influence each environmental covariate has on stage-specific productivity or capacity, our method allows for the propagation of estimation uncertainty in those relationships forward when those model parameters are used to predict future abundance trends under alternative climate, marine productivity, or water use scenarios.

METHODS UNCERTAINTY – AICC SELECTIONS AND MCMC METHODS

In order to test a range of hypotheses regarding which environmental covariates influence the survival of seven populations of Sacramento River Chinook, we constructed a stage-structured statistical population dynamics model. When fit to available adult and juvenile abundance data, this model estimates the magnitude and direction of influence that a set of environmental covariates has on two components of Chinook survival, namely life-stage specific productivity (maximum survival) rates and capacities. In the process of fitting population dynamics models to data as part of our analysis, there were two sources of uncertainty that we considered directly. The first was structural uncertainty, or uncertainty in the subset of environmental covariates that best represent the processes driving changes in abundance over time. The second is estimation uncertainty, or uncertainty in our ability to identify the true direction and magnitude of the effect each environmental covariate imposes on Chinook survival. To address structural uncertainty in our analysis, we used a process of forward stepwise model building, based upon an AICc criteria, with replication to ensure complete evaluation of model space, or the range of potential models that may be used to describe trends in abundance over time. This process allowed us to define the "best" model or subset of potential environmental covariates (hypotheses) for describing observed population dynamics. To address the second type of uncertainty in our analysis, estimation uncertainty, we employed Markov Chain Monte-Carlo estimation methods to quantify the probability distributions for the coefficients describing the effect of each environmental covariate on survival.

Stepwise AICc Model Selection

In total 37 separate environmental covariates were identified by the study team as potential drivers of interannual variation in Sacramento Chinook survival. Describing the effects of these 37 environmental covariates on separate populations in the form of either population-specific effects or common influences on groups of populations, resulted in a total 59 covariate-by-population effects, whose influence on survival may be estimated based on their ability to explain observed Chinook abundance data. Each of these 59 covariate-by-population effects represents an alternative hypothesis to be tested in our analysis.

Hypotheses for covariate-by-population effects on Chinook survival may be compared to a "null" model that attempts to explain variation in the time-series' of observed juvenile and adult abundance data based on only observed ocean harvest rates, hatchery release numbers, estimated productivities (maximum survival rates) for populations in the first life-stage, and annual capacities specified by the juvenile capacity modelling (Hendrix et al. 2014). The null model represents the base case, without any influence from environmental covariates. However, in order to define the model with the best potential to provide accurate predictions for population responses to future environmental, climate, and water management scenarios it was necessary to find the most parsimonious model, or subset of explanatory covariates. Model parsimony is defined by the balance between the ability to accurately explain variation in observed data, while estimating the fewest parameters possible. The Akaike information criterion, corrected for small sample sizes (AICc, Eq. I.19), quantifies model parsimony and provides a metric for selecting amongst competing models (Burnham and Anderson 2002). Competing models incorporating

alternative combinations of covariate effects were compared based on their AICc values in order to define a "best-fit" model for generating predictions for future abundance trends.

With a total of 59 independent covariate-by-population effects to be tested for their ability to explain variation in historical Sacramento Chinook survival, the number of possible combinations of these effects, or potential models, is quite large. It becomes unrealistic to fit every possible model permutation to the available data and compare AICc values. Therefore we used a method for exploring the model space, or the range of potential models incorporating different combinations of these effects, which involved a forward stepwise model building with AICc as the selection criteria. Forward stepwise model building begins first by fitting the null model, without any covariate effects, to the available data. Second, a covariate is selected at random from amongst the set of 59 possible covariate-by-population effects and included in the model, and this model is subsequently fit to the data. Third, the AICc value for this new model is compared to that of the null model. If a reduction in AICc value for the model including the additional covariate of greater than 2 units is observed ($\Delta\text{AICc} \leq 2$), when the old model is compared to the model incorporating the new covariate, that covariate is kept, otherwise it is removed from the model. Moving forward, this process of randomly sampling covariates without replacement, fitting the model to data, and evaluating $\Delta AICc$, (i.e. steps two and three) are repeated until all covariates have been tested for their ability to improve model parsimony (see Fig. I.4).

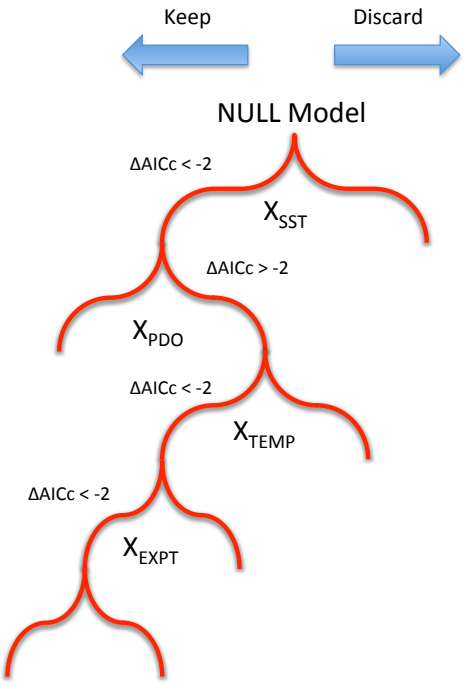

Figure I.4. Diagram of forward stepwise AICc model building process. Starting from the null model, covariates (X_{TEMP}, X_{PDO} etc.) are sampled at random without replacement from the set of 59 possible hypotheses and included in the statistical model. The model is then fit to abundance data and the difference in AICc values between the old and new models dictates whether that covariate is kept or discarded, and the next iteration begins.

The result of one round of forward stepwise AICc model building, or fitting the null model and 59 alternative models sequentially, is one realization of a best-fit model based upon the AICc criteria. However, experience indicates that given even small correlations among some environmental covariates, the order in which covariates are introduced has a subtle influence on the resulting model. Therefore, in order to more fully explore the uncertainty in model selection, we repeated the forward stepwise AICc process 1,000 times. By evaluating the frequency with which specific covariates appear in best-fit models across these 1,000 realizations, it is possible to determine which covariates are most important in explaining historical variation in Chinook survival. Furthermore, by repeating the stepwise AICc process 1,000 times, we are thoroughly exploring the model space and among these independently built models can determine the single model that has the lowest AICc among the candidate best-fit models.

Markov Chain Monte-Carlo Estimation Methods

The second critical piece of uncertainty in our analysis is estimation uncertainty. Estimation uncertainty describes variation in the estimated value of model parameters, and is a function of how well model parameters are informed by the available data. In order to quantify the level of estimation uncertainty in our analyses, particularly as it pertains to estimates of the coefficients describing the influence of environmental covariates on Chinook survival, we employed Bayesian estimation methods in addition to the maximum likelihood approach described above. Bayes' Theorem (Eq. I.21) describes the probability of a hypothesis θ, in our case a set of parameter values, given the data, which in our case are both adult spawning abundance ($A_{t,p}$) and juvenile abundance (J_t) observations.

$$P\left(\theta \mid data\right) = \frac{P\left(data \mid \theta\right)P\left(\theta\right)}{\int P\left(data \mid \theta\right)P\left(\theta\right)} \quad \text{(I.21)}$$

The prior probability on logit transformed coefficients was normal with a mean of zero and standard deviation equal to 2.5, as per recommendations by King et al. (2010). Bounded uniform priors were assumed for all other estimated model parameters. Estimated initial (log) abundances 1967-1969 were bounded on the (0, 100) interval, basal stage productivities ($\beta_{s,p,0}$) were bounded on the (-25, 25) interval, and basal stage capacities ($\gamma_{s,p.0}$) bounded on the (-100, 100) interval. Bayesian estimation methods allow the posterior probability distribution for derived and estimated parameters to be calculated, and from it the full range of parameter uncertainty. The posterior probability distribution for model parameter i (θ_i) describes the probability that the true value of that parameter is equal to a specific value. Based upon the posterior probability distributions for model parameters, we are able to calculate the expected values for model parameters as well the uncertainty in those parameter estimates.

Markov Chain Monte-Carlo (MCMC) methods are commonly used numerical algorithms employed to draw samples from the posterior distributions for parameters in Bayesian models (Gelman et al. 2004). We employed the Random Walk Metropolis-Hastings (RW-MH) MCMC algorithm implemented in AD Model Builder (Fournier et al. 2012) to draw samples from posterior distributions of parameters in population dynamics model. The RW-MH MCMC algorithm is a widely applicable MCMC algorithm that accounts for correlations among model

parameters. As implemented in ADMB, the RW-MH MCMC algorithm begins by finding the parameter values that maximize the complete data likelihood, or posterior modes, and then uses the estimated covariance matrix for model parameters to create a multivariate proposal distribution. Based upon this multivariate proposal distribution randomly drawn parameter sets, or MCMC jumps, are proposed and either accepted or rejected based upon comparison of the ratio of the proposed posterior density to that of the current state, with a random uniform (0,1) deviate. In this way, the RW-MH MCMC algorithm in ADMB begins as the posterior mode and samples the joint posterior.

MCMC chains were run for 5,000,000 iterations with a thinning rate of 1/1,000 to reduce posterior correlation. The first 30% of the chain was removed as a burn-in period, during which the chain approached the stationary distribution for model parameters. To ensure MCMC results converged to their stationary distribution, three independent chains were run simultaneously. Model convergence was tested in three separate ways. First, traceplots of MCMC samples were evaluated for the presence of discernable trends that would indicate a lack of convergence to the true stationary distribution. Second, posterior correlations at differing lags were calculated, wherein significant correlation would indicating a lack of convergence. Finally, Gelman and Rubin's convergence diagnostic (Gelman and Rubin 1992, Brooks and Gelman 1998) was used to compare within and among chain variance to determine if all three chains had indeed converged to the same stationary distribution.

RESULTS MODEL FITS

Model Selection Results

In order to define the set of environmental covariates that best explains historical patterns in abundance for the seven populations of Sacramento Chinook, we employed a process of iterative forward stepwise AICc model selection. This process was meant to test the full range of alternative hypotheses for drivers of Sacramento Chinook survival, and define the most coherent set of covariates with the greatest explanatory power and predictive potential. Each iteration of model selection results in a candidate best-fit model, however it in order to fully explore model space it was necessary to repeat this process many times with a randomized order of covariate proposal in each iteration. By comparing the percent of times any particular covariate appeared across the 1,000 candidate best-fit models, we are able to determine which covariates or hypotheses have the greatest support from the data. Table I.3, describes the percentage of candidate best-fit models that incorporated each specific covariate.

Hypothesis	Covariate	Sum	Percent	Hypothesis	Covariate	Sum	Percent	Hypothesis	Covariate	Sum	Percent
58	spring.butte - sacAirTemp.spring	998	100%	37	spring.deer - sacAirTemp.spring	186	19%	22	.1.2.3.4.5.6.7-pdo.late	11	1%
51	.5.6.7-spring.size.chipps	945	95%	40	.5.6.7-freeport.sed.conc	185	19%	24	fall.battle.creek - sacAirTemp.spring	11	1%
17	.1.2.3.4-upwelling.south.early	783	78%	11	.1.2.3.4-fall.dayflow.cd	182	18%	14	.1.2.3.4-fall.farallon.temp.late	9	1%
21	.1.2.3.4.5.6.7-pdo.early	657	66%	15	.1.2.3.4-upwelling.north.early	169	17%	31	fall.feather - feather.oronville.discharge	9	1%
57	spring.butte - sacAirTemp.summer	571	57%	6	.1.2.3.4-freeport.sed.conc	159	16%	59	spring.butte - butte.discharge	8	1%
48	.5.6.7-spring.dayflow.export	541	54%	56	spring.mill - mill.discharge	131	13%	13	.1.2.3.4-fall.farallon.temp.early	7	1%
9	.1.2.3.4-fall.dayflow.export	484	48%	7	.1.2.3.4-bass.cpue	107	11%	5	.1.2.3.4-yolo.wood.peak.streamflow	3	0%
10	.1.2.3.4-fall.dayflow.expin	374	37%	38	.5.6.7-verona.peak.streamflow	96	10%	16	.1.2.3.4-upwelling.north.late	2	0%
41	.5.6.7-bass.cpue	362	36%	49	.5.6.7-spring.dayflow.expin	95	10%	23	fall.battle.creek - sacAirTemp.summer	2	0%
36	spring.deer - sacAirTemp.summer	359	36%	43	.5.6.7-upwelling.north.late	94	9%	54	spring.mill - sacAirTemp.summer	2	0%
55	spring.mill - sacAirTemp.spring	316	32%	4	.1.2.3.4-verona.peak.streamflow	87	9%	25	fall.battle.creek - keswick.discharge	1	0%
46	spring.deer - deer.discharge	282	28%	3	fall.sac.mainstem - keswick.discharge	85	9%	26	fall.battle.creek - battle.discharge	1	0%
20	.1.2.3.4.5.6.7-curl.late	275	28%	2	fall.sac.mainstem - sacAirTemp.spring	83	8%	27	fall.battle.creek - battle.peak.gage.ht	0	0%
44	.5.6.7-upwelling.south.early	222	22%	29	fall.feather - sacAirTemp.spring	77	8%	28	fall.feather - sacAirTemp.summer	0	0%
50	.5.6.7-spring.dayflow.cd	220	22%	52	.5.6.7-spring.farallon.temp.early	62	6%	30	fall.feather - keswick.discharge	0	0%
18	.1.2.3.4-upwelling.south.late	205	21%	45	.5.6.7-upwelling.south.late	48	5%	32	fall.american - sacAirTemp.summer	0	0%
53	.5.6.7-spring.farallon.temp.late	202	20%	39	.5.6.7-yolo.wood.peak.streamflow	46	5%	33	fall.american - sacAirTemp.spring	0	0%
42	.5.6.7-upwelling.north.early	199	20%	1	fall.sac.mainstem - sacAirTemp.summer	45	5%	34	fall.american - keswick.discharge	0	0%
47	.5.6.7-spring.dayflow.geo	194	19%	12	.1.2.3.4-fall.size.chipps	36	4%	35	fall.american - american.discharge	0	0%
19	.1.2.3.4.5.6.7-curl.early	193	19%	8	.1.2.3.4-fall.dayflow.geo	17	2%				

Table I.3. Model selection results. Percent inclusion rate for environmental covariate effects across 1,000 candidate best-fit models, each resulting from one round of forward stepwise-AICc model building. Note the covariate name includes the single population name, or the numbers for multiple populations upon whose survival the effect of the environmental covariate is shared. For reference population numbers are: 1) fall-run mainstem Sacramento wild-run Chinook, 2) fall-run Battle Creek Coleman National Fish Hatchery produced Chinook, 3) fall-run Feather River Hatchery produced Chinook, 4) fall-run American River Nimbus Hatchery produced Chinook, 5) spring-run Deer Creek wild Chinook, 6) spring-run Mill Creek wild Chinook, and 7) spring-run Butte Creek wild Chinook.

Results of the iterative forward stepwise-AICc model selection (Table I.3) indicate that the set of environmental covariates (hypotheses) which best describe historical variation in Sacramento Chinook abundance encompass a wide range of locations within the life cycle, populations, and ecological processes. A higher inclusion rate across best-fit models for a specific covariate by population(s) effect may be interpreted as greater weight of evidence from the data that this covariate explains variation in survival and therefore may be of ecological importance (Table I.3). Foremost, it should be noted that the influence of spring air temperature at the city of Sacramento on survival of the Butte Creek population (spring.butte – sacAirTemp.spring) was included as an AICc-selected covariate in 998 of 1,000 best-fit models. This covariate represents air temperature during juvenile rearing (January – March) at the city of Sacramento, and is included as a surrogate for Butte Creek stream temperature. Additional covariates which were represented in 60% or greater of iteratively built models include: 1) the combined influence of the size of out-migrating spring-run juveniles on the survival of Deer, Mill and Butte Creek spring-run populations (.5.6.7-spring.size.chipps), 2) the combined influence of near-shore upwelling during the period of ocean entry (April – June) upon the survival of the four fall-run populations (.1.2.3.4-upwelling.south.early), and 3) the combined influence of the Pacific Decadal Oscillation during winter (January – May average) of the first year of marine residence (.1.2.3.4.5.6.7-pdo.early) on the survival of all four fall-run and three spring-run populations. The 5th most frequently included covariate was the effect of summer (July – September) air temperature at Sacramento during the brood year, on survival of Butte Creek spring-run Chinook (spring.butte-sacAirTemp.summer). This covariate was included to test hypothesis that high over-summer water temperatures may have a negative impact on the survival and successful spawning of adult spring-run Chinook holding in tributaries.

With respect to the representation of anthropogenic drivers of Chinook survival across the 1,000 forward-AICc built models, covariates describing the influence of water exports on spring and fall-run survival were the 6th, 7th, and 8th most often included. The combined effect of average water exports from the Sacramento – San Joaquin Delta between February and April quantified by the Dayflow QEXPORTS metric on survival of spring-run Chinook (.5.6.7-spring.dayflow.export), appeared in 54% of forward stepwise-AICc built models. Similarly, the covariate representing the combined effect of March – May average Sacramento – San Joaquin water exports on the survival of the four fall-run Chinook populations (.1.2.3.4-fall.dayflow.export) was included in 48% of stepwise-AICc built models, with the ratio of water exports to total Delta water inflow (Dayflow: EXPIN) during this same period (.1.2.3.4-fall.dayflow.expin) following closely with a 37% inclusion rate. Other covariates highlighting the influence of water routing and supply in the Sacramento – San Joaquin Delta were included in a smaller subset of stepwise-AICc built models. The influence of average net channel depletion (Dayflow: QCD) between February and April on the grouped spring-run Chinook populations (.5.6.7-spring.dayflow.cd) was included in 22% of the 1,000 stepwise-AICc built models. In addition, the combined influence of the average flow into Georgiana Slough and the Delta Cross Channel (Dayflow: QXGEO) February – April on the spring-run populations (.5.6.7-spring.dayflow.geo) was included in 19% of candidate best-fit models.

While the inclusion rate of specific covariate-by-population effects across the 1,000 stepwise-AICc built models provides an indication of the relative weight of evidence from the data, that each covariate holds some ability to explain historical patterns in survival, we consider the model with the lowest AICc value to have the best predictive ability. The single

model with the lowest AICc value represents the most parsimonious fit to the data, explaining the greatest amount of observed variation in adult and juvenile abundance, while estimating the fewest parameters. This lowest AICc or "final" model provides the best basis for predicting future trends in abundance under alternative climate, marine production, and water management scenarios. The final model included 14 covariate-by-population effects, spanning both the freshwater and marine portions of the life cycle (Table I.4). In addition, the effects incorporated in the final model include both single-population effects as well as shared effects of environmental covariates across multiple populations. In total five of the covariates included in the final (lowest AICc) model were related to survival in the 1st (upriver) stage, six were related to the 2nd stage representing environmental effects on survival through the Sacramento – San Joaquin Delta, two were related to the 3rd stage influencing survival in the nearshore environment, and only one covariate was related to survival during subsequent years of marine residence.

Hypothesis Number	Covariate	Covariate Description	Model Stage	Populations
3	fall.sac.mainstem - keswick.discharge	Average January - March water discharge (cfs) at Keswick Dam	Upstream	Fall Sacramento Mainstem Wild
24	fall.battle.creek - sacAirTemp.spring	Sacramento air temperature during spring (January - March) emergence year	Upstream	Fall Battle Creek (CNFH) Hatchery
46	spring.deer - deer.discharge	Average October - December water discharge (cfs) at Deer Creek	Upstream	SpringDeer Creek
57	spring.butte - sacAirTemp.summer	Sacramento air temperature during summer (July - September) of the brood year	Upstream	Spring Butte Creek
58	spring.butte - sacAirTemp.spring	Sacramento air temperature during spring (January - March) emergence year	Upstream	Spring Butte Creek
40	.5.6.7-freeport.sed.conc	Average February - April monthly sediment concentration (mg/L)	Sacramento - San Joaquin Delta	Spring Deer Creek
				Spring Mill Creek
				Spring Butte Creek
48	.5.6.7-spring.dayflow.export	Dayflow: Total Delta Exports and Diversions/Transfers (QEXPORTS). February - April average	Sacramento - San Joaquin Delta	Spring Deer Creek
				Spring Mill Creek
				Spring Butte Creek
51	.5.6.7-spring.size.chipps	Average size of spring-run Chinook at ocean entry from Chipps Island Trawl	Sacramento - San Joaquin Delta	Spring Deer Creek
				Spring Mill Creek
				Spring Butte Creek
6	.1.2.3.4-freeport.sed.conc	Average February - April monthly sediment concentration (mg/L)	Sacramento - San Joaquin Delta	Fall Sacramento Mainstem Wild
				Fall Battle Creek (CNFH) Hatchery
				Fall Feather River Hatchery
				Fall American River (Nimbus) Hatchery
10	.1.2.3.4-fall.dayflow.expin	Dayflow: Export/Inflow Ratio (EXPIN). March - May average	Sacramento - San Joaquin Delta	Fall Sacramento Mainstem Wild
				Fall Battle Creek (CNFH) Hatchery
				Fall Feather River Hatchery
				Fall American River (Nimbus) Hatchery
11	.1.2.3.4-fall.dayflow.cd	Dayflow: Net Channel Depletion (QCD). March - May average	Sacramento - San Joaquin Delta	Fall Sacramento Mainstem Wild
				Fall Battle Creek (CNFH) Hatchery
				Fall Feather River Hatchery
				Fall American River (Nimbus) Hatchery
17	.1.2.3.4-upwelling.south.early	NOAA Index for upwelling at Southern Location (36 N, 122 W), average of SPRING months (April - June)	Nearshore Region	Fall Sacramento Mainstem Wild
				Fall Battle Creek (CNFH) Hatchery
				Fall Feather River Hatchery
				Fall American River (Nimbus) Hatchery
20	.1.2.3.4.5.6.7-curl.late	NOAA Wind Stress Curl for upwelling at Northern Location (39 N, 125 W), average of FALL months (July - December)	Nearshore Region	Fall Sacramento Mainstem Wild
				Fall Battle Creek (CNFH) Hatchery
				Fall Feather River Hatchery
				Fall American River (Nimbus) Hatchery
				Spring Deer Creek
				Spring Mill Creek
				Spring Butte Creek
21	.1.2.3.4.5.6.7-pdo.early	Pacific Decadal Oscillation (PDO), average of January - May monthly indices during first year of mearine residence	1st Ocean Year	Fall Sacramento Mainstem Wild
				Fall Battle Creek (CNFH) Hatchery
				Fall Feather River Hatchery
				Fall American River (Nimbus) Hatchery
				Spring Deer Creek
				Spring Mill Creek
				Spring Butte Creek

Table I.4. Fourteen covariate-by-population effects included in the final AICc-selected model.

Of the covariate-by-population effects on upstream survival incorporated in the final model three were related to atmospheric temperature, used as a proxy for tributary-specific water temperatures, and two were related to water flow conditions. The three temperature-related covariate-by-population effects were all based on air temperature at Sacramento, CA and included: 1) the effect of average spring air temperature (January - March) on survival of the fall-run Battle Creek population in the year of emergence (fall.battle.creek - sacAirTemp.spring), 2) the effect of average summer air temperature (July – September) during the brood year on offspring production and oocyte through juvenile survival for the Butte Creek spring-run population (spring.butte - sacAirTemp.summer), and 3) the effect of average spring air temperature (January – March) in the year of emergence on survival of Butte Creek spring-run Chinook (spring.butte - sacAirTemp.spring). The two upstream covariate effects related to water flow conditions included, the influence of average water

discharge rates (cfs^{-1}) at Keswick Dam during the period between January and March on the survival of Sacramento mainstem spawning wild fall-run Chinook (fall.sac.mainstem - keswick.discharge), and the effect of average water discharge in Deer Creek between October and December on the brood year survival of spring-run Chinook spawning in that tributary (spring.deer - deer.discharge).

The range of covariates which best describe historical patterns in juvenile Chinook survival through the Sacramento – San Joaquin Delta stage included factors both anthropogenic and natural in origin. Interestingly, the winter (February-April) concentration of sediment (mg/L) measured at Freeport, CA was selected based upon the AICc criteria as an important explanatory covariate for both grouped fall-run (.1.2.3.4-freeport.sed.conc) and spring-run (.5.6.7-freeport.sed.conc) populations. Two other covariate effects on the combined survival of fall-run Chinook populations which relate to water flow and management in the Sacramento – San Joaquin Delta were also identified in the final model, including average March – May Dayflow metrics for: 1) QCD or net channel depletion for in-delta consumptive use (.1.2.3.4-fall.dayflow.cd), and 2) EXPIN or the ratio of total delta exports to freshwater inflows (.1.2.3.4-fall.dayflow.expin) (CDWR 2014). In addition to sediment concentration, two other covariate effects on the combined survival of the Deer, Mill, and Butte Creek spring-run populations in the Sacramento – San Joaquin Delta were present in the AICc-selected final model. These included the influence of average monthly water exports and diversions from the delta (February – April) as quantified by the Dayflow metric QEXPORTS (CDWR 2014), which represents the sum of Central Valley Project exports, State Water Project exports, Contra Costa Water District diversions, and North Bay Aqueduct exports (.5.6.7-spring.dayflow.export), and the average size of juvenile spring-run Chinook caught in the Chipps Island Trawl (.5.6.7-spring.size.chipps).

Based on the AICc criteria and thorough exploration of model space using replicate stepwise model building, the final model identified three covariates able to explain some of variance in Chinook survival in the nearshore region following ocean entry and survival during subsequent years of marine residency. Survival for the four fall-run Chinook populations in the nearshore region was explained in part by upwelling patterns during the spring months (April – June) at the southern NOAA/PFEL monitoring site located at 36°N latitude and 122°W longitude (.1.2.3.4-upwelling.south.early). Additionally, the effect of average wind stress curl during July – December of the year of ocean entry on the survival of all seven combined spring and fall-run populations was included in the final model (.1.2.3.4.5.6.7-curl.late). The last covariate present in the final model linked to broad-scale marine climate patterns was the effect of the average Pacific Decadal Oscillation Index during the winter of the first year at sea (January – May) on the combined survival of all seven populations (.1.2.3.4.5.6.7-pdo.early).

These fourteen population-by-covariate effects, spanning freshwater and marine portions of the Chinook life cycle and all seven analyzed Chinook populations, represent the most parsimonious explanation for historical patterns in Chinook survival and observed juvenile and adult abundance. This final model was used as the basis for the subsequent Bayesian analysis of the effect of each of these covariates and their realized survival influence, and used for predicting future trends in abundance under alternative water management scenarios, predictions for future climate change, and marine production patterns.

Estimation Results

In order to estimate the direction and magnitude of the 14 covariate effects identified by AICc selection criteria across 1,000 stepwise-AICc built models (Table I.4), we have employed Bayesian methods with a MCMC sampler. Separate stage-structured models were used to represent each of the seven populations, however common effects across populations for specific covariates were estimated, and shared capacity constraints in the Sacramento – San Joaquin Delta were assumed for the four fall-run and three spring-run populations separately. Estimation of model parameters was informed by juvenile and adult abundance data, reconstructed to account for observed stray rates between hatchery and wild populations. Figure I.6 displays observed adult abundance data for the four fall-run Chinook populations and three spring-run populations as well as the posterior predictive distribution from the Bayesian population dynamics model. The posterior predictive distribution represented by the red line and shaded regions, describe the median, 50% and 95% credible intervals for the predicted adult spawning abundance or hatchery returns for each population in each year.

Results indicate that the model predicts the pattern for Deer and Mill Creek spring-run populations which exhibit higher adult abundances, relative to the time series, through 1984 followed by a period of lower adult abundance through the mid-1990s, followed by higher relative abundances through 2006 (Fig. I.5). Similarly for the Butte Creek spring-run population, the model captures the period of lower spawning abundance prior 1985 followed by a pronounced increase in abundance, ending with a relative plateau in the early 2000's (Fig. I.5). Model predictions for Sacramento Mainstem spawning wild fall-run Chinook and Feather River hatchery fall Chinook both fail to capture the low returns in 1998 – 1999, but capture the reduction in abundance observed in 2007 – 2008. In general for all seven populations of spring and fall-run Chinook included in the analysis, model predictions do not explicitly capture interannual variation, but explain much of the general trend in abundance across the time series (Fig. I.5).

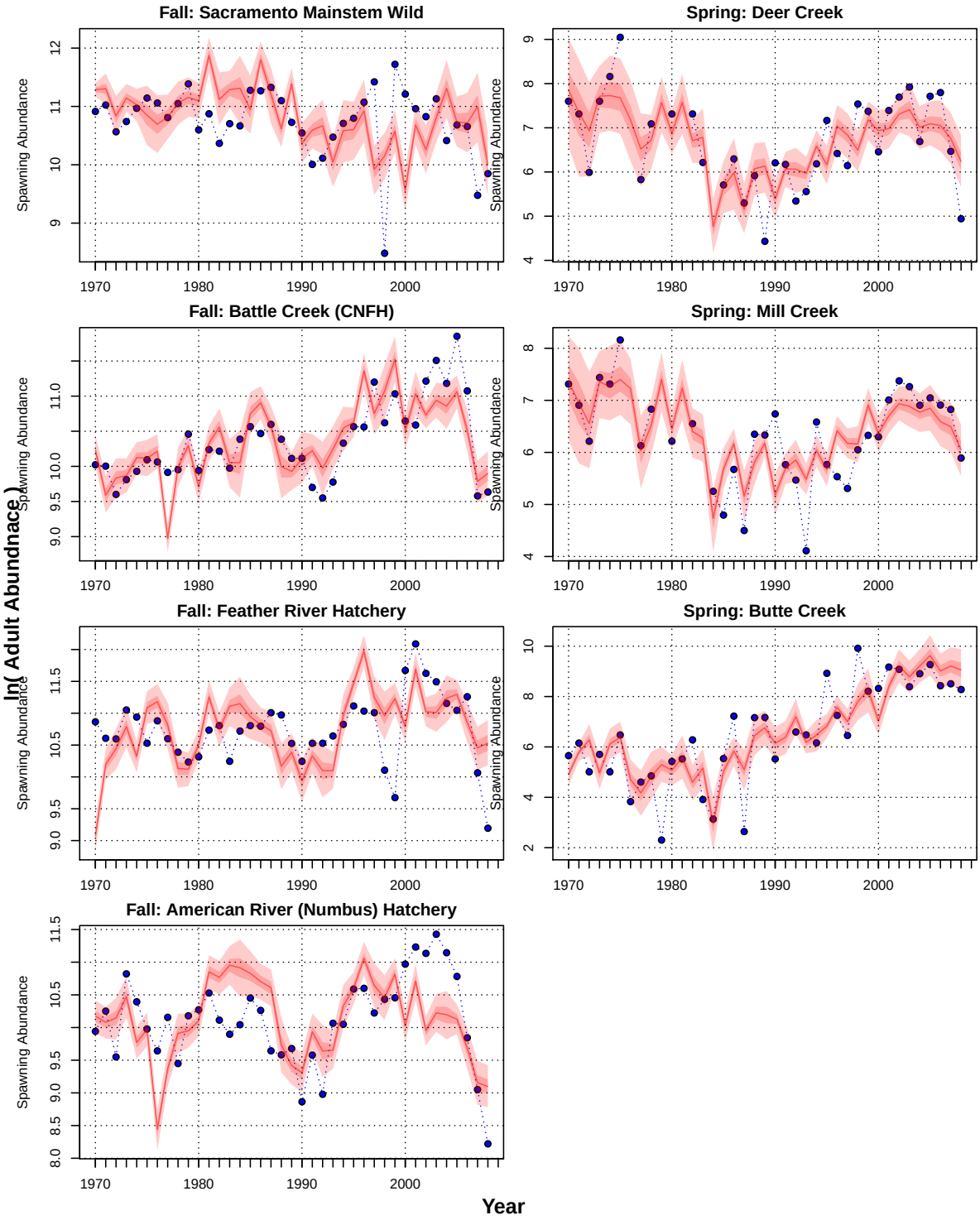

Figure I.5. Bayesian population dynamics model fit to adult abundance data. Blue points and dashed lines indicate the observed adult abundance in each year on the spawning grounds or at the hatchery, reconstructed to account for average stray rates observed from coded wire tagging data (Kormos et al. 2012, Palmer-Zwahlen and Kormos 2013). Red shaded regions are the 95% and 50% credible intervals for the model predicted abundance in each year, and the red line describes the median of the posterior predictions for abundance in each year. Observed and predicted abundances are presented in natural log space.

Posterior distributions for coefficients describing the direction and magnitude of influence each environmental covariate has on a specific population or group of populations were sampled, along with those for other model parameters including survival rate during the first (upstream) life-stage. Bayesian posterior distributions describe the estimated probability that a particular estimated or derived model parameter has a specific value. Figure I.6 displays posterior distributions for coefficients describing the influence of environmental covariates on survival, as well as those for parameters describing the base survival rate to Sacramento – San Joaquin Delta entry. In this figure, samples from posterior distributions arising from the three separate MCMC chains are drawn in different colors. Each parameter estimate is illustrated as a caterpillar plot whose median is described by a point, 50% credible interval by a thick line, and 95% credible interval by a thin line. The concordance of the parameter medians and credible intervals across the three MCMC chains, along with Gelman-Rubin test statistic values for all parameters ≤ 1.05, provide evidence that all three chains have converged to the same stationary distribution.

The bottom panel of figure I.6 displays model predictions for the value of the basal productivity parameter ($\beta_{s,p,0}$) in the upstream stage (Eq. I.5), or maximum survival rate to Sacramento – San Joaquin Delta entry. It should be noted that for the four wild-spawning populations (i.e. Mainstem Sacramento fall-run, and Deer, Mill, and Butte Creek spring runs), this parameter represents the maximum survival rate from egg to Delta entry, while for the three hatchery produced populations (Battle Creek (CNFH), Feather River, and American River (Nimbus) fall-run) this parameter represents the maximum survival rate from hatchery release to Delta entry. Parameter values in logit space are listed on the x-axis below the lower panel, while back transformed maximum survival rate values appear above the lower panel. Several things are clear from this figure I.6. First, the similarity in posterior distributions from each of the three chains again indicates that all three have converged to the same stationary distribution despite differing random walk trajectories through parameter space. Second, basal productivity or maximum survival rate for the upstream stage is both significantly higher and more variable for the three hatchery-reared populations. Higher maximum survival rates for these populations are to be expected given that they only represent mortality incurred after release, not mortality from fertilization to the date of release. However, the greater variance in maximum survival rate for the hatchery populations is easily discernable.

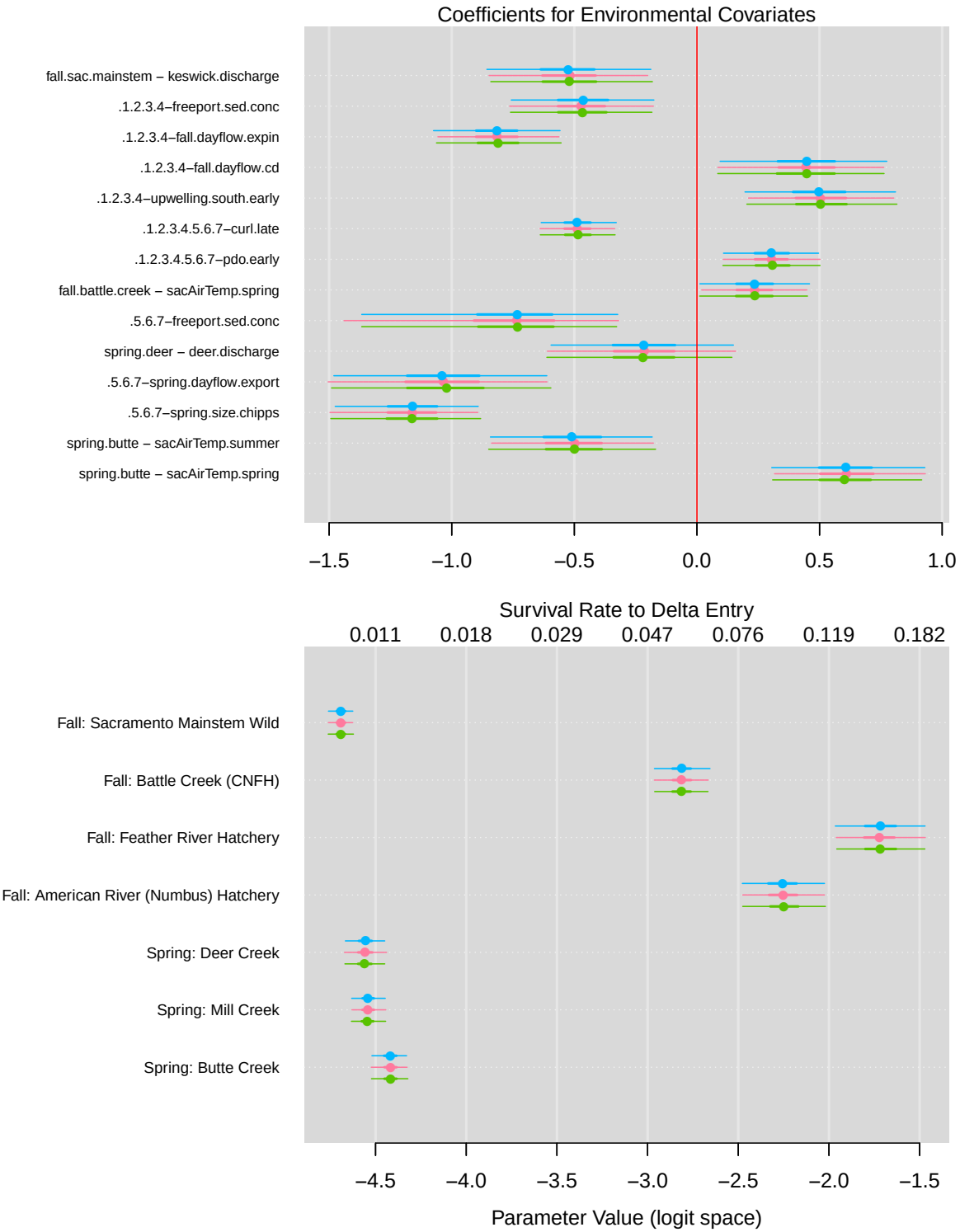

Figure I.6. Posterior probability distributions for coefficients describing the influence of environmental covariates on survival (top) and the maximum survival rate from egg (or hatchery release) to Sacramento – San Joaquin Delta entry. Caterpillar plots describe the median (dot), 50% credible interval (thick line), and 95% credible interval (thin line) of each posterior. Posteriors from each of the independent MCMC chains are depicted with different colours.

Posterior estimates for the value of the coefficients ($\beta_{s,p,c}$) describing the influence of each environmental covariate on a specified population, or group of populations, provide an indication of whether each covariate has a positive or negative influence on survival (Fig. 6, top panel). Table I.5 shows the estimated value for each of the coefficients along with their variance, and quantile range for each posterior distribution. These results indicate that of the 14 covariates included in the final model, 8 covariates were estimated to have a negative impact on stage-specific productivity (maximum survival rate), 5 were estimated to have a positive influence, and 1 was estimated to have a negative influence on average but with a 95% credible interval range overlapping zero. The covariates whose survival impact is estimated to be negative include the effect of: 1) water discharge (cfs-1) from Keswick Dam on Mainstem Sacramento spawning fall-run Chinook (fall.sac.mainstem - keswick.discharge), 2) sediment concentration at Freeport, CA (mg/L) on the combined survival of the four fall-run populations (.1.2.3.4-freeport.sed.conc), 3) the export to inflow ratio in the Sacramento – San Joaquin Delta on combine survival of the fall-run populations (.1.2.3.4-fall.dayflow.expin), 4) wind stress curl on the combined survival of all seven populations of spring and fall-run Chinook (.1.2.3.4.5.6.7-curl.late), 5) spring Freeport, CA sediment concentrations on the combined survival of the three spring-run Chinook populations (.5.6.7-freeport.sed.conc), 6) water exports from the Sacramento – San Joaquin Delta on the combined survival of the three spring-run populations (.5.6.7-spring.dayflow.export), 7) the average size of juvenile spring-run Chinook on combined spring-run survival (.5.6.7-spring.size.chipps), and 8) Sacramento air temperature during summer months of the brood year on survival of Butte Creek spring-run Chinook (spring.butte - sacAirTemp.summer).

Covariate	Mean	sd	CV	2.50%	25%	50%	75%	97.50%
fall.sac.mainstem - keswick.discharge	-0.52	0.17	0.32	-0.85	-0.63	-0.52	-0.41	-0.19
.1.2.3.4-freeport.sed.conc	-0.47	0.15	0.32	-0.76	-0.57	-0.47	-0.37	-0.18
.1.2.3.4-fall.dayflow.expin	-0.81	0.13	0.16	-1.06	-0.90	-0.81	-0.73	-0.56
.1.2.3.4-fall.dayflow.cd	0.44	0.17	0.39	0.09	0.33	0.45	0.56	0.77
.1.2.3.4-upwelling.south.early	0.50	0.15	0.31	0.20	0.40	0.50	0.61	0.81
.1.2.3.4.5.6.7-curl.late	-0.49	0.08	0.16	-0.64	-0.54	-0.49	-0.43	-0.33
.1.2.3.4.5.6.7-pdo.early	0.30	0.10	0.33	0.11	0.24	0.31	0.37	0.50
fall.battle.creek - sacAirTemp.spring	0.23	0.11	0.47	0.01	0.16	0.24	0.31	0.45
.5.6.7-freeport.sed.conc	-0.76	0.27	0.35	-1.38	-0.90	-0.73	-0.59	-0.32
spring.deer - deer.discharge	-0.22	0.19	0.87	-0.61	-0.34	-0.22	-0.09	0.15
.5.6.7-spring.dayflow.export	-1.04	0.23	0.22	-1.49	-1.18	-1.03	-0.88	-0.61
.5.6.7-spring.size.chipps	-1.17	0.15	0.13	-1.49	-1.26	-1.16	-1.06	-0.89
spring.butte - sacAirTemp.summer	-0.51	0.17	0.34	-0.84	-0.62	-0.50	-0.39	-0.17
spring.butte - sacAirTemp.spring	0.61	0.16	0.26	0.31	0.50	0.61	0.71	0.93

Table I.5. Values for the posterior probability distributions for coefficients describing the influence of environmental covariates ($\beta_{s,p,c}$) on productivity (maximum survival rate).

Five of the coefficient values were estimated to be positive (Table I.5), indicating that an increase in the value of those covariates leads to an increase in the maximum survival rate for the associated population or group of populations. These covariates which are estimated to positively influence survival include the effect of: 1) upwelling in the nearshore region during spring of the ocean entry year on the combined survival of the fall-run Chinook populations (.1.2.3.4-upwelling.south.early), 2) spring air temperature at Sacramento, CA on the survival of fall-run Battle Creek (CNFH) Chinook (fall.battle.creek - sacAirTemp.spring), 3) spring air temperature at Sacramento, CA on the survival of Butte Creek spring-run Chinook (spring.butte - sacAirTemp.spring), 4) net channel depletion in the Sacramento – San Joaquin Delta resulting from within-delta consumptive use as quantified by the Dayflow

metric QCD on the combined survival of the four fall-run Chinook populations (.1.2.3.4-fall.dayflow.cd), and 5) the magnitude of the Pacific Decadal Oscillation during winter (January – May) of the first year at in the ocean on the combined survival of all seven spring and fall-run Chinook populations (.1.2.3.4.5.6.7-pdo.early). For the 13 covariates classified above as having either a distinct positive or negative effect on survival, the posterior distribution describing the probability of the true value for each coefficient had a 95% credible interval that was completely above or below zero. Although the estimated median value for the coefficient describing the effect of Deer Creek discharge (cfs^{-1}) on Deer Creek spring-run Chinook survival (spring.deer - deer.discharge) is less than zero (i.e. -0.22, Table I.5) indicating an negative influence on survival, the 95% credible interval overlaps with zero indicating a significant probability (p=0.121) of the covariate having either no influence or a positive influence on survival.

While posterior probability distributions for coefficients representing the influence of each environmental covariate on stage and population-specific productivity ($\beta_{s,p,c}$) describe the model estimate for how much an increase or decrease in the value of that covariate is expected to change stage-specific productivity parameter of the Beverton-Holt equation (Eq. I.4), it is difficult to directly compare these estimated coefficient values for several reasons. First, the basal productivity rate ($\beta_{s,p,0}$) for each stage is population-specific, meaning that the magnitude of estimated coefficients ($\beta_{s,p,c}$) is always relative to the to the basal productivity rate for the population of interest. Second, coefficient values and basal productivity rates are estimated in logit space to ensure the resultant productivity value is smoothly scaled between 0 and 1 (Eq. I.5), and comparing coefficients and basal productivity rates in logit space may be difficult to interpret. Therefore, we have endeavored to translate the magnitude of the estimated environmental covariate effects into more easily interpretable changes in survival.

In order to translate the value of estimated coefficients describing the influence of environmental covariates into predictions for realized changes in survival, we calculated the survival rate for the seven populations from egg, or hatchery release, through adults returning to freshwater under a range of scenarios. Survival rates for each population were calculated by tracking a set number of individuals forward in time across life-stages, assuming no harvest mortality, and using parameter values sampled from the joint posterior for the estimation model. One thousand independent sets of model parameter values were sampled from their joint posterior in order to preserve posterior correlation, and used to quantify the variation in predictions for the influence of each environmental covariate on survival, arising from estimation uncertainty. Survival rate was calculated as the sum of spawning adults across return years, divided by the number of eggs or hatchery releases. The spawning abundance, used as the basis for calculating survival rates, was the 1970 – 2010 average for the wild-spawning populations (i.e. mainstem Sacramento fall-run, as well as Deer, Mill, and Butte Creek spring-run) and the average release numbers for the most recent 10 years for the Battle Creek (CNFH), Feather River, and American River (Nimbus) hatchery populations. Likewise, the most recent 10-year average was used for capacity of wild juvenile fall-run Chinook in the Sacramento mainstem and for the total capacity for spring-run and fall-run Chinook rearing in the Sacramento – San Joaquin Delta.

The distribution of survival rate predictions for each population (p), across the 1,000 independent sets of parameter values (i), was first calculated for a base case ($Sbase_{p,i}$). Under the base case the value for all environmental covariates was set at zero, which for z-standardized covariates is equal to the long-term average. Subsequently the covariate-specific

survival ($Scov_{p,i,c}$) of each population across the 1,000 parameter sets was determined, as each covariate (c) was sequentially changed to have a value of 1. Covariate-specific survival ($Scov_{p,i,c}$) thus represents the population (p) and sample (i) specific survival rate when covariate c is increased in value to 1 standard deviation above the long-term mean. From this, the percentage difference in survival for each population resulting from an increase in the value of an environmental covariate was calculated as: $\%\ difference\ in\ Survival_{p,i,c} = \frac{(Scov_{p,i,c} - Sbase_{p,i})}{Sbase_{p,i}} * 100$. Table I.6 displays the mean and standard deviation for the expected percentage change in survival for each population across the sampled parameter sets, when each covariate is increased in value by 1 SD from the mean.

Covariate	Fall: Sacramento Mainstem Wild	Fall: Battle Creek (CNFH)	Fall: Feather River Hatchery	Fall: American River (Numbus) Hatchery	Spring: Deer Creek	Spring: Mill Creek	Spring: Butte Creek
fall.sac.mainstem - keswick.discharge	-50.2 (12.5)	0.5 (0.1)	0.5 (0.1)	0.5 (0.1)	0 (0)	0 (0)	0 (0)
.1.2.3.4-freeport.sed.conc	-36.5 (10)	-36.5 (10)	-36.5 (10)	-36.5 (10)	0 (0)	0 (0)	0 (0)
.1.2.3.4-fall.dayflow.expin	-57 (6.6)	-57 (6.6)	-57 (6.6)	-57.1 (6.6)	0 (0)	0 (0)	0 (0)
.1.2.3.4-fall.dayflow.cd	43.3 (17.5)	43.3 (17.5)	43.3 (17.5)	43.3 (17.5)	0 (0)	0 (0)	0 (0)
.1.2.3.4-upwelling.south.early	51.1 (16.7)	51.1 (16.7)	51.1 (16.7)	51.1 (16.7)	0 (0)	0 (0)	0 (0)
.1.2.3.4.5.6.7-curl.late	-38.5 (5.4)	-38.5 (5.4)	-38.5 (5.4)	-38.5 (5.4)	-38.5 (5.4)	-38.5 (5.4)	-38.5 (5.4)
.1.2.3.4.5.6.7-pdo.early	29.8 (10.4)	29.8 (10.4)	29.8 (10.4)	29.8 (10.4)	29.8 (10.5)	29.8 (10.5)	29.8 (10.5)
fall.battle.creek - sacAirTemp.spring	-0.2 (0.1)	38.2 (19.4)	-0.2 (0.1)	-0.2 (0.1)	0 (0)	0 (0)	0 (0)
.5.6.7-freeport.sed.conc	0 (0)	0 (0)	0 (0)	0 (0)	-53.8 (13.3)	-53.8 (13.3)	-53.8 (13.3)
spring.deer - deer.discharge	0 (0)	0 (0)	0 (0)	0 (0)	-24.4 (20)	0 (0)	0 (0)
.5.6.7-spring.dayflow.export	0 (0)	0 (0)	0 (0)	0 (0)	-67.2 (9.1)	-67.2 (9.1)	-67.2 (9.1)
.5.6.7-spring.size.chipps	0 (0)	0 (0)	0 (0)	0 (0)	-72.5 (5.3)	-72.5 (5.3)	-72.5 (5.3)
spring.butte - sacAirTemp.summer	0 (0)	0 (0)	0 (0)	0 (0)	0 (0)	0 (0)	-38.4 (10.2)
spring.butte - sacAirTemp.spring	0 (0)	0 (0)	0 (0)	0 (0)	-0.1 (0)	-0.1 (0)	132.8 (47.6)

Table I.6. Percentage change in egg (or hatchery release) to adult survival resulting from covariate variation. Values in the table are the mean (sd) differences in survival between the base case and a scenario where the value of a specific covariate (row) is increased by 1 standard deviation from the long-term mean.

Figure I.7 displays the effect of each environmental covariate on each Chinook population, as the distribution of percentage change in egg (or hatchery release) to adult survival, expected when the value of a specific covariate is 1 SD above the long-term mean. Each panel in figure I.7 describes the influence of a single covariate, while each row within a panel is the survival change expected for a specific population. Within each panel the seven population-specific caterpillar plots describe the distribution of expected survival difference, with the point demarking the median, and the thick and thin lines defining the 50% and 95% credible intervals for the prediction. Two aspects of this analysis are important to consider. First, the figure describes the difference in survival between the base case (all covariates at the mean) and that when a single covariate value is changed, and although the survival differences may be the same across populations, this should not be not be taken as evidence that population-specific survival rates are also estimated to be the same. Second, an estimated survival difference at or near zero does not imply there is no survival effect, only that this interaction was not included in the final AICc-selected model. Any small, but non-zero survival effects are the result of changes in the survival of another population in response to the covariate, with which the focal population shares a capacity constraint at some point in the life cycle.

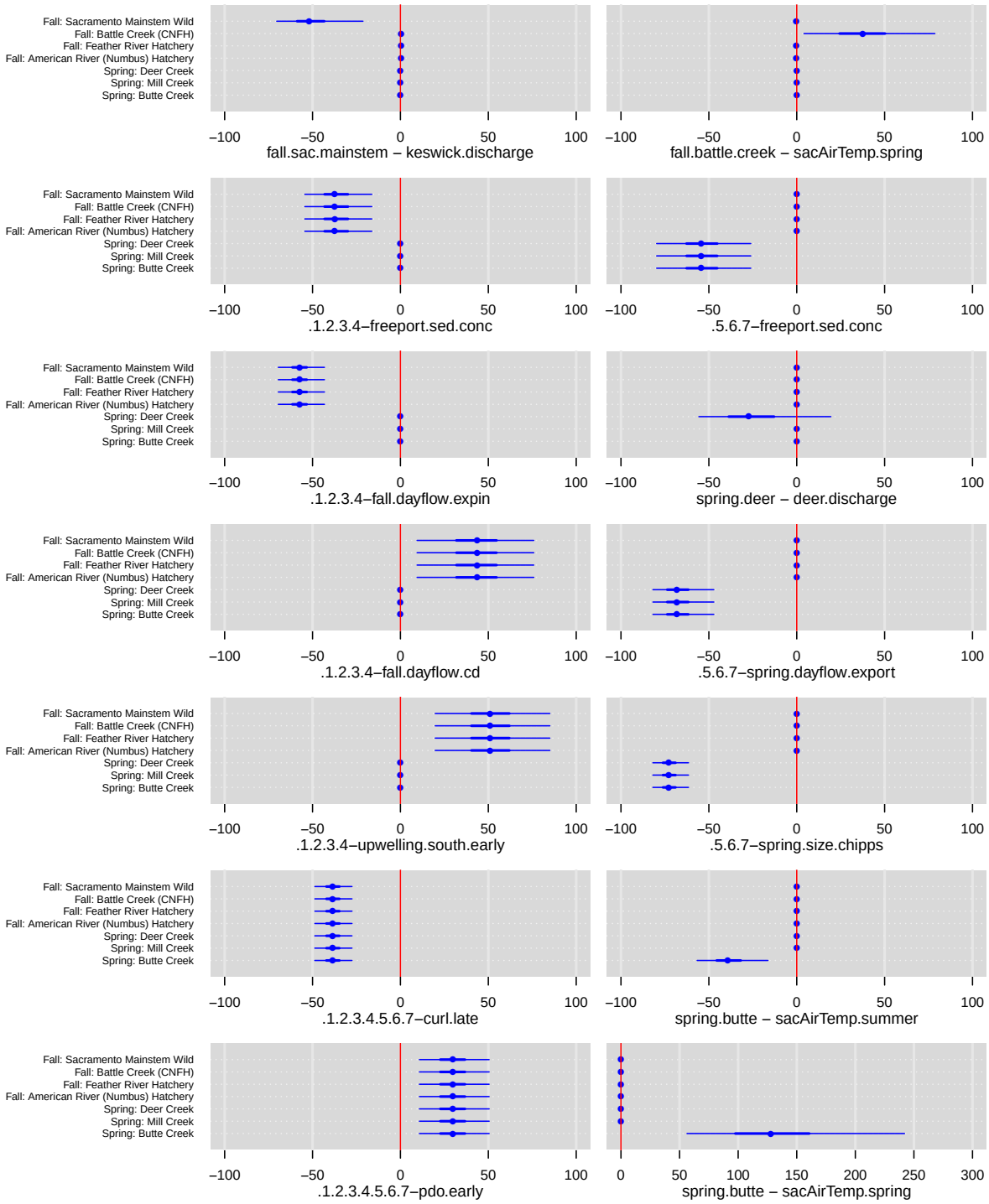

Figure I.7. Percentage change in egg (or hatchery release) to adult survival resulting from a 1 standard deviation increase in covariate values. Each panel represents the outcome of increasing the value of a specific covariate (listed below the x-axis), with each caterpillar plot describing the effect on each population (y-axis). Plotted values are the difference in survival between a scenario where the covariate value is increased and a base case where all covariates are equal to their long-term mean. Caterpillar plots describe the median (dot), 50% interval (thick line), and 95% interval (thin line) for each survival difference accounting for estimation uncertainty.

Results of this analysis of the environmental drivers of survival for Sacramento River fall and spring-run Chinook salmon indicate that several factors have the potential to significantly influence survival in the upstream portion of juvenile migration. Keswick Dam discharge is predicted to reduce egg to adult survival by 52.2%, for each increase in discharge rate of 1 SD. Increased air temperatures in the spring months following emergence are expected to increase the survival of Battle Creek (CNFH) fall-run Chinook by 37.5%, although the 95% credible interval for this predictions ranges from a moderate a modest 4.4% increase to a 79.8% increase indicating significant uncertainty in this prediction. Spring time air temperatures are expected to influence the early juvenile survival of Butte Creek spring-run Chinook in a similar direction but to a much greater extent with a predicted 124.7% increase. Conversely, increased summertime air temperatures during the period of adult upstream holding and egg development are expected to reduce survival by 39.4%, indicating that summertime temperatures may be reaching lethal levels or affecting adult fertility. The final environmental variable linked to the upstream stage and early juvenile survival is water discharge in Deer Creek, which is expected to reduce survival for Deer Creek spring-run Chinook by a modest 26.2%. However, it is important to note that there is significant uncertainty in this prediction with an increase in Deer Creek discharge by 1 SD predicted to have result in anywhere between a 59.4% reduction in survival and a 27% increase in survival 95% of the time.

Later in the life cycle for Sacramento River Chinook, several factors are expected to significantly influence juvenile survival in the Sacramento – San Joaquin Delta. A 1 SD increase in the concentration of sediment (mg/L) at Freeport, CA is expected to result in a 37.1% reduction in the survival of the four fall-run Chinook populations. Sediment concentration is predicted to have a slightly larger influence on survival of the three spring-run populations, with a 54.3% reduction in egg to adult survival. Water exports from the Sacramento – San Joaquin Delta, although quantified through different metrics, are expected to reduce survival of both spring and fall-run juvenile Chinook. An increase in total exports of 1 SD from the 1967-2010 average is predicted to result in a 68.1% reduction in the survival of Deer, Mill, and Butte Creek spring-run Chinook. Similarly, an increase in the ratio of Delta water exports to Delta inflow of 1 SD is expected to reduce survival of the four fall-run populations by 57.8%. Interestingly however, net channel depletion or the quantity of water removed from Delta channels to meet consumptive needs (Dayflow: QCD) is predicted to increase the survival of fall-run Chinook by 43.7%. The final covariate linked to survival of spring-run Chinook in the Sacramento – San Joaquin Delta is the average size of spring-run Chinook in the Chipps Island Trawl survey. Each increase in the average size of juvenile Chinook by 1 SD from the mean (1967-2010) is predicted to reduce survival by 72.9%.

Environmental conditions in the nearshore and marine portions of the Chinook life cycle were also found to have a significant impact on survival to adulthood. An increase in average nearshore upwelling during late spring (April – June) in the region south of San Francisco Bay of 1 SD above the mean, is expected to increase survival to adulthood by 51.2% for the four wild and hatchery-reared fall-run Chinook populations. Also related to marine patterns of nutrient transport and productivity, an increase average wind stress curl during the fall (July – December) of the first year of marine residency was estimated to reduce survival for the seven populations of spring and fall-run Chinook by 39%. The final covariate linked to Chinook survival in the marine environment was the Pacific Decadal Oscillation index during winter (January – May) of the first year of marine residence. An increase in PDO value of 1 SD above the 1967 – 2010 mean is predicted to increase survival of the seven populations of spring and fall-run Chinook by 30%, however there exists

significant uncertainty in this prediction with the 95% credible interval ranging from 10.1 - 51% increase in egg or hatchery release to adult survival.

PART I DISCUSSION

This evaluation of the putative environmental drivers of survival for seven populations of spring and fall-run Chinook spawning within the Sacramento River watershed was comprised of two essential components. The first component was model selection or the process of determining the weight of evidence from the data for which subset of the 59 hypothesized covariate-by-population effects were able to best explain historical variation in Chinook salmon survival, and are therefore informative for predicting future trends in abundance. One thousand potential best-fit models were built using forward stepwise based upon AICc as the selection criteria. The percentage of the 1,000 best-fit models resulting from stepwise-AICc building which included a specific covariate provide a good indication of the relative amount of support each of these competing hypotheses had from the adult and juvenile abundance data (Table I.3). The fact that a range of covariates influencing both grouped and single Chinook populations at all points in the life cycle were present amongst those with a high inclusion rate provide evidence that there not exist a single population bottleneck within the life cycle. This indicates that variation in environmental factors a multiple points within the life cycle play a role in determining interannual survival to adulthood. Of further importance is the observation that both natural covariates, including temperature, water flow, and marine productivity patters, as well as those of anthropogenic origin (i.e. water exports, export/inflow ratio, and water routing) appear amongst the set with the highest inclusion rate. This finding indicates that variation in survival of Sacramento River Chinook population in not driven by natural or anthropogenic processes in isolation. The final model (Table I.4), chosen based on having the lowest AICc value amongst the 1,000 candidate best-fit models, likewise includes a range of covariates throughout the life cycle representing both natural and anthropogenic processes are statistically important predictors of survival.

The influence of striped bass (*Morone saxatilis*) on survival of spring-run Chinook was of particular interest given findings by Lindley and Mohr (2003), which indicated that higher future abundances of striped bass were likely to lead to greater extinction potential for winter-run Chinook. While the effect of striped bass on survival on spring-run Chinook was included in 36% candidate best-fit models, it did not appear in the final (lowest AICc) model. When included alongside other covariates in the final model, the estimated effect of striped bass abundance was centered near zero, indicating an inability to estimate a distinctly negative impact on grouped survival of spring-run Chinook. This result indicates that while striped bass abundance does explain some of the variation in spring-run Chinook survival, other explanatory covariates provide a better alternative explanation for historical abundance observations.

The estimated effect that water exports from the Sacramento – San Joaquin Delta on juvenile Chinook survival through this region was also of importance. While the effect of average water export levels on spring-run Chinook survival and the influence of export/inflow ratio on fall-run Chinook survival both appear in the final model, these two covariate effects have a 54% and 37% inclusion rates across the 1,000 candidate best-fit models. The fact that these export-related covariate effects do not appear at the top of the list of most often included covariates, indicates that while they have substantial potential to

explain historical patterns in spring and fall-run Chinook survival, as indicated by distinctly negative survival effects whose 95% credible intervals do not overlap zero (Figure I.7 and Table I.6), there are other environmental covariate which explain a greater proportion of variation in historical abundance.

The second component of this evaluation was to estimate the direction and magnitude of change in survival rates resulting from variation in each of the covariates in the final model using Bayesian methods. When evaluating population dynamics model estimates for the effect of environmental covariates on survival, it is important to place each result in the proper biological context and determine if there exists a rational mechanistic explanation. The effect of Sacramento air temperatures on several populations appeared as AICc-selected explanatory covariates for several populations. Sacramento air temperature was employed as a proxy for water temperatures in upstream regions of the Sacramento River watershed for two reasons. First, significant and often linear relationships exist for between stream temperatures and air temperatures in most regions. Second, stream temperature data were not available continuously for the requisite time series (1967 – 2010) for all locations, resulting in the necessity for interpolation based on the relationship with air temperature. Therefore, for consistency in the covariate time-series and to reduce the risk of introducing additional uncertainty into the estimation process, we elected to use air temperatures as covariates in place of interpolated water temperatures. Results indicate a positive influence of increased spring (January - March) air temperatures on the survival of Battle Creek (CNFH) fall-run Chinook and Butte Creek spring-run Chinook. This temperature metric coincides with the period prior to and during which juvenile Chinook are rearing. The estimated positive influence of spring temperatures on Chinook survival could result indirectly from the increase in primary production fostered by increased water temperatures and subsequent effects on food availability. In this way growth potential for juvenile Chinook in freshwater depends indirectly on temperature in the rearing environment through food availability, and directly through effects on metabolism as warmer conditions allow juveniles to approach their bioenergetic optimum. Finally, there is some evidence that acclimation to higher temperatures early in life my facilitate higher thermal tolerance later in life, although research in this area has primarily focused on Great Lakes rainbow trout and has not been explicitly evaluated in Chinook (Myrick and Chech 1998). While spring time temperatures were estimated to have a positive influence at this point in the lifecycle, it is important to note that higher temperatures experienced later in the lifecycle during summer months may approach upper tolerance limits, resulting in negative survival impacts. However, the effect of increased summertime temperatures on juvenile survival was not evaluated as part of this analysis.

Contrary to the estimated positive effect of spring temperatures, air temperature during the summer months (July - September) of the brood year were found to have a negative impact on the survival of Butte Creek spring-run Chinook (Table I.6). For Butte Creek spring-run Chinook this time period coincides with the point in the life-cycle when adults are holding in freshwater prior to spawning. Prior to the creation of impassable barriers to upstream migration, the life history of spring-run Chinook was adapted to make use of high spring runoff events from snowmelt to migrate upstream into high elevation streams with tolerable temperature regimes where they could successfully mature during the summer months and await spawning when waters cooled to below 14 – 15^{0}C (Williams 2006). However, in Butte Creek mortality rates during the holding period were observed to exceed 20-30% in 2002 and 65% in 2003 during high temperature events (Ward et al. 2003). This is likely the result of the increased metabolic demands for adult spring-run Chinook while

holding in freshwater during high temperature events, and the increased rate of disease onset and parasite load observed in other members of the *Oncorhynchus* genus exposed to high temperatures (Kocan et al. 2009).

Water flow conditions during juvenile rearing were also found to be important predictors of Chinook survival. Water discharge rates at Keswick Dam were found to negatively influence survival of mainstem spawning wild fall-run Chinook, and water discharge in Deer Creek was found to reduce survival of the Deer Creek spring-run population although to a lesser extent (Table I.6). While it is reasonable to assume that higher discharge rates could lead to greater access to valuable off-channel rearing habitat, water flow conditions additionally have the potential to influence foraging ability by juveniles through the availability of drifting food sources (Neuswanger et al. 2014). None the less the finding that fall-run Chinook survival was negatively influenced by increased water flow contradicts findings by Stevens and Miller (1983) and Newman and Rice (2002). With respect to the influence of water discharge on the survival of Deer Creek spring-run Chinook, this tributary is prone to concentrated high flow events due to flood control levees and a lack of riparian vegetation in its lower reaches (Tompkins 2006). For Deer Creek this may indicate that high water flow rates reduce foraging opportunities for juvenile Chinook, rather than enhancing them, as would be the case in a system with greater floodplain connectivity.

Findings related to the influence of environmental covariates on survival of fall and spring-run Chinook in the Sacramento – San Joaquin Delta are of particular interest in this study. First, the effect of sediment concentration in waters at Freeport, California appeared in the final AICc-selected model, and increases in sediment concentration were estimated to have a substantial negative influence on the survival of both spring and fall-run populations. This finding is contrary to a priori expectations that increased sediment concentrations might provide a survival benefit, if they limit the efficacy of visual predators such as striped bass. We remain limited in our ability to explain the estimated negative effect of sediment concentrations save for the fact that increased sediment influx might be linked to production potential for phytoplankton and the benthic periphyton which form the basis for the aquatic food web. Similarly, the estimated negative influence of average juvenile spring-run Chinook size on the common survival of the three spring-run populations appears contrary to a priori expectations. In the review of size selective mortality in teleost fishes Sogard (1997) found general support for the “bigger is better” hypothesis across taxa. Claiborne et al. (2011) also found that juvenile to adult survival of yearling Chinook from the Willamette River Hatchery increased with size at ocean entry. However, in an evaluation of the effect of size on survival from analysis of scale samples from Chinook returning to the same hatchery, Ewing and Ewing (2002) found either no significant size difference between juveniles at the hatchery and those at ocean entry, or in the case of the 1989 – 1990 brood years evidence for greater survival of smaller individuals. It is important to note that spring-run juvenile size data was unavailable until 1976. As a result we were forced to assume the long-term average for this covariate prior that year which may have influenced results related to this particular covariate.

Results of this analysis related to the influence of water exports from the Sacramento – San Joaquin Delta indicate a negative influence of the export/inflow ratio on the combined survival of the four fall-run Chinook populations and a negative influence increased total Delta exports on the combined survival of spring-run Chinook populations (Table I.6). These findings indicate that higher export rates lead to reduced survival for Sacramento River Chinook on average, however a mechanistic explanation remains elusive. Direct entrainment

mortality seems an unlikely mechanism given the success of reclamation and transport procedures, even given increased predation potential at the release site. Changes to water routing may provide a more reasonable explanation for the estimated survival influence of Delta water exports. Higher exports, or export/inflow ratio, result in greater water diversion into the interior delta where survival has been observed to be substantially lower than that in the Sacramento River mainstem (Perry et al. 2010), potentially resulting from an increased encounter rate with predators or prolonged residence in areas with suboptimal feeding opportunities or dissolved oxygen concentrations.

In conjunction with freshwater drivers of survival for spring and fall-run Chinook populations of the Sacramento River watershed, results of this analysis indicate that several attributes of the marine environment have a significant influence on survival. Two covariates related to nearshore and offshore ocean current patterns and resultant nutrient movement within the water column were included as part of the final AICc-selected model. These covariates were the strength of nearshore upwelling and wind stress curl. Nearshore upwelling results in deep, cooler, and nutrient rich waters moving toward limnetic zone, with onshore transport and convergence fostering higher nearshore productivity during spring and summer. Conversely, wind stress curl is associated with offshore divergent transport (Wells et al. 2008). Our results indicate that increased nearshore upwelling during April – June of the year of ocean entry results in an increase in the combined survival of the four fall-run Chinook populations. Four alternative covariates quantifying upwelling patterns were evaluated as competing hypotheses for fall-run Chinook survival at different locations and quantifying time periods. Covariates were constructed using information from PFEL/NOAA monitoring sites both north and south of San Francisco Bay and for both the spring (April – June) and fall (July – December) periods. The AICc-selected covariate that appeared in the final model used the upwelling index data for spring time-period and at the southern location. Interestingly, although the effect of upwelling at the southern location in the spring months on the combined survival of spring-run Chinook appeared in 22% of candidate best-fit models, it did not appear in the final (lowest AICc) model, indicating that while upwelling may also be an important predictor of spring-run Chinook survival it appears to explain more variation in fall-run Chinook survival.

Wind stress curl was found to have a negative influence on the combined survival of all seven spring and fall-run Chinook populations. These results are not unexpected given findings by Wells et al. (2007) that indicate greater Chinook growth in the first year of life with increased nearshore upwelling and decreased wind stress curl. Wells et al. (2008) likewise found that reductions in wind stress curl were linked to increased production of rockfish species although they note this may be more related to dispersal of juvenile rockfish. The estimated reduction in survival for Chinook associated with greater wind stress curl is likely explained by trophic interactions, with findings by Macias et al. (2012) indicating that biomass concentrations for phytoplankton and zooplankton are likely to be substantially higher with coastal upwelling as opposed to wind stress curl driven upwelling offshore.

The Pacific Decadal Oscillation (PDO) describes a persisting periodicity in sea surface temperature, mixed layer depth, and strength and direction of ocean currents (Mantua and Hare 2002). Estimates for the influence of the PDO during January – May of the first year at sea indicating for the seven spring and fall-run Chinook populations, indicate increased survival is likely to be observed in during positive PDO events. This result is contrary to findings by Hare et al. (1999) which indicate positive PDO conditions favor production in Alaskan salmon stocks and disfavor the productivity of West Coast stocks, as

well as findings by Wells et al. (2006) which highlight the negative covariation between size of Columbia River Chinook size and PDO values.

PART II SIMULATION OF FUTURE ABUNDANCE UNDER ALTERNATIVE CLIMATE, OCEANOGRAPHIC, AND WATER USE SCENARIOS

INTRODUCTION

The purpose of conducting forward population projections was to simulate future survival for Sacramento River Chinook under alternative climate, oceanographic, and water management scenarios. Simulating the four populations of fall-run and three populations of spring-run Chinook forward in time, provides a means for weighing differences in future survival under alternative water export levels, relative to the uncertainty in future climate change and ocean productivity. In order to generate predictions for future survival, we integrated results from the Bayesian estimation model with expectations for future environmental conditions under two alternative future ocean production trends, two predictions for future climate change, and at four potential levels of future water exports (see Appendix B). In addition to differences in future Chinook survival arising from natural and anthropogenic environmental factors, we have also propagated both estimation and process uncertainty forward in our predictions for future abundance and realized survival rates.

Future climate scenarios were based upon the U.S. Bureau of Reclamation's (USBR) Operations and Criteria Plan (OCAP) Study (USBR 2008). Two alternative scenarios for overland climate change were evaluated, the OCAP Study 9.2 and 9.5. The OCAP Study 9.2 (referenced as: **cc92**) describes a wetter and cooler prediction for future climate change, with a mean increase in temperature of 0.42° C and an increase in precipitation of 12.5%. Conversely, the OCAP Study 9.5 (referenced as: **cc95**) describes a dryer and warmer outlook for future climate change in the Central Valley, with a mean increase in temperature of 1.56° C and a decrease in precipitation of 12%. In addition to differing scenarios regarding climate change, two alternative predictions for future ocean conditions were explored. These two scenarios, one representing traditional perceptions of positive growth conditions for Chinook (referenced as **oceanUP**) and the other representing negative growth conditions (referenced as **oceanDOWN**), describe alternative patterns in nearshore upwelling and temperature, and future trends in broad-scale ocean currents.

Paired with these alternative scenarios for future climate change and ocean production, were four scenarios related to the magnitude of future water exports from the Sacramento-San Joaquin Delta. The four future scenarios for total water exports included: 1. **expAVG** (future exports equal to the 1967 – 2010 average), 2. **expZERO** (zero future water exports), 3. **expUP30** (an increase in future exports to 30% above the historical average), and 4. **expDOWN30** (a decrease in future exports to 30% below the historical average). While it is clear that some of these water export scenarios are economically infeasible (i.e. expZERO) they were included as part of the population projections to bound the range of potential biological outcomes from management actions. All export scenarios are based upon the historical export values calculated as the average of March – May Dayflow (QEXPORT) values for fall-run Chinook, and the average of February – April values for spring-run Chinook.

In total, these 2 onshore climate change scenarios, 2 ocean production scenarios, and 4 water export scenarios, resulted in 16 different realizations of the future environment for Chinook populations of the Sacramento River watershed. These sixteen environmental scenarios were subsequently translated into future covariate values (see Appendix B), for use as inputs in projecting the populations forward in time and determining realized future survival rates.

Simulation Methods

Realized future survival rates were simulated by projecting all seven populations of Sacramento River Chinook forward in time for 50 years (2007 – 2057). The structure of the population dynamics model utilized to estimate stage-specific survival rates and the direction and magnitude of response by populations (or groups of populations) to environmental covariates, formed the basis for these forward population projections. Population and brood year specific cohorts of Chinook were tracked forward in time through the same six spatio-temporal life-stages (i.e. upstream/tributaries, Sacramento-San Joaquin Delta, nearshore, and the 1st, 2nd, and 3rd years in the ocean). In the same way as the estimation model, both the wild-spawning and hatchery production life cycles were represented in population projections, with wild-spawning populations linked to future cohort production through a fixed fecundity per individual, and hatchery production fixed at the population-specific average of releases from the most recent 10-year period. Stage-specific capacities for Sacramento mainstem-spawning fall-run Chinook in the upstream stage, and the grouped spring-run and fall-run populations in the Sacramento-San Joaquin Delta, were fixed at the average of estimates from Hendrix et al. (2014) for the most recent 10-year period. Estimated values for population dynamics model parameters including stage and population-specific productivity rates, and coefficients describing the direction and magnitude of influence that environmental covariates have on stage-specific productivity (maximum survival) rates, were used when simulating future trends in abundance.

When simulating future trends in Chinook abundance in order to evaluate differences in realized survival, it was necessary to account the two major sources of uncertainty in our analysis and propagate this uncertainty forward into predictions under alternative environmental and export scenarios. The first source of uncertainty in generating robust predictions for future abundance is uncertainty in the estimates of population dynamics model parameters. This includes uncertainty in the estimated value of life-stage and population specific basal productivity rates, as well as coefficients describing the influence of environmental covariates on survival. Estimation uncertainty arises when estimated values for model parameters are poorly informed by the available data, leading to broad posterior probability distributions indicating a broad range of parameter values with similar probabilities of being correct given the data. To account for estimation uncertainty in model parameters, we drew 1,000 independent sets of model parameter values from the joint posterior sampled by the Bayesian estimation model. By drawing parameter sets from the joint posterior, and repeating the 50-year forward projection of the seven populations using each of the independent parameter sets, we are able to capture the influence of both the true uncertainty in parameter values and posterior correlations between estimated parameters.

The second source of uncertainty that was integrated into forward projects was process uncertainty, or temporal variation in the state of future population dynamics. For each

of the 1,000 replicate forward simulations, a random process deviate was introduced in the calculation for initial abundance in the first model stage (Eq. II.2, II.3).

$$N_{y,s=1,p,e,i} = A_{t=y,p,a,e,i} * fec * \exp\left(\varepsilon_{y,p,i} - \frac{\sigma_p^2}{2}\right)$$
$$\varepsilon_{y,p,i} \sim N\left(0, \sigma_p\right) \quad \text{(II.2)}$$

Equation II.2 describes how process uncertainty is introduced into the wild-spawning life cycle used to represent the Sacramento mainstem fall-run, and Deer, Mill, and Butte Creek spring-run Chinook populations. The number of individuals entering the upstream (1st) model stage ($N_{y,s=1,p,e,i}$), of brood year y, population p, in simulation i of environmental scenario e, is a function of the number of spawning adults returning in calendar year t = y of population p ($A_{t=y,p,e,i}$), the fixed fecundity rate of 2,000 eggs/individual ($fec = 2{,}000$), and the exponentiated brood year y, population p, and simulation i specific process deviate ($\varepsilon_{y,p,i}$). Conversely, equation II.3 describes how initial abundance in the first model stage was calculated with process errors for the three populations of hatchery-produced fall-run Chinook, where RH_p is the fixed level of hatchery releases for each population.

$$N_{y,s=1,p,e,i} = RH_p * \exp\left(\varepsilon_{y,p,i} - \frac{\sigma_p^2}{2}\right)$$
$$\varepsilon_{y,p,i} \sim N\left(0, \sigma_p\right) \quad \text{(II.3)}$$

Process deviates ($\varepsilon_{y,p,i}$) for each brood year y, population p, and replicate simulation i, were generated as random draws from a normal distribution with mean equal to 0, and population-specific standard deviations (σ_p). The standard deviations for the process error distributions (σ_p) were the maximum likelihood estimates for the residual observation uncertainty from fitting the original population dynamics model to historical abundance data. In total 1,000 randomly drawn process deviates, corresponding to the replicate simulations using parameter sets drawn from the joint posterior, were generated for each population in each of the 50 years of the forward simulation. To ensure comparability, the same set sets of brood year and population specific process deviates were used across environmental scenarios.

When simulating future trends in Sacramento Chinook abundance and evaluating realized survival rates, it was necessary to incorporate the likely impact of future fishery removals. Fishing mortality was simulated based upon the current Reasonable and Prudent Alternative (RPA) management scheme for Central Valley Chinook (see “Simulation of Harvest Rates” below). Annual allowable harvest rates for fall-run Chinook are established based upon the Sacramento Index (SI), however maximum harvest rates are further contingent upon minimum abundance requirements for ESA listed winter-run Chinook. When projecting populations forward in time, it was necessary to simultaneously model the future dynamics of winter-run Chinook in response to the 16 environmental scenarios under evaluation. Results from the evaluation of Sacramento River winter-run Chinook using the OBAN model (see Appendix D) which was run in parallel with the spring and fall run model, were used to simulate the future abundance of Sacramento River winter-run Chinook across the same 50-year time-series in response to differences in future climate change, marine

production, and water exports across scenarios. Moving forward in time, future harvest rates depended on the model-predicted abundance of fall-run Chinook and winter-run Chinook (see "Simulation of Harvest Rates"). Spring-run harvest rates were scaled at 95% of fall-run harvest rates.

SIMULATION OF FUTURE HARVEST RATES

Background

The Pacific Fisheries Management Council (Council) manages the harvest of salmon on the coasts of California, Oregon, and Washington. The ocean salmon fishery targets Chinook, coho, and pink salmon species, which include Sacramento River Chinook salmon. The Sacramento River Chinook stocks overlap with Klamath River Chinook salmon in a mixed stock fishery. Furthermore, the Sacramento River fall Chinook (SRFC) is an indicator stock for the Central Valley Fall complex and Klamath River fall Chinook (KRFC) is an indicator stock for the Oregon/Northern California Chinook complex. As indicator stocks, the Council calculates both acceptable biological catches (ABC) and annual catch limits (ACL) for the SRFC and KRFC.

Both Sacramento River and Klamath River Chinook are composed of stocks supported by hatchery production and stocks that are listed as a conservation concern under the Endangered Species Act (ESA). In the Sacramento River and Klamath River mixed fishery, the Sacramento winter-run (federally listed as threatened in 1990 and as endangered in 1994 under ESA), Central Valley spring-run (listed as threatened under ESA in 1999) and the California coastal (listed in 1999) may limit harvest rates. Target harvest rates for the Sacramento fall run are determined annually via a forecast of abundance indexes of Chinook salmon to both rivers. Management of the fishery occurs through a series of spatially explicit openings and closures to structure the harvest effort in such a manner to ensure conservation of portions of the stocks that may be at low abundances while allowing harvest of those stocks that are healthy. There are a series of Council meetings to review the forecasted abundance and possible management alternatives.

NMFS developed a Biological Opinion in 2010 (2010 Opinion) to evaluate the effects of the ocean salmon fishery on winter run stock (Biological Opinion on the Authorization of Ocean Salmon Fisheries Pursuant to the Pacific Coast Salmon Fishery Management Plan and Additional Protective Measures as it affects the Sacramento River Winter Chinook Salmon (winter-run) Evolutionary Significant Unit (NMFS 2010)). In the 2010 Opinion, NMFS identified that winter-run cohorts could be reduced (i.e., decrease in the number of spawners relative to the number of spawners in the absence of the fishery) by 10 to 25% due to the ocean salmon harvest with an average rate of 20%. Most of the impacts occur south of Point Arena, CA from contacts with the recreational fishery (O'Farrell 2012).

To avoid a jeopardy conclusion on the operation of the ocean salmon fishery, NMFS developed a Reasonable and Prudent Alternative (RPA) to allow explicit control of the management process to reduce impacts when extinction risk of winter run increases (e.g., due to low stock size or periods of decline). After the issuance of the 2010 Opinion, the Council was given options to either increase size limits or enact seasonal closures to reduce the fishery impacts on winter-run in 2010 and 2011.

In 2012, NMFS performed a Management Strategy Evaluation (MSE) for different control rules based on the abundance of winter-run Chinook for setting the allowable harvest rate on the mixed stock fishery (Winship et al. 2012). The control rules set allowable impacts of age-3 winter-run south of point Arena as: 1) 0 impact (a closed fishery south of Point Arena); 2) 25% impact, which is the historical estimate of impact rate; 3) 20% impact, which is the current rate; and four alternatives (4-7) that reduce impact rates at certain winter-run thresholds. These MSE compared the impact rate under each of the control rules relative to the potential for increasing extinction risk of winter-run Chinook.

Management of Sacramento River Chinook

Fall-run

The fishery impact rate for SRFC is set by evaluating the Sacramento Index (SI) in each year. The SI is calculated as the sum of a) harvest south of Cape Falcon, OR; b) SRFC impacts due to non-retention in ocean fisheries; c) harvest in the recreational fishery in the Sacramento River basin; and d) SRFC spawner escapement. The SI is forecasted each year using a regression model with an autocorrelated error term that uses the number of SRFC jacks from the previous year as the dependent variable.

The estimates of the SI are subsequently used to determine the status of the fishery as overfished, approaching overfished, rebuilding, or rebuilt. The important metrics for determining the status are the minimum stock size threshold (MSST) (91,500 for SRFC) and the stock size at maximum sustainable yield (122,000). Given the status of the fishery, the allowable biological catch, annual catch limit, and the overfished limit can then be calculated.

The determination of the fishing rate is described as follows (PFMC 2014). The discrete fishing rate (F) at the overfishing limit, F_{OFL}, is defined as being equal to F_{MSY} (or the maximum fishery mortality threshold) and the spawner size (S) at the overfishing limit, $S_{OFL} = N \times (1 - F_{MSY})$. Because, SRFC is a Tier-2 fishery, the fishing rate consistent with the allowable biological catch $F_{ABC} = F_{MSY} \times 0.90$ and $S_{ABC} = N \times (1 - F_{ABC})$, where N is the spawner equivalent units. Finally, the fishing rate consistent with the allowable catch limits, F_{ACL}, is equivalent to F_{ABC} and $S_{ACL} = N \times (1-F_{ACL})$, which results in $S_{ACL} = S_{ABC.}$. The impact rate is determined by the SRFC control rule as a function of the potential spawner abundance (in this case the spawner abundance is the Sacramento Index = SI) (Figure II.1).

Winter-run

The current RPA (NMFS 2012) uses a fishery control rule with a reduction in fishery impact as a function of 3-year geometric average of winter-run escapement. The escapement is defined as the total male and female, natural-origin and hatchery-origin escapement as estimated by an annual carcass survey (USFWS 2011). The fishery control rule has the following threshold definitions (Figure II.1): A) from escapement of 0 to 500, the allowable impact rate south of Point Arena is 0; B) from escapement of 501 to 4000, the impact rate is linearly increasing from 0.1 to 0.2; C) from escapement of 4000 to 5000, the impact rate is 0.2. The impact rate for escapement > 5000 is undefined. For purposes of the MSE, NMFS assumed that the impact rate would be 0.2 for any 3-year geometric mean of escapement > 4000 as described on pg. 57 of Winship et al. (2012). We assumed the same upper bound of 0.2 for age-3 impact when the 3-year geometric average escapement was > 5000.

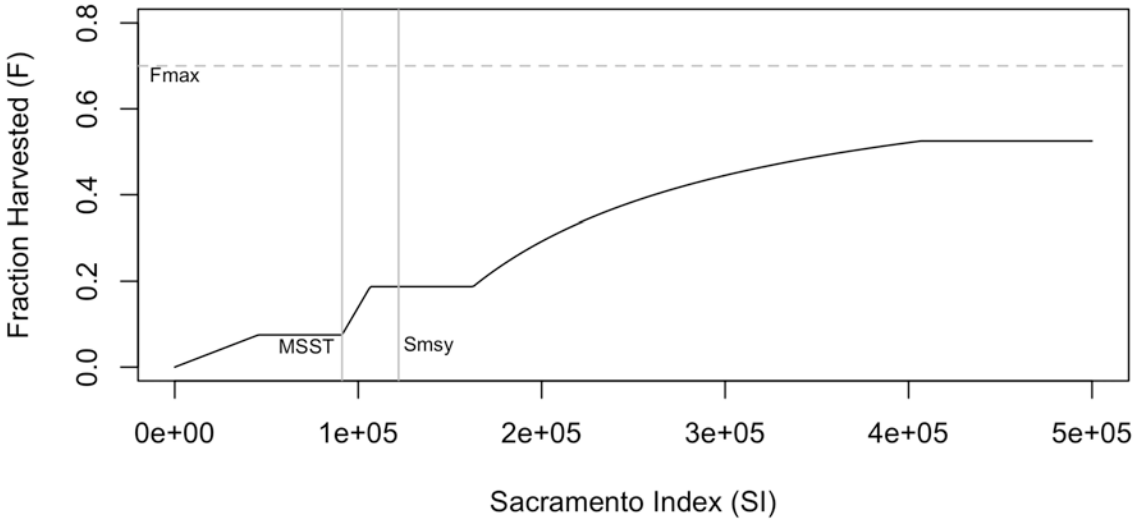

Figure II.1. Fishery control rule as a function of the potential spawner abundance (Sacramento Index) used for setting impact rates for Sacramento River fall-run Chinook.

The fishery control rule defines the impact rates south of Point Arena, which largely encompasses the winter-run marine distribution. Fall-run Chinook are found north of Point Arena, and the fishery control rule for those areas is dependent upon the abundance index for fall run.

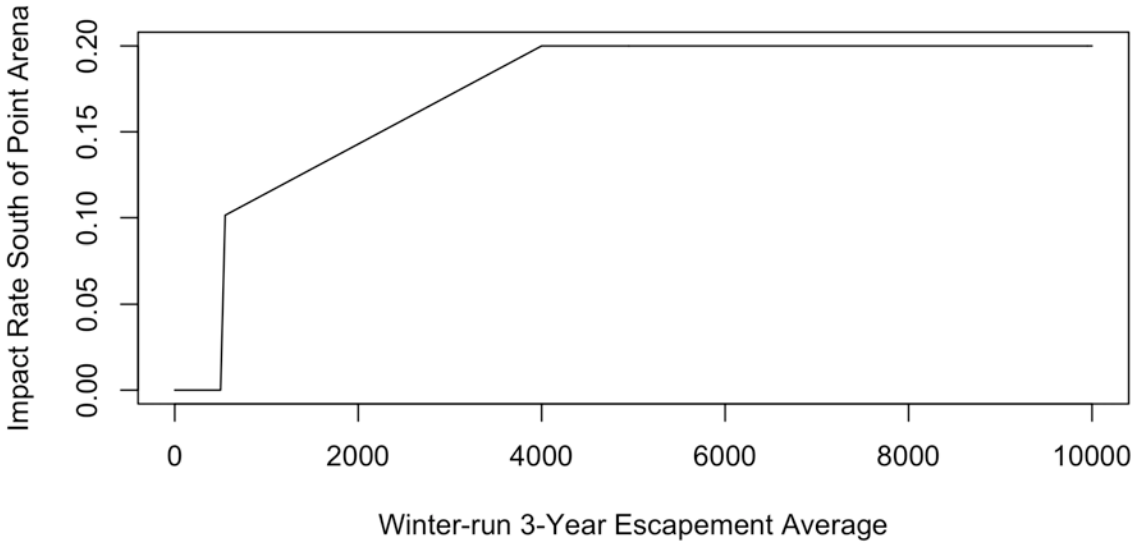

Figure II.2. Fishery control rule as a function of the trailing 3-year geometric average of winter-run abundance.

For example, the SI forecast in 2014 was 634,650 (PFMC 2014). The spawner escapement associated with overfishing in 2014 is 139,623, which is calculated as a function of F_{MSY} (0.78) and the SI abundance forecast of 634,650. The SRFC is a Tier 2 stock, so the $F_{ABC} = F_{MSY} * 0.90 = 0.70$, and the spawner escapement associated the allowable biological catch was forecasted to be $S_{ABC} = N(1-F_{ABC}) = 190,395$.

In 2014, the 3-year geometric mean of winter-run abundance was 2,380, which resulted in a maximum forecasted impact rate on age-3 winter-run of 15.4% (in comparison it was 13.7% in 2012 and 12.9% in 2013).

Reducing the maximum impact rate on age-3 winter-run may have important consequences for the actual harvest rates on SRFC. Recently, Satterthwaite et al. (2013) compared the ocean distribution of fall-run, winter-run, and spring-run during the summer and fall, which provides some understanding of the spatial differences in the relative contacts per unit effort of the fishery, which is a proxy for the spatial distribution of each run. Sacramento River fall-run have relative contacts per unit effort of approximately 0.2 for management areas located south Latitude 42 N at the CA OR border, and 0.1 north of Latitude 42 N and Cape Falcon at the OR WA border. These results suggest that the closing of fishing south of Point Arena, as would be required for winter-run 3-year average escapement of less than 500, can have potential consequences for the total fall-run impact rate. For more information, please see PFMC (2014).

Spring Run

There are no explicit fishery management rules for spring run, though it has been noted in past NMFS Biological Opinions (e.g., NMFS 2010) that protections for winter run are likely to be beneficial for spring run. Comparisons of ocean and river impact rates of spring-run relative to SRFC by US Fish and Wildlife Service for the purposes of meeting the goals of the Central Valley Project Improvement Act (CVPIA) indicated equivalent ocean fishery rates were assumed for sprint-run and fall-run, whereas river impact rates were consistently lower for spring-run (Chinookprod_032011.xlsx obtained from http://www.fws.gov/stockton/afrp/). Overall, total fishing impact rates for spring-run were approximately 0.95 of fall-run.

Harvest Model

The management of SRFC requires annual management rules to optimize the fishery due to changing abundances of winter-run and Klamath River stock sizes in addition to the status of other stocks (e.g., PFMC 2014). The management process can be simplified by making several assumptions about the fishery management dynamics:

- Klamath River Fall Chinook do not limit the values of F_{ABC} calculated annually for SRFC.
- The Klamath River fall age 4 harvest rate limits, intended to protect California Coastal Chinook, do not limit the values of F_{ABC} calculated annually for SRFC.
- Abundance of age-3 SRFC and winter-run are obtained from the spring-run & fall-run life cycle model and the winter-run models, respectively. In the actual management of SRFC, estimates of an adult (age 3-5) abundance index in year *t* are calculated from regressions to age-2 abundances in year *t*-1.

- The fishery acts without error; thus, management overfishing (i.e., total annual exploitation rate exceeds the maximum fishing mortality threshold of 0.78) cannot occur.

The following steps were developed for calculating the annual impact rate for SRFC (F_{FR}), and Sacramento winter-run Chinook (F_{WR}).

1. Calculate an estimate of the Sacramento Index as the sum of the four components identified previously.
2. Determine the fall-run impact rate F_{FR} based on the fishery control rule for SRFC (Figure II.1). The control rule specifies that even if the stock is approaching an overfished condition (the SRFC stock has a 3 year geometric average (t-2, t-1, current year) that is below the threshold of 91,500), a *de minimis* fishery will occur at the rate defined by the fisheries control rule.
3. Calculate the trailing 3-year geometric average of winter-run abundance.
4. Depending upon the 3-year geometric value, set the fishery impact rate for winter-run (Figure II.2). If the winter-run impact rate is 0, reduce F_{FR} by 25% to account for lost fishing opportunities south of Point Arena.
5. Set the impact rate for spring-run $F_{SR} = 0.95F_{FR}$ to reflect reduced river impact rates.

RESULTS

Future trends in abundance for seven populations of fall and spring-run Chinook spawning in tributaries of the Sacramento River watershed were simulated under different scenarios for future climate change and ocean productivity, and alternative levels of water export from the Sacramento-San Joaquin Delta. Results from a Bayesian multi-stock population dynamics model, fit to historical abundance data, were used to parameterize forward simulations. In addition, future trends in abundance for Sacramento winter-run Chinook were also simulated to allow for implementation of the current fishery management process. All eight populations were simulated forward in time for 50 years in response to the 16 alternative environmental scenarios (combinations of future climate, ocean productivity, and water exports), subject to capacity interactions arising from juvenile competition, and accounting for estimation uncertainty and process error in future predictions. The forward simulation for each environmental scenario was replicated 1,000 times with randomly drawn process deviates and model parameter values.

Differences in future outcomes for these populations in response to the 16 scenarios are best quantified through comparison of realized survival rates within populations and across scenarios. Realized survival rate was calculated in two ways depending on the life history of the individual populations. First, for wild-spawning Chinook stocks (mainstem Sacramento fall-run, and Deer, Mill and Butte Creek spring-run), realized survival was calculated as the as the survival rate from egg to spawning adult, or the sum of spawning adults from a brood year across return years, divided by the spawning abundance producing that cohort multiplied by the assumed fecundity (Eq. II.4).

$$RS_{y,p,e,i} = \frac{\sum_{a=1}^{Nages} A_{t,p,a,e,i}}{E_{y,p,e,i}} \quad \text{(II.4)}$$

$$t = y + \tau_a$$

In equation II.4, realized survival ($RS_{y,p,e,i}$) from brood year y, of population p, for environmental scenario e, and simulation i, is a function of the adult abundance surviving both natural and fishing mortality and returning to spawn ($A_{t,p,a,e,i}$) in calendar year t, of population p and age a, resulting from simulation i of environmental scenario e, and the number of eggs ($E_{y,p,e,i}$) resulting from brood year y for that population, scenario and simulation. τ_a represents the difference between brood year y and the calendar year of return t, for individuals returning at each age a.

Realized survival for the hatchery-produced populations (Battle Creek (CNFH), Feather River, and American River (Nimbus) fall-run) is determined by the ratio of returning adult spawners ($A_{t,p,a,e,i}$) to the number of hatchery for that population (RH_p), which is assumed constant in the future (Eq. II.5)

$$RS_{y,p,e,i} = \frac{\sum_{a=1}^{Nages} A_{t,p,a,e,i}}{RH_p} \quad \text{(II.5)}$$

$$t = y + \tau_a$$

Predictions for future realized survival rates for the three spring-run (Fig. II.3) and four fall-run (Fig. II.4) populations across years and replicate scenarios, accounting for future fishing mortality, across environmental and export scenarios show some consistent patterns. As expected, survival rates for the hatchery-produced Chinook populations were much higher than those predicted for the wild-spawning populations, given that realized survival was measured as survival from release to spawning adult, as opposed to egg to adult survival (Table II.1). For the fall-run Chinook populations, the final model estimated a net positive impact of nearshore upwelling on survival, as a result these four populations show higher average survival rates for scenarios which included a 10% increase in upwelling (oceanUP) across both future climate change and water export scenarios. Across fall-run populations, simulated positive upwelling conditions in the future resulted in an average increase in realized survival of between 12% and 67% (mean: + 44%) across export scenarios, when compared with those scenarios incorporating a 20% reduction in nearshore upwelling (oceanDOWN, Table II.1). With respect to the spring-run Chinook populations, substantially smaller differences in realized survival rates in response to the oceanUP scenarios were observed, with 5 – 17% decreases in average realized egg to adult survival (Fig. II.3). Winter-run Chinook on the other hand, were predicted to exhibit higher survival in response to the increased upwelling under the oceanUP scenario, with 7 – 36% higher survival (Table II.1)

Predictions for differences in realized survival rate across water export scenarios indicated similar general trends across both populations and potential differences in future climate change. For all populations realized survival rates were predicted to be highest under the zero export scenario, followed by scenarios simulating a 30% reduction in exports, average exports, and a 30% increase in water exports (Fig. II.3, II.4). When compared to scenarios simulating future survival in response to water export levels at the 1967 – 2010 average, spring-run Chinook populations are expected to exhibit a higher average realized survival in response to a 30% reduction in export volumes, with survival 27 – 48% higher for Deer Creek, 29 – 51% higher for Mill Creek, and 19 – 38% higher for Butte Creek Chinook, across environmental scenarios. Fall-run Chinook populations are predicted to exhibit somewhat smaller increases in survival under a 30% export reduction (expDOWN30) relative to average water exports in the future (expAVG), with realized survival higher by 12 – 26% for Sacramento mainstem wild-spawning Chinook, and between 14% and 27% for the three hatchery-produced fall-run Chinook populations across environmental scenarios (Table II.2). Winter-run Chinook are predicted to respond to a 30% reduction in future water exports, with only a 3 – 9% increase in survival relative to the average export scenario (Table II.2).

When future dynamics of Sacramento Chinook populations were simulated with a 30% increase in water exports (expUP30), compared to the average export scenario the mainstem Sacramento wild-spawning Chinook were predicted to experience 16 – 28% lower median realized survival rates from egg to spawning adult, while the three hatchery-produced populations were predicted to exhibit a 14 – 25% reduction in future survival from release to adulthood, depending on the climate change and ocean production scenario (Fig II.4, Table II.2). Simulation of future Deer, Mill, and Butte Creek survival indicated that, relative to the average water export scenario, average realized egg to adult survival was predicted to be 39 – 53% lower in the presence of a 30% increase in future water exports (Fig. II.3, Table II.2). The simulation results again indicate that the response by winter-run Chinook to altered export levels is minimal, with a 0 – 3% reduction in average realized egg to adult survival, across environmental scenarios.

Predictions for realized survival under the zero future export scenario (expZERO) were higher for all populations, however the magnitude of the difference in survival between this and the average export scenario (expAVG) was largely contingent upon the climate change scenario and population of interest. The Deer and Mill Creek spring-run populations exhibited the largest difference in realized survival between the zero and average export scenarios, under the OCAP 9.2 climate change prediction and positive ocean conditions (cc92.oceanUP) (Fig. II.3). Predicted survival in the absence of exports was 79% higher for Deer Creek, 85% higher for Mill Creek, and 59% higher for Butte Creek Chinook, compared to average exports (Table II.2). Interestingly, the Butte Creek spring-run Chinook population also showed one of the smallest responses to the zero export scenario across populations, with only 27% higher survival compared to the average export scenarios under the OCAP 9.5 climate change and lower ocean production environmental scenario (cc95.oceanDOWN). This increase in predicted survival is quite minimal when compared to the 62 – 83% higher survival predicted for the fall-run Chinook populations with zero exports, under the same environmental scenario (Table II.2). In general however, average realized survival for fall-run Chinook under the zero export scenario is expected to be 28 – 62% higher for the mainstem Sacramento wild-spawning population and 44 – 83% higher for the hatchery-produced populations, when compared to expectations under the average export scenario. While results indicated that realized winter-run Chinook survival would be minimally influenced by a 30% increase or reduction in future exports, the zero export scenario is predicted to increase survival by 28 – 91%, most appreciably when combined with a cooler and wetter future climate change scenario and positive future marine conditions (cc92.oceanUP).

In addition to higher median realized survival rates, the zero export scenario is also predict to also produce more variable survival in the future. While most pronounced for the spring-run Chinook populations, when the variability in realized survival is compared across export scenarios it is consistently higher for the zero export case, across all populations (Fig. II.3, Fig. II.4). The Butte Creek population exhibits the greatest variation in future survival, specifically under the zero export scenario, and for the OCAP 9.2 climate change pathway across export scenarios (Fig. II.3).

While these forward simulation results suggest that higher and more variable realized survival can be expected under the zero export scenario, across populations, climate change trajectories, and ocean productivity patterns, it is also evident that a 30% reduction in water exports (expDOWN30) is likely to achieve an increase in realized survival of a substantial magnitude in many cases. For example, on average across environmental scenarios the Butte Creek population is expected to exhibit a 41% increase in average realized survival under the zero export scenario, and a similarly large increase of 27%, with a 30% reduction in spring export volumes (Fig. II.3, Table II.2). This amounts to a difference of only a 14 percentage points in the predicted survival rate increase; between the zero export and 30% export reduction scenarios. Results are similar for the other spring-run populations, with a difference of 25 percentage points for Mill and Deer Creek spring-run Chinook. Improvements in survival under the zero export scenario, relative to the 30% export reduction scenario (expDOWN30), are on average greater for the hatchery-produced fall-run Chinook populations, but likewise suggest that on average across environmental scenarios, a difference in survival of only 26 – 43 percentage points is likely to be observed (Table II.2).

The percentage difference in realized survival increase, for the zero export and 30% reduction scenarios, relative to the average export scenario, is most variable for the winter-run Chinook population. The percentage increase in survival difference between expZERO

and expDOWN30 is smallest under cc95.oceanDOWN scenario at 25, and greatest under the cc92.oceanUP scenario. This indicates that under a cooler and wetter future climate with greater upwelling (cc92.oceanUP), the ceasing all exports (expZERO) is likely to have a substantially higher survival benefit relative to reducing exports by 30% (expDOWN30). While, in the face of a hotter and drier future climate with reduced nearshore upwelling (cc95.oceanDOWN) where survival is severely limited by natural processes, both before and after the delta, the benefits of a 30% reduction and zero exports are more similar (Table II.2). This same pattern is predicted for the spring-run Chinook populations, but not the fall-run populations.

With respect to the influence of climate change on predictions for future realized survival, differences in outcomes amongst climate change scenarios differed across populations and were smaller on average when compared differences resulting from alternative export scenarios. The Butte Creek spring-run Chinook population is predicted to have consistently higher realized survival under the OCAP 9.2 climate change forecast, which represents a slightly slower rate of warming paired with increased precipitation (Fig. II.3). Conversely, both the spring-run Deer Creek and fall-run Sacramento mainstem wild-spawning populations show slightly, but consistently, higher survival under the OCAP 9.2 climate change trajectory which describes a greater increase in temperature paired with lower levels of future precipitation (Table II.1).

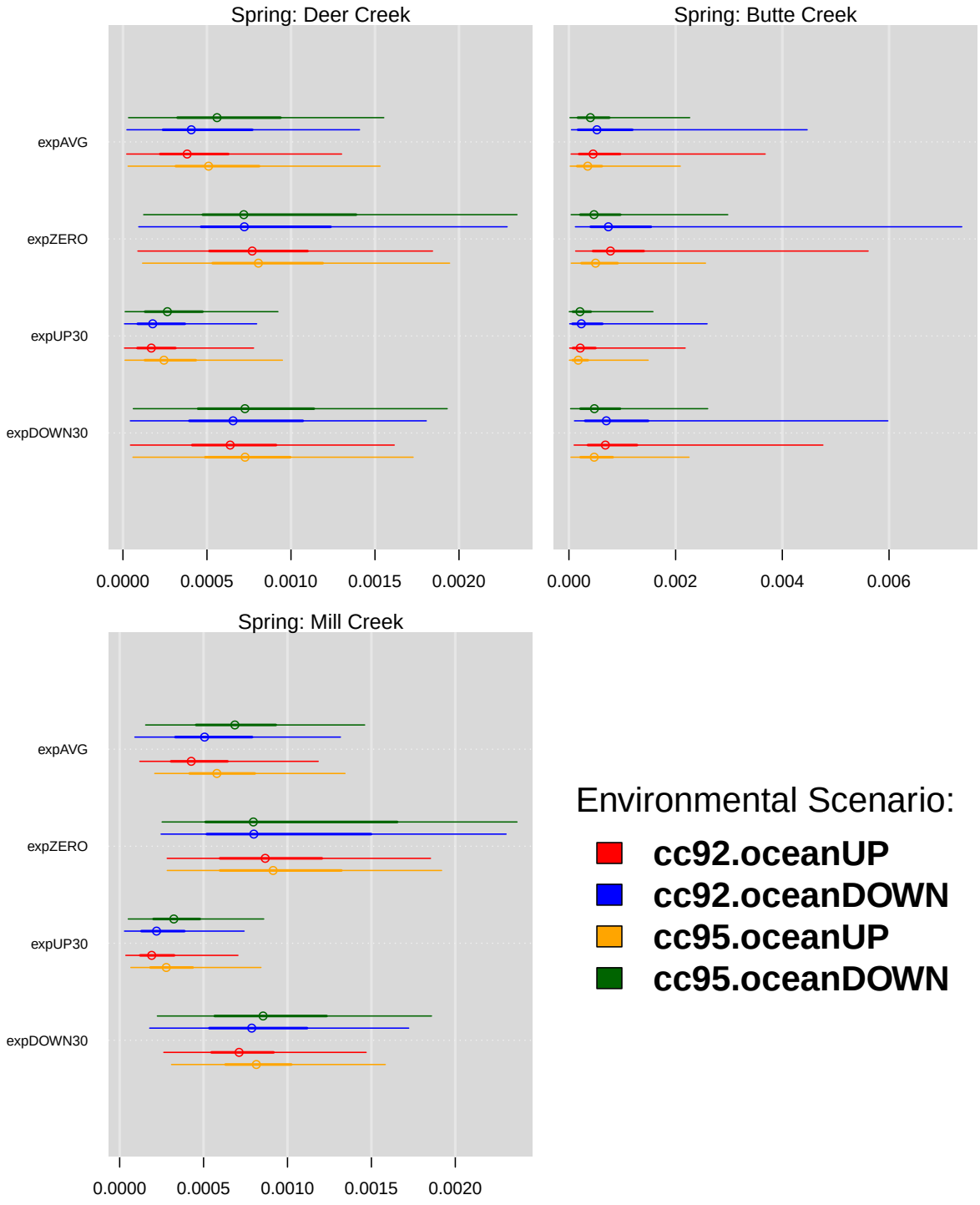

Figure II.3. Caterpillar plots describing the predicted distribution of realized survival to return, across years and simulations, for spring-run Chinook populations. The circle, thick line, and thin line describe the median, 50% credible interval and 95% credible interval for the predictions.

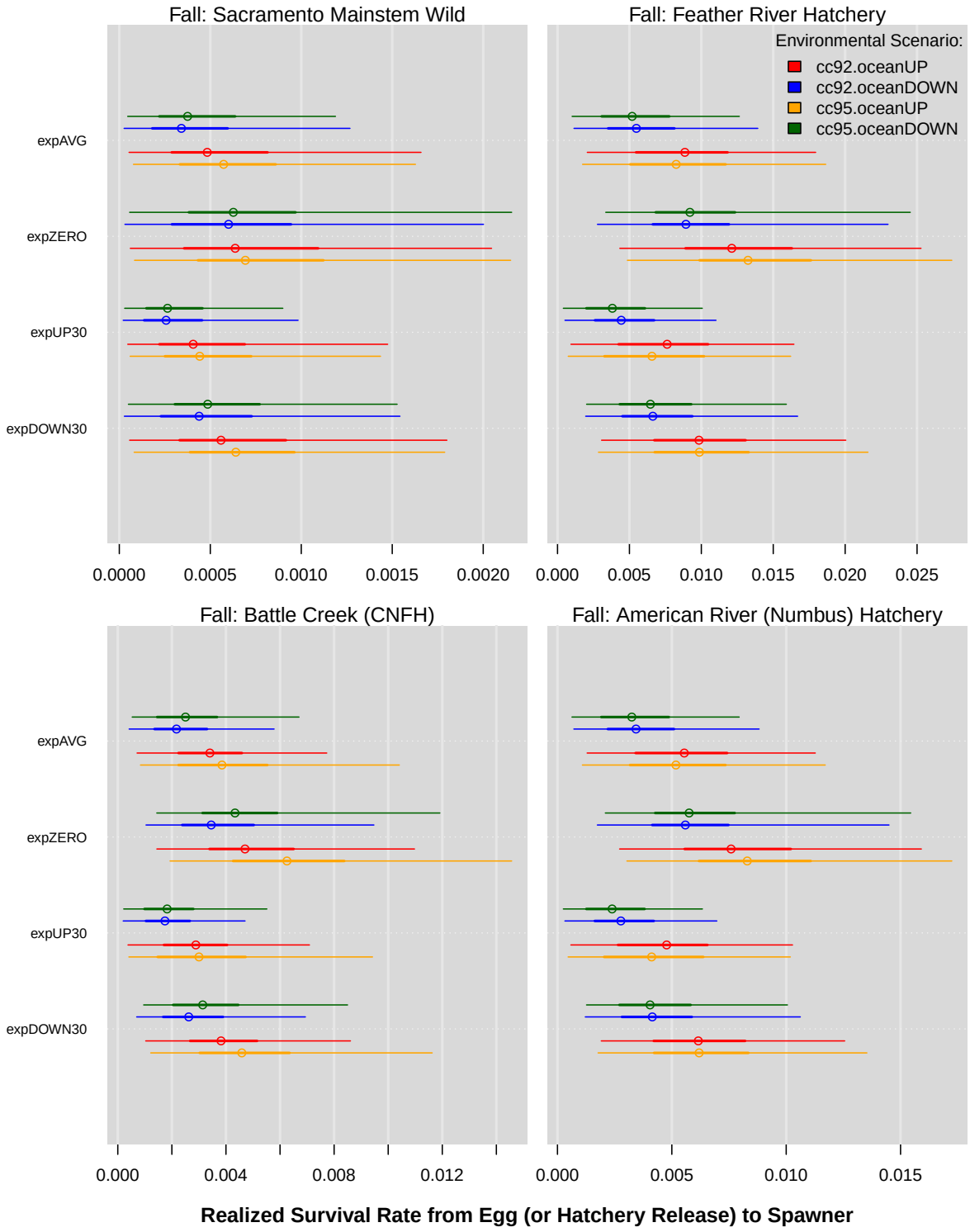

Figure II.4. Caterpillar plots describing the predicted distribution of realized survival to return, across years and simulations, for four fall-run Chinook populations. The circle, thick line, and thin line describe the median, 50% credible interval and 95% credible interval for the predictions.

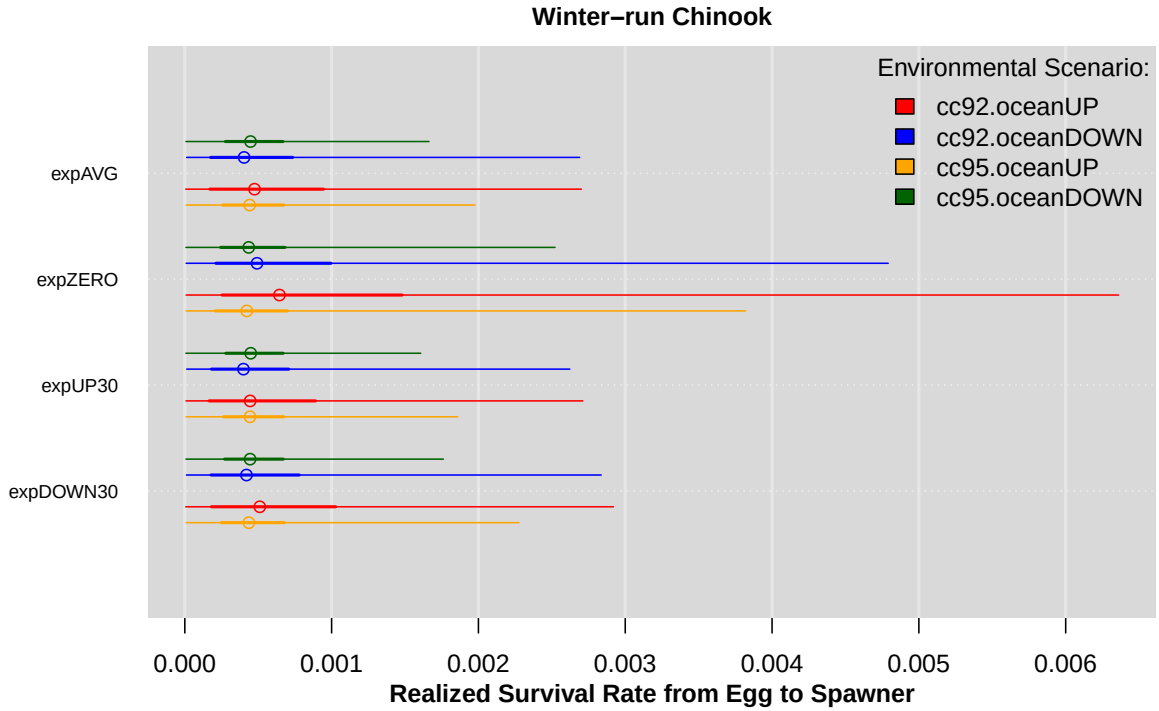

Figure II.5. Caterpillar plots describing the predicted distribution of realized survival to return, across years and simulations, for winter run Chinook populations. The circle, thick line, and thin line describe the median, 50% credible interval and 95% credible interval for the predictions.

Population	Export Scenario	cc92.oceanUP	cc92.oceanDOWN	cc95.oceanUP	cc95.oceanDOWN
Fall: Sacramento Mainstem Wild	expAVG	0.060%	0.043%	0.064%	0.046%
	expZERO	0.077%	0.068%	0.083%	0.074%
	expUP30	0.050%	0.033%	0.053%	0.033%
	expDOWN30	0.067%	0.052%	0.072%	0.058%
Fall: Battle Creek (CNFH)	expAVG	0.355%	0.245%	0.420%	0.274%
	expZERO	0.513%	0.394%	0.665%	0.484%
	expUP30	0.303%	0.195%	0.342%	0.205%
	expDOWN30	0.406%	0.295%	0.500%	0.346%
Fall: Feather River Hatchery	expAVG	0.894%	0.605%	0.867%	0.562%
	expZERO	1.292%	0.983%	1.411%	1.026%
	expUP30	0.764%	0.483%	0.700%	0.420%
	expDOWN30	1.019%	0.731%	1.040%	0.713%
Fall: American River (Numbus) Hatchery	expAVG	0.560%	0.380%	0.543%	0.352%
	expZERO	0.810%	0.617%	0.885%	0.643%
	expUP30	0.479%	0.303%	0.439%	0.263%
	expDOWN30	0.639%	0.459%	0.652%	0.447%
Spring: Deer Creek	expAVG	0.047%	0.052%	0.059%	0.065%
	expZERO	0.083%	0.090%	0.089%	0.095%
	expUP30	0.023%	0.025%	0.031%	0.033%
	expDOWN30	0.069%	0.075%	0.077%	0.082%
Spring: Mill Creek	expAVG	0.050%	0.058%	0.064%	0.071%
	expZERO	0.092%	0.100%	0.098%	0.105%
	expUP30	0.024%	0.027%	0.033%	0.036%
	expDOWN30	0.075%	0.084%	0.085%	0.092%
Spring: Butte Creek	expAVG	0.077%	0.092%	0.051%	0.058%
	expZERO	0.122%	0.136%	0.068%	0.074%
	expUP30	0.041%	0.049%	0.031%	0.034%
	expDOWN30	0.106%	0.121%	0.062%	0.069%
Winter-run Chinook	expAVG	0.069%	0.061%	0.059%	0.055%
	expZERO	0.133%	0.098%	0.085%	0.070%
	expUP30	0.067%	0.060%	0.058%	0.055%
	expDOWN30	0.076%	0.064%	0.062%	0.056%

Table II.1. Median of simulations for the predicted percent realized survival from egg or hatchery release to spawning adult, across water export and future environmental scenarios. Matrix of scenario-specific realized survival predictions for each population are shaded from red (low) to green (high) for ease of interpretation.

Population	Export Scenario	cc92.oceanUP	cc92.oceanDOWN	cc95.oceanUP	cc95.oceanDOWN
Fall: Sacramento Mainstem Wild	expZERO	30%	59%	28%	62%
	expUP30	-16%	-23%	-18%	-28%
	expDOWN30	12%	23%	12%	26%
Fall: Battle Creek (CNFH)	expZERO	44%	61%	58%	77%
	expUP30	-15%	-20%	-18%	-25%
	expDOWN30	14%	21%	19%	26%
Fall: Feather River Hatchery	expZERO	45%	62%	63%	83%
	expUP30	-14%	-20%	-19%	-25%
	expDOWN30	14%	21%	20%	27%
Fall: American River (Numbus) Hatchery	expZERO	45%	63%	63%	83%
	expUP30	-15%	-20%	-19%	-25%
	expDOWN30	14%	21%	20%	27%
Spring: Deer Creek	expZERO	79%	72%	50%	46%
	expUP30	-50%	-52%	-47%	-49%
	expDOWN30	48%	44%	29%	27%
Spring: Mill Creek	expZERO	85%	74%	53%	47%
	expUP30	-51%	-53%	-49%	-50%
	expDOWN30	51%	46%	32%	29%
Spring: Butte Creek	expZERO	59%	47%	32%	27%
	expUP30	-46%	-47%	-39%	-41%
	expDOWN30	38%	31%	21%	19%
Winter-run Chinook	expZERO	91%	60%	44%	28%
	expUP30	-3%	-2%	-1%	0%
	expDOWN30	9%	5%	5%	3%

Table II.2. Percent difference in median realized survival from average export (expAVG) scenario, across environmental scenarios. Values shaded from red (low) to green (high) for ease of interpretation.

In addition to estimates for future realized survival rates, for wild-spawning populations the average productivity of populations across years and replicate scenarios was also evaluated. Figure II.6, displays the average number of recruits per spawner for the Sacramento mainstem wild-spawning fall-run Chinook population, and the Deer, Mill, and Butte Creek spring-run populations and winter run, under alternative water export scenarios and environmental conditions. Scenarios that predict average productivity of less than 1 recruit-per-spawner, indicate that those populations are unlikely to remain viable in the future and will tend toward extinction in the presence of environmental stochasticity. Forward simulation results for the mainstem Sacramento fall-run Chinook population indicate that under the average (expAVG) and 30% increase (expUP30) water export scenarios, average productivity in the face unfavorable ocean conditions producing a 20% reduction in future upwelling (oceanDOWN) is expected to be less than one recruit-per-spawner (Fig. II.6). However, under both of these future export scenarios average recruits-per-spawner is expected to expected to exceed one under favorable future ocean conditions (oceanUP).

Predicted future realized productivity (recruits-per-spawner) for the Deer, Mill, and Butte Creek spring-run populations is predicted to be significantly lower under the scenario representing a 30% increase in future exports (expUP30). For both the Deer Creek and Mill Creek populations, average realized productivity (recruits-per-spawner) is predicted to be less than one with a 30% increase in water exports (expUP30), across all four combinations of future climate change and marine conditions (Fig. II.6). Predictions for future productivity of the Butte Creek population indicate that with the more gradual climate warming and greater future precipitation under the OCAP 9.2 scenario indicate that even with a 30% increase in water exports (expUP30) the population may be expected to produce at or near 1 recruit-per-spawner, and therefore remain viable.

Average future productivity (recruits-per-spawner) is expected to be highest across environmental scenarios under the zero export (expZERO) and 30% reduction in future exports (expDOWN30). However, realized productivity is predicted to vary across populations in response to future climate change and ocean production scenarios. For the mainstem Sacramento wild-spawning fall-run population, future productivity in the face of positive ocean conditions and specifically increased nearshore upwelling (oceanUP) is predicted to be highest and exceed one recruit-per-spawner, independent of the climate change or export scenario. The form of future climate change is predicted to have the greatest impact on the Butte Creek spring-run Chinook population, with higher productivity, in terms of recruits-per-spawner, under the OCAP 9.2 scenario (Fig. II.6). This results from the fact that this population was found to be particularly sensitive to summertime temperatures, which are predicted to increase more precipitously under the OCAP 9.5 climate change scenario leading to reduced over-summer survival of adults holding prior to spawning. Spring run stocks are much more sensitive to exports than fall and winter run, but both fall and winter do see slight improvement under export restrictions.

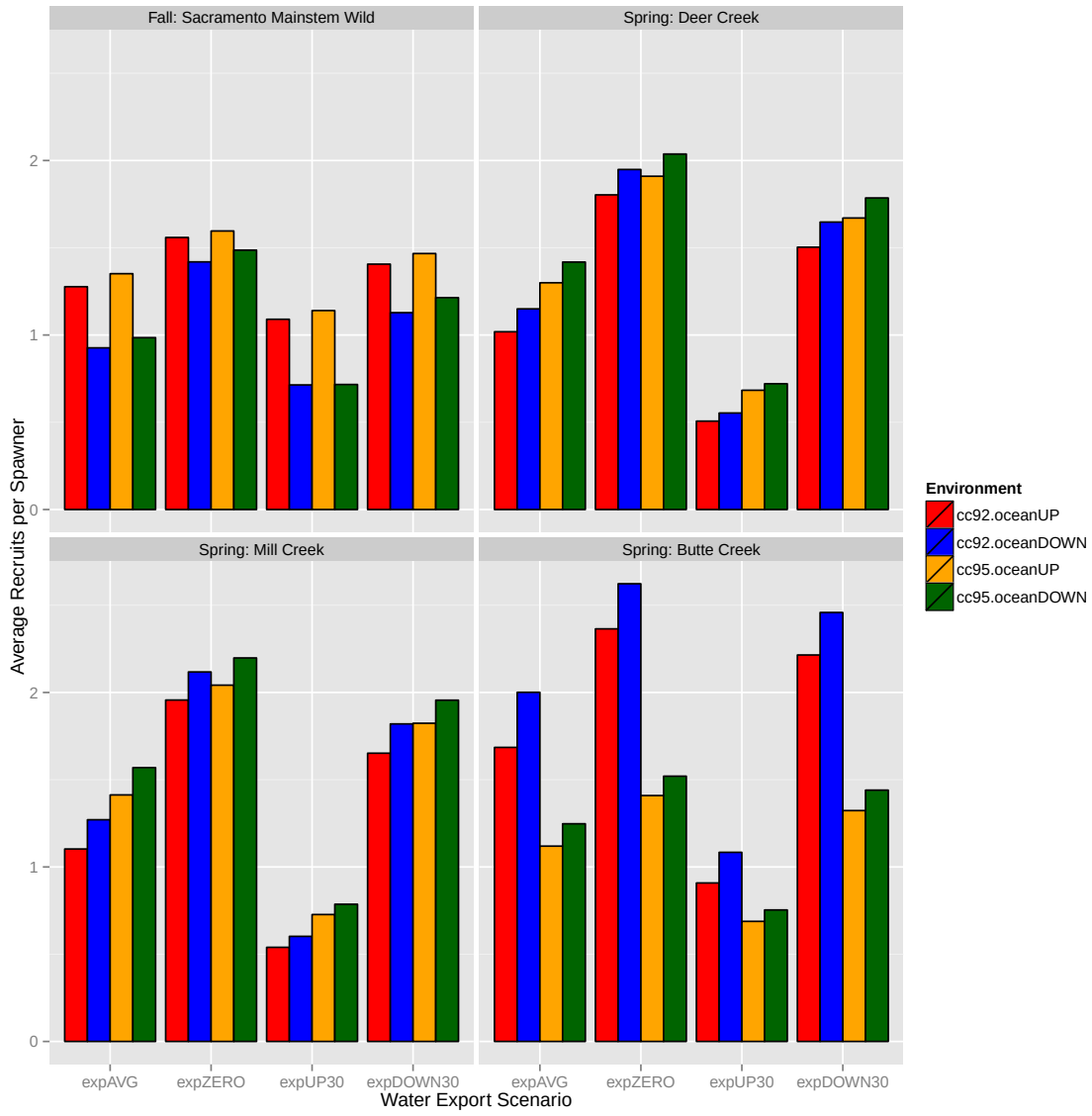

1720

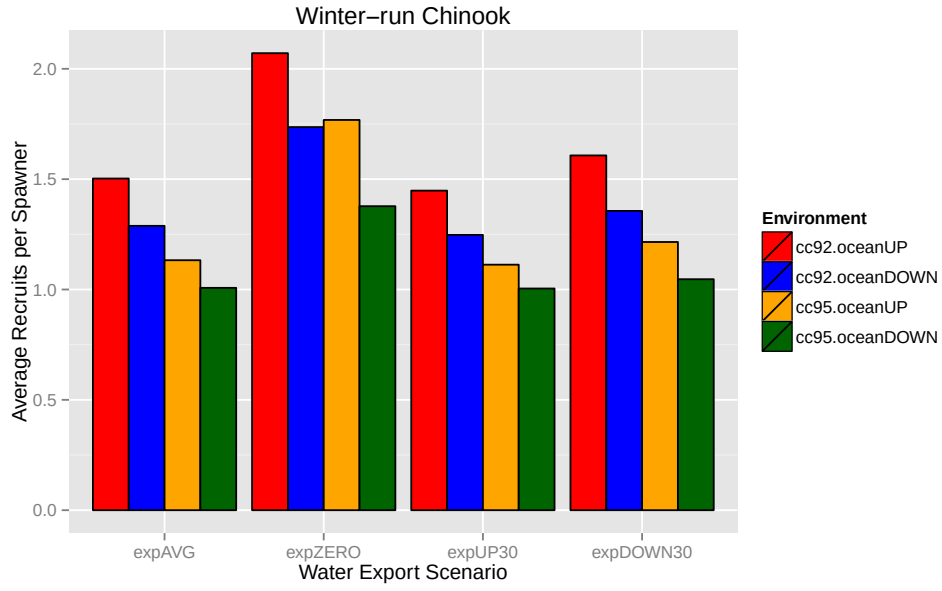

1721

1722 **Figure II.6. Average number of realized recruits per spawner, across populations, environmental and**
1723 **export scenarios**

PART II DISCUSSION

Results from a Bayesian population dynamics model estimating the stage and population specific maximum survival rates and changes in survival in response to natural and anthropogenic environmental covariates were used to parameterize simulations for future trends in population-specific abundance under alternative water export, climate change, and ocean production scenarios. Both estimation and process uncertainty were incorporated into future predictions by, first sampling model parameter values from the joint posterior, and second incorporating stochastic process deviations into the first modeled life-stage. One thousand replicate simulations of the 50-year future time series were used to fully quantify the influence of these two sources of uncertainty. The likely impact from future ocean harvest of Chinook was incorporated by simultaneously modeling the future trends in abundance for winter-run Chinook in the Sacramento system and replicating the current fishery management decision rules. We did not explore the impacts of modifying the harvest regime, but obviously any change in the fraction of fish harvested would have an analogous impact to increasing survival via changing exports or other environmental factors.

Results from these forward simulations in the form of estimates for future realized survival rates from egg, or hatchery release, to spawning adult, and estimates for realized productivity (recruits-per-spawner) indicate that while all populations are sensitive to differences in future water exports from the Sacramento-San Joaquin Delta, differences in the future environment are likely to have substantial population-specific impacts. The observation that predicted realized survival and productivity are generally higher for the fall-run populations and equal or lower for the spring-run populations under the oceanUP scenario results from several characteristics of the forward simulation model. The oceanUP scenario represents a 10% increase in future nearshore upwelling, paired with a smaller increase in future water temperatures at the Farallon Islands. While nearshore upwelling was found by the estimation model to significantly increase survival in the nearshore region for fall-run Chinook populations, this covariate was not AICc-selected for the spring-run populations. As a result, predictions for future realized survival for the fall-run Chinook populations show as consistently higher survival and productivity patterns in response to the oceanUP scenario. This prediction for higher realized survival for fall-run Chinook populations agrees with insights by Lindley et al. (2009) pointing to unusually low nearshore upwelling patterns as one of the proximate causes of the failure of the 2004 – 2005 fall-run brood years. In addition, the grouped survival of all seven Chinook populations was found to have a positive relationship with the Pacific Decadal Oscillation. The oceanUP scenario described an initial negative PDO phase, followed by a positive PDO phase, resulting in lower marine survival initially followed by higher marine survival in later years for the populations. The opposite pattern in marine survival was observed for the seven Chinook populations under the oceanDOWN scenario in response to the PDO pattern simulated in the opposite direction.

Future climate change scenarios had mixed impacts across populations as a result of the estimated response by populations to the environmental covariates impacted by the OCAP 9.2 and 9.5 predictions. The cooler and wetter OCAP 9.2 scenario had a particularly strong influence on the Butte Creek population, because a strong negative influence of high summertime temperatures was predicted for this population. However, the increase in water flow associated with the OCAP 9.2 scenario resulted in increased sediment concentration at Freeport, CA. Given the negative relationship between sediment concentration at this location

and survival for both fall and spring-run Chinook, this aspect of the OCAP 9.2 scenario did result in some reduction in survival for all populations, although in some cases this effect was outweighed by the interaction with temperature.

Across all combinations of future export and environmental scenarios predictions for both realized survival and productivity (recruits-per-spawner) were highly variable. While we have focused on predicted differences in median survival and average productivity, the 95% credible intervals for these predictions overlap in almost all cases. This indicates that the combination of both estimation and process uncertainty introduced in the forward simulation process leads to significant variability in future abundance and our quantified metrics. This is particularly pronounced in future predictions of realized survival for the Butte Creek population, which are extremely right skewed (Fig. II.3).

Quantifying results of forward simulations for wild-spawning Chinook populations in terms of average productivity (recruits-per-spawner) provided an efficient means for determining under what water export scenarios and environmental conditions specific populations are expected to persist (recruits-per-spawner > 1), or decline toward extinction (Fig. II.5). For several of the populations under the 30% increase in future water export scenario (expUP30), and for the fall-run mainstem Sacramento wild-spawning population under the average export scenario paired with decreased future upwelling (oceanDOWN), average productivity was predicted at less than one. While this result suggests that under those conditions specific populations may be expected to decline in abundance, it is important to fully understand the assumptions involved in this prediction. First, the forward simulations assume that future fishing mortality rates will vary in accordance with current management practices, as influenced by the Sacramento Index and harvest limitations based upon the abundance of winter-run Chinook. A reduction in future fishing mortality rate may be sufficient to increase the productivity of these populations above 1 recruit-per-spawner and facilitate persistence. Second, predictions for future productivity do not account for the stray rates amongst hatchery and wild populations leading to source-sink dynamics (Johnson et al. 2012). These effects may be most important for the Sacramento mainstem wild-spawning fall-run Chinook population, which was found in 2010 and 2011 to have 20 – 27% of its observed spawning abundance resulting from hatchery-reared strays (Kormos et al. 2012, Palmer-Zwahlen and Kormos 2013). Whether the contribution of straying individuals may be enough to facilitate persistence of populations under environmental and export scenarios that are predicted by these analysis to lead to decline (recruits-per-spawner < 1), remains unknown.

REFERENCES

Battin, J., M. W. Wiley, M. H. Ruckelshaus, R. N. Palmer, E. Korb, K. K. Bartz, and H. Imaki. 2007. Projected impacts of climate change on salmon habitat restoration. Proc Natl Acad Sci U S A **104**:6720-6725.

Beverton, R. J. H., and S. J. Holt. 1957. On the dynamics of exploited fish populations.

Brooks, S. P., and A. Gelman. 1998. General methods for monitoring convergence of iterative simulations. Journal of Computational and Graphical Statistics **7**:434-455.

Burnham, K. P., and D. R. Anderson. 2002. Model selection and multimodel inference : a practical information-theoretic approach. 2nd edition. Springer, New York.

CDF&W. 2014. GrandTab 2014.04.22: California Central Valley Chinook population report. California Department of Fish and Wildlife.

CDWR. 2014. DAYFLOW Data.*in* C. D. o. W. Resources, editor.

Claiborne, A. M., J. P. Fisher, S. A. Hayes, and R. L. Emmett. 2011. Size at release, size-selective mortality, and age of maturity of Willamette River Hatchery yearling Chinook salmon. Transactions of the American Fisheries Society **140**:1135-1144.

Ewing, R. D., and G. S. Ewing. 2002. Bimodal length distributions of cultured chinook salmon and the relationship of length modes to adult survival. Aquaculture **209**:139-155.

Fournier, D. A., H. J. Skaug, J. Ancheta, J. Ianelli, A. Magnusson, M. N. Maunder, A. Nielsen, and J. Sibert. 2012. AD Model Builder: using automatic differentiation for statistical inference of highly parameterized complex nonlinear models. Optimization Methods and Software **27**:233-249.

Gelman, A., J. B. Carlin, H. S. Stern, and D. B. Rubin. 2004. Bayesian data analysis. 2nd edition. Chapman & Hall/CRC, Boca Raton, Fla.

Gelman, A., and D. B. Rubin. 1992. Inference from iterative simulation using multiple sequences. Statistical Science **7**:457-511.

Hare, S. R., N. J. Mantua, and R. C. Francis. 1999. Inverse production regimes: Alaska and West Coast Pacific salmon. Fisheries **24**:6-14.

Hendrix, N., E. Danner, C. M. Greene, H. Imaki, and S. T. Lindley. 2014. Life cycle modeling framework for Sacramento River Winter-run Chinook salmon. NOAA Technical Memorandum.

Hilborn, R., and M. Mangel. 1997. The ecological detective: confronting models with data. Princeton University Press, Princeton, NJ.

1839 Honea, J. M., J. C. Jorgensen, M. M. McClure, T. D. Cooney, K. Engie, D. M. Holzer, and R.
1840 Hilborn. 2009. Evaluating habitat effects on population status: influence of
1841 habitat restoration on spring-run Chinook salmon. Freshwater Biology **54**:1576-
1842 1592.

1843 Huber, E. R., and S. M. Carlson. in review. Temporal trends of California Central Valley
1844 fall run Chinook salmon hatchery release practices.

1845 Johnson, R. C., P. K. Weber, J. D. Wikert, M. L. Workman, R. B. MacFarlane, M. J. Grove,
1846 and A. K. Schmitt. 2012. Managed metapopulations: do salmon hatchery 'sources'
1847 lead to in-river 'sinks' in conservation? PLoS ONE **7**:e28880.

1848 King, R., B. Morgan, O. Gimenez, and S. Brooks. 2010. Bayesian analysis for population
1849 ecology. CRC Press.

1850 Kocan, R., P. Hershberger, G. Sanders, and J. Winton. 2009. Effects of temperature on
1851 disease progression and swimming stamina in Ichthyophonus-infected rainbow
1852 trout, Oncorhynchus mykiss (Walbaum). Journal of Fish Diseases **32**:835-843.

1853 Kormos, B., M. Palmer-Zwahlen, and A. Low. 2012. Recover of coded-wire tags from
1854 Chinook salmon in California's Central Valley escapement and ocean harvest
1855 2010. California Deparment of Fish and Game, Sacramento, Calfornia.

1856 Lindley, S. T., C. B. Grimes, M. S. Mohr, W. Peterson, J. Stein, J. T. Anderson, L. W.
1857 Botsford, D. L. Bottom, C. A. Busack, T. K. Collier, J. Ferguson, J. C. Garza, A. M.
1858 Grover, D. G. Hankin, R. G. Kope, P. W. Lawson, A. Low, R. B. Macfarlane, K. Moore,
1859 M. Palmer-Zwahlen, F. B. Schwing, J. Smith, C. Tracy, R. Webb, B. K. Wells, and T.
1860 H. Williams. 2009. What caused the Sacramento River fall Chinook stock
1861 collapse?

1862 Lindley, S. T., and M. S. Mohr. 2003. Modeling the effect of striped bass (*Morone saxatilis*)
1863 on the population viability of Sacramento River winter-run chinook salmon
1864 (*Oncorhynchus tshawytscha*). FISHERY BULLETIN **101**:321-331.

1865 Macias, D., P. J. S. Franks, M. D. Ohman, and M. R. Landry. 2012. Modeling the effects of
1866 coastal wind- and wind-stress curl-driven upwellings on plankton dynamics in
1867 the Southern California current system. Journal of Marine Systems **94**:107-119.

1868 Mantua, N. J., and S. R. Hare. 2002. The Pacific decadal oscillation. Journal of
1869 Oceanography **58**:35-44.

1870 Moussalli, E., and R. Hilborn. 1986. Optimal Stock Size and Harvest Rate in Multistage
1871 Life-History Models. Canadian Journal of Fisheries and Aquatic Sciences **43**:135-
1872 141.

1873 Myrick, C. A., and J. J. Chech. 1998. Temperature effects on Chinook salmon and
1874 Steelhead: a review focusing on California's Central Valley populations. Bay-Delta
1875 Modeling Forum.

1876 Neuswanger, J., M. S. Wipfli, A. E. Rosenberger, and N. F. Hughes. 2014. Mechanisms of
1877 drift-feeding behavior in juvenile Chinook salmon and the role of inedible debris
1878 in a clear-water Alaskan stream. Environmental Biology of Fishes **97**:489-503.

1879 Newman, K. B., and P. L. Brandes. 2010. Hierarchical Modeling of Juvenile Chinook
1880 Salmon Survival as a Function of Sacramento-San Joaquin Delta Water Exports.
1881 North American Journal of Fisheries Management **30**:157-169.

1882 Newman, K. B., and J. Rice. 2002. Modeling the survival of Chinook salmon smolts out-
1883 migrating through the lower Sacramento River system. Journal of the American
1884 Statistical Association **97**:983-993.

1885 Palmer-Zwahlen, M., and B. Kormos. 2013. Recovery of coded-wire tags from Chinook
1886 salmon in California's Central Valley escapement and ocean harvest in 2011.
1887 California Department of Fish and Wildlife, Sacramento, California.

1888 Perry, R. W., J. R. Skalski, P. L. Brandes, P. T. Sandstrom, A. P. Klimley, A. Ammann, and B.
1889 MacFarlane. 2010. Estimating survival and migration route probabilities of
1890 juvenile Chinook salmon in the Sacramento-San Joaquin River Delta. North
1891 American Journal of Fisheries Management **30**:142-156.

1892 Poytress, W. R., J. J. Gruber, F. D. Carrillo, and S. D. Voss. 2014. Compendium report of
1893 Red Bluff Diversion Dam rotary trap juvenile anadromous fish production
1894 indices for years 2002-2012. Report of U.S. Fish and Wildlife Service to California
1895 Department of Fish and Wildlife and US Bureau of Reclamation.

1896 Scheuerell, M. D., R. Hilborn, M. H. Ruckelshaus, K. K. Bartz, K. M. Lagueux, A. D. Haas,
1897 and K. Rawson. 2006. The Shiraz model: a tool for incorporating anthropogenic
1898 effects and fish-habitat relationships in conservation planning. Canadian Journal
1899 of Fisheries and Aquatic Sciences **63**:1596-1607.

1900 Sogard, S. M. 1997. Size-selective mortality in the juvenile stage of teleost fishes: A
1901 review. Bulletin of Marine Science **60**:1129-1157.

1902 Stevens, D. E., and L. W. Miller. 1983. Effects of river flow on abundance of young
1903 Chinook salmon, American Shad, Longfin Smelt, and Delta Smelt in the
1904 Sacramento-San Joaquin River system. North American Journal of Fisheries
1905 Management **3**:425-437.

1906 Tompkins, M. R. 2006. Floodplain connectivity and river corridor complexity:
1907 Implications for river restoration and planning for floodplain management.
1908 University of California, Berkley.

1909 USBR. 2008. Central Valley Project and State Water Project Operations Criteria and Plan
1910 Biological Assessment. U.S. Department of the Interior, Bureau of Reclamation,
1911 Mid-Pacific Region, Sacramento, California.

1912 Ward, P. D., T. R. McReynolds, and C. E. Garman. 2003. Butte Creek spring-run Chinook
1913 salmon, *Oncorhynchus tshawytscha* pre-spawn mortality evaluation, 2003.
1914 California Department of Fish and Game, Chico, California.

1915 Wells, B. K., J. C. Field, J. A. Thayer, C. B. Grimes, S. J. Bograd, W. J. Sydeman, F. B. Schwing,
1916 and R. Hewitt. 2008. Untangling the relationships among climate, prey and top
1917 predators in an ocean ecosystem. Marine Ecology-Progress Series **364**:15-29.

1918 Wells, B. K., C. B. Grimes, J. C. Field, and C. S. Reiss. 2006. Covariation between the
1919 average lengths of mature coho (*Oncorhynchus kisutch*) and Chinook salmon (*O.*
1920 *tshawytscha*) and the ocean environment. Fisheries Oceanography **15**:67-79.

1921 Wells, B. K., C. B. Grimes, and J. B. Waldvogel. 2007. Quantifying the effects of wind,
1922 upwelling, curl, sea surface temperature and sea level height on growth and
1923 maturation of a California Chinook salmon (Oncorhynchus tshawytscha)
1924 population. Fisheries Oceanography **16**:363-382.

1925 Williams, J. G. 2006. Central valley salmon: a perspective on Chinook and steelhead in
1926 the Central Valley of California. San Francisco Estuary & Watershed Science **4**.

1927 Zar, J. H. 2010. Biostatistical analysis. 5th edition. Prentice-Hall/Pearson, Upper Saddle
1928 River, N.J.

1929 Zeug, S. C., P. S. Bergman, B. J. Cavallo, and K. S. Jones. 2012. Application of a Life Cycle
1930 Simulation Model to Evaluate Impacts of Water Management and Conservation
1931 Actions on an Endangered Population of Chinook Salmon. Environmental
1932 Modeling & Assessment **17**:455-467.

1933

1934

APPENDIX A LINKAGES TO THE CENTRAL VALLEY LIFE CYCLE MODEL

BACKGROUND

The National Marine Fisheries Service (NMFS) Southwest Fisheries Science Center (SWFSC) initiated a project to develop life-cycle models of salmon populations in the Central Valley. The project objective is to build a framework to quantitatively evaluate how the management and operation of the Federal Central Valley Project (CVP) and California State Water Project (SWP) affect Central Valley salmon populations. The modeling framework will evaluate the current operations of the CVP and SWP, i.e., Operational Plan and Criteria (OCAP), and evaluate future water conveyance structures as proposed in the Bay Delta Conservation Plan (BDCP). The NMFS Central Valley Life Cycle Model (CVCLCM) targeted winter-run as the first race of Chinook for model development (Hendrix et al. 2014).

The CVCLCM framework is a stage-structured model. Stages in the model were based on developmental state as well as geographic location (e.g., smolts in the delta, smolts in the mainstem river, or smolts in a floodplain). State transitions among life-history stages are defined by a modified Beverton-Holt (Beverton 1957) that allows individuals exceeding the capacity of a habitat to move to a different geographic location rather than die in that habitat (Greene and Beechie 2004). The Beverton-Holt with movement function is defined by a survival rate, capacity, and movement rate (Figure A.1). Each of these parameters can be modeled as a function of environmental or anthropogenic factors that may be influenced by management (e.g., spatial extent of floodplain habitat as it affects capacity) and operational actions (e.g., flow as it affects movement or water temperature as it affects survival).

Capacity estimates for the river and delta habitats from the CVCLCM were used in the current fall-run and spring-run model. In addition, there are several products from the current model that will be useful to the CVCLCM, which is developing fall-run and spring-run life cycle models.

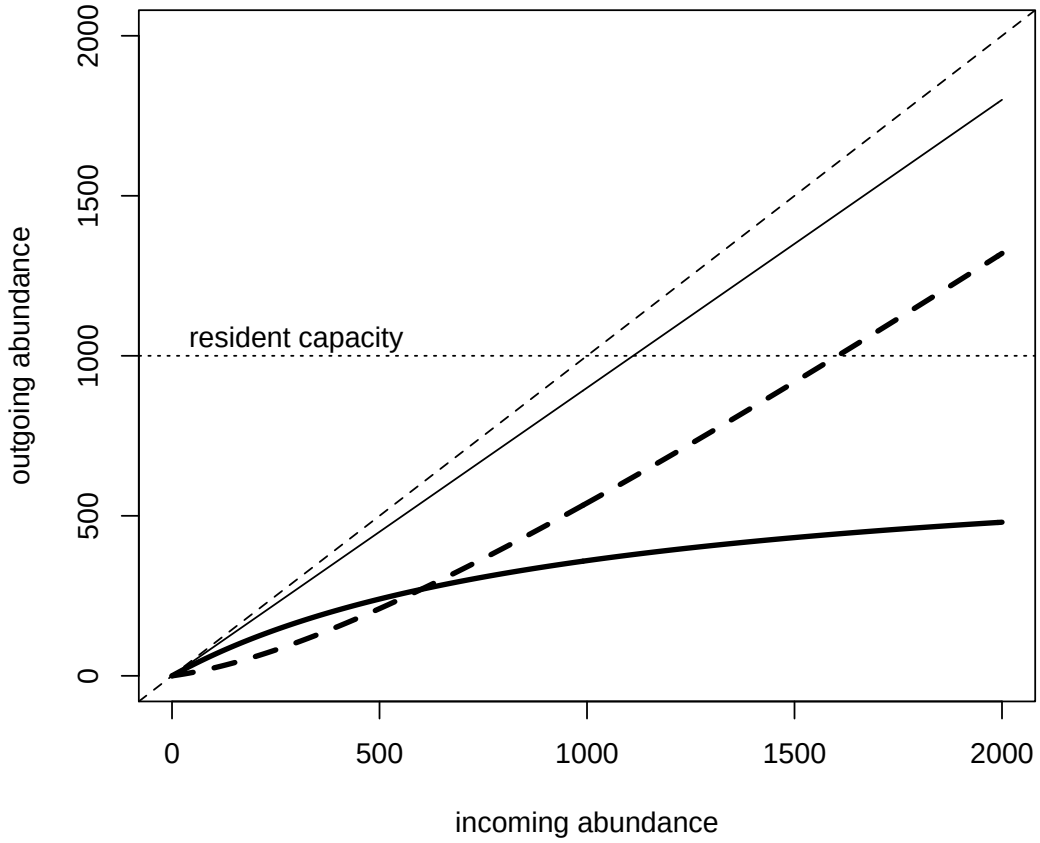

Figure A.1. Beverton-Holt with movement transition function. Outgoing abundance (thin solid line) is composed of migrants (thick dashed line) and residents (thick solid line), which are affected by the resident capacity (dotted horizontal line). Those fish that are not residents leave as migrants. The 1:1 line (thin dashed) is also plotted for reference.

PRODUCTS FROM THE CVCLCM USED IN THE FALL-RUN AND SPRING-RUN MODEL

Capacities

The CVCLCM developed estimates of monthly capacities for use in the Beverton-Holt transition function. The capacities were estimated in four habitats/geographic areas: 1) Sacramento River from headwaters to the city of Sacramento (river), 2) Yolo bypass (floodplain), 3) delta (city of Sacramento to Chipps Island) and 4) Chipps Island to the Golden Gate Bridge (bay). Two of these areas were used in the current fall-run and spring-run life-cycle model. The Sacramento River monthly capacity estimates were used for the Sacramento River mainstem spawning fall-run population in Stage 1 and the delta capacity estimates were used in fall-run (average delta capacity March to May) and spring-run (average delta capacity February to April) capacities for Stage 2.

Capacities for the river, floodplain, delta, and bay habitats were calculated in the CVCLCM as a function of habitat-specific capacity models (Hendrix et al. 2014). We provide details on the river and delta calculations and habitat capacity estimates, because they were included in the fall-run and spring-run model. In particular, the calculation of River capacity was modified since the publishing of the methods in Hendrix et al. (2014). Although the initial model development in the CVCLCM was focused on winter-run, the estimates of capacity are applicable to all races of Chinook in the Central Valley.

River Capacities

The River capacities were defined as a function of velocity and depth. For each variable preferred versus not-preferred categories were defined (Table A.1). The possible combinations of the 2 levels of 2 variables provided 4 categories of habitat quality for rearing Chinook salmon. The Central Valley is primarily a hatchery-dominated system with fish released at smolt size for rapid migration to the ocean, and natural stocks are at historically low levels; therefore, current estimates of fish density from the Central Valley may not be indicative of densities at capacity. As a result, densities from the Skagit River, WA were used to inform the maximum density estimates for each category (Greene et al. 2005). Two densities were used to calculate capacities: the 90th percentile and the 95th percentile of the distribution of densities by habitat category in the Skagit River.

Table A.1. Habitat variables used to define the River capacity.

Variable	Preferred or Not-preferred	Range
Velocity	Preferred	$\leq$ 0.15 m/s
	Not preferred	> 0.15 m/s
Depth	Preferred	> 0.2 m and $\leq$ 1m
	Not preferred	$\leq$ 0.2m or > 1m

Areas of habitat under each of the 4 categories were calculated by running the HEC-RAS model on a series of Sacramento River cross-sections that define cells. Each cell in the cross-section has a depth and velocity, and altering the flow changes the depth and velocity of a particular cell. The area of each cell that corresponded to a specific combination of velocity and depth category was tabulated for each monthly flow associated with a cross-section. The appropriate density of Chinook salmon for each of the 4 categories was applied to arrive at a density estimate for the Sacramento River in each month (Figure A.2).

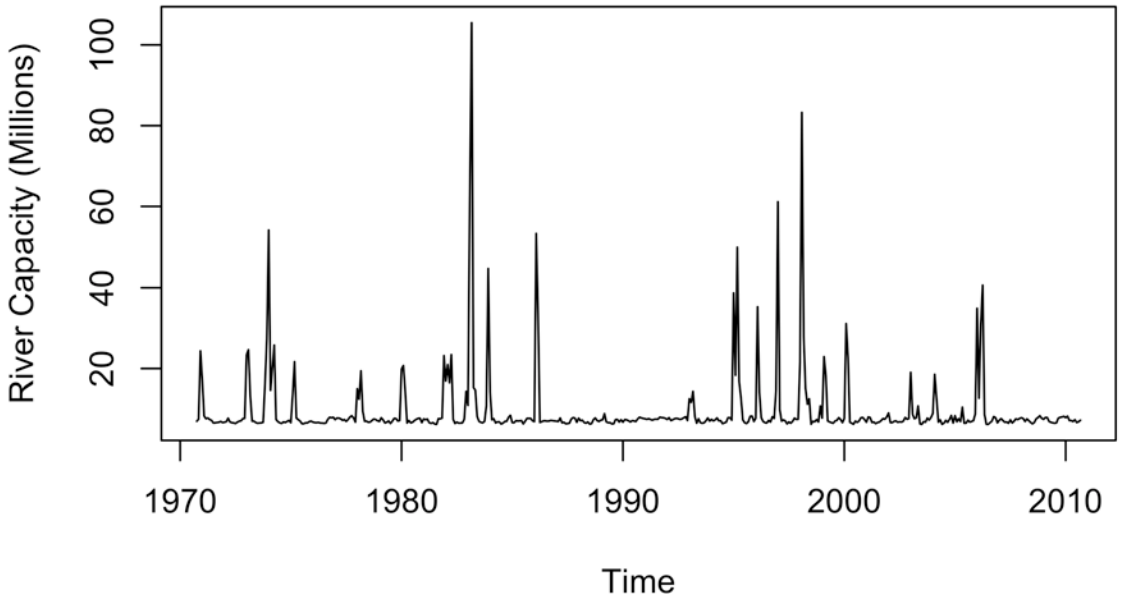

Figure A.2. Monthly capacity of Chinook salmon in the Sacramento River using a 90th percentile estimate of fish density.

Delta Capacities

The monthly capacities in the delta were defined as a function of several habitat attributes including: channel type, cover, shoreline type, blind channel area, salinity and vegetated cover along riverbanks. Analysis was conducted by using Geographic Information System (GIS) data layers. Habitat quality was determined by defining binary High/Low ranges for each axis of habitat quality, similar to the Preferred and Not-preferred approach used in the river habitat. In the delta, 8 categories of habitat quality were defined, each with an associated maximum density. Because not all habitats are accessible by rearing Chinook, a subsequent analysis was conducted to restrict habitat areas based on connectivity. Using beach seine data collected by US Fish and Wildlife Service (Speegle et al. 2013), a generalized linear model was used to estimate the probability of juvenile habitat use by seining location. This model was subsequently used to restrict habitat use by juvenile salmonids throughout the delta. Monthly estimates of capacity in the delta reflected the restricted access to particular areas of the delta and the seasonal absence of juvenile salmonids during the summer months (Figure A.3). Additional details on the capacity calculations can be found in Hendrix et al. (2014).

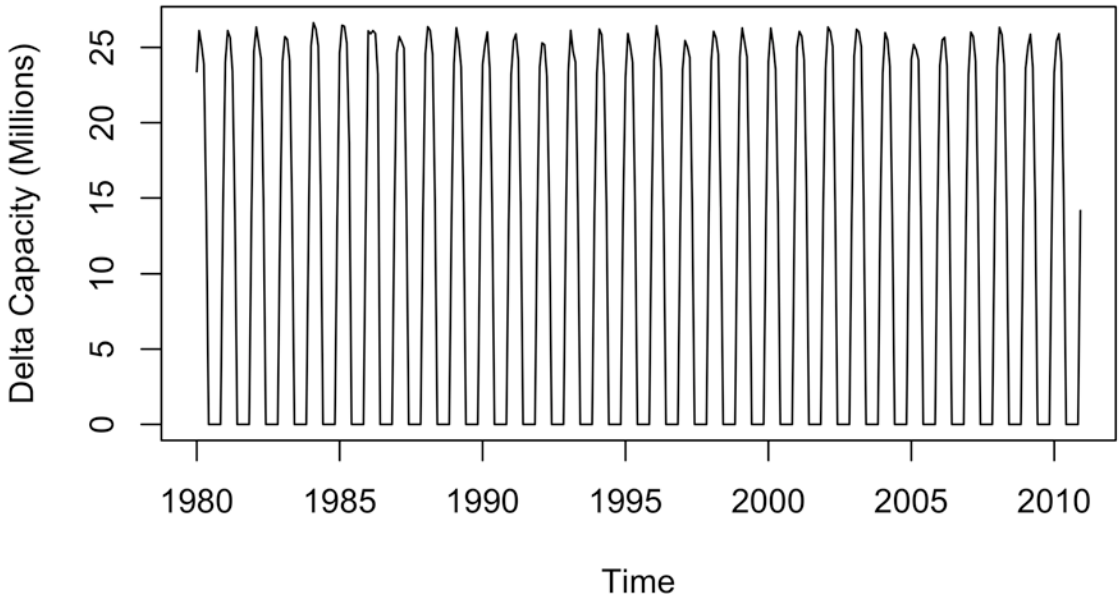

Figure A.3. Monthly capacities of Chinook salmon in the delta using a 90th percentile estimate of fish density.

Products from the fall-run and spring-run model that could benefit the CVCLCM

In the current project, we are using a model for fall and spring-run that incorporates competition through density dependence via a Beverton-Holt transition. This interaction effectively removes some capacity for each of the interacting races. Initial model evaluations indicated that an external capacity value improves the ability to estimate an interaction effect e.g., between fall-run and spring-run or between hatchery and natural. Although the Beverton-Holt function in the CVCLCM incorporates a movement component, understanding the importance of both of these interactions is important in the context of the CVCLCM models for fall-run and spring-run Chinook.

The NMFS scientists developing the fall-run and spring-run CVCLCM models will benefit from interacting with the current fall-run and spring-run model. The current model uses the CVCLCM capacities for certain stages, but these can also be modeled as functions of covariates to allow further hypothesis evaluation. In addition, the time series of observations is greater for the current model than the CVCLCM, which is restricted to 1980 to 2010. Thus earlier escapement data can be used to help parameterize the CVCLCM. Finally, the speed with which alternative hypotheses can be developed and fit to the fall-run and spring-run escapement data provides a useful tool for model construction in the CVCLCM. Hypotheses can be developed and tested on the order of minutes to hours, whereas running the full CVCLCM under a new set of environmental drivers can take on the order of days.

REFERENCES

Beverton, R. J. H., and S. J. Holt. 1957. On the dynamics of exploited fish populations.

Greene, C. M. and T. J. Beechie. 2004. Consequences of potential density-dependent mechanisms on recovery of ocean-type Chinook salmon (*Oncorhynchus tshawytscha*). Canadian Journal of Fisheries and Aquatic Sciences 61(4):590-602.

Greene, C. M., D. W. Jensen, G. R. Pess, E. A. Steel, and E. Beamer. 2005. Effects of environmental conditions during stream, estuary, and ocean residency on Chinook salmon return rates in the Skagit River, Washington. Transactions of the American Fisheries Society 134(6):1562-1581.

Hendrix, N., Danner, E., Greene, C. M., Imaki, H., & Lindley, S. T. 2014. Life cycle modeling framework for Sacramento River Winter-run Chinook salmon. NOAA Technical Memorandum NOAA -TM-NMFS-SWFSC-530.

Speegle, J., Kirsch, J., & Ingram, J. 2013. Annual Report: Juvenile fish monitoring during the 2010 and 2011 field seasons within the San Francisco Estuary, California.

APPENDIX B CLIMATE CHANGE SCENARIO PROJECTIONS

Climate change scenario projections were used to explore the level of impact that California's Central Valley Project (CVP) and State Water Project (SWP) operations can have on spring, fall and winter run Chinook under favorable and unfavorable climate forecasts. Model covariates were divided into three categories: overland covariates (river flows, river temperatures, air temperatures), nearshore ocean covariates (upwelling, PDO, wind stress curl, Farallon ocean temperatures), and anthropogenic water use covariates (exports, export/inflow ratios). Overland model covariates reflected two climate change scenarios: a warmer/drier scenario, and a cooler/wetter scenario. Nearshore ocean covariates explored two situations: favorable nearshore conditions for Chinook at ocean entry (increases in upwelling, PDO in negative phase, less warming of nearshore oceans), and unfavorable conditions (decreases in upwelling, PDO in positive phase, greater warming of nearshore oceans). Anthropogenic water use levels were modified with regard to exports to create four options: 1. future exports=mean historical exports; 2. future exports=mean historical exports +30%; 3. future exports=mean historical exports – 30%, and 4. future exports=0. A total of 16 climate change scenarios were generated using all combinations of overland covariates, nearshore ocean covariates and anthropogenic water use covariates (Table B.1).

METHODS

As the basis for our climate change scenarios, we used the United States Bureau of Reclamation's (USBR) Operations Criteria and Plan (OCAP) Study 9.2 and 9.5 (USBR 2008). OCAP Study 9.2 reflects a mean increase in temperature of 0.75° F (=0.42° C) and an increase of 12.5% in precipitation. OCAP Study 9.5 reflects a mean increase in temperature of 2.8° F (=1.56° C) and a decrease in precipitation of 12%. These temperature and precipitation changes represent a mean 30-year change between 1971-2000 and projected 2011-2040 levels. Study 9.2 and 9.5 are the extreme corners of a bounding box that captures the 10^{th} and 90^{th} percentiles for temperature increase and precipitation change that were predicted by 112 climate projections from a variety of climate models and greenhouse gas emission levels (USBR 2008). USBR used the following methodology to generate OCAP Study 9.2 and 9.5:

1. Plot temperature change (ΔT) vs. precipitation change (ΔP) over central California for each of 112 archived Downscaled CMIP3 Climate Projections (Downscaled CMIP3 Climate Projections Archive website).
2. Determine the 10^{th} and 90^{th} percentiles for predicted temperature and precipitation change.
3. Identify the levels of ΔT and ΔP associated with the 10^{th} and 90^{th} percentiles in the climate projections. The intersection of the 10^{th} and 90^{th} percentiles for ΔT with the 10^{th} and 90^{th} percentiles for ΔP form a bounding box with four corners.
4. Choose climate projections that most closely reflect the four corners of the bounding box. OCAP Study 9.2 reflects the mildest climate change conditions over central California (less warming/ wetter), while OCAP Study 9.5 reflects the most dramatic climate change conditions over central California (more warming/ drier).
5. Modify CalSim-II hydrology inputs and Sacramento River Water Quality Model (SRWQM) inputs based on temperature and precipitation values generated by the climate projections.

6. Run CalSim-II and SRWQM models using historical data that has been modified to reflect climate change, but is still run retrospectively.

We used CalSim-II and SRWQM outputs for OCAP Study 9.2 and 9.5 (USBR 2008 Appendix R zipped data), but projected the hindcast covariate values from 1946-2002 onto years 2007-2063 to obtain a forward projection, while retaining year-to-year variability in covariate values and the covariance structures present in the natural system. OCAP Study 9.2 and 9.5 provided two types of scenario outputs:

1. Streamflows and controlled discharges from dams and weirs: The CalSim-II model predicts mean monthly streamflows and discharges at various points throughout the Sacramento River system and the Delta, including the following covariates from the spring, fall and winter run Chinook models:
    a. **Keswick Dam discharge** (fall run): CalSim-II channel flows at C5 from OCAP Study 9.2 and 9.5 were used for years 1946-2002, averaged over January-March. Averaged values were then projected forward to become scenario values for 2007-2063 (Fig. B.1, Table B.2D).
    b. **Deer Creek discharge** (spring run): CalSim-II channel flows for Deer Creek were not available in OCAP Study 9.2 and 9.5. Instead, CalSim-II channel flows at C11305 (just past the confluence of Mill Creek, Deer Creek, Antelope Creek and discharge point D11305) from OCAP Study 9.2 and 9.5 were used for years 1946-2002, averaged over October-December. Deer Creek was separated from the other constituents of C11305 using the following methodology:
        i. CalSim-II channel flows at C11309 (Deer Creek), C11305 and D11305 were obtained from OCAP scenario NAA_Existing (no action alternative) for years 1946-2002, averaged over October-December. Deer Creek flow C11309 was divided by the sum of D11305 and C11305 to determine which proportion of Deer + Mill + Antelope Creek flows should be attributed to Deer Creek.
        ii. CalSim-II values C11305 + D11305 from OCAP Study 9.2 and 9.5 were multiplied by the vector of proportions for Deer Creek, one for each year (mean over all years=0.42, sd=0.05). These values were then projected forward to become scenario values for 2007-2063 (Fig. B.2, Table B.2D).
    c. **Exports / Inflow Ratio** (fall run): CalSim-II delta inflows (INFLOW-DELTA parameter) from OCAP Study 9.2 and 9.5 for 1946-2002, averaged over March-May, were used as the denominator in the Exports/Inflow ratio, while the four export scenarios (see *8. CVP and SWP Dayflow Exports*; and *8b. Mean Daily Exports March-May*, below) formed the numerator (Fig. B.3, Table B.2E).
    d. **Bend Bridge minimum monthly flow** (winter run): CalSim-II channel flows at C109 from OCAP Study 9.2 and 9.5 were used over years 1946-2002, selecting the minimum monthly flow between August-November. Minimum flow values were then projected forward to become scenario values for 2007-2063 (Fig. B.4, Table B.3A).
    e. **Freeport sediment concentration as a function of Freeport flow** (spring and fall run): Sediment concentrations at Freeport, averaged annually over February-April, were modelled as a linear function of Freeport flows (also averaged annually over February-April) from CalSim-II scenario

NAA_Existing at C169. The linear model equation, with intercept set to zero, is:

Freeport sediment conc. = CalSim-II flow at Freeport * 0.0022487

The R-squared value for the regression is 0.834 (Fig. B.5). Freeport flows from OCAP Study 9.2 and 9.5 for years 1946-2002, averaged over February-April, were then used in conjunction with the linear model to generate sediment concentrations. These were projected forward to years 2007-2063 (Fig. B.6, Table B.2D).

2. River temperatures: SRWQM generates mean monthly river temperatures at various nodes along major rivers in the Sacramento River system (USBR 2008 Appendix R zipped data)
    a. **Sacramento River temperature at Bend Bridge** (winter run): SRWQM outputs for OCAP Study 9.2 and 9.5 were extracted along the Sacramento River at Bend Bridge for 1946-2002. Model predictions were averaged for months July-September and projected onto years 2007-2063 (Fig. B.7, Table B.3B).

In addition to the OCAP Study 9.2 and 9.5 scenario outputs, we also used several other sources of data to generate scenario covariates:

3. Nearshore ocean upwelling estimates: Upwelling indices were obtained from NOAA's Pacific Fisheries Environmental Laboratory (PFEL Upwelling website). We increased and decreased historic values (1946-2002) of upwelling by +10% and -20% to account for a range of changes to upwelling that might occur under climate change (N. Mantua pers. comm., 12/8/14). These altered historic values were then projected onto years 2007-2063.
    a. **Upwelling at 36° N, 122° W** (spring and winter run): NOAA upwelling index values at 36° N, 122° W (southwest of Monterey, CA) were averaged over April-June for years 1946-2002, and adjusted up or down before being projected onto 2007-2063 (Fig. B.8, Tables B.2B & B.3A).
4. Pacific Decadal Oscillation (PDO) index: PDO indices were obtained from the Joint Institute for the Study of the Atmosphere and Oceans (Mantua and Hare). Over the last century, the PDO has displayed a 20-30 year autocorrelation pattern (Mantua et al. 1997). To capture the future impact of positive (warm) and negative (cold) PDO cycles on Chinook populations, we used two ranges of historic PDO data and projected them forward to years 2007-2063: one was a sequence that began with a positive PDO phase before flipping to a negative PDO phase, while the other began with a negative PDO phase and then flipped to a positive PDO phase. Pacific Northwest and West coast salmon production is enhanced during the negative phase of the PDO, and tends to decline during positive phases of the PDO (Mantua et al. 1997, Hare et al. 1999).
    a. **PDO** (spring and fall run): PDO values between 1900 and 2013 were averaged annually over January-May, and two sequences with opposite patterns were selected for future scenarios (Fig. B.9). The sequence of years between 1922-1978 began with a positive PDO phase, flipping to a negative phase around 1947. The sequence of years between 1946-2002 began with a negative PDO phase, flipping to a positive phase around 1977 (Fig. B.10, Table B.2B).

5. Wind Stress Curl Index: Calculated values for NOAA wind stress curl index for upwelling at Northern Location (39° N, 125° W) were obtained from NOAA's Pacific Fisheries Environmental Laboratory (PFEL Derived Winds website).
    a. **Curl Index** (spring and fall run): Historic curl index values from 1946-2002 averaged over July-December were increased or decreased by 20% and plotted as forward projections for 2007-2063 (Fig. B.11). Curl trajectories from 1967-2063 suggested a long-term autocorrelation pattern (Fig. B.11). Because we did not have compelling reasons to believe that future curl values would follow the same pattern as historic values, we set the future scenario curl index equal to mean curl from 1967-2010 (standardized curl index = 0) (Table B.2B).
6. Farallon Islands ocean temperature: Water temperature data at the Farallon Islands (37° 41.8' N, 122° 59.9' W) were not available for all years between 1946 and 2002, so the methodology of projecting covariate values from 1946-2002 under climate change onto years 2007-2063 could not be used. Instead, we calculated the mean water temperature over February-April for 1967-2012, and increased it by 0.42° C (=0.75° F) to correspond with OCAP Study 9.2, and by 1.56° C (=2.8° F) to correspond with OCAP Study 9.5.
    a. **Farallon Islands ocean temperature** (winter run): Mean water temperature from February-April during years 1967-2012 was 11.8° C. This was increased to 12.3° C and 13.4° C to match with OCAP Study 9.2 and 9.5, respectively (Fig. B.12, Table B.3B).
7. Sacramento air temperatures: Sacramento air temperature projections for 2007-2063 were obtained from the Downscaled CMIP3 Climate Projections archive (Downscaled CMIP3 Climate Projections Archive website) for the same climate projections that were used to generate OCAP Study 9.2 and 9.5. Air temperatures were obtained for the modelled grid cell containing Sacramento's latitude/ longitude (38.5556° N, 121.4689° W). OCAP Study 9.2 was based on climate model mri cgcm2.3.2a with A2 emissions, simulation #5, and OCAP Study 9.5 was based on climate model ukmo hadcm3 with A2 emissions, simulation #1.
    a. **Sacramento air temperature - spring** (spring and fall run): Climate projections for the modelled cell over Sacramento were averaged annually over January-March and adjusted up by 4.55 °F to spatially downscale climate projections to match with historic Sacramento air temperature data. The adjustment factor was obtained for each climate projection by subtracting mean projected air temperature between 1960-2010 (averaged over January-March) from mean historical Sacramento air temperature over the same period. Resulting differences were averaged for the two scenarios to obtain an adjusting value of 4.55 °F (Fig. B.13, Table B.2A).
    b. **Sacramento air temperature - summer** (fall run): Climate projections for the modelled cell over Sacramento for July-September were adjusted up by 8.82° F to spatially downscale climate projections to match with historic Sacramento air temperature data. Methodology for obtaining the adjustment factor was the same as for spring Sacramento air temperatures (see above) (Fig. B.13, Table B.2A).
8. CVP and SWP Dayflow Exports: Dayflow data for exports from the Delta were obtained from California's Department of Water Resources (CA DWR Dayflow website). Average daily exports were calculated for 1967-2010 and modified to generate four future export scenarios: 1. future exports = mean historical exports; 2.

future exports = mean historical exports +30%; 3. future exports = mean historical exports – 30%; and 4. future exports = 0.

a. **Mean daily exports February-April** (spring run): Dayflow exports were averaged annually over February-April for years 1967-2010 to form the historical export level, which was then modified for scenarios (Fig. B.14, Table B.2C).
b. **Mean daily exports March-May, for Export/Inflow ratio** (fall run): Dayflow exports were averaged annually over March-May for years 1967-2010 to form the historical export level for the Export/Inflow ratio (see Fig. B.3 and Table B.2E for the Export/Inflow ratio).
c. **Total daily exports December-June** (winter run): Dayflow exports were summed over all days between December and June, then averaged over 1967-2007 to form the mean historical export level, which was then modified for scenarios (Fig. B.15, Table B.3A).

9. Daily stream flows: Streamflow data are collected daily at select locations by USGS (USGS National Water Information System website). In order to generate future predictions for OCAP Study 9.2 and 9.5, the daily stream flow data had to be correlated to an appropriate CalSim-II output using linear models.
   a. **Number of days Sacramento River flow at Verona > 56,000 cfs** (winter run): A linear model was generated to relate CalSim-II monthly flows at Verona (C160 from OCAP scenario NAA_Existing) for 1967-2003 averaged over December-March, to the total number of days between December and March that Sacramento River flow at Verona exceeded 56,000 cfs (data from USGS National Water Information System website). The linear model is:

      # Days flow > 56,000 = -25.19 + CalSim-II flow at Verona * 0.001646

      with R-squared = 0.9285. This relationship was used in conjunction with CalSim-II flows at Verona (C160) for December 1946-March 2003, averaged over December-March, to generate future scenario values (projected onto 2007-2063) for number of days that Sacramento River flow at Verona exceeds 56,000 cfs (Fig. B.16, Table B.3B)
10. Water management operations: Discharges from dams, weirs and gates are managed in California to optimize diverse interests, including efforts to increase winter run Chinook populations.
    a. **Proportion of time Delta Cross Channel gate is open, December-March** (winter run): The current operations plan is to close the Delta Cross Channel (DCC) gate while winter run Chinook are out-migrating. As a result, future scenarios assume that the proportion of time that the DCC gate is open between December and March is zero (Table B.3B).
11. Parameters for which no future conditions could be generated:
    a. **Channel Depletion** (fall run): The net channel depletion is the quantity of water removed from the Delta channels to meet consumptive use, averaged over March-May. Since future population growth may be countered by water-saving technologies and measures, we set the future value of channel depletion equal to the mean value over 1967-2010 (or a standardized value of 0) (Table B.2A).
    b. **Smolt Size at Chipps Island** (spring run): For this parameter, we assumed that size of out-migrating smolt caught at Chipps Island will not change over

future years, so smolt size for the scenario projections was set equal to mean size over 1967-2010 (standardized value of 0) (Table B.2A).

ACKNOWLEDGEMENTS

We would like to thank Nate Mantua (NMFS – SWFSC) for advice on climate change impacts to physical characteristics of oceans, and Andrew Pike (NMFS – SWFSC) for his assistance with understanding and obtaining CalSim-II and SRWQM OCAP model outputs. For climate projection outputs that were used for scenario covariates, we acknowledge the modeling groups, the Program for Climate Model Diagnosis and Intercomparison (PCMDI) and the WCRP's Working Group on Coupled Modelling (WGCM) for their roles in making available the WCRP CMIP3 multi-model dataset. Support of the CMIP3 dataset is provided by the Office of Science, U.S. Department of Energy. Lastly, we thank Nate Mantua and Steve Hare for access to their historic PDO index values.

CITATIONS

California Department of Water Resources Dayflow Data. Accessed online Dec. 20, 2014. http://www.water.ca.gov/dayflow/output/Output.cfm

Downscaled CMIP3 Climate Projections Archive. Accessed online Dec. 15, 2014. http://gdo-dcp.ucllnl.org/downscaled_cmip_projections/dcpInterface.html#Projections:%20Subset%20Request

Hare, S.R., Mantua, N.J., Francis, R.C. (1999). Inverse production regimes: Alaska and West Coast Salmon. *Fisheries* 24(1): 6-14.

Mantua, N., Hare, S.R., Zhang, Y., Wallace, J.M., Francis, R.C. (1997). A Pacific interdecadal climate oscillation with impacts on salmon production. *Bulletin of the American Meteorological Society* 78: 1069-1079.

Mantua, N. and Hare, S.R., PDO Index Monthly Values: January 1900-present. Joint Institute for the Study of the Atmosphere and Ocean (University of Washington). Accessed online Dec. 30, 2014. http://jisao.washington.edu/pdo/PDO.latest

Pacific Fisheries Environmental Laboratory (NOAA) Coastal Upwelling Indices. Accessed online Dec. 20, 2014. http://www.pfeg.noaa.gov/products/PFEL/modeled/indices/upwelling/NA/upwell_menu_NA.html

Pacific Fisheries Environmental Laboratory (NOAA) Derived Winds and Ocean Transports. Accessed online Dec. 30, 2014. http://www.pfeg.noaa.gov/products/PFEL/modeled/indices/transports/transports.html

U.S. Bureau of Reclamation, 2008. Central Valley Project and State Water Project Operations Criteria and Plan Biological Assessment. U.S. Department of the Interior, Bureau of Reclamation, Mid-Pacific Region. Sacramento, California. Chapter 9 and Appendix R. http://www.usbr.gov/mp/cvo/OCAP/docs/OCAP_BA_2008.pdf

U.S. Bureau of Reclamation, 2008. Central Valley Project and State Water Project Operations Criteria and Plan Biological Assessment. U.S. Department of the Interior, Bureau of Reclamation, Mid-Pacific Region. Sacramento, California. Appendix R, zipped data. Accessed online Dec. 15, 2014. http://www.usbr.gov/mp/cvo/ocap_page.html

FIGURES

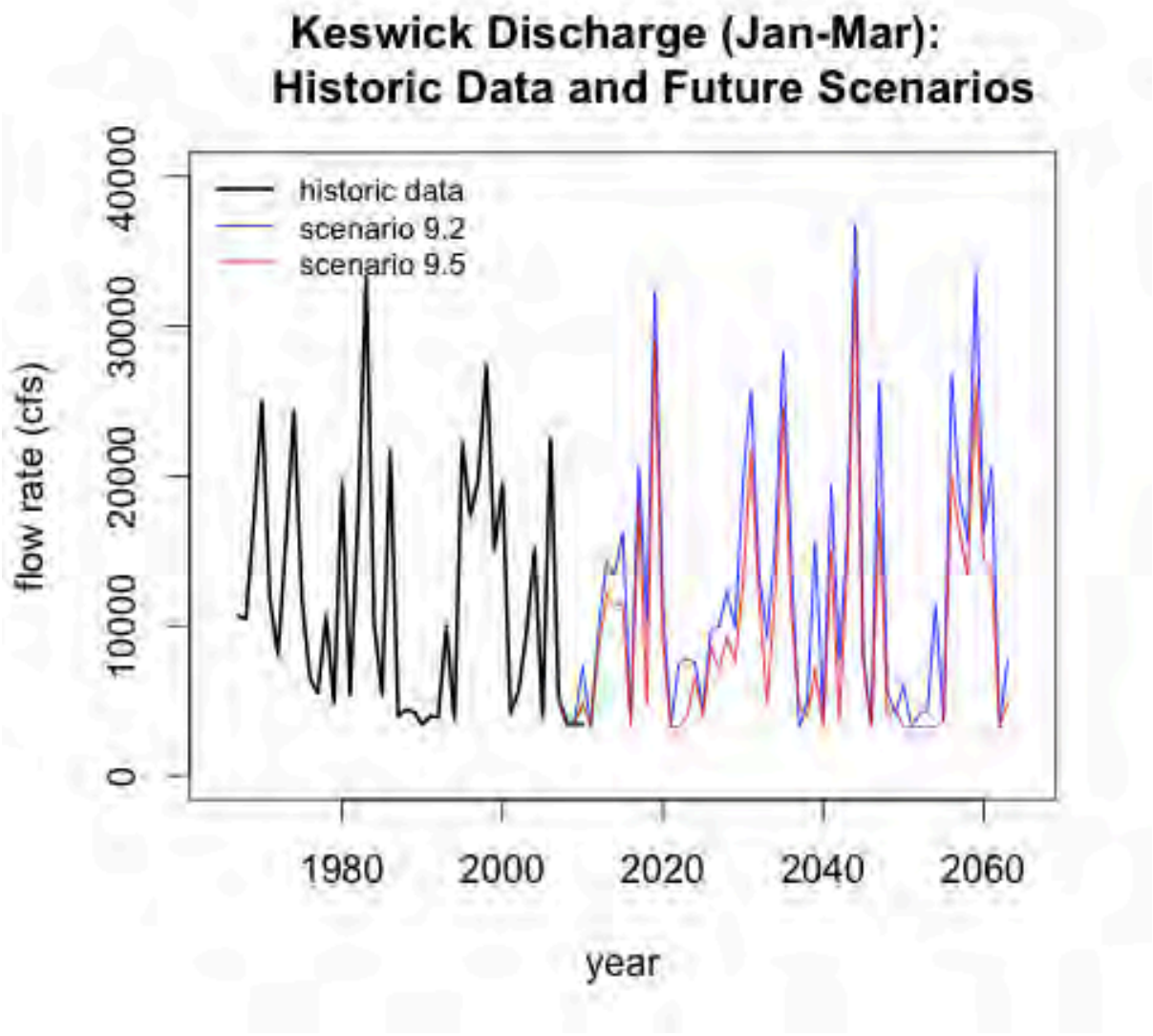

Figure B.1. Mean annual discharge (cubic feet per second, cfs) from Keswick Dam for January-March: historic data from 1967-2010 and climate change scenarios 9.2 and 9.5. Climate change scenarios were based on CalSim-II OCAP Study 9.2 and 9.5 values from 1946-2002, which were projected forward to 2007-2063.

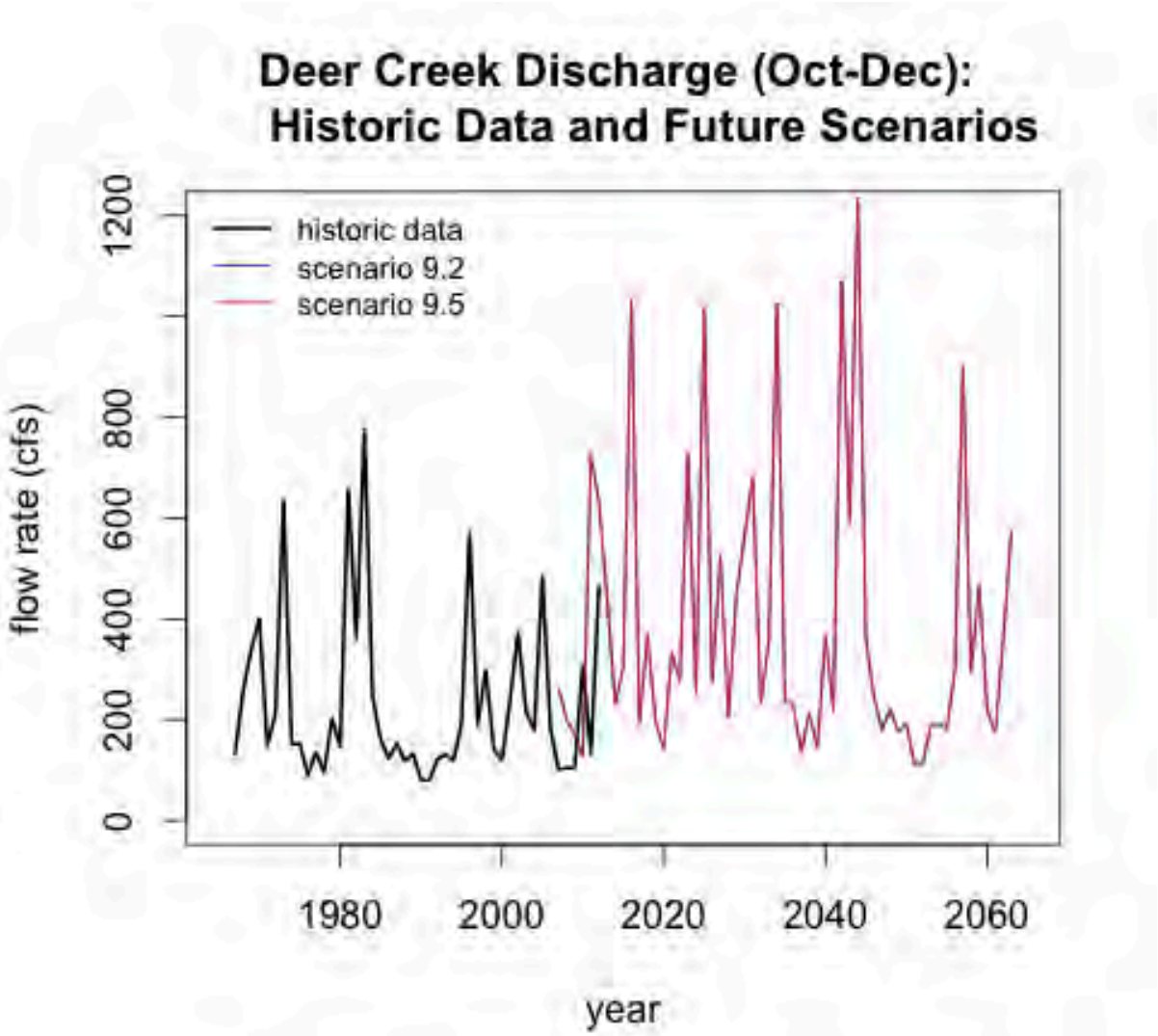

Figure B.2. Mean annual discharge (cfs) from Deer Creek for October-December: historic data from 1967-2012 and climate change scenarios 9.2 and 9.5. Climate change scenarios were based on CalSim-II OCAP Study 9.2 and 9.5 values from 1946-2002, which were projected forward to 2007-2063. Note that there is no difference in projection values between scenarios 9.2 and 9.5.

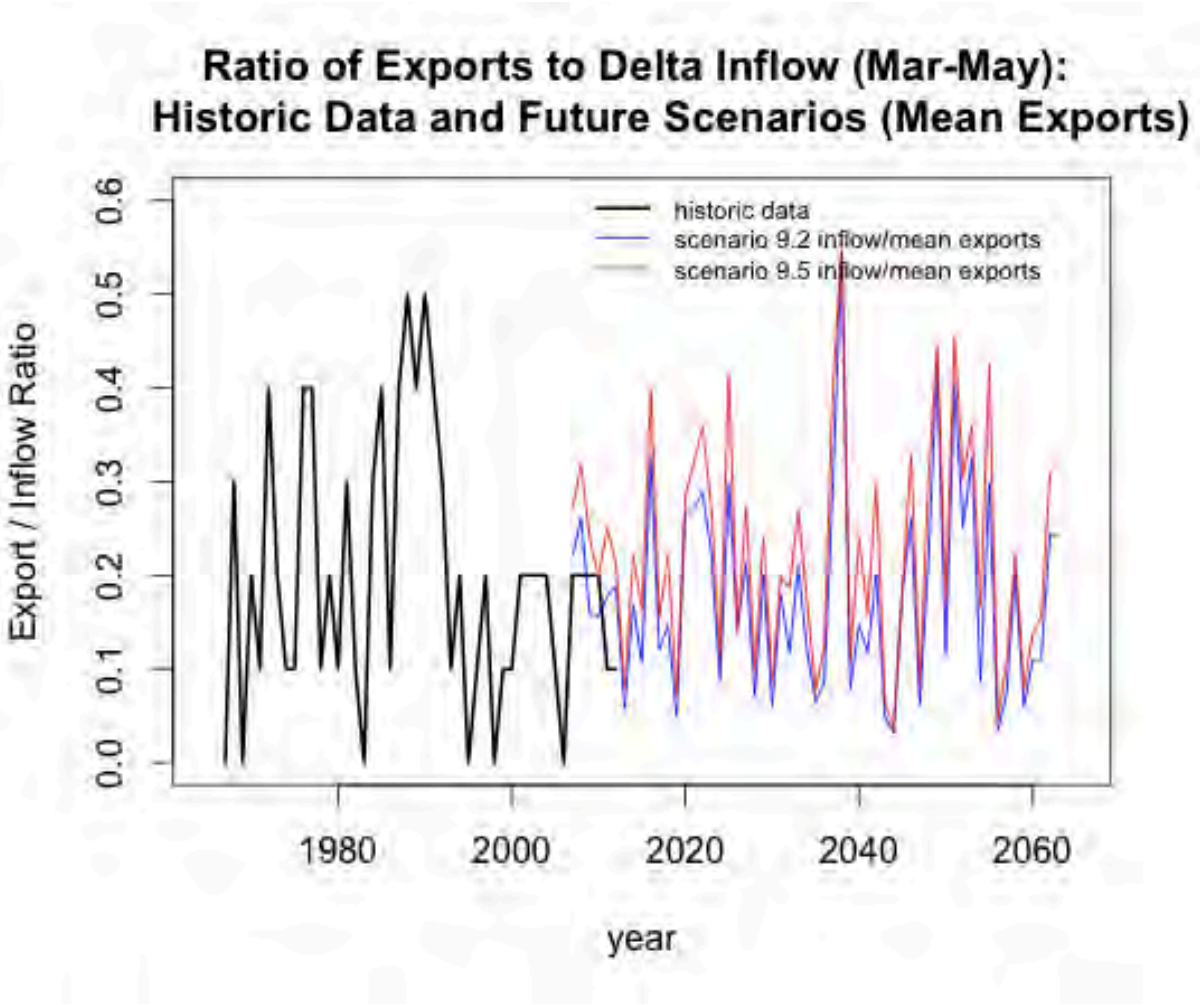

Figure B.3. Exports to inflow ratio for the Delta, averaged over March-May: historic data from 1967-2012 and climate change scenarios 9.2 and 9.5. Historic values are based on Dayflow data ((QCVP + QSWP – BBID)/ QTOT). Climate change scenarios use mean exports from 1967-2010 for the numerator, and CalSim-II Delta inflow values from OCAP Study 9.2 and 9.5 for the denominator. The CalSim-II Delta inflow values were from years 1946-2002, projected forward to 2007-2063.

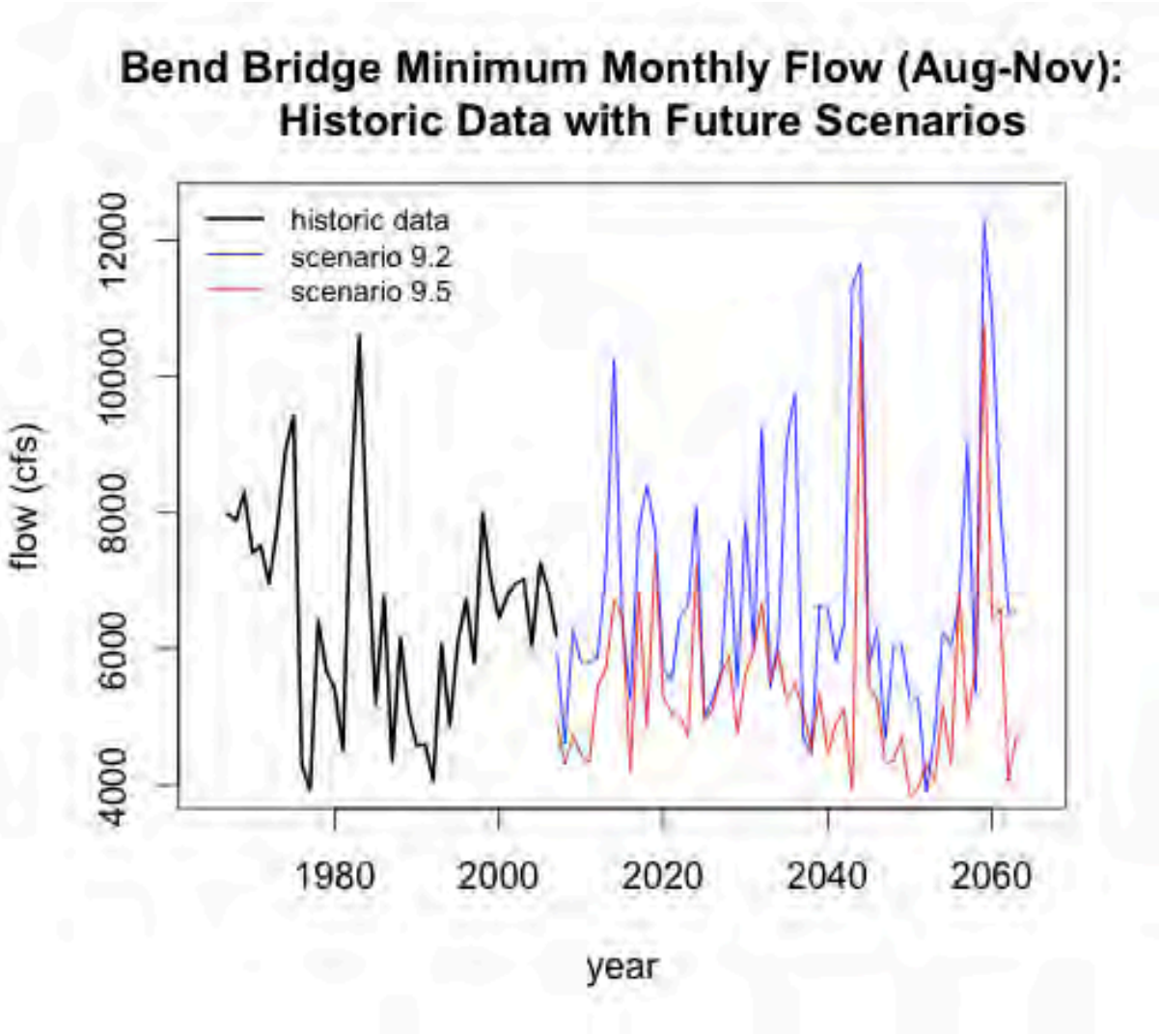

Figure B.4. Minimum monthly flow (cfs) at Bend Bridge for August-November: historic data from 1967-2007 and climate change scenarios 9.2 and 9.5. Climate change scenarios were based on CalSim-II OCAP Study 9.2 and 9.5 values from 1946-2002, which were projected forward to 2007-2063.

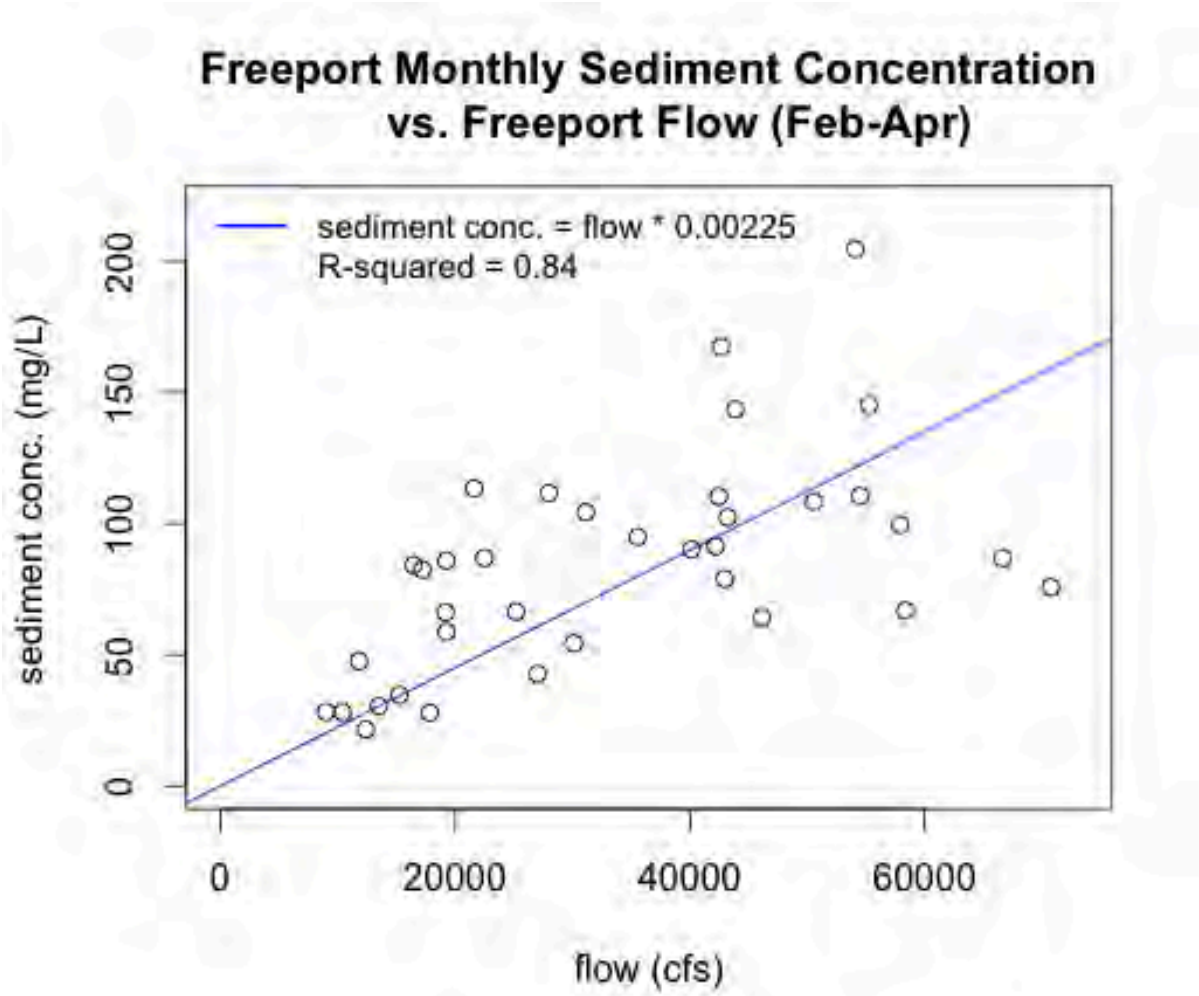

2384

2385

2386 **Figure B.5.** Average monthly sediment concentration (mg/L) at Freeport for years 1967-
2387 2002, as a function of modelled Freeport flows (cfs) from CalSim-II OCAP scenario
2388 NAA_Existing at node C169. Each point represents one year of data, averaged over months
2389 February-April. A linear model was fit to the points, with a specified intercept of 0 (blue
2390 line):

2391 Freeport sediment concentration = Freeport flow * 0.0022487

2392 The adjusted R-squared for the linear model is 0.84.

2393

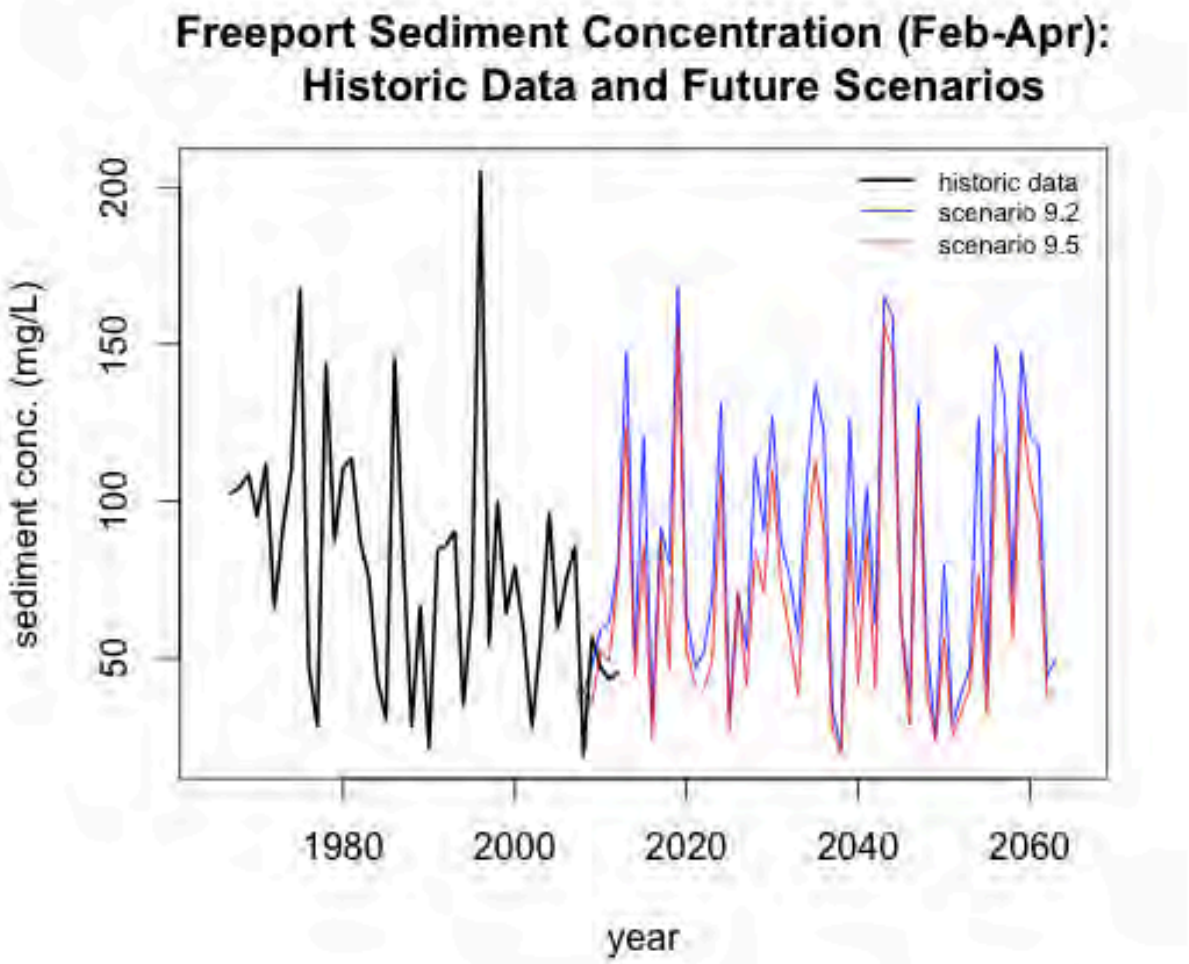

Figure B.6. Freeport sediment concentrations (mg/L) averaged over February-April: historic data from 1967-2012 and climate change scenarios 9.2 and 9.5. Climate change scenario values were obtained using Freeport flow predictions (at C169) from CalSim-II OCAP Study 9.2 and 9.5 for 1946-2002, and multiplying these values by 0.0022487 to correlate them to sediment concentrations (see Fig. B.5). The 1946-2002 climate change scenario sediment predictions were then projected forward to 2007-2063.

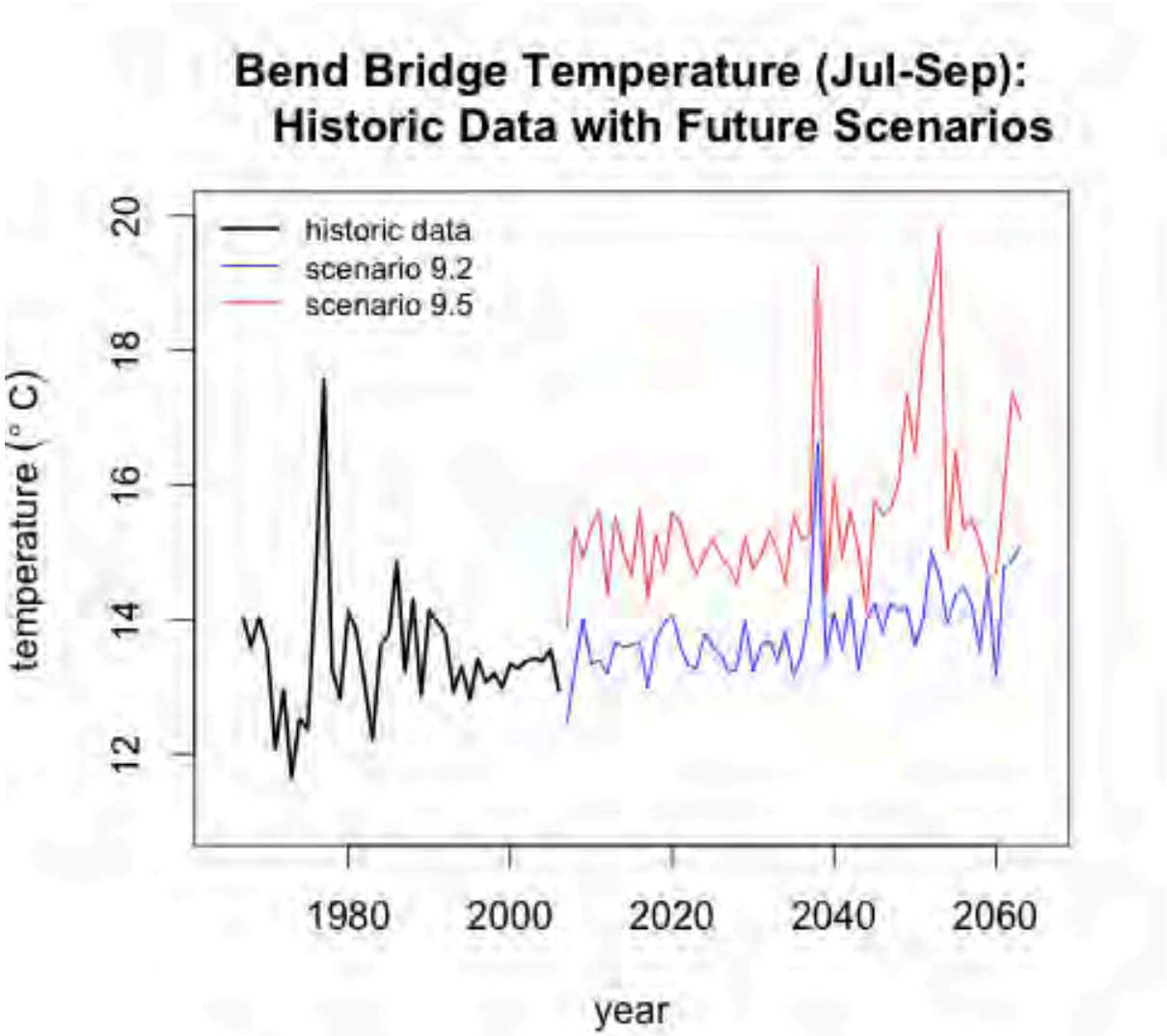

2405

2406 **Figure B.7.** Sacramento River average water temperature (° C) at Bend Bridge, averaged
2407 over July-September: historic data from 1967-2006 and climate change scenarios 9.2 and 9.5.
2408 Climate change scenarios were based on the SRWQM OCAP Study 9.2 and 9.5 values from
2409 1946-2002, which were projected forward to 2007-2063.

2410
2411

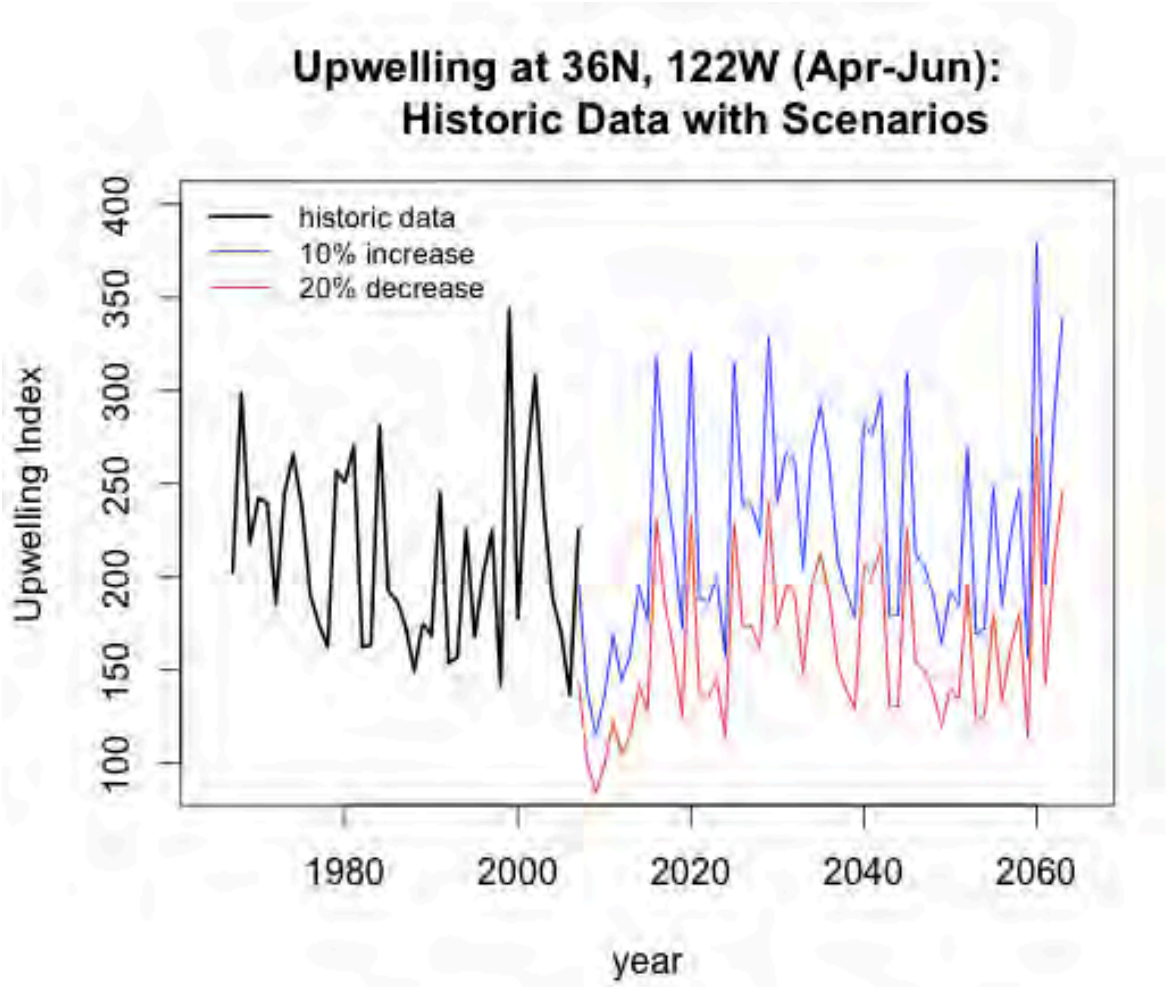

2412

2413 **Figure B.8.** NOAA upwelling index at station 36° N, 122°W averaged over April-June:
2414 historic data from 1967-2007 and two climate change scenarios. Climate change scenarios
2415 were based on historic upwelling values from 1946-2002, which were adjusted up (+20%) or
2416 down (-10%) and projected forward to 2007-2063.

2417

2418

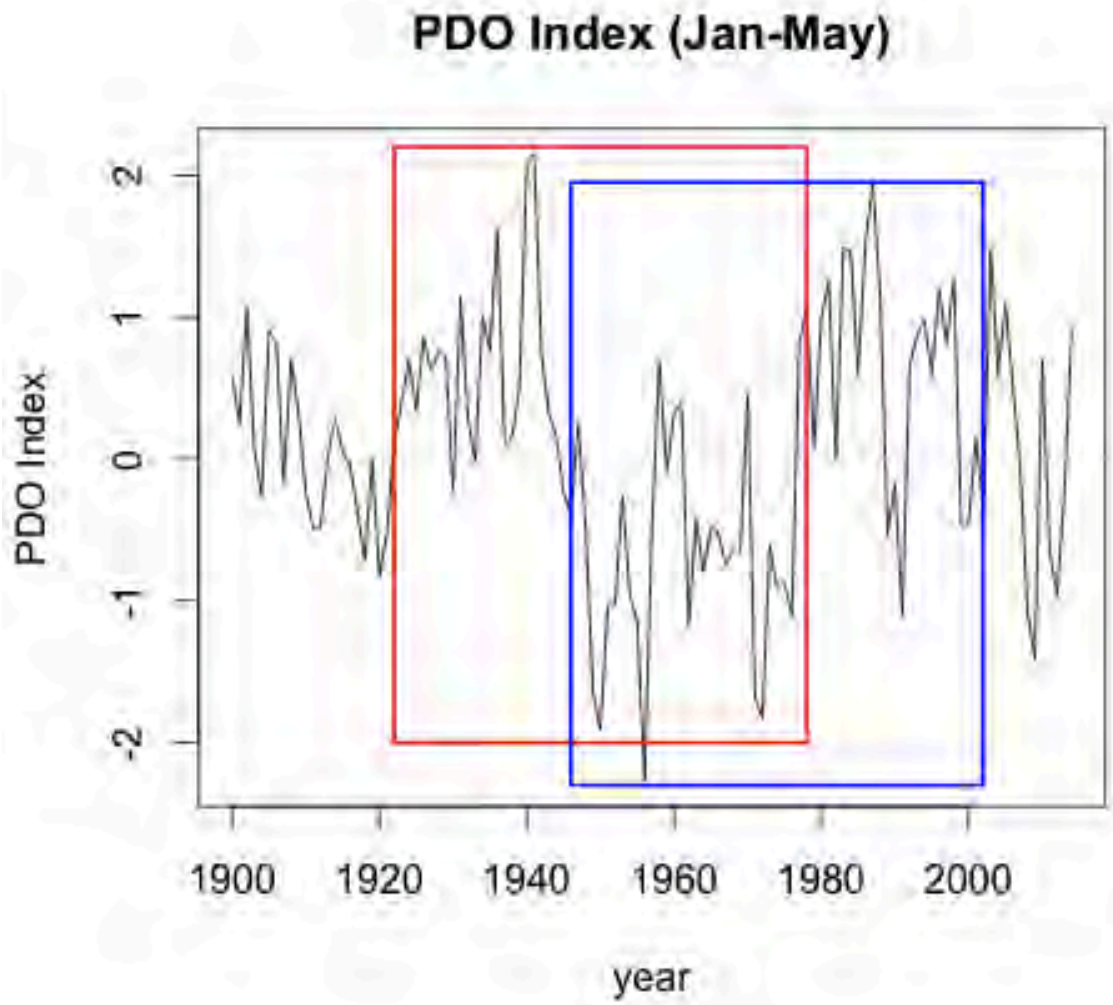

Figure B.9. Historic values of the PDO index, averaged annually over January-May. West coast salmon stocks have higher productivity during negative (cool) phases of the PDO, and lower productivity during positive (warm) phases. The sequence of years from 1922-1978 (red box) was projected forward to 2007-2063 to represent a scenario where the PDO begins in a positive cycle, while the sequence of years from 1946-2002 (blue box) was projected forward to represent a scenario where the PDO begins in a negative cycle.

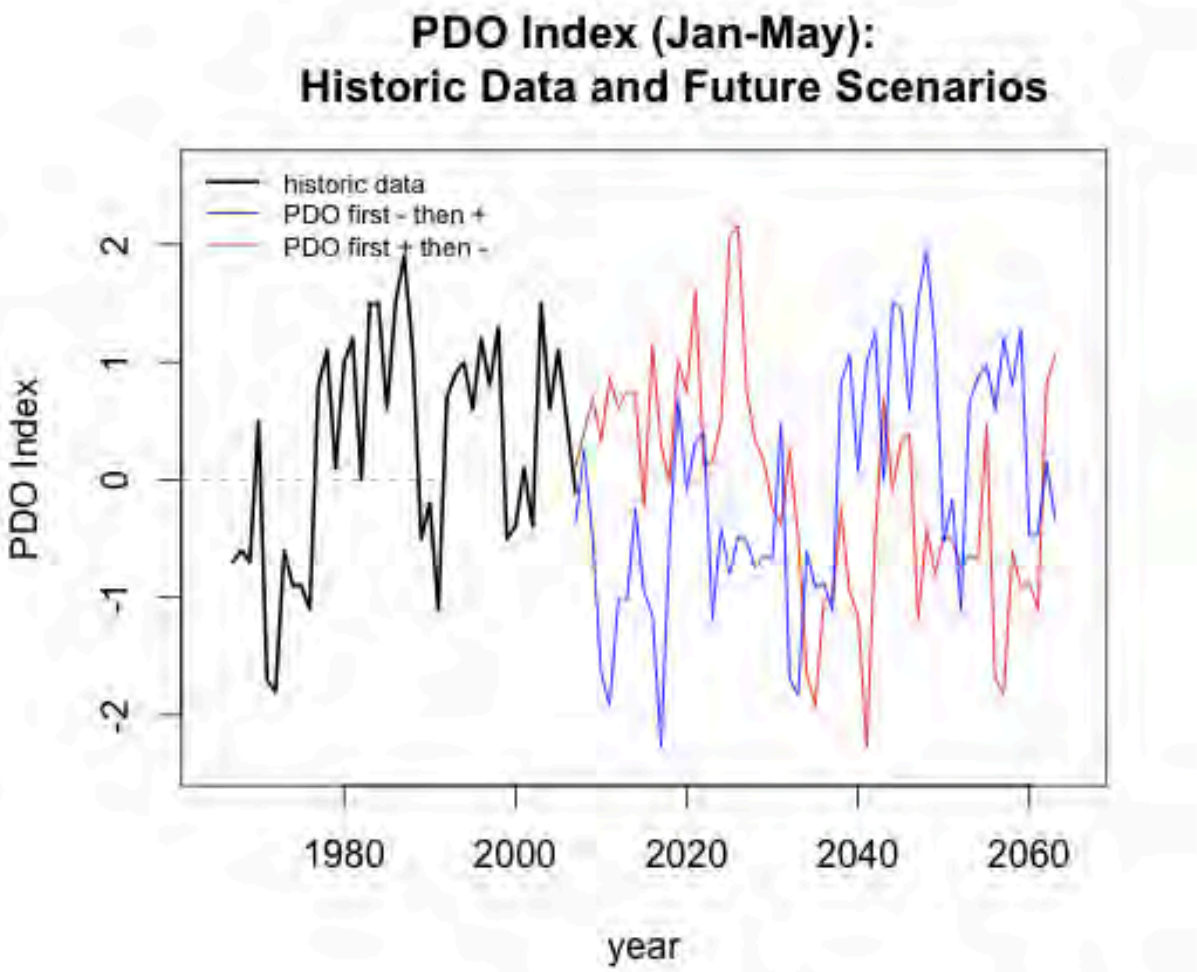

2426

2427 **Figure B.10.** PDO index averaged annually over January-May: historic data from 1967-2007
2428 and two future scenarios. Future scenarios were projected onto 2007-2063 and consist of: 1.)
2429 a historic sequence that begins with a negative PDO index, then flips to a positive PDO index
2430 halfway through the time series (blue line: historic values from 1922-1978); and 2.) a historic
2431 sequence that begins with a positive PDO index, then flips to a negative PDO index (red line:
2432 historic values from 1946-2002).

2433

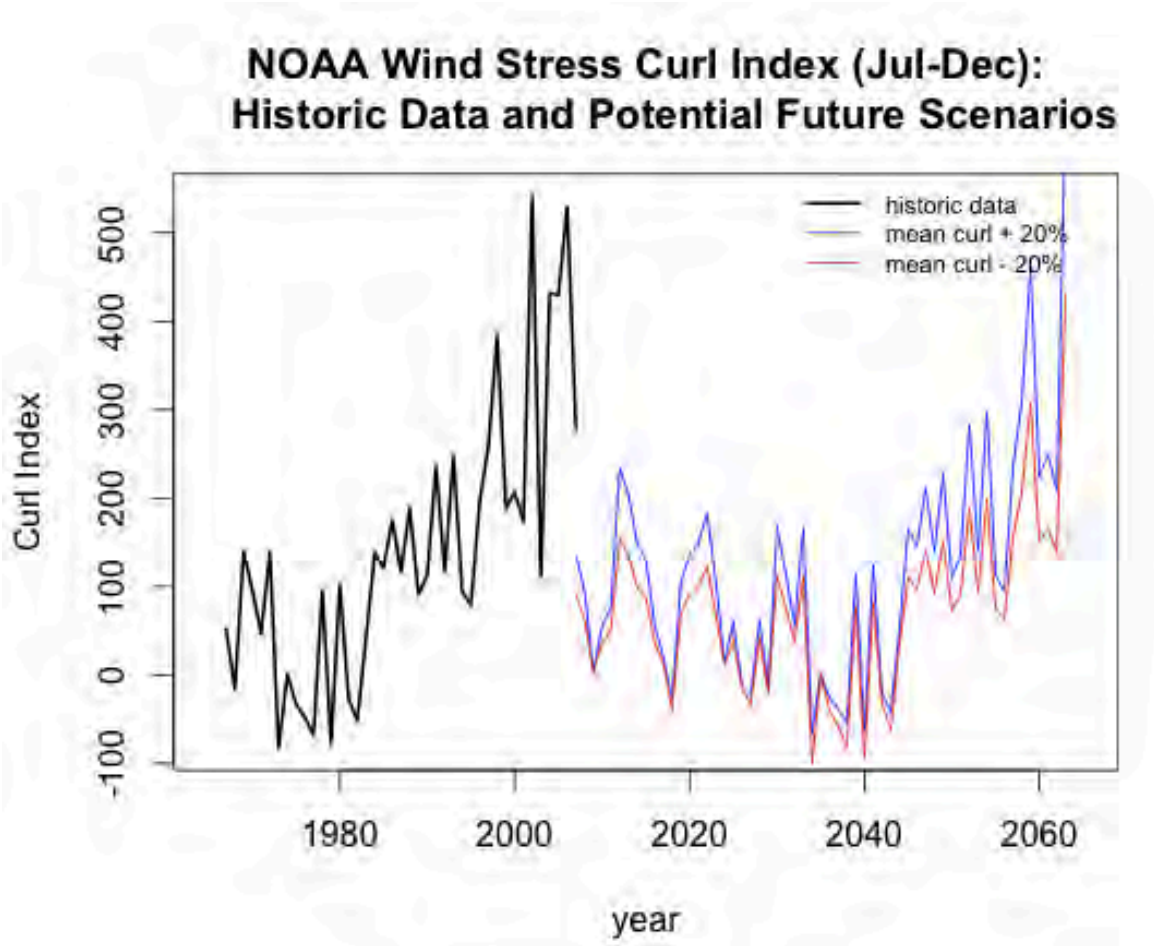

Figure B.11. NOAA wind stress curl index averaged over July-December: historic data for 1967-2007 and potential scenario values. Potential scenario values were generated by increasing (+20%) or decreasing (-20%) curl data from 1946-2002 according to the equations below, then projecting the values onto 2007-2063:

Curl + 20% = historic curl + abs value(historic curl) * 0.2

Curl – 20% = historic curl – abs value(historic curl) * 0.2

Curl index trajectories from 1967-2063 suggest a long-term autocorrelation pattern. Because we did not have compelling reasons to believe that future curl values would follow the same pattern as historic values, we set the standardized curl projections for future scenarios to 0.

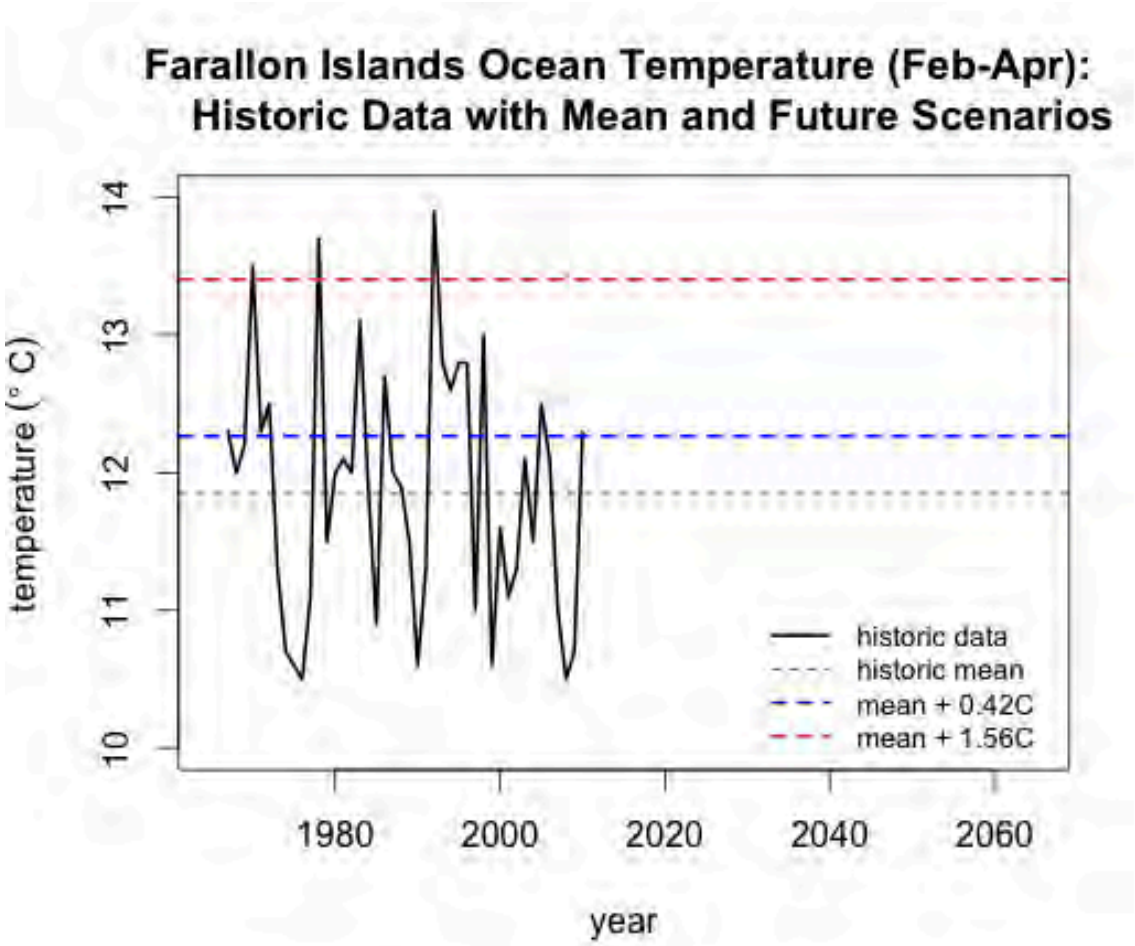

2447

2448 **Figure B.12.** Ocean temperature at the Farallon Islands averaged over February-April:
2449 historic data with mean for 1967-2010, and two climate projections: mean +0.42° C (=0.75°
2450 F, the average temperature increase for OCAP Study 9.2), and mean +1.56° C (=2.8° F, the
2451 average temperature increase for OCAP Study 9.5).

2452

2453
2454

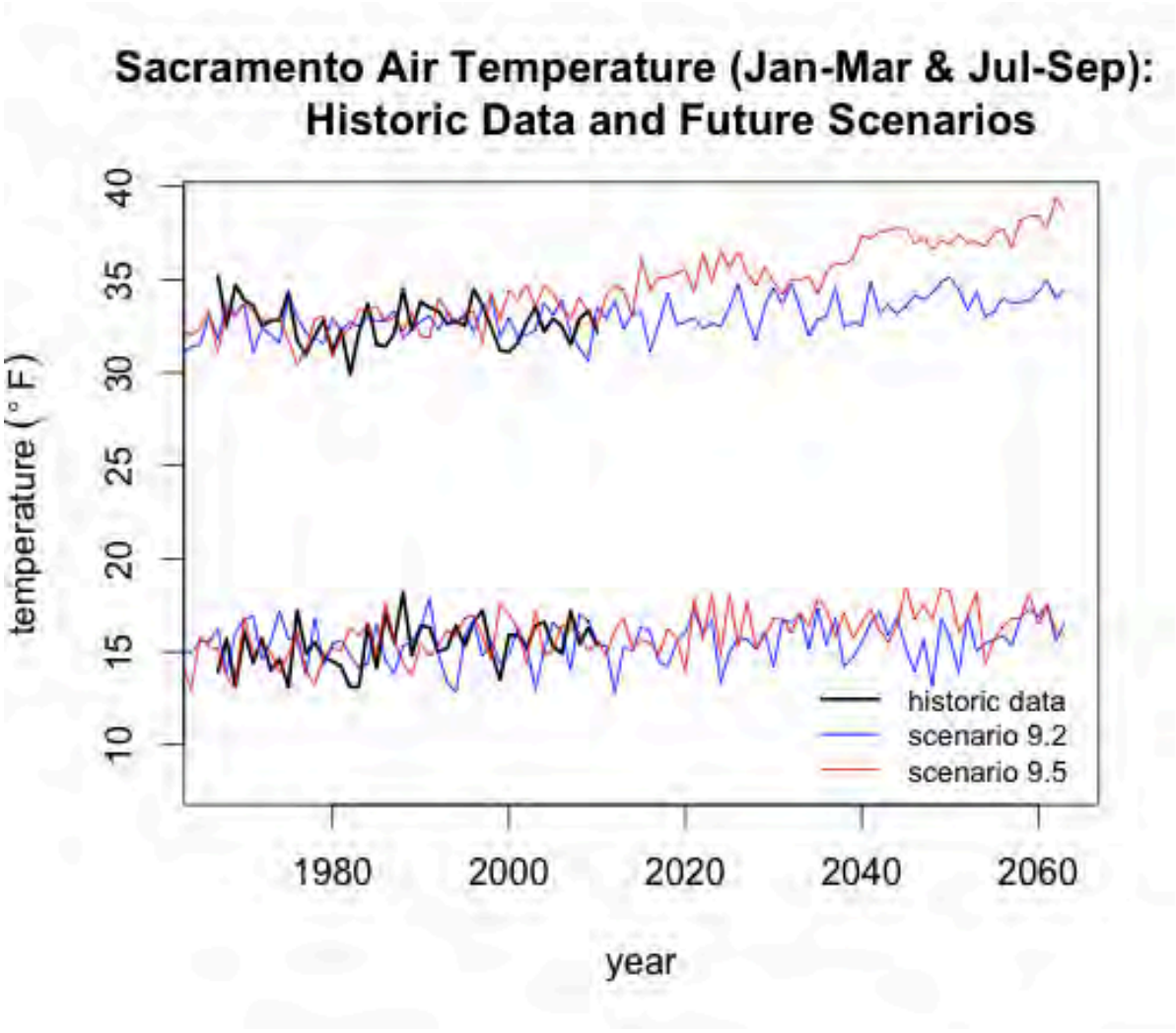

2455

2456 **Figure B.13.** Sacramento air temperature averaged over spring months (January-March,
2457 bottom lines) and summer months (July-September, top lines): historic data for 1967-2010,
2458 and future climate change predictions based on CMIP3 climate projections. CMIP3 air
2459 temperature predictions for the model cell over Sacramento were adjusted by + 4.55° F for
2460 the spring, and + 8.82° F for the summer, to spatially downscale climate projections from
2461 1967-2010 to match the range of historic Sacramento air temperature data.

2462

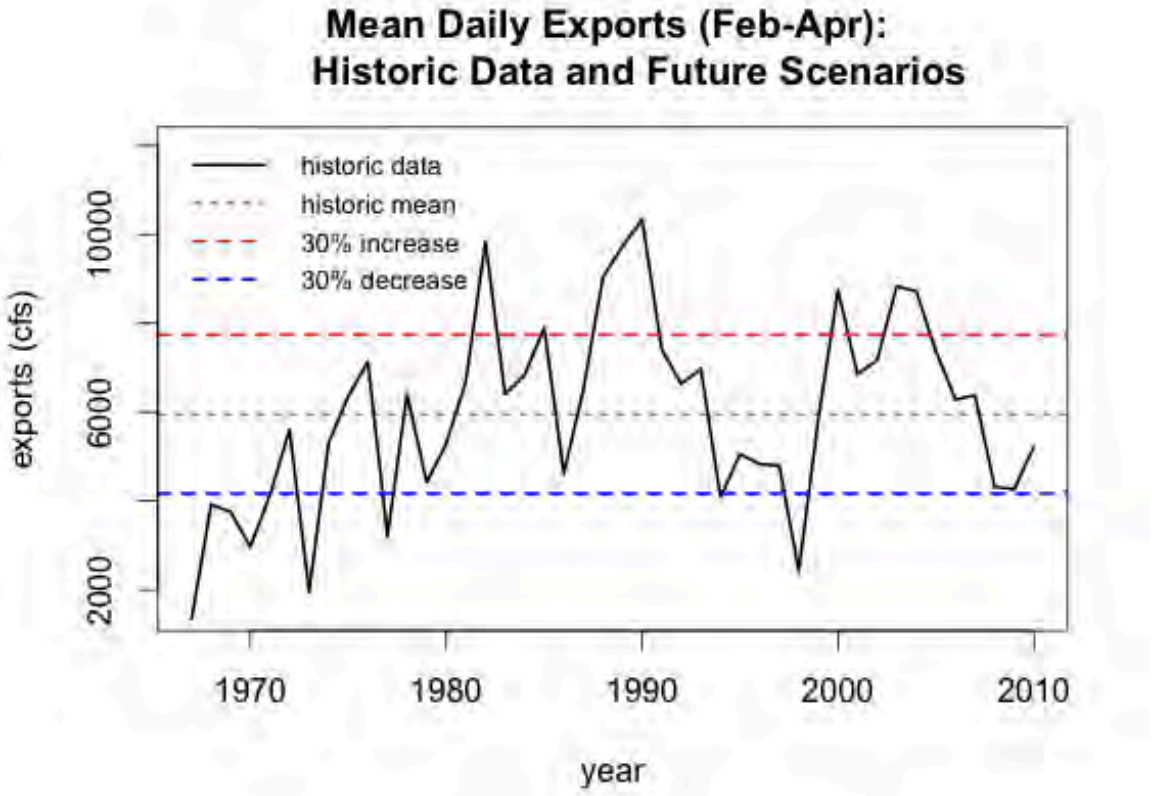

2463

2464 **Figure B.14.** Mean daily exports (cfs) averaged annually from February-April: historic data
2465 and future scenarios. Scenarios represent the following options: mean exports (1967-2010),
2466 zero exports, mean exports + 30%, mean exports - 30%.

2467

2468

2469
2470

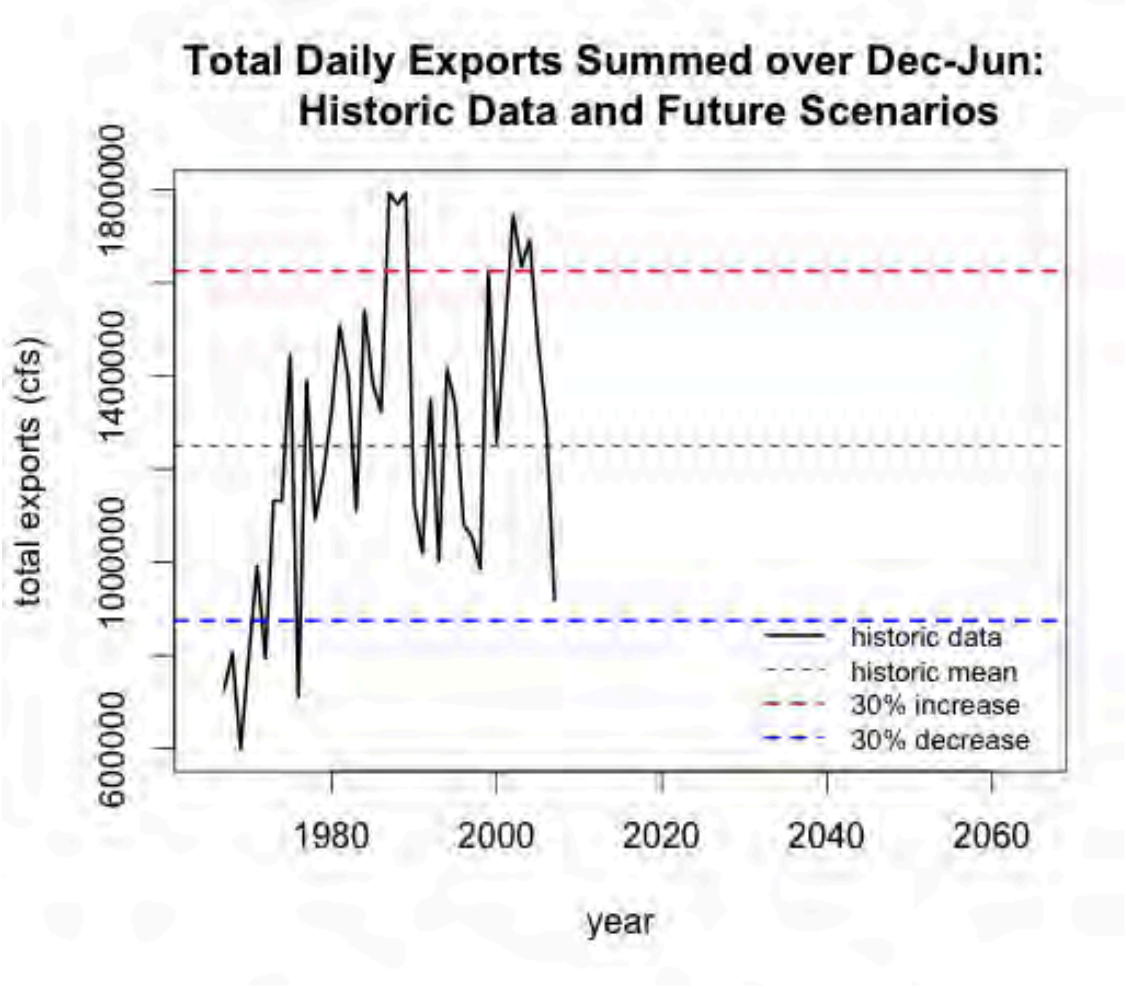

Figure B.15. Total daily exports summed over December-June: historic data and future scenarios. Scenarios represent the following options: mean total exports (1967-2010), zero exports, mean total exports + 30%, mean total exports - 30%.

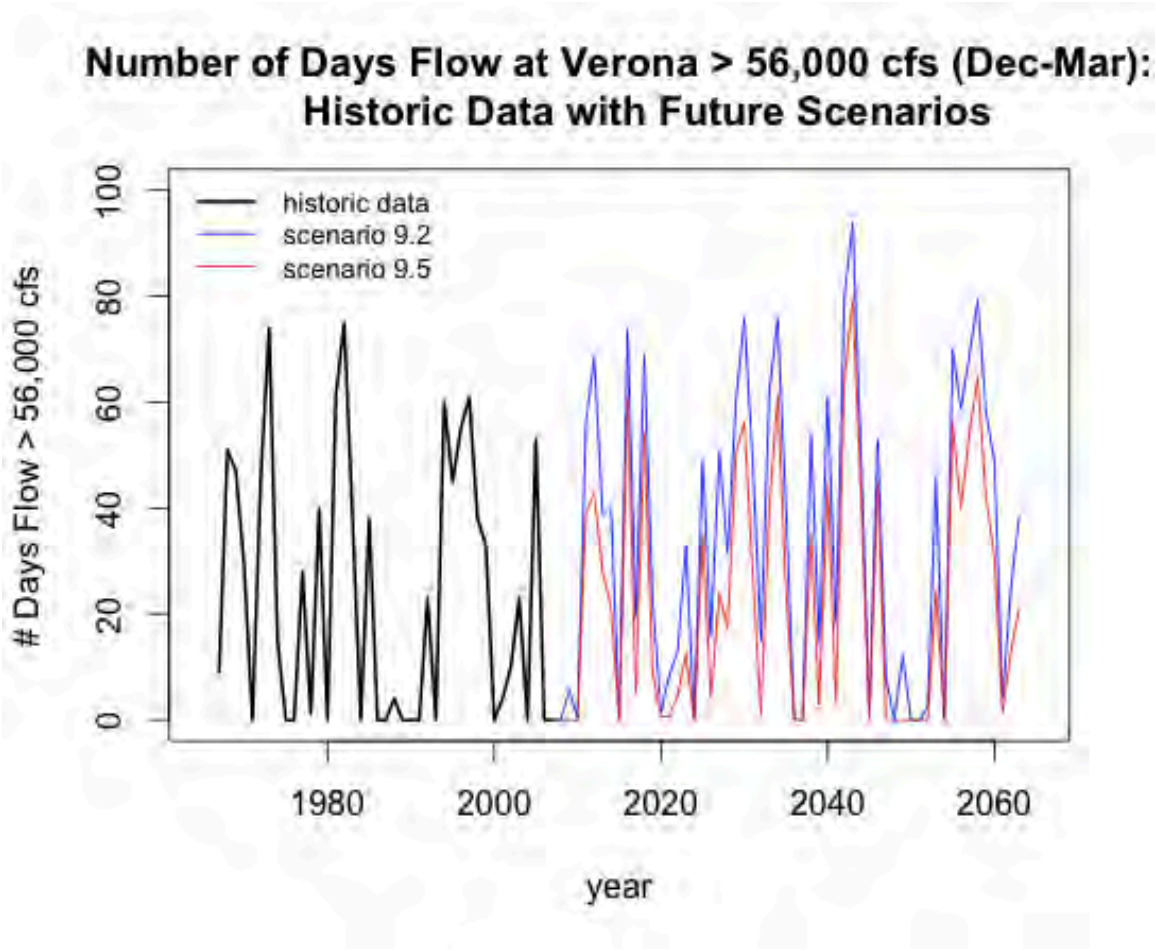

Figure B.16. Total number of days from December-March that Sacramento River flow at Verona exceeds 56,000 cfs: historic data from 1967-2007 and climate change scenarios 9.2 and 9.5. Climate change scenario values were obtained using Verona flow predictions (at C160) from CalSim-II OCAP Study 9.2 and 9.5 for 1946-2002 averaged over December-March, and adjusting these values per the linear model:

$$\#\text{ Days flow} > 56{,}000 = -25.19 + \text{CalSim-II flow at Verona} * 0.001646$$

to correlate them to the number of days that flow exceeds 56,000 cfs. The 1946-2002 climate change scenario predictions were then projected forward to 2007-2063.

TABLES

Table B.1. Scenario list with values drawn for each category of covariate.

	OCAP Study	Upwelling	Farallon Temp	PDO Index	Exports
Scenario 1	9.2	+ 10%	+ 0.42° C	- then +	Mean Level
Scenario 2	9.2	- 20%	+ 1.56° C	+ then -	Mean Level
Scenario 3	9.2	+ 10%	+ 0.42° C	- then +	Zero
Scenario 4	9.2	- 20%	+ 1.56° C	+ then -	Zero
Scenario 5	9.2	+ 10%	+ 0.42° C	- then +	Mean + 30%
Scenario 6	9.2	- 20%	+ 1.56° C	+ then -	Mean + 30%
Scenario 7	9.2	+ 10%	+ 0.42° C	- then +	Mean - 30%
Scenario 8	9.2	- 20%	+ 1.56° C	+ then -	Mean - 30%
Scenario 9	9.5	+ 10%	+ 0.42° C	- then +	Mean Level
Scenario 10	9.5	- 20%	+ 1.56° C	+ then -	Mean Level
Scenario 11	9.5	+ 10%	+ 0.42° C	- then +	Zero
Scenario 12	9.5	- 20%	+ 1.56° C	+ then -	Zero
Scenario 13	9.5	+ 10%	+ 0.42° C	- then +	Mean + 30%
Scenario 14	9.5	- 20%	+ 1.56° C	+ then -	Mean + 30%
Scenario 15	9.5	+ 10%	+ 0.42° C	- then +	Mean - 30%
Scenario 16	9.5	- 20%	+ 1.56° C	+ then -	Mean - 30%

Table B.2A. Fall and spring covariate values for Sacramento air temperature, channel depletion and smolt size at Chipps Island.

	Sacramento Air Temp (°F, Jan-Mar)		Sacramento Air Temp (°F, Jul-Sep)		Channel Depletion (cfs, Mar-May)	Size at Chipps Island (mm, Jan)
Year	Study 9.2	Study 9.5	Study 9.2	Study 9.5	Mean	Mean
2007	14.0	16.3	32.1	32.9	521	94.1
2008	17.1	16.0	31.3	34.1	521	94.1
2009	16.7	15.0	30.6	33.2	521	94.1
2010	15.5	15.6	33.5	32.5	521	94.1
2011	15.3	14.8	32.9	34.1	521	94.1
2012	12.8	16.1	33.9	34.7	521	94.1
2013	15.3	16.8	32.3	34.4	521	94.1
2014	15.0	15.2	33.2	33.0	521	94.1
2015	16.4	15.6	33.2	36.1	521	94.1
2016	16.1	15.5	31.1	34.5	521	94.1
2017	14.5	14.8	32.6	35.1	521	94.1
2018	14.2	16.2	34.3	35.1	521	94.1
2019	15.5	15.7	32.6	35.3	521	94.1
2020	16.0	13.9	32.7	35.6	521	94.1
2021	17.3	17.8	32.9	34.3	521	94.1
2022	16.0	15.7	32.4	36.4	521	94.1
2023	16.7	18.1	32.7	34.9	521	94.1
2024	13.3	14.8	32.5	36.5	521	94.1
2025	15.0	18.1	33.5	35.6	521	94.1
2026	15.8	15.3	34.8	36.5	521	94.1
2027	15.7	17.7	32.9	35.3	521	94.1
2028	15.2	15.2	31.7	34.7	521	94.1
2029	16.1	15.8	33.6	35.6	521	94.1
2030	14.2	16.8	34.5	34.9	521	94.1
2031	16.7	16.8	33.7	34.2	521	94.1
2032	16.6	16.0	34.8	35.0	521	94.1
2033	17.0	17.0	33.5	35.0	521	94.1
2034	15.1	16.4	32.0	35.2	521	94.1
2035	17.3	17.8	32.9	34.2	521	94.1
2036	15.4	17.3	33.0	35.3	521	94.1
2037	16.8	15.8	34.6	35.9	521	94.1
2038	14.2	17.1	32.4	35.8	521	94.1
2039	14.7	15.7	32.8	36.1	521	94.1
2040	15.5	16.5	32.5	37.3	521	94.1

Table B.2A (continued). Fall and spring covariate values for Sacramento air temperature, channel depletion and smolt size at Chipps Island.

	Sacramento Air Temp (°F, Jan-Mar)		Sacramento Air Temp (°F, Jul-Sep)		Channel Depletion (cfs, Mar-May)	Size at Chipps Island (mm, Jan)
Year	Study 9.2	Study 9.5	Study 9.2	Study 9.5	Mean	Mean
2041	16.5	17.3	34.9	37.2	521	94.1
2042	17.1	16.1	33.2	37.6	521	94.1
2043	15.9	15.5	33.6	37.6	521	94.1
2044	16.9	16.4	33.2	37.8	521	94.1
2045	15.2	18.5	33.5	37.7	521	94.1
2046	13.9	16.8	34.2	36.9	521	94.1
2047	15.7	17.5	33.9	37.3	521	94.1
2048	13.2	16.7	34.3	36.6	521	94.1
2049	16.8	18.4	34.9	37.1	521	94.1
2050	15.7	18.2	35.1	36.9	521	94.1
2051	13.8	16.0	34.5	37.4	521	94.1
2052	17.0	16.9	33.4	37.0	521	94.1
2053	15.0	18.2	34.3	37.0	521	94.1
2054	15.4	14.3	33.0	36.8	521	94.1
2055	15.6	15.7	33.3	37.5	521	94.1
2056	15.9	16.4	34.0	37.7	521	94.1
2057	15.3	16.8	33.7	36.7	521	94.1
2058	16.8	16.8	33.8	38.2	521	94.1
2059	17.3	18.1	33.9	38.4	521	94.1
2060	16.9	16.5	34.3	38.4	521	94.1
2061	17.5	17.4	35.0	37.8	521	94.1
2062	15.6	16.1	34.0	39.4	521	94.1
2063	16.6	16.0	34.4	38.7	521	94.1

Table B.2B. Fall and spring covariate values for upwelling index, wind stress curl and PDO index.

	Upwelling Index (36N, 122W, Apr-Jun)		NOAA Wind Stress Curl Index (39N, 125W, Jul-Dec)	PDO Index (Jan-May)	
Year	Up 10%	Down 20%	Mean	+ then -	- then +
2007	199	145	151	0.10	-0.38
2008	139	101	151	0.40	0.24
2009	116	84	151	0.70	-0.49
2010	136	99	151	0.33	-1.64
2011	169	123	151	0.86	-1.92
2012	144	105	151	0.61	-1.02
2013	158	115	151	0.75	-1.03
2014	195	142	151	0.72	-0.26
2015	177	129	151	-0.23	-0.95
2016	318	231	151	1.14	-1.15
2017	256	186	151	0.29	-2.27
2018	220	160	151	-0.02	-0.50
2019	173	126	151	1.01	0.69
2020	320	233	151	0.76	-0.10
2021	189	138	151	1.61	0.32
2022	186	135	151	0.12	0.40
2023	200	145	151	0.16	-1.18
2024	157	114	151	0.49	-0.42
2025	314	229	151	2.07	-0.80
2026	239	174	151	2.15	-0.48
2027	239	174	151	0.74	-0.52
2028	223	162	151	0.32	-0.74
2029	329	239	151	0.16	-0.64
2030	240	174	151	-0.24	-0.67
2031	267	194	151	-0.38	0.46
2032	263	191	151	0.24	-1.69
2033	205	149	151	-0.49	-1.83
2034	270	196	151	-1.64	-0.60
2035	292	213	151	-1.92	-0.91
2036	262	190	151	-1.02	-0.88
2037	209	152	151	-1.03	-1.10
2038	192	139	151	-0.26	0.82
2039	179	130	151	-0.95	1.06
2040	282	205	151	-1.15	0.07

Table B.2B (continued). Fall and spring covariate values for upwelling index, wind stress curl and PDO index.

	Upwelling Index (36N, 122W, Apr-Jun)		NOAA Wind Stress Curl Index (39N, 125W, Jul-Dec)	PDO Index (Jan-May)	
Year	Up 10%	Down 20%	Mean	+ then -	- then +
2041	276	201	151	-2.27	1.00
2042	297	216	151	-0.50	1.25
2043	179	130	151	0.69	-0.01
2044	180	131	151	-0.10	1.50
2045	309	225	151	0.32	1.46
2046	212	154	151	0.40	0.59
2047	206	150	151	-1.18	1.52
2048	191	139	151	-0.42	1.95
2049	165	120	151	-0.80	1.15
2050	193	140	151	-0.48	-0.53
2051	186	135	151	-0.52	-0.17
2052	270	196	151	-0.74	-1.09
2053	169	123	151	-0.64	0.66
2054	173	126	151	-0.67	0.87
2055	248	180	151	0.46	0.98
2056	185	134	151	-1.69	0.60
2057	222	161	151	-1.83	1.20
2058	248	180	151	-0.60	0.81
2059	157	114	151	-0.91	1.27
2060	378	275	151	-0.88	-0.48
2061	195	142	151	-1.10	-0.45
2062	285	207	151	0.82	0.15
2063	339	246	151	1.06	-0.35

2515 **Table B.2C.** Fall and spring covariate values for mean daily exports.

2516

	Mean Daily Exports (cfs, Feb-Apr)			
Year	Mean	None	Up 30%	Down 30%
2007	5954	0	7740	4168
2008	5954	0	7740	4168
2009	5954	0	7740	4168
2010	5954	0	7740	4168
2011	5954	0	7740	4168
2012	5954	0	7740	4168
2013	5954	0	7740	4168
2014	5954	0	7740	4168
2015	5954	0	7740	4168
2016	5954	0	7740	4168
2017	5954	0	7740	4168
2018	5954	0	7740	4168
2019	5954	0	7740	4168
2020	5954	0	7740	4168
2021	5954	0	7740	4168
2022	5954	0	7740	4168
2023	5954	0	7740	4168
2024	5954	0	7740	4168
2025	5954	0	7740	4168
2026	5954	0	7740	4168
2027	5954	0	7740	4168
2028	5954	0	7740	4168
2029	5954	0	7740	4168
2030	5954	0	7740	4168
2031	5954	0	7740	4168
2032	5954	0	7740	4168
2033	5954	0	7740	4168
2034	5954	0	7740	4168
2035	5954	0	7740	4168
2036	5954	0	7740	4168
2037	5954	0	7740	4168
2038	5954	0	7740	4168
2039	5954	0	7740	4168
2040	5954	0	7740	4168

2517

2518
2519

2520 **Table B.2C (continued).** Fall and spring covariate values for mean daily exports.

2521

	Mean Daily Exports (cfs, Feb-Apr)			
Year	Mean	None	Up 30%	Down 30%
2041	5954	0	7740	4168
2042	5954	0	7740	4168
2043	5954	0	7740	4168
2044	5954	0	7740	4168
2045	5954	0	7740	4168
2046	5954	0	7740	4168
2047	5954	0	7740	4168
2048	5954	0	7740	4168
2049	5954	0	7740	4168
2050	5954	0	7740	4168
2051	5954	0	7740	4168
2052	5954	0	7740	4168
2053	5954	0	7740	4168
2054	5954	0	7740	4168
2055	5954	0	7740	4168
2056	5954	0	7740	4168
2057	5954	0	7740	4168
2058	5954	0	7740	4168
2059	5954	0	7740	4168
2060	5954	0	7740	4168
2061	5954	0	7740	4168
2062	5954	0	7740	4168
2063	5954	0	7740	4168

2522

2523

2524
2525

Table B.2D. Fall and spring covariate values for Freeport sediment concentration, Keswick discharge and Deer Creek discharge.

	Freeport Sediment Concentration (mg/L, Feb-Apr)		Keswick Discharge (cfs, Jan-Mar)		Deer Creek Discharge (cfs, Oct-Dec)	
Year	Study 9.2	Study 9.5	Study 9.2	Study 9.5	Study 9.2	Study 9.5
2007	39.4	38.0	5243	5300	263	263
2008	39.0	36.0	3434	3304	199	199
2009	47.7	35.6	3641	3428	171	171
2010	59.0	52.4	7253	4820	127	127
2011	61.4	49.0	3250	3250	725	725
2012	79.7	75.7	9926	8546	631	631
2013	147.8	123.3	14349	12033	442	442
2014	50.6	44.4	13435	11368	230	230
2015	120.5	86.0	16243	11469	303	303
2016	30.0	24.3	3953	3250	1034	1034
2017	91.6	87.0	20651	18332	192	192
2018	79.6	45.9	10356	4860	370	370
2019	168.1	155.8	32284	29055	196	196
2020	63.6	52.3	11435	9122	142	142
2021	47.2	41.4	3250	3250	333	333
2022	51.4	39.9	7469	3250	276	276
2023	69.0	48.8	7814	3994	730	730
2024	131.0	108.6	7531	6533	252	252
2025	32.2	26.3	4428	3992	1016	1016
2026	69.7	71.0	9841	8544	275	275
2027	53.1	41.2	9921	7004	525	525
2028	113.4	84.9	12309	9262	207	207
2029	90.5	70.8	9851	7587	449	449
2030	127.2	110.0	19597	12796	564	564
2031	87.1	74.1	25746	21687	683	683
2032	76.1	57.8	13406	11874	233	233
2033	57.3	38.2	9342	4974	355	355
2034	106.2	87.0	15483	12171	1025	1025
2035	137.0	112.5	28265	24483	238	238
2036	121.7	90.0	14762	11115	229	229
2037	33.0	26.7	3250	4583	135	135
2038	20.8	19.5	4865	3933	213	213
2039	126.1	91.5	15667	6976	144	144
2040	67.2	42.1	3896	3250	367	367

Table B.2D (continued). Fall and spring covariate values for Freeport sediment concentration, Keswick discharge and Deer Creek discharge.

	Freeport Sediment Concentration (mg/L, Feb-Apr)		Keswick Discharge (cfs, Jan-Mar)		Deer Creek Discharge (cfs, Oct-Dec)	
Year	Study 9.2	Study 9.5	Study 9.2	Study 9.5	Study 9.2	Study 9.5
2041	104.3	89.4	19408	14964	217	217
2042	60.7	39.8	7729	3740	1069	1069
2043	164.6	155.7	16139	14051	591	591
2044	159.0	147.5	36756	33072	1237	1237
2045	60.7	61.4	8095	7268	358	358
2046	37.1	28.7	3250	3250	245	245
2047	130.5	123.5	26225	17841	179	179
2048	53.8	39.3	5643	3915	221	221
2049	24.6	23.4	4105	4498	177	177
2050	79.5	56.3	6010	3250	191	191
2051	28.5	25.4	3250	3306	111	111
2052	38.8	32.7	4180	3250	111	111
2053	46.9	40.3	4337	3320	187	187
2054	126.9	76.3	11370	3250	192	192
2055	41.6	31.4	3618	3701	180	180
2056	149.1	115.9	26699	19849	297	297
2057	133.7	114.9	18602	16308	903	903
2058	70.5	56.5	15811	13367	292	292
2059	147.6	130.2	33555	26125	470	470
2060	120.2	107.2	16191	14408	216	216
2061	118.0	93.0	20572	13863	173	173
2062	44.3	37.5	3250	3250	361	361
2063	49.3	39.9	7795	4871	576	576

2539 **Table B.2E.** Fall and spring covariate values for export/inflow ratios.

2540

	Mean Daily Export/Inflow Ratio (Mar-May), Inflows for Study 9.2, Various Export Values				Mean Daily Export/Inflow Ratio (Mar-May), Inflows for Study 9.5, Various Export Values			
Year	E=Mean	Zero	Mean+30%	Mean-30%	E=Mean	Zero	Mean+30%	Mean-30%
2007	0.22	0	0.29	0.15	0.27	0	0.35	0.19
2008	0.26	0	0.34	0.18	0.32	0	0.41	0.22
2009	0.16	0	0.20	0.11	0.24	0	0.31	0.17
2010	0.16	0	0.20	0.11	0.20	0	0.26	0.14
2011	0.18	0	0.23	0.12	0.25	0	0.33	0.18
2012	0.19	0	0.24	0.13	0.21	0	0.28	0.15
2013	0.06	0	0.07	0.04	0.08	0	0.10	0.06
2014	0.17	0	0.22	0.12	0.22	0	0.29	0.15
2015	0.11	0	0.14	0.07	0.16	0	0.21	0.11
2016	0.33	0	0.42	0.23	0.40	0	0.52	0.28
2017	0.12	0	0.16	0.08	0.16	0	0.20	0.11
2018	0.15	0	0.19	0.10	0.22	0	0.29	0.15
2019	0.05	0	0.06	0.03	0.07	0	0.09	0.05
2020	0.27	0	0.35	0.19	0.29	0	0.37	0.20
2021	0.27	0	0.35	0.19	0.32	0	0.42	0.22
2022	0.29	0	0.37	0.20	0.36	0	0.47	0.25
2023	0.22	0	0.29	0.16	0.27	0	0.35	0.19
2024	0.09	0	0.11	0.06	0.11	0	0.15	0.08
2025	0.30	0	0.39	0.21	0.42	0	0.54	0.29
2026	0.14	0	0.19	0.10	0.14	0	0.18	0.10
2027	0.21	0	0.28	0.15	0.27	0	0.36	0.19
2028	0.07	0	0.09	0.05	0.10	0	0.13	0.07
2029	0.20	0	0.26	0.14	0.24	0	0.31	0.17
2030	0.06	0	0.08	0.04	0.09	0	0.11	0.06
2031	0.18	0	0.23	0.12	0.20	0	0.26	0.14
2032	0.12	0	0.15	0.08	0.19	0	0.24	0.13
2033	0.21	0	0.27	0.15	0.27	0	0.35	0.19
2034	0.12	0	0.16	0.08	0.17	0	0.23	0.12
2035	0.07	0	0.08	0.05	0.08	0	0.10	0.05
2036	0.09	0	0.11	0.06	0.12	0	0.16	0.09
2037	0.30	0	0.39	0.21	0.40	0	0.52	0.28
2038	0.55	0	0.71	0.38	0.55	0	0.71	0.38
2039	0.08	0	0.10	0.06	0.11	0	0.14	0.08
2040	0.15	0	0.19	0.10	0.24	0	0.31	0.17

2541

2542
2543

Table B.2E (continued). Fall and spring covariate values for export/inflow ratios.

	Mean Daily Export/Inflow Ratio (Mar-May), Inflows for Study 9.2, Various Export Values				Mean Daily Export/Inflow Ratio (Mar-May), Inflows for Study 9.5, Various Export Values			
Year	E=Mean	Zero	Mean+30%	Mean-30%	E=Mean	Zero	Mean+30%	Mean-30%
2041	0.12	0	0.15	0.08	0.16	0	0.21	0.11
2042	0.20	0	0.26	0.14	0.30	0	0.39	0.21
2043	0.05	0	0.06	0.03	0.06	0	0.08	0.04
2044	0.03	0	0.04	0.02	0.04	0	0.05	0.03
2045	0.18	0	0.24	0.13	0.18	0	0.24	0.13
2046	0.26	0	0.34	0.18	0.33	0	0.43	0.23
2047	0.06	0	0.08	0.04	0.09	0	0.11	0.06
2048	0.22	0	0.28	0.15	0.30	0	0.39	0.21
2049	0.42	0	0.55	0.30	0.45	0	0.58	0.31
2050	0.12	0	0.15	0.08	0.17	0	0.22	0.12
2051	0.40	0	0.52	0.28	0.45	0	0.59	0.32
2052	0.25	0	0.33	0.18	0.30	0	0.40	0.21
2053	0.32	0	0.42	0.23	0.36	0	0.47	0.25
2054	0.09	0	0.11	0.06	0.17	0	0.22	0.12
2055	0.30	0	0.39	0.21	0.43	0	0.55	0.30
2056	0.03	0	0.04	0.02	0.05	0	0.06	0.03
2057	0.07	0	0.10	0.05	0.11	0	0.14	0.07
2058	0.20	0	0.26	0.14	0.22	0	0.29	0.16
2059	0.06	0	0.08	0.04	0.08	0	0.10	0.06
2060	0.11	0	0.14	0.08	0.14	0	0.18	0.10
2061	0.11	0	0.14	0.08	0.15	0	0.20	0.11
2062	0.24	0	0.32	0.17	0.31	0	0.40	0.22
2063	0.24	0	0.31	0.17	0.31	0	0.41	0.22

Table B.3A. Winter covariate values for total exports, upwelling index and Bend Bridge flows.

	Total Exports (Σ daily exports (cfs), Dec-Jun)				Upwelling Index (36N, 122W, Apr-Jun)		Bend Bridge Monthly Minimum Flow (cfs, Aug-Nov)	
Year	Mean	Zero	Up 30%	Down 30%	Up 10%	Down 20%	Study 9.2	Study 9.5
2007	1250154	0	1625201	875108	199	145	5975	4968
2008	1250154	0	1625201	875108	139	101	4616	4309
2009	1250154	0	1625201	875108	116	84	6284	4737
2010	1250154	0	1625201	875108	136	99	5791	4441
2011	1250154	0	1625201	875108	169	123	5804	4343
2012	1250154	0	1625201	875108	144	105	5881	5458
2013	1250154	0	1625201	875108	158	115	7166	5699
2014	1250154	0	1625201	875108	195	142	10262	6713
2015	1250154	0	1625201	875108	177	129	6383	6500
2016	1250154	0	1625201	875108	318	231	5261	4191
2017	1250154	0	1625201	875108	256	186	7764	6807
2018	1250154	0	1625201	875108	220	160	8409	4863
2019	1250154	0	1625201	875108	173	126	7717	7413
2020	1250154	0	1625201	875108	320	233	5722	5274
2021	1250154	0	1625201	875108	189	138	5521	5071
2022	1250154	0	1625201	875108	186	135	6478	5026
2023	1250154	0	1625201	875108	200	145	6631	4723
2024	1250154	0	1625201	875108	157	114	8097	7236
2025	1250154	0	1625201	875108	314	229	5008	4950
2026	1250154	0	1625201	875108	239	174	5264	5109
2027	1250154	0	1625201	875108	239	174	5638	5641
2028	1250154	0	1625201	875108	223	162	7568	5882
2029	1250154	0	1625201	875108	329	239	5454	4745
2030	1250154	0	1625201	875108	240	174	7893	5639
2031	1250154	0	1625201	875108	267	194	5985	5977
2032	1250154	0	1625201	875108	263	191	9251	6681
2033	1250154	0	1625201	875108	205	149	5422	5516
2034	1250154	0	1625201	875108	270	196	6129	5944
2035	1250154	0	1625201	875108	292	213	9035	5224
2036	1250154	0	1625201	875108	262	190	9760	5488
2037	1250154	0	1625201	875108	209	152	4699	5090
2038	1250154	0	1625201	875108	192	139	4457	4557
2039	1250154	0	1625201	875108	179	130	6642	5340
2040	1250154	0	1625201	875108	282	205	6591	4465

Table B.3A (continued). Winter covariate values for total exports, upwelling index and Bend Bridge flows.

	Total Exports (Σ daily exports (cfs), Dec-Jun)				Upwelling Index (36N, 122W, Apr-Jun)		Bend Bridge Monthly Minimum Flow (cfs, Aug-Nov)	
Year	Mean	Zero	Up 30%	Down 30%	Up 10%	Down 20%	Study 9.2	Study 9.5
2041	1250154	0	1625201	875108	276	201	5831	4908
2042	1250154	0	1625201	875108	297	216	6375	5114
2043	1250154	0	1625201	875108	179	130	11342	3907
2044	1250154	0	1625201	875108	180	131	11658	10590
2045	1250154	0	1625201	875108	309	225	5762	5427
2046	1250154	0	1625201	875108	212	154	6286	5278
2047	1250154	0	1625201	875108	206	150	4686	4327
2048	1250154	0	1625201	875108	191	139	6023	4359
2049	1250154	0	1625201	875108	165	120	6061	4687
2050	1250154	0	1625201	875108	193	140	5220	3852
2051	1250154	0	1625201	875108	186	135	5289	3963
2052	1250154	0	1625201	875108	270	196	3900	4303
2053	1250154	0	1625201	875108	169	123	4743	4086
2054	1250154	0	1625201	875108	173	126	6268	5149
2055	1250154	0	1625201	875108	248	180	6027	4313
2056	1250154	0	1625201	875108	185	134	6689	6797
2057	1250154	0	1625201	875108	222	161	9018	4929
2058	1250154	0	1625201	875108	248	180	5361	5755
2059	1250154	0	1625201	875108	157	114	12261	10749
2060	1250154	0	1625201	875108	378	275	10876	6441
2061	1250154	0	1625201	875108	195	142	8025	6568
2062	1250154	0	1625201	875108	285	207	6552	4070
2063	1250154	0	1625201	875108	339	246	6536	4757

Table B.3B. Winter covariate values for number of days that Verona flow > 56,000 cfs, Bend Bridge water temperatures, Farallon Island ocean temperatures, and proportion of time that the Delta Cross Channel gates are open.

	# Days (Dec-Mar) that Verona Flow > 56,000 cfs		Bend Bridge Average Water Temperature (°C, Jul-Sep)		Farallon Islands Ocean Temperature (°C, Feb-Apr)		Prop. of Time Delta Cross Channel Gates are Open (Dec-Mar)
Year	Study 9.2	Study 9.5	Study 9.2	Study 9.5	+ 0.42° C	+ 1.56° C	Mean
2007	0	0	12.5	13.8	12.3	13.4	0
2008	0	0	13.3	15.4	12.3	13.4	0
2009	6	0	14.0	14.9	12.3	13.4	0
2010	0	0	13.3	15.4	12.3	13.4	0
2011	56	39	13.4	15.6	12.3	13.4	0
2012	68	43	13.2	14.4	12.3	13.4	0
2013	39	28	13.7	15.5	12.3	13.4	0
2014	40	21	13.6	15.0	12.3	13.4	0
2015	0	0	13.6	14.6	12.3	13.4	0
2016	74	60	13.7	15.6	12.3	13.4	0
2017	20	5	13.0	14.3	12.3	13.4	0
2018	69	54	13.7	15.3	12.3	13.4	0
2019	23	9	13.9	14.7	12.3	13.4	0
2020	2	1	14.1	15.6	12.3	13.4	0
2021	8	1	13.6	15.4	12.3	13.4	0
2022	13	4	13.3	15.0	12.3	13.4	0
2023	33	12	13.3	14.7	12.3	13.4	0
2024	0	0	13.8	15.0	12.3	13.4	0
2025	49	35	13.6	15.2	12.3	13.4	0
2026	16	4	13.5	14.9	12.3	13.4	0
2027	51	24	13.2	14.8	12.3	13.4	0
2028	32	17	13.3	14.5	12.3	13.4	0
2029	60	50	14.0	15.2	12.3	13.4	0
2030	76	56	13.2	14.7	12.3	13.4	0
2031	49	28	13.6	15.0	12.3	13.4	0
2032	15	1	13.7	15.3	12.3	13.4	0
2033	62	40	13.4	15.0	12.3	13.4	0
2034	76	61	13.8	14.6	12.3	13.4	0
2035	40	25	13.1	15.5	12.3	13.4	0
2036	0	0	13.5	15.2	12.3	13.4	0
2037	0	0	14.2	15.2	12.3	13.4	0
2038	54	35	16.6	19.2	12.3	13.4	0
2039	14	3	13.4	14.4	12.3	13.4	0
2040	61	45	14.1	16.0	12.3	13.4	0

Table B.3B (continued). Winter covariate values for number of days that Verona flow > 56,000 cfs, Bend Bridge water temperatures, Farallon Island ocean temperatures, and proportion of time that the Delta Cross Channel gates are open.

	# Days (Dec-Mar) that Verona Flow > 56,000 cfs		Bend Bridge Average Water Temperature (°C, Jul-Sep)		Farallon Islands Ocean Temperature (°C, Feb-Apr)		Prop. of Time Delta Cross Channel Gates are Open (Dec-Mar)
year	Study 9.2	Study 9.5	Study 9.2	Study 9.5	+ 0.42° C	+ 1.56° C	Mean
2041	18	4	13.6	14.9	12.3	13.4	0
2042	80	64	14.3	15.6	12.3	13.4	0
2043	94	79	13.3	15.1	12.3	13.4	0
2044	50	43	14.0	14.1	12.3	13.4	0
2045	2	0	14.2	15.8	12.3	13.4	0
2046	53	45	13.8	15.6	12.3	13.4	0
2047	8	0	14.2	15.6	12.3	13.4	0
2048	0	0	14.1	16.1	12.3	13.4	0
2049	12	0	14.2	17.3	12.3	13.4	0
2050	0	0	13.6	16.5	12.3	13.4	0
2051	0	0	14.0	18.0	12.3	13.4	0
2052	2	0	15.0	18.7	12.3	13.4	0
2053	46	24	14.6	19.7	12.3	13.4	0
2054	0	0	13.9	15.0	12.3	13.4	0
2055	70	56	14.4	16.5	12.3	13.4	0
2056	59	40	14.5	15.3	12.3	13.4	0
2057	69	54	14.2	15.5	12.3	13.4	0
2058	79	65	13.5	15.2	12.3	13.4	0
2059	58	42	14.6	14.7	12.3	13.4	0
2060	49	31	13.2	14.7	12.3	13.4	0
2061	4	1	14.8	15.9	12.3	13.4	0
2062	25	13	14.9	17.4	12.3	13.4	0
2063	39	21	15.1	17.0	12.3	13.4	0

APPENDIX C: GROWTH ANALYSIS AND MODELLING

In this appendix we provide a description of the methods we used to collect and analyze length information from various state and federal collection facilities in the Sacramento drainage. We assembled time series of lengths, both upstream and downstream, for both hatchery fish and combined hatchery and wild aggregates. Where possible, we used upstream and downstream lengths to obtain annual growth estimates. In the absence of a downstream growth measurement, we assembled a time series of downstream lengths. We performed regressions on growth and length estimates, evaluating impacts of environmental conditions on growth.

INTRODUCTION

The life-cycle modeling analysis in this project attempts to attribute variability in survival to environmental factors during different parts of the life history. Survival can be affected by the environment in complex ways, and can be mediated through biotic and abiotic processes. We posit that size can play a role in predicting survival, and that growth itself can be an indicator of survival as well. An obvious mechanism for size effects on survival would be that larger fish are less vulnerable to predation than smaller fish. A mechanism for growth being a predictor of survival would be that faster growing fish are likely to be experiencing better feeding conditions and bioenergetic advantages, and therefore should survive better.

In this appendix we look for relationships between environmental conditions and growth, but because growth requires two measurements (a capture and a recapture, or a release and recapture), we are not always able to get an estimate of a growth increment. Some length estimates obtained from survey data cannot be connected to later surveys, and therefore a growth estimate can't be derived from the measurements. An example of this occurs with rotary screw traps operating in tributaries, where juvenile size samples are obtained during rearing and migration. Those sizes are not directly comparable to later samples obtained downstream, because the downstream samples are aggregates of all the independent upstream sampled lengths. We might be able to document a pattern in upstream sizes over the years, but growth to the downstream measurement can't be inferred. We therefore treat size as a surrogate for growth, with the assumption that annual variability in juvenile size is in actual fact a measurement of annual variability in growth since all fish must at some point have emerged from the gravel at roughly the same sizes.

METHODS

We performed an analysis of length and growth patterns for Spring and Fall run Chinook in the Sacramento River in relation to environmental factors. We collected size at release and recapture data from state and federal agencies. We compiled records into average sizes at release for several different stock aggregates that provided adequate sample sizes for the years the data were available. In some case, it was possible to associate the length of a downstream recaptured fish with a known upstream release size to obtain a growth increment

estimate, but in other cases only the downstream size record was available. Upstream length records were obtained from hatchery release information, from screw traps operated in tributaries, and from seine surveys operated throughout the Sacramento drainage. The farthest downstream sizes were obtained from Chipps Island, where mid-water trawl surveys collected size information and recorded the race of the fish based on the presence of a CWT or a length based estimated based on the length of the fish at the time the sample was obtained.

Data compilation

Length data

The Pacific States Marine Fisheries Commission manages and supports the Regional Mark Processing Center (RMPC; http://www.rmpc.org/), which in turn manages the Regional Mark Information System (RMIS). Agencies and organizations throughout the Western United States report CWT data directly to the RMIS. The Delta Juvenile Fish Monitoring Program (DJFMP) was initiated in the 1970s and is managed by the US Fish and Wildlife Service (USFWS, 2014). The program has a stated objective to monitor the effects of water projects in the Bay Delta on juvenile Chinook.

The number of juvenile salmon leaving freshwater during the spring has been sampled annually since 1978 by means of mid-water trawling in the estuary near Chipps Island (Brandes and McLain 2001). The Trawl site in Suisun Bay is sampled three days per week year round. It is sometimes sampled daily and at times two shifts per day for a total of 20 tows per day during May and June. During December and January, trawls occur 7 days per week with ten 20 minute trawls conducted daily. Catch limits are imposed when Delta Smelt catches exceed 8 individual Delta Smelt. The trawl survey records fish length at capture and creates a record of the race, origin and release location if a coded wire tag is detected.

We used data that had been collected since 1979 in mid-water boat trawls at Chipps Island, Suisun Bay (Zone 10 S UTM, 4211218N, 595531E). Data from the DJFMP is available online (http://www.fws.gov/stockton/jfmp/). USFWS tables available online contained metrics of juvenile Chinook salmon that had been marked with CWTs, released throughout the Sacramento - San Joaquin Basin and then recovered near Chipps Island in Suisun Bay (Coded *Wire Tag 1978 -2011.xls* and *Coded Wire Tag 2012 -2013.xls*). Survey records not containing CWTs can be found in the spreadsheets *Chipps Island Trawls 1976-2011.xlsx and Chipps Island Trawls 2012-2014.xlsx*.

We used the records from the Chipps Island trawls to create a database of fish lengths and growths increments for all fish with CWTs (referred to as the CWT table). Each fish with a CWT is of a known origin, so the race and the source (hatchery or wild stock origin) are also known. We used the remaining records from the Chipps Island survey to construct a database table of Chinook known to be of a given race, but where the origin is not known. These records were assembled into a table we refer to as the TRAWL table, which only distinguishes between Fall and Spring runs.

We compiled juvenile salmon length data from the Sacramento watershed and the San Francisco Bay Delta into a relational database in order to determine growth of hatchery Fall Chinook and hatchery and wild juvenile Spring Chinook. Wild Spring stocks included Deer, Mill and Butte creeks. Butte Creek fish were release and recaptured in Butte Creek, the Sutter

Bypass or near Chipps Island in Suisun Bay. Release and recovery data were compiled from three sources: California Department of Fish and Wildlife (CDFW), US Fish and Wildlife Service's Delta Juvenile Fish Monitoring Program (DJFMP) and the Regional Mark Processing Center (RMPC).

From 1995 to 2001, the CDFW captured, measured, marked, and released wild spring-run Chinook on Butte Creek (CDFG, 1999; CDFG, 2004-2; CDFG, 2004-3). The purpose of the CDFW program was to estimate adult escapement, monitor timing and abundance of juvenile outmigration, and monitor relative growth rates in the Butte Creek system. Fish were captured and marked with adipose fin clips and coded wire tags at the Parrot-Phelan Diversion Dam (PPDD; Zone 10 S UTM, 4396287N, 611463E). Releases took place at three locations, but varied from year to year. Release sites were: PPDD, Baldwin Construction Yard (approximately one mile downstream of the PPDD) and Adams Dam (approximately 7 miles downstream of PPDD). After release, marked fish were subject to recapture and sacrifice at downstream locations in Butte Creek, the Sutter Bypass and the Sacramento Delta near Chipps Island. Rotary screw traps were used to recapture fish at all locations and an off-stream fish screen outfitted with a trap box was used to collect fish at the PPDD site. Recaptured fish were sacrificed, measured for fork length and their CWTs were extracted and read. We received programmatic data formatted in a Microsoft Access database directly from the CDFW (C. Garman, personal communication, 1/30/2014).

We queried the RMIS database for juvenile Chinook that had been marked and released at any location in the Sacramento drainage. The RMIS table was then related by CWT code to Chipps Island mid-water trawl and Sacramento River recoveries. In this way, we queried recoveries with release locations only within the Sacramento Basin.

We obtained tributary measurements of juvenile lengths from rotary screw traps (RSTs) operating in Butte creek, Mill creek and Deer creek. Rotary screw traps were operated by the US Fish and Wildlife Service in Mill and Deer creeks, and by the California Department of Fish and Wildlife in Butte creek. Screw trap operation spanned 1995-2010 in the records used in this analysis. We used samples obtained from January to June of each year to obtain estimates of tributary outmigration size.

Environmental data

We compiled time series of environmental variables that pertain to the experiences of downstream migration juveniles. For Spring Run, we used discharge at the three creeks (Deer, Mill and Butte), flow, exports volumes and other export indices, and a CPUE index of bass abundance. Flow temperature and discharge were obtained from USGS gauging stations (http://waterdata.usgs.gov/nwis/inventory). Exports and other dayflow parameters were obtained from water project data available on the California department of water resources website (http://www.water.ca.gov/dayflow/output/Output.cfm). Environmental variables were normalized by subtracting the mean and dividing by the standard deviation. The variables are summarized in Table C.1 for Spring run and in Table C.2 for Fall run.

Table C.1 Environmental variables used in length and growth analysis of Spring Chinook.

Covariate	Description	Location	Data Origin
Deer discharge	Average monthly water discharge (cfs) at Deer Creek	Vinna, Deer Creek	USGS 11383500 DEER C NR VINA CA
Mill discharge	Average monthly water discharge (cfs) on Mill Creek	Molinos, Mill Creek	USGS 11381500 MILL C NR LOS MOLINOS CA
Butte discharge	Average monthly water discharge (cfs) on Butte Creek	Chico, Butte Creek	USGS 11390000 BUTTE C NR CHICO CA
Yolo flow	Peak (maximum) streamflow into YOLO Bypass at Woodland, CA	Into Yolo at Woodland, CA	USGS 11453000 YOLO BYPASS NR WOODLAND CA
Bass	Index of Striped Bass abundance as number of striped bass kept. This is NOT effort standardized, but effort data is not available <1980	Delta	Marty Gingris personal comm.
GEO	The amount of water reaching the Mokelumne River system from the Sacramento River via the Delta Cross Channel and Georgiana Slough	Delta cross channel and Georgiana Slough	Dayflow: Delta Cross Channel and Georgiana Slough Flow Estimate (QXGEO)
EXP	Accounts for all water diverted from the Delta by the Federal and State governments to meet water agreements and contracts. These include Central Valley Project pumping at Tracy (QCVP), the Contra Costa Water District Diversions at Middle River (new for WY 2010; data begin on 01AUG2010), Rock Slough, and Old River (QCCC), the North Bay Aqueduct export (QNBAQ), and State Water Project exports (Banks Pumping Plant or Clifton Court Intake, QSWP).	South Delta	Dayflow: Total Delta Exports and Diversions/Transfers (QEXPORTS).
EXPIN	The Export/Inflow Ratio is the combined State and Federal Exports divided by the total Delta inflow (QTOT). EXPIN = (QCVP+QSWP-BBID)/QTOT (8)	Delta	Dayflow: Export/Inflow Ratio (EXPIN)

CD	The Dayflow parameter net channel depletion (QCD) is an estimate of the quantity of water removed from Delta channels to meet consumptive use (QGCD)	Delta	Dayflow: Net Channel Depletion (QCD)
CVP	Dayflow parameter for Central Valley Project pumping at Tracy (QCVP)	Delta	

2696

2697 **Table C.2 Environmental variables used in length and growth analysis of Fall Chinook**

Covariate Name	Description	Location	Data Origin
Keswick discharge	Average monthly water discharge (cfs) at Keswick Dam	Keswick Dam	USGS 11370500 SACRAMENTO R A KESWICK CA
Battle discharge	Average monthly water discharge (cfs) on Battle Creek	Cottonwood, Battle Creek	USGS 11376550 BATTLE C BL COLEMAN FISH HATCHERY NR COTTONWOOD CA
Battle height	Peak gauge height for the water year	Cottonwood, Battle Creek	USGS 11376550 BATTLE C BL COLEMAN FISH HATCHERY NR COTTONWOOD CA
Feather discharge	Average monthly water discharge (cfs) on the Feather River	Oronville, Feather River	USGS 11407000 FEATHER R A OROVILLE CA
Feather temp	Feather River average maximum temperature from USGS gage with (daily) interpolations from Sacramento, CA air temperature (1992+)	Oronville, Feather River	USGS 11407000 FEATHER R A OROVILLE CA
American temp	American River average maximum temperature from USGS gage with (daily) interpolations from Sacramento, CA air temperature (~1978-1998)	Fair Oaks, American River	USGS 11446500 AMERICAN R A FAIR OAKS CA
Yolo flow	Peak (maximum) streamflow into YOLO Bypass at Woodland, CA	Into Yolo at Woodland, CA	USGS 11453000 YOLO BYPASS NR WOODLAND

			CA
Bass	Index of Striped Bass abundance as number of striped bass kept. This is NOT effort standardized, but effort data is not available <1980	Delta	Marty Gingris personal comm.
GEO	The amount of water reaching the Mokelumne River system from the Sacramento River via the Delta Cross Channel and Georgiana Slough	Delta: DCC and Georgiana Slough	Dayflow: Delta Cross Channel and Georgiana Slough Flow Estimate (QXGEO)
EXP	Accounts for all water diverted from the Delta by the Federal and State governments to meet water agreements and contracts. These include Central Valley Project pumping at Tracy (QCVP), the Contra Costa Water District Diversions at Middle River (new for WY 2010; data begin on 01AUG2010), Rock Slough, and Old River (QCCC), the North Bay Aqueduct export (QNBAQ), and State Water Project exports (Banks Pumping Plant or Clifton Court Intake, QSWP).	South Delta	Dayflow: Total Delta Exports and Diversions/Transfers (QEXPORTS).
EXPIN	The Export/Inflow Ratio is the combined State and Federal Exports divided by the total Delta inflow (QTOT). EXPIN = (QCVP+QSWP-BBID)/QTOT (8)	Delta	Dayflow: Export/Inflow Ratio (EXPIN)
CD	The Dayflow parameter net channel depletion (QCD) is an estimate of the quantity of water removed from Delta channels to meet consumptive use (QGCD)	Delta	Dayflow: Net Channel Depletion (QCD)
CVP	Dayflow parameter for Central Valley Project pumping at Tracy (QCVP)	Delta	Dayflow: Central Valley Project Pumping (QCVP)
SWP	Dayflow parameter for State Water Project exports (Banks Pumping	Delta	Dayflow: State Water Project Pumping

	Plant or Clifton Court Intake, QSWP)		(QSWP)

Length and Growth analysis

We examined environmental factors affecting length at recapture at Chipps Island of fish with known and unknown release lengths. Where length at release was known, we examined growth rates. We associated each size and growth record with environmental factors experienced by each race of salmon each year the sizes were recorded. We compared fall and spring length at capture at Chipps Island from two separate surveys. The CWT table provided an estimate of growth for fall and spring hatchery releases. The mid-water trawls did not distinguish between wild and hatchery fish, so those analyses pertain to the race as a whole, without distinction about release locations or wild/hatchery distinctions. We also obtained sizes from DJFMP seines in Region 1 (upstream from the Delta) and compared those sizes with Chipps Island size information. Since seine samples do not distinguish between populations, growth obtained from subtracting upstream seine sizes from Chipps Island trawl sizes provide estimates of aggregate Fall and Spring run sizes, but cannot distinguish between release locations or between wild and hatchery releases.

SEINE/TRAWL - growth by race from mid-Sacramento to Chipps Island.

We queried the DJFMP seine database to obtain estimates of growth for Spring and Fall runs. Region 1 of the DJFMP beach seine runs from Colusa State Park to Elkhorn. We averaged lengths of Spring and Fall seine lengths for each year for fish collected between January and June, and compared those to Chipps Island midwater trawl sizes. The trawl survey assigned fish to Fall and Spring runs based on size ranges and records indicated that all collections occurred in May and June. We calculated the growth for each race of fish each year as the difference between the average trawl length and the average seine length. We refer to these growth estimates as the SEINE/TRAWL dataset.

We examined growth patterns in relation to environmental variables listed in Tables C.1 and C.2. We performed stepwise linear regressions of growth in relation to each variable, adding variables according to best p-value, and stopping when no further significant variables were found.

CWT –growth and length by hatchery source.

When hatchery fish are released, the average size of a sample of the release batch is used as the release length of record for fish in the batch. When recaptures occur at Chipps Island, a record for each fish recaptured can be compared to a release length record on the basis of CWT codes. To get reasonable sample sizes for recaptures, we were forced to aggregate hatchery releases such that release locations were ignored. We aggregated all release locations within the Sacramento drainage for each hatchery source. Since a release batch contains a range of lengths, it is possible for the smallest recaptured fish to be smaller than the average released fish. The growth record for each year was calculated as the average of all the recapture lengths minus the average release length. The average of release length was calculated as the weighted release length, weighted by the number released at each location at each time of release. We refer to the length and growth estimates from this method as the CWT dataset.

We tested for statistical relationships between size at recapture and environmental variables for Spring and Fall hatchery releases from Coleman National Fish Hatchery (CNFH) and Feather Fish Hatchery (FFH). We examined growth and length patterns in relation to environmental variables listed in Tables C.1 and C.2. We performed stepwise linear regressions of growth and length in relation to each variable, adding variables according to best p-value, and stopping when no further significant variables were found.

TRAWL – length by race at Chipps Island.

We selected records that were not limited to CWT tagged fish (the TRAWL dataset in this analysis) from Chipps Island, and assembled all records of Spring and Fall chinook to look at the size. By not being limited to CWT matches, the sample size was much larger than for the CWT matched database, but for the TRAWL dataset, the origin of fish could not be determined. The race of the fish was assigned by a length/timing criteria established by the DJFMP (the "Race Table" found at www.fws.gov/stockton/jfmp). Using these records we looked for temporal trends, comparisons between Spring and Fall runs, and relationships between size at capture and environmental factors. Annual average size records for Spring and Fall Chinook do not distinguish between hatchery and wild, and there is no growth estimate because the size at release is not known, and there is no way to distinguish between Butte, Mill, and Deer creeks. The TRAWL dataset provides an aggregate estimate of length at Chipps Island by race alone.

We examined growth patterns in relation to environmental variables listed in Tables C.1 and C.2. We performed stepwise linear regressions of length in relation to each variable, adding variables according to best p-value, and stopping when no further significant variables were found. We treat length as a surrogate for growth on the assumption that some initial length can be treated as a constant across and all variability can be thought of as occurring after that initial length.

RST – Lengths in tributaries

Deer, Mill, and Butte creek rotary screw trap records were queried to obtain estimates of out-migrating juvenile sizes. We took the average size of all samples obtained from the traps between January and June of each migration year. We attempted to match CWT releases from Butte Creek each year to recoveries within the Sacramento basin to obtain growth estimates at various sample locations, but found that recoveries were too few to obtain good estimates of growth. Butte Creek CWT release records with Chipps Island recapture events began in 1996, but recaptures amounted to fewer than 10 fish per year at Chipps Island. It was not possible to relate RST lengths to downstream lengths at Chipps Island for a growth estimate. We therefore limited our examination of RST data to showing temporal trends of sizes of Deer, Mill and Butte creeks.

RESULTS

SEINE/TRAWL - growth by race from mid-Sacramento to Chipps Island.

The average growth of Spring and Fall Chinook are shown in Figure C.1 along with the time elapsed between Seine surveys and mid-water trawls. The temporal trend in growth is shown in Figure C.2. Fall Chinook appear to be slightly larger and on average seen in seine surveys about half of a month later. Predominantly, Fall Chinook appear to grow slightly

more between Seine and mid-water trawl surveys, which is noteworthy, since they do so in less time as seen in the average month seined calculation.

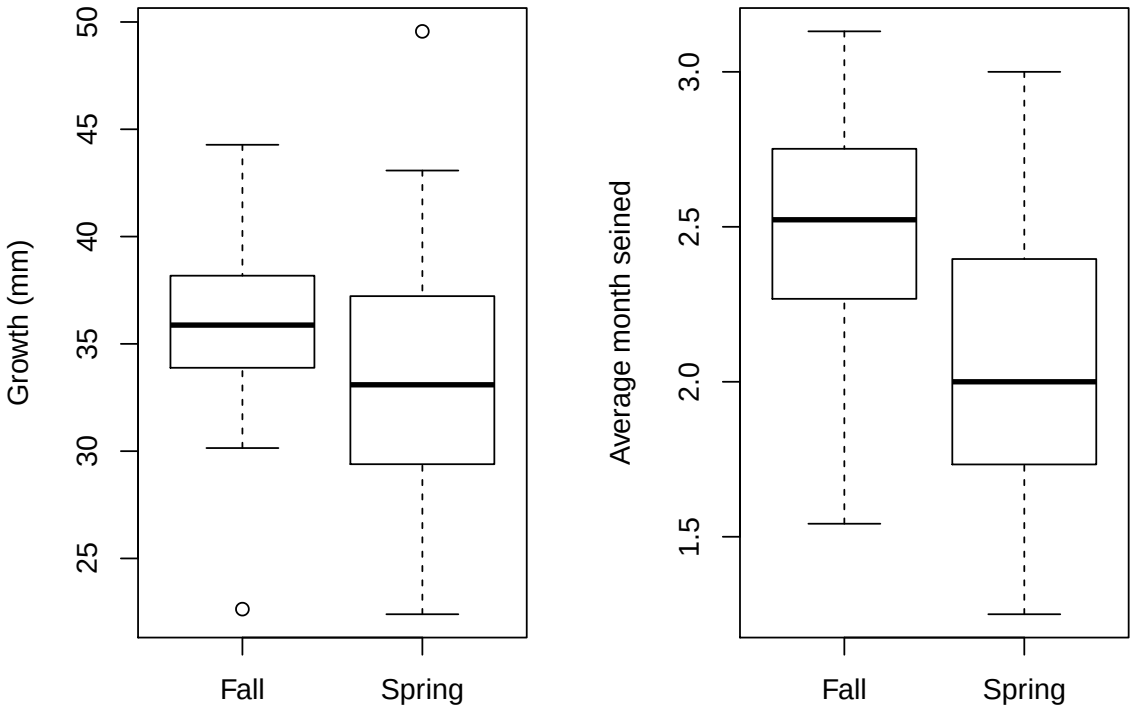

Figure C.1 Growth between release and sampling at Chipps Island (left panel) and month at which Region 1 seine was sampled (right panel).

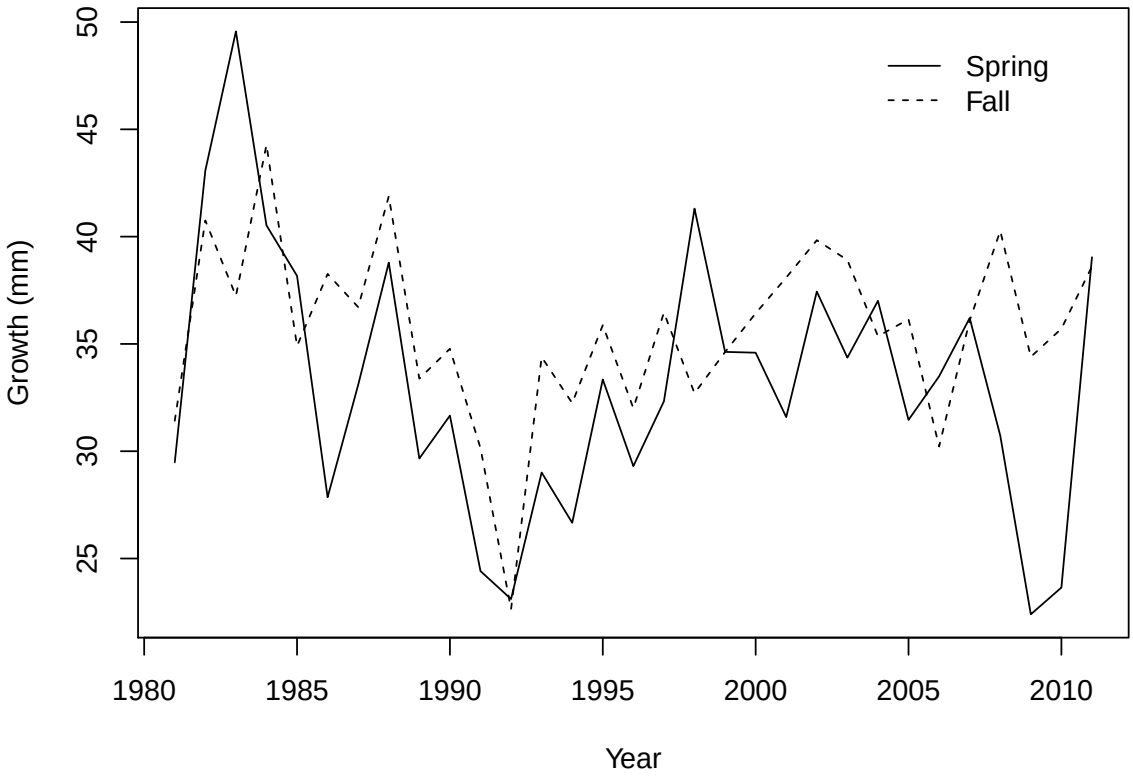

Figure C.2 Temporal trends in Spring and Fall Chinook growth evaluated from beach seine and mid-water trawl surveys.

Table C.3 shows the results of stepwise linear regressions. The regression results show that there are significant effects of Bass, Central Valley Project exports, race (spring or fall run) , and the export to inflow ratio (EXPIN). The bass index shows a positive effect on growth. Central Valley Project exports also show a positive effect, but the export to inflow ratio shows a negative effect. The adjusted R-squared value for the fit was 0.4068. The diagnostic plot of the fit is shown in Figure C.3.

Table C.3 Regression results of growth in SEINE/TRAWL data in relation to environmental variables. Intercept in parentheses.

Coefficients:	Estimate	Std. Error	t value	Pr(>|t|)	Signif
(int-Fall)	38.3357	0.9227	41.546	<2.00E-16	***
Bass	5.4229	1.3838	3.919	0.000241	***
CVP	3.8959	0.7293	5.342	1.67E-06	***
Spring	-3.5728	1.0712	-3.335	0.001503	**
EXPIN	-1.3115	0.6071	-2.16	0.034961	*

*** p<0.001, **p<0.01, *p<0.05, . p<0.1

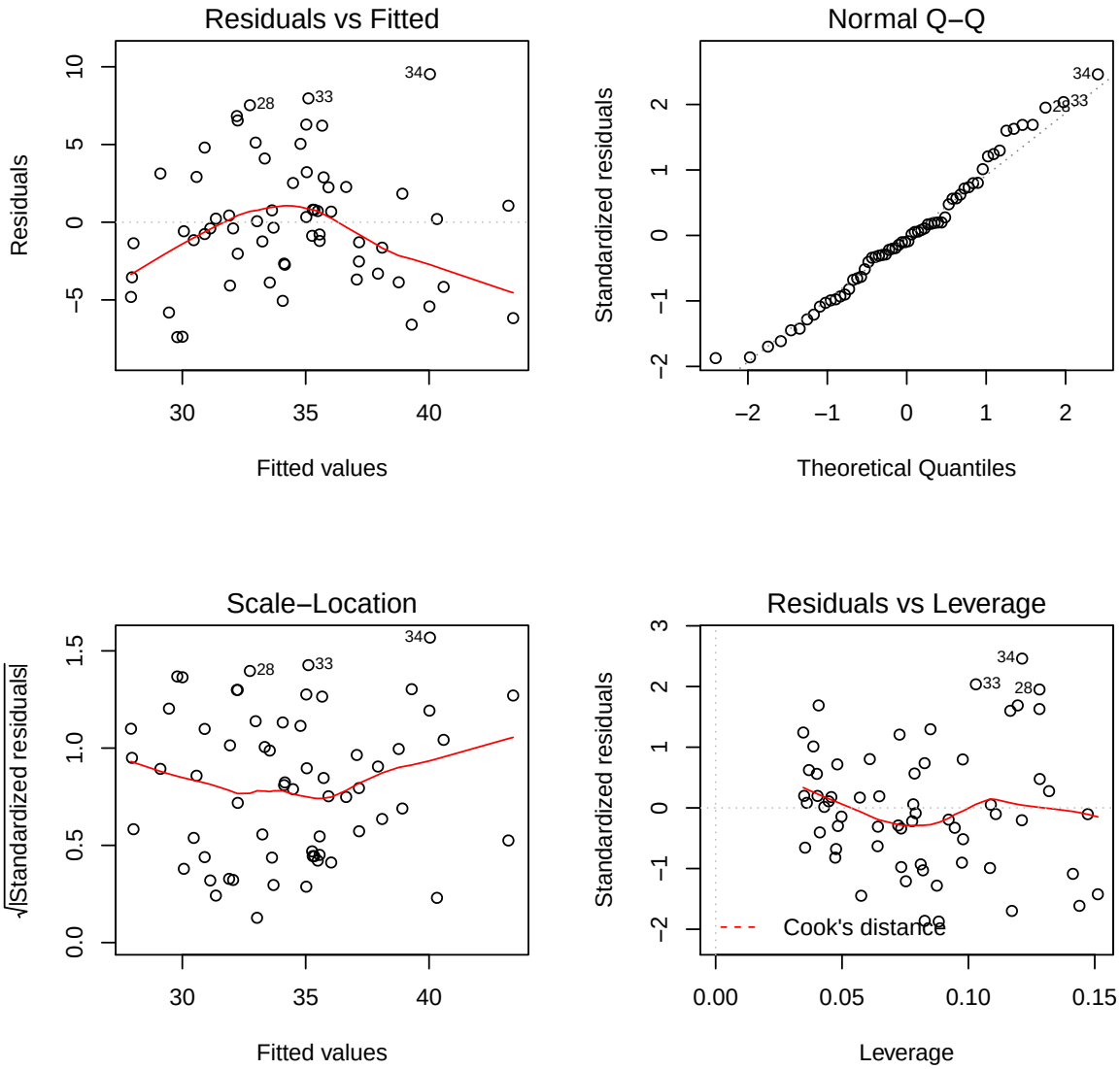

Figure C.3 Diagnostic plot of best fitting model of seine-trawl growth of Spring and Fall chinook.

CWT –growth and length by hatchery source.

Feather Fish Hatchery (FFH) spring Chinook and Coleman National Fish Hatchery (CNFH) fall Chinook growth and lengths at Chipps Island are shown in Figure C.4. We see that there is considerable variability in growth, and that Spring run fish appear to have grown faster than Fall run until the early 1990's, but are now growing less than Fall run (see Figure C.4 upper panel). Table C.4 shows the results of stepwise regressions of length against all Spring and Fall run covariates. The export to inflow ratio was the only significant predictor of catch length in the Chipps Island trawl, with EXPIN having a positive effect. The adjusted R-squared for the best fitting model shown was 0.3414. Diagnostic plots of the best fit are shown in Figure C.5, where we can see that the residuals are normal. Regressions show a

hatchery effect, finding that FFH fish arrive at Chipps Island 3.5 mm larger than CNFH fish, but FFH fish included Spring run, which were larger. Despite growth of Spring run recoveries appearing to decline from 1985, the lengths of Spring run fish at Chipps Island appears to be relatively constant. We found no significant relationships between growth and environmental variables.

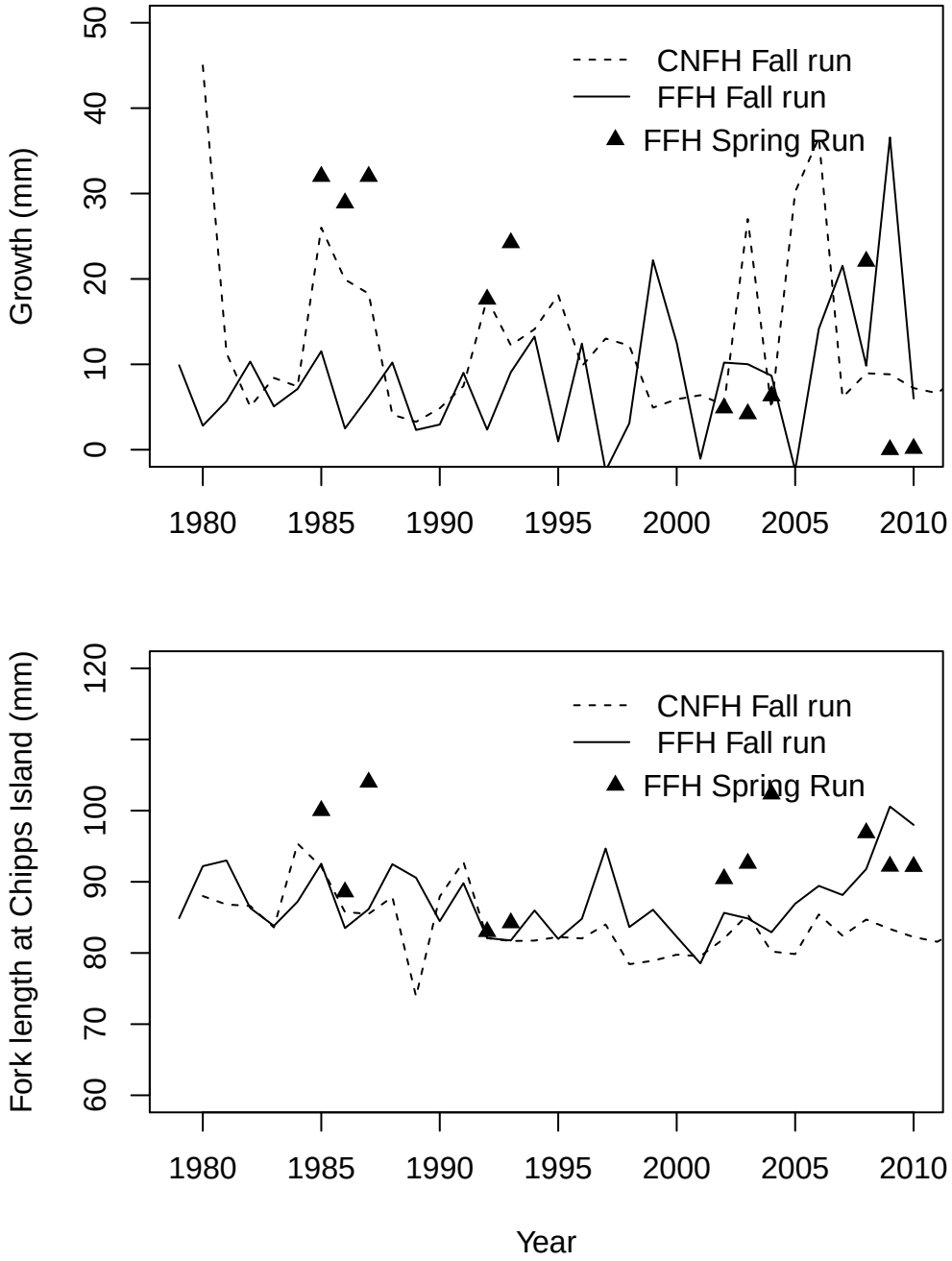

Figure C.4 Growth of CNFH and FFH Fall runs, and FFH Spring run (upper panel) and length at Chipps Island (lower panel).

Table C.4 Regression results of relationship between CWT length at Chipps Island and environmental variables. Intercept in parentheses for Fall CNFH.

Coefficients:	Estimate	Std. Error	t value	Pr(>|t|)	Signif
(Intercept)	83.8357	0.8361	100.27	<2.00E-16	***
Race Spring	5.6019	1.6816	3.331	0.00137	**
EXPIN	1.7117	0.5764	2.969	0.00405	**
Source FFH	3.4654	1.1919	2.907	0.00484	**

*** p<0.001, **p<0.01, *p<0.05, . p<0.1

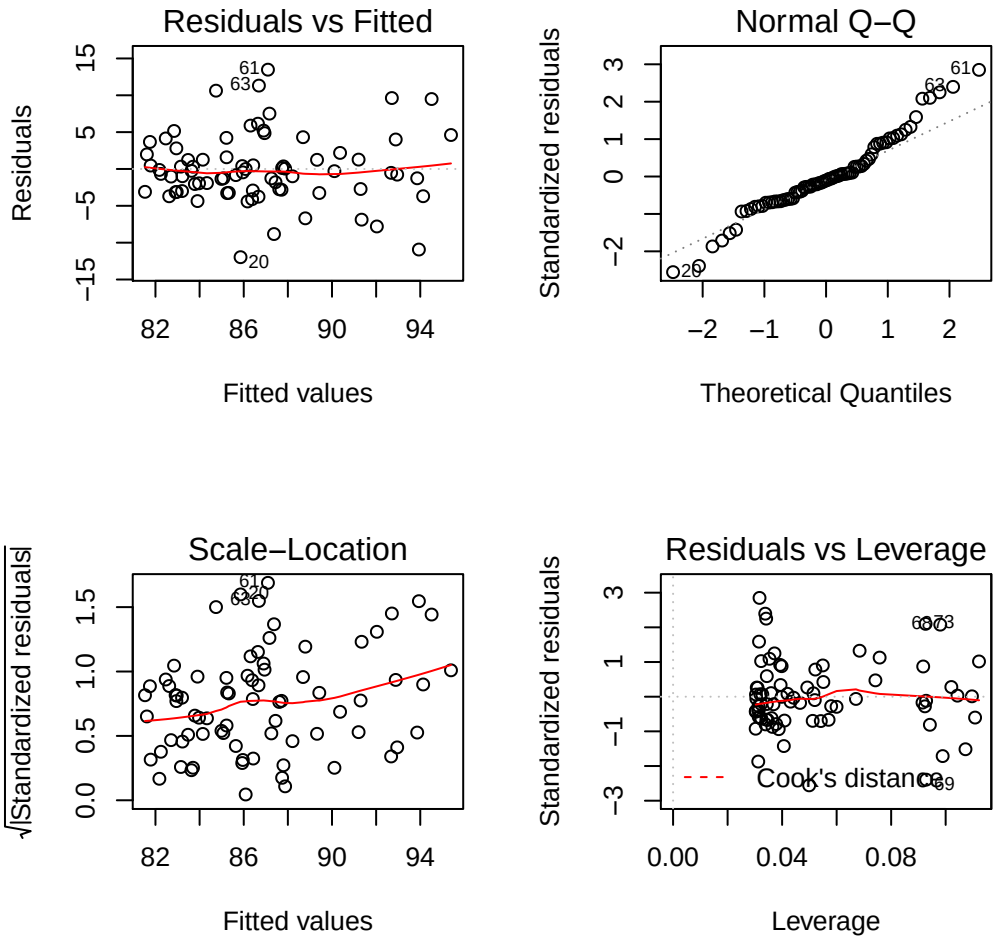

Figure C.5 Diagnostic plots of best fit of length at recapture at Chipps Island to environmental variables.

TRAWL – length by race at Chipps Island.

Unlike the CWT lengths from hatchery specific releases, the aggregated relative Spring and Fall lengths remain consistent from the 1980's until present. Spring run appear to be consistently larger that Fall run (see Figure C.6). Regression results are shown in Table C.5 and indicate that Yolo flow, the Central Valley Project exports, the export to inflow ratio, water passing via the Delta Cross Channel, and the bass index are all significant predictors of size. The Adjusted R-squared of the best fit shown is 0.785. The diagnostic plots of the best

fit is shown in Figure C.7. The TRAWL dataset had the largest samples, and despite being aggregated wild and hatchery fish, and despite not identifying source drainages, the regression results yield the highest R-squared. The diagnostics show normality in residuals as well as the majority of residuals concentrated on predicted theoretical quantiles.

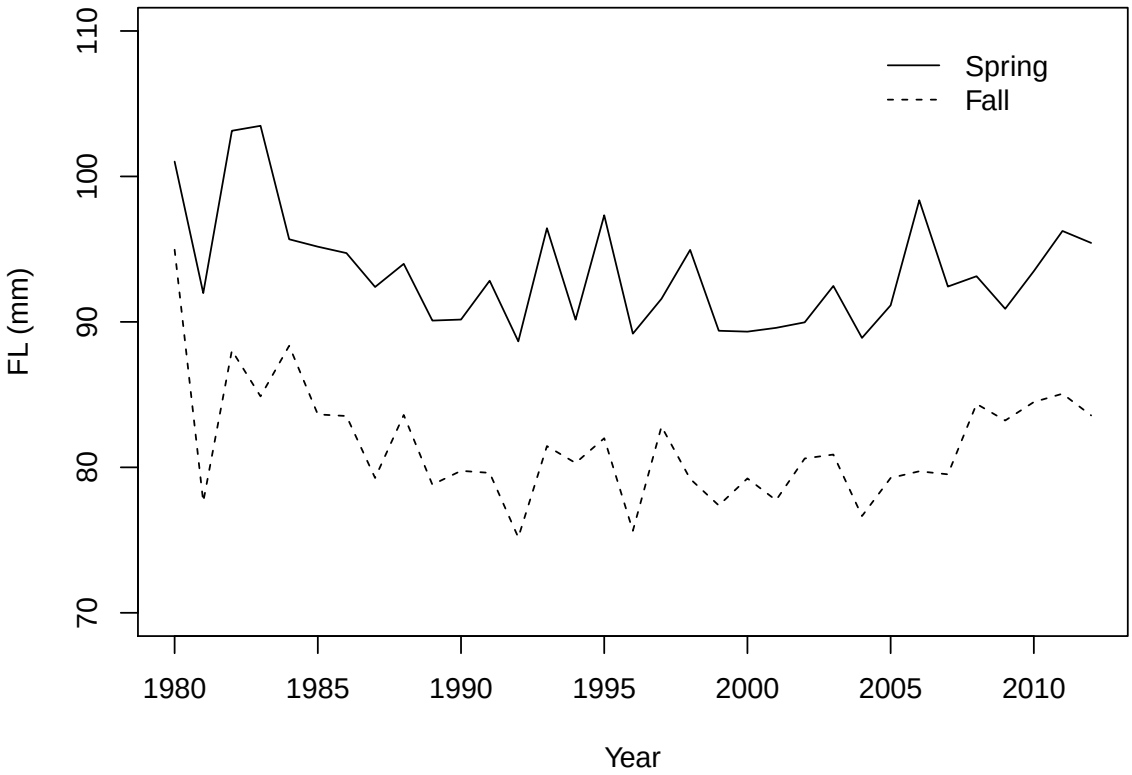

Figure C.6 Lengths of Spring and Fall aggregates at Chipps Island in TRAWL data.

Table C.5 Regression results of best fit of trawl lengths to environmental variables.

Coefficients:	Estimate	Std. Error	t value	Pr(>|t|)	Signif
(Intercept)	80.9897	0.7322	110.604	<2.00E-16	***
race Spring	11.4344	0.8359	13.678	<2.00E-16	***
Yolo flow	0.99	0.5468	1.811	0.075288	.
CVP	2.6729	0.7082	3.774	0.000375	***
EXPIN	-2.5741	0.7566	-3.402	0.001206	**
GEO	-1.4716	0.6551	-2.246	0.028449	*
BASS	-1.8643	1.0438	-1.786	0.079228	.

*** p<0.001, **p<0.01, *p<0.05, . p<0.1

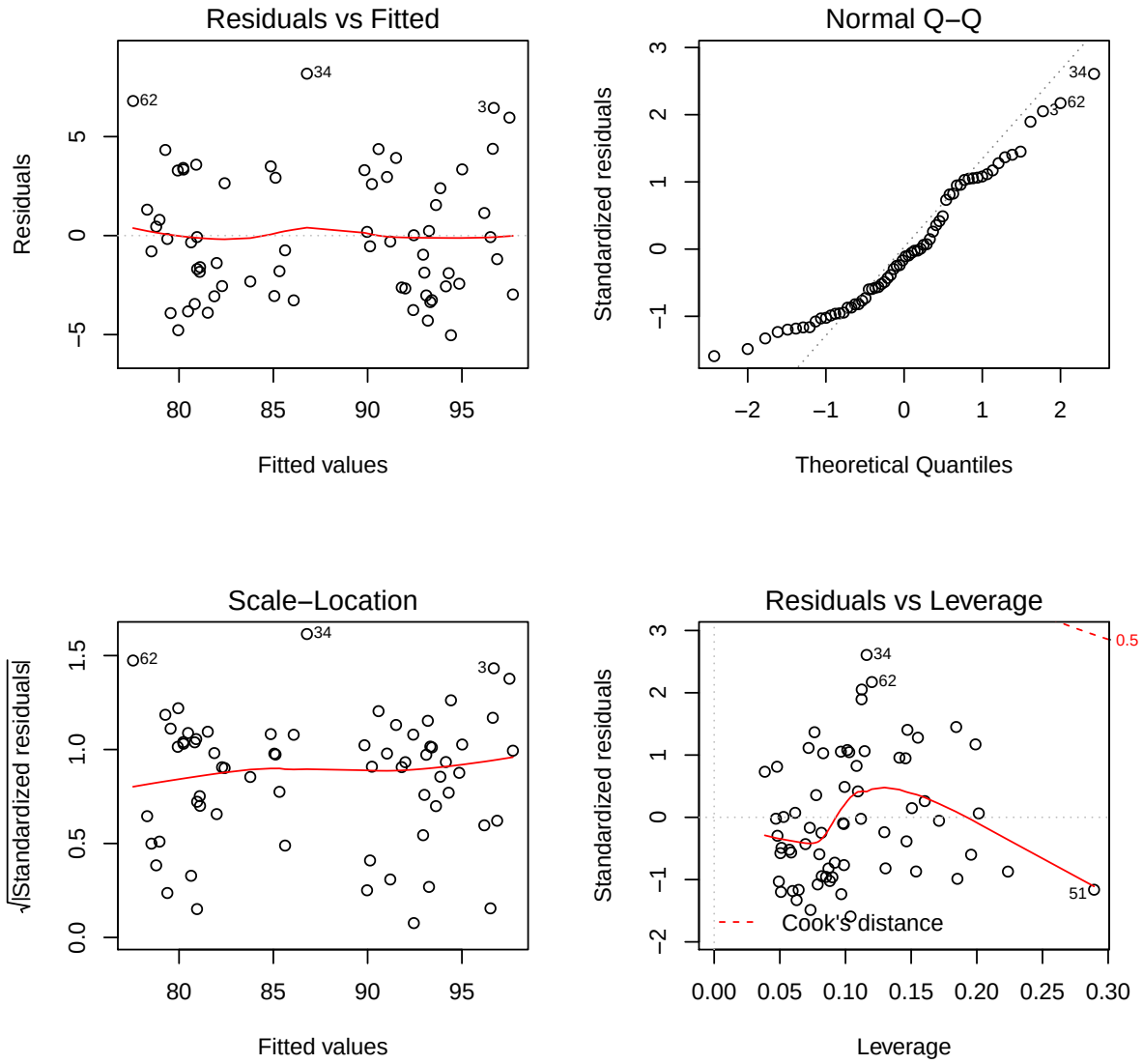

Figure C.7 Diagnostic plot of best fitting model of relationship between length at Chipps Island mid-water trawl and environmental variables.

RST – Lengths in tributaries

Mill, Deer, and Butte creek Spring run average fish sizes from rotary screw trap operations are shown in Figure C.8. We see that Mill, Deer and Butte creeks are on average about 45-55 mm in length between January and June when records were aggregated for outmigration estimates. The temporal pattern in sizes is shown in Figure C.9. We see no major trend in size in tributaries between January and June, only that Butte creek fish appear to run a bit smaller.

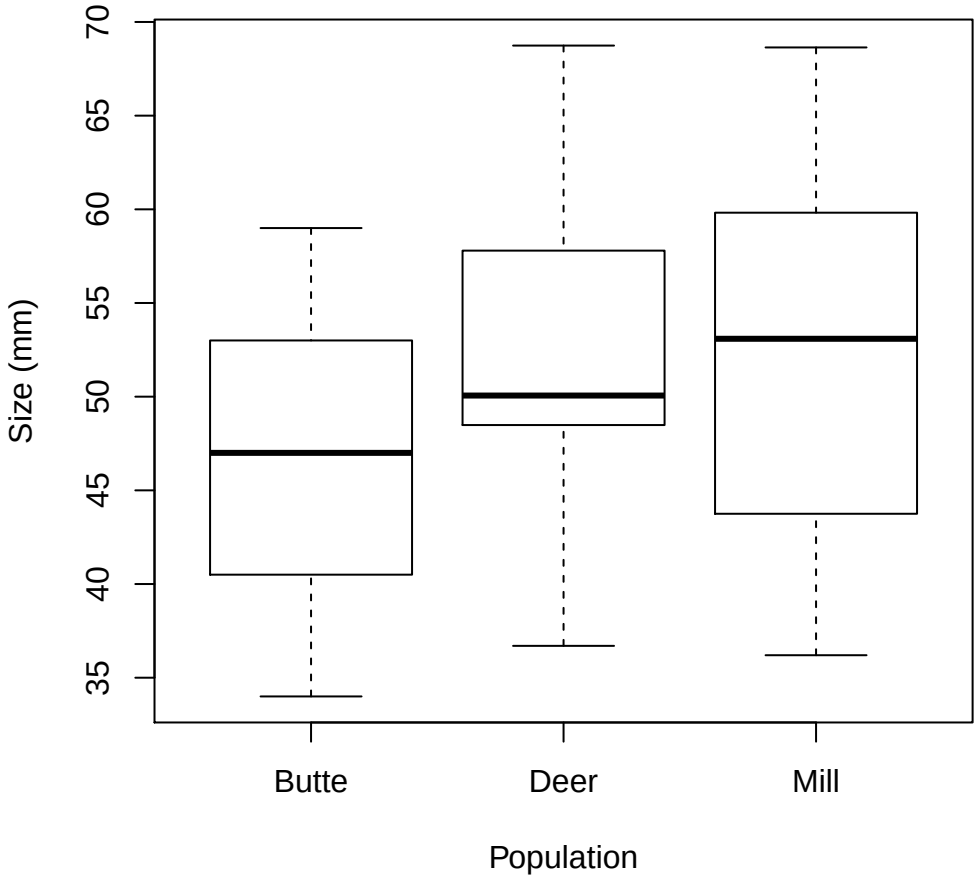

Figure C.8 Average size of juveniles obtained from rotary screw traps operating in Butte, Deer and Mill creeks between January and June.

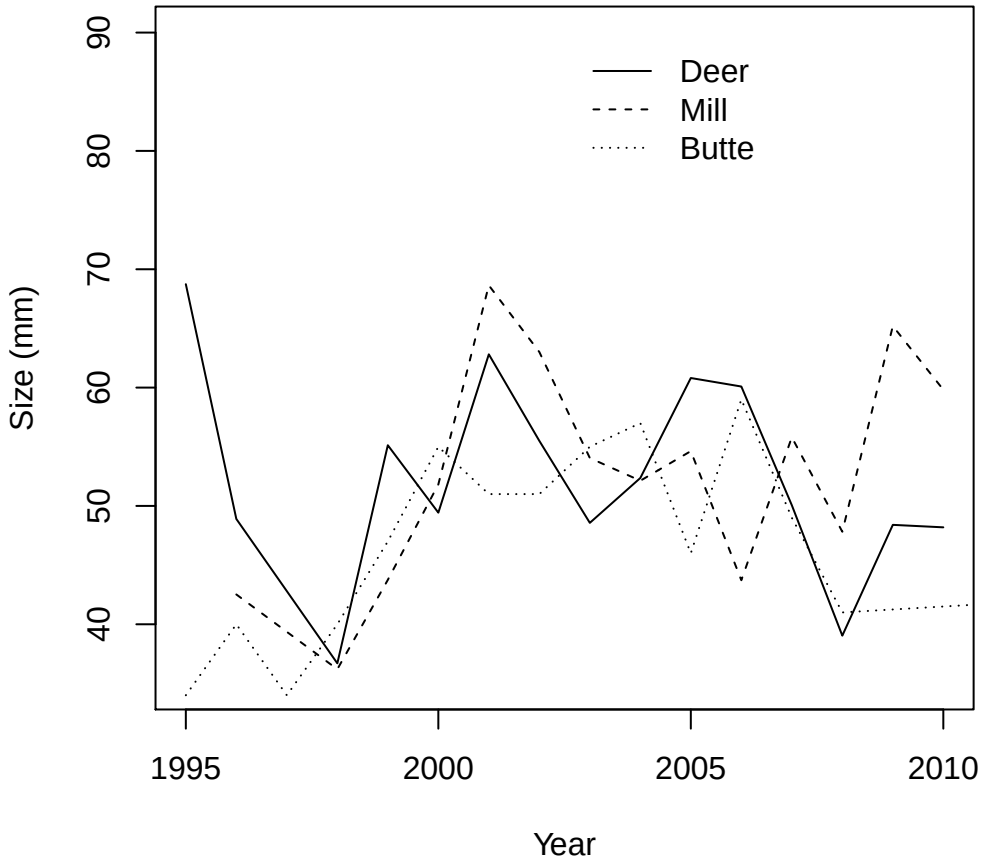

Figure C.9 Temporal trend in juvenile sizes obtained from rotary screw traps operating in Deer, Butte and Mill creeks between January and June.

DISCUSSION

This analysis drew upon varied sources of fish length information in the Sacramento River drainage. The summary of rotary screw trap lengths indicates that Spring run out-migrating Chinook from Deer, Mill and Butte creeks are approximately the same size, and have been stable at approximately 55 mm in recent years. Regression analysis of recoveries from mid-water trawl surveys at Chipps Island indicates that growth of fish from North of the Delta to Chipps Island, as well as the length at recapture in Chipps Island trawls varied in relation to environmental variables. Regression analyses showed that the length at Chipps Island from the perspective of two different types of length statistics proved to be related to environmental variables regardless of the data source of the length estimates.

We used two different growth metrics. One growth metric came from lengths of CWT recoveries and releases of hatchery fish, and the other came from seine and trawl surveys. The CWT growth was derived from average recovery length at Chipps Island and average release lengths at various release locations and times. The average recovery length is a statistic based on a very small sample size relative to the release length statistic. If you

consider the how many fish are released relative to recaptured, and if you consider that tagged fish are released at various locations and at different times, it is easy to see how biased the growth estimate might be. The SEINE/TRAWL growth estimate made no distinction between hatchery and non-hatchery fish and it represents an estimate of the growth of all Fall or Spring run fish between Region 1 seines and Chipps Island. In comparison to the CWT estimate, it will be more complex in it's stock composition (with hatchery and non-hatchery fish of all origins), but it is much simpler in upstream capture and release size sampling. All stocks were sampled from the same locations for sizing regardless of origin. We found a relationship between SEINE/TRAWL growth and environmental variables, but no relationship between CWT growth and environmental variables. This may be due to the complexity of how the release length was calculated for the CWT growth estimate.

The environmental predictors that best explained growth were the Central Valley Project exports (CVP), the ratio of combined state and federal exports to the total Delta inflow (EXPIN), and the bass index. CVP and EXPIN are both related to flows in complex ways. CVP is related to flow because exports would tend to be less restricted at higher flows, but would have its highest impact when flows are low. We would expect that juvenile salmon growth could be high when CVP is highest under that logic. EXPIN is related to flow by a similar logic, but since EXPIN is a ratio, we would expect the largest fraction of flows to be exported when flows are low (for a given level of exports). We would expect juvenile salmon growth to be lowest when EXPIN is highest at the lowest flows.

Figure C.10 illustrates some the general patterns in environmental covariation. In the upper left panel we see that CVP has the greatest degree of variability at the lowest flows (with Yolo flow being used as a surrogate for average flow at export locations). Across a range of flow values we can see that the lower bound of CVP increases. This is consistent with a general tendency of reducing exports at lower flows. The relative impact of exports at a given flow is seen with EXPIN, which we see (lower left) diminishes at higher flows. We also see that more water reaches downstream to the Mokelumne river when EXPIN is lower (lower right panel). Finally, there is a general pattern of CVP being larger when EXPIN is higher, but recall that the highest EXPIN may coincide with low flows.

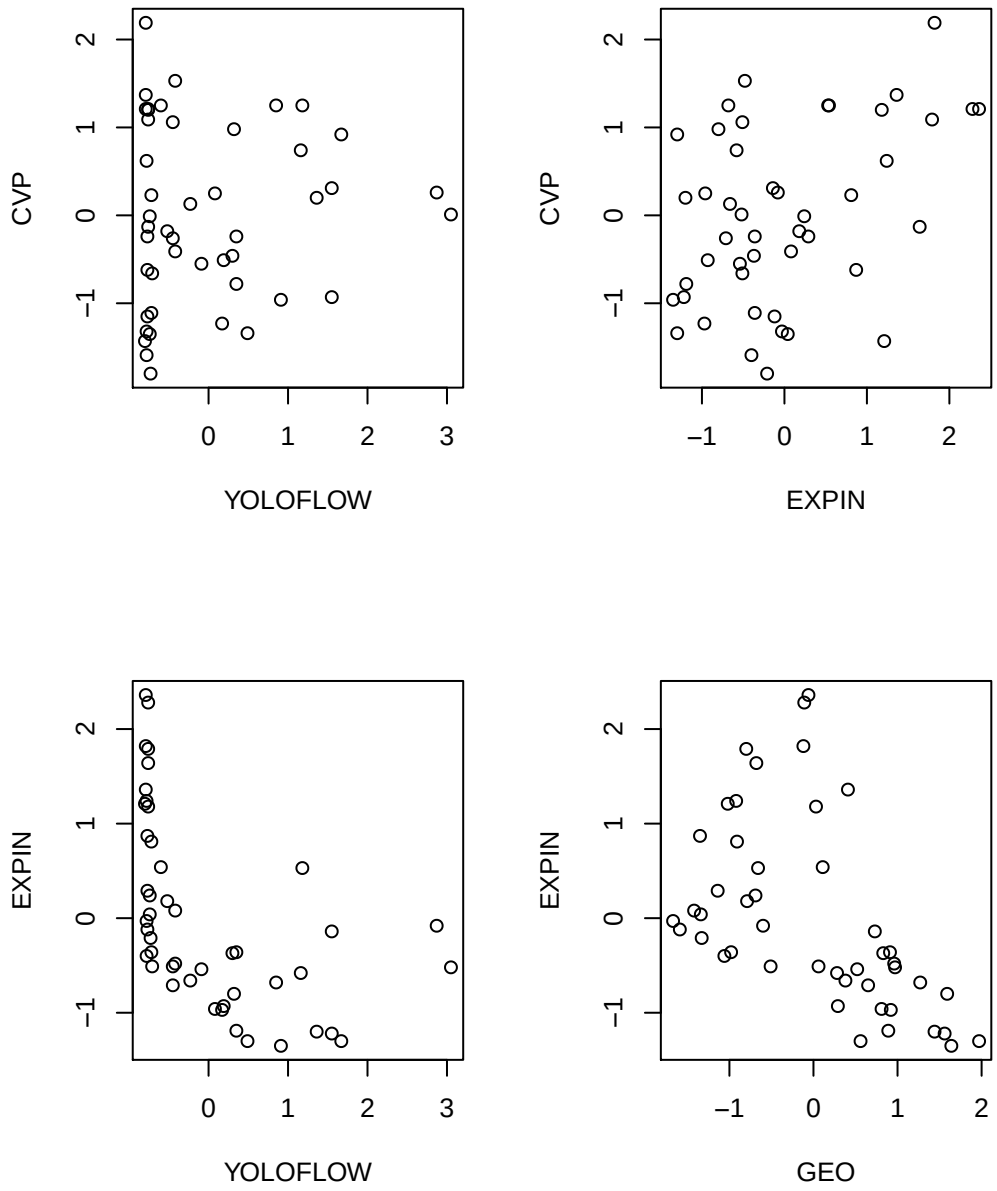

Figure C.10 Covariation between significant environmental predictors.

EXPIN was a significant predictor of length when both CWT and TRAWL datasets were used. It was significant with $p<0.01$ in both cases. EXPIN was also a significant predictor ($p<0.01$) of growth estimates of Fall and Spring aggregates obtained from the SEINE/TRAWL dataset. The CWT length regression is in conflict with the SEINE/TRAWL growth regression and the TRAWL length regression though. The CWT result predicts a positive effect of EXPIN, versus a negative effect for the other two regression analyses. A possible reason for this would be that the CWT dataset was exclusively measuring hatchery fish (although hatchery fish would also have been present in the other two analyses). If EXPIN has a positive effect on hatchery fish length at Chipps Island as shown in the CWT length regression, and a negative effect on the aggregate of both hatchery and non-hatchery fish seen in the TRAWL length and SEINE/TRAWL growth analysis, it might suggest that that the negative effect on non-hatchery growth is even stronger than seen in the TRAWL

surveys. It could also be a size related issue. If hatchery fish are smaller and more vulnerable to entrainment, removal of the smaller fish from the out-migrating cohort would make it appear as if they grew on average, when in fact it was just the smaller ones that did not make it into the downstream survey sample.

The relationship between flows and exports, and resulting growth and survival are complex. We found that growth and length are negatively related to EXPIN, but positively related to CVP. A possible mechanism, is that there is a threshold flow/export relationship where in smaller fish become more vulnerable to entrainment. Such a mechanism would predict that more larger fish than smaller fish make it downstream to be sampled at Chipps Island, which has the effect of making the growth appear larger on the basis of the average recovery size. This would appear to be favorable growth conditions despite the fact that all individuals did not grow better on those conditions. If a relatively high CVP export year were where to coincide with an average flow year, and if more small fish were entrained, it would appear that fish where larger at Chipps Island.

Results also indicated that Spring run were longer at Chipps Island, despite the fact that the SEINE/TRAWL regression showed that Spring run growth was less than Fall run. Total Central Valley Projects (combined state and federal) exports showed positively effect on growth in the SEINE/TRAWL regression and length in the TRAWL analysis. Since there was a negative effect from the export to inflow ratio, it may be suggest that total flows have a positive effect, and that there may be a relationship between exports and flows that is dictated by water extraction policies.

It is interesting that regression results show that bass has a positive effect on the growth estimates evaluated from the SEINE/TRAWL, yet has a negative effect on lengths estimated from the TRAWL data. Since the bass index is not standardized to effort, it can't imply a direct predation rate change on a size class of Chinook juveniles, but depending on the relationship between the index and the size of the bass caught, it might imply a shift in the size of Chinook vulnerable to bass predation at a given abundance of bass. It could be that smaller fish are more vulnerable and predation biases the growth estimate by removing smaller fish.

Our examination of length/growth sensitivity to environmental variation points to a few results. First, EXPIN is a statistically significant predictor of size and growth, with a negative effect on both. Our samples conflate the story a bit, but if you consider that the only positive effect was seen in the length of hatchery fish, and if you consider that the CWT dataset had race and hatchery factors, the positive effect of EXPIN in the regression result of the CWT data should not detract from the regression results found in both the SEINE/TRAWL and TRAWL dataset. It should be noted however, that the highest regression coefficient value for an environmental effect in any of our regressions was about 5, meaning that about 5 mm per standard deviation was the maximum variability in size predicted by variability in an environmental effect. This implies that at the extreme of 2 standard deviations, only 10 mm of net difference in size at Chipps Island would be predicted. Still, two standard deviations explains about 95% of the variation in environmental factors, and 10 mm explains 10-15% of the variability in length at Chipps Island (assuming 85 mm length at Chipps Island). Since the same environmental variables explain significant variation in rearing survival, it is feasible that length may be an instrumental in the mechanism of rearing survival.

REFERENCES

Brandes, P.L. and J.S. McLain. 2001. Juvenile Chinook salmon abundance, distribution, and survival in the Sacramento-San Joaquin Estuary. Pages 39 – 138 *in* R.L. Brown, editor. Contributions to the Biology of Central Valley Salmonids, Volume 2, Fish Bulletin 179. California Department of Fish and Game, Sacramento, California.

California Department Of Fish And Game. 1998. Butte Creek Spring-Run Chinook Salmon, *Oncorhynchus Tshawytscha*, Juvenile Outmigration And Life History 1995-1998. Administrative Report No. 99-5.

California Department Of Fish And Game. 2000. Butte And Big Chico Creeks Spring-Run Chinook Salmon, *Oncoryhnchus Tshawytscha* Life History Investigation 1998-2000. Administrative Report No. 2004-2.

California Department Of Fish And Game. 2004. Butte And Big Chico Creeks Spring-Run Chinook Salmon, *Oncoryhnchus Tshawytscha* Life History Investigation 2000-2001. Administrative Report No. 2004-3.

Garman, C.E and T. R. McReynolds. 2008. Spring-Run Chinook Salmon, Oncoryhnchus tshawytscha, Life History Investigation. California Department of Fish and Game. Inland Fisheries Administrative Report No. 2009-1.

U.S. Fish and Wildlife Service – Stockton Fish and Wildlife Office. March 2014. Metadata for the Stockton Fish and Wildlife Office's Delta Juvenile Fish Monitoring Program. http://www.fws.gov/stockton/jfmp/.

APPENDIX C: GROWTH ANALYSIS AND MODELLING

In this appendix we provide a description of the methods we used to collect and analyze length information from various state and federal collection facilities in the Sacramento drainage. We assembled time series of lengths, both upstream and downstream, for both hatchery fish and combined hatchery and wild aggregates. Where possible, we used upstream and downstream lengths to obtain annual growth estimates. In the absence of a downstream growth measurement, we assembled a time series of downstream lengths. We performed regressions on growth and length estimates, evaluating impacts of environmental conditions on growth.

INTRODUCTION

The life-cycle modeling analysis in this project attempts to attribute variability in survival to environmental factors during different parts of the life history. Survival can be affected by the environment in complex ways, and can be mediated through biotic and abiotic processes. We posit that size can play a role in predicting survival, and that growth itself can be an indicator of survival as well. An obvious mechanism for size effects on survival would be that larger fish are less vulnerable to predation than smaller fish. A mechanism for growth being a predictor of survival would be that faster growing fish are likely to be experiencing better feeding conditions and bioenergetic advantages, and therefore should survive better.

In this appendix we look for relationships between environmental conditions and growth, but because growth requires two measurements (a capture and a recapture, or a release and recapture), we are not always able to get an estimate of a growth increment. Some length estimates obtained from survey data cannot be connected to later surveys, and therefore a growth estimate can't be derived from the measurements. An example of this occurs with rotary screw traps operating in tributaries, where juvenile size samples are obtained during rearing and migration. Those sizes are not directly comparable to later samples obtained downstream, because the downstream samples are aggregates of all the independent upstream sampled lengths. We might be able to document a pattern in upstream sizes over the years, but growth to the downstream measurement can't be inferred. We therefore treat size as a surrogate for growth, with the assumption that annual variability in juvenile size is in actual fact a measurement of annual variability in growth since all fish must at some point have emerged from the gravel at roughly the same sizes.

METHODS

We performed an analysis of length and growth patterns for Spring and Fall run Chinook in the Sacramento River in relation to environmental factors. We collected size at release and recapture data from state and federal agencies. We compiled records into average sizes at release for several different stock aggregates that provided adequate sample sizes for the years the data were available. In some case, it was possible to associate the length of a downstream recaptured fish with a known upstream release size to obtain a growth increment

estimate, but in other cases only the downstream size record was available. Upstream length records were obtained from hatchery release information, from screw traps operated in tributaries, and from seine surveys operated throughout the Sacramento drainage. The farthest downstream sizes were obtained from Chipps Island, where mid-water trawl surveys collected size information and recorded the race of the fish based on the presence of a CWT or a length based estimated based on the length of the fish at the time the sample was obtained.

Data compilation

Length data

The Pacific States Marine Fisheries Commission manages and supports the Regional Mark Processing Center (RMPC; http://www.rmpc.org/), which in turn manages the Regional Mark Information System (RMIS). Agencies and organizations throughout the Western United States report CWT data directly to the RMIS. The Delta Juvenile Fish Monitoring Program (DJFMP) was initiated in the 1970s and is managed by the US Fish and Wildlife Service (USFWS, 2014). The program has a stated objective to monitor the effects of water projects in the Bay Delta on juvenile Chinook.

The number of juvenile salmon leaving freshwater during the spring has been sampled annually since 1978 by means of mid-water trawling in the estuary near Chipps Island (Brandes and McLain 2001). The Trawl site in Suisun Bay is sampled three days per week year round. It is sometimes sampled daily and at times two shifts per day for a total of 20 tows per day during May and June. During December and January, trawls occur 7 days per week with ten 20 minute trawls conducted daily. Catch limits are imposed when Delta Smelt catches exceed 8 individual Delta Smelt. The trawl survey records fish length at capture and creates a record of the race, origin and release location if a coded wire tag is detected.

We used data that had been collected since 1979 in mid-water boat trawls at Chipps Island, Suisun Bay (Zone 10 S UTM, 4211218N, 595531E). Data from the DJFMP is available online (http://www.fws.gov/stockton/jfmp/). USFWS tables available online contained metrics of juvenile Chinook salmon that had been marked with CWTs, released throughout the Sacramento - San Joaquin Basin and then recovered near Chipps Island in Suisun Bay (Coded *Wire Tag 1978 -2011.xls* and *Coded Wire Tag 2012 -2013.xls*). Survey records not containing CWTs can be found in the spreadsheets *Chipps Island Trawls 1976-2011.xlsx and Chipps Island Trawls 2012-2014.xlsx*.

We used the records from the Chipps Island trawls to create a database of fish lengths and growths increments for all fish with CWTs (referred to as the CWT table). Each fish with a CWT is of a known origin, so the race and the source (hatchery or wild stock origin) are also known. We used the remaining records from the Chipps Island survey to construct a database table of Chinook known to be of a given race, but where the origin is not known. These records were assembled into a table we refer to as the TRAWL table, which only distinguishes between Fall and Spring runs.

We compiled juvenile salmon length data from the Sacramento watershed and the San Francisco Bay Delta into a relational database in order to determine growth of hatchery Fall Chinook and hatchery and wild juvenile Spring Chinook. Wild Spring stocks included Deer, Mill and Butte creeks. Butte Creek fish were release and recaptured in Butte Creek, the Sutter

Bypass or near Chipps Island in Suisun Bay. Release and recovery data were compiled from three sources: California Department of Fish and Wildlife (CDFW), US Fish and Wildlife Service's Delta Juvenile Fish Monitoring Program (DJFMP) and the Regional Mark Processing Center (RMPC).

From 1995 to 2001, the CDFW captured, measured, marked, and released wild spring-run Chinook on Butte Creek (CDFG, 1999; CDFG, 2004-2; CDFG, 2004-3). The purpose of the CDFW program was to estimate adult escapement, monitor timing and abundance of juvenile outmigration, and monitor relative growth rates in the Butte Creek system. Fish were captured and marked with adipose fin clips and coded wire tags at the Parrot-Phelan Diversion Dam (PPDD; Zone 10 S UTM, 4396287N, 611463E). Releases took place at three locations, but varied from year to year. Release sites were: PPDD, Baldwin Construction Yard (approximately one mile downstream of the PPDD) and Adams Dam (approximately 7 miles downstream of PPDD). After release, marked fish were subject to recapture and sacrifice at downstream locations in Butte Creek, the Sutter Bypass and the Sacramento Delta near Chipps Island. Rotary screw traps were used to recapture fish at all locations and an off-stream fish screen outfitted with a trap box was used to collect fish at the PPDD site. Recaptured fish were sacrificed, measured for fork length and their CWTs were extracted and read. We received programmatic data formatted in a Microsoft Access database directly from the CDFW (C. Garman, personal communication, 1/30/2014).

We queried the RMIS database for juvenile Chinook that had been marked and released at any location in the Sacramento drainage. The RMIS table was then related by CWT code to Chipps Island mid-water trawl and Sacramento River recoveries. In this way, we queried recoveries with release locations only within the Sacramento Basin.

We obtained tributary measurements of juvenile lengths from rotary screw traps (RSTs) operating in Butte creek, Mill creek and Deer creek. Rotary screw traps were operated by the US Fish and Wildlife Service in Mill and Deer creeks, and by the California Department of Fish and Wildlife in Butte creek. Screw trap operation spanned 1995-2010 in the records used in this analysis. We used samples obtained from January to June of each year to obtain estimates of tributary outmigration size.

Environmental data

We compiled time series of environmental variables that pertain to the experiences of downstream migration juveniles. For Spring Run, we used discharge at the three creeks (Deer, Mill and Butte), flow, exports volumes and other export indices, and a CPUE index of bass abundance. Flow temperature and discharge were obtained from USGS gauging stations (http://waterdata.usgs.gov/nwis/inventory). Exports and other dayflow parameters were obtained from water project data available on the California department of water resources website (http://www.water.ca.gov/dayflow/output/Output.cfm). Environmental variables were normalized by subtracting the mean and dividing by the standard deviation. The variables are summarized in Table C.1 for Spring run and in Table C.2 for Fall run.

2014 **Table C.1 Environmental variables used in length and growth analysis of Spring**
2015 **Chinook.**

Covariate	Description	Location	Data Origin
Deer discharge	Average monthly water discharge (cfs) at Deer Creek	Vinna, Deer Creek	USGS 11383500 DEER C NR VINA CA
Mill discharge	Average monthly water discharge (cfs) on Mill Creek	Molinos, Mill Creek	USGS 11381500 MILL C NR LOS MOLINOS CA
Butte discharge	Average monthly water discharge (cfs) on Butte Creek	Chico, Butte Creek	USGS 11390000 BUTTE C NR CHICO CA
Yolo flow	Peak (maximum) streamflow into YOLO Bypass at Woodland, CA	Into Yolo at Woodland, CA	USGS 11453000 YOLO BYPASS NR WOODLAND CA
Bass	Index of Striped Bass abundance as number of striped bass kept. This is NOT effort standardized, but effort data is not available <1980	Delta	Marty Gingris personal comm.
GEO	The amount of water reaching the Mokelumne River system from the Sacramento River via the Delta Cross Channel and Georgiana Slough	Delta cross channel and Georgiana Slough	Dayflow: Delta Cross Channel and Georgiana Slough Flow Estimate (QXGEO)
EXP	Accounts for all water diverted from the Delta by the Federal and State governments to meet water agreements and contracts. These include Central Valley Project pumping at Tracy (QCVP), the Contra Costa Water District Diversions at Middle River (new for WY 2010; data begin on 01AUG2010), Rock Slough, and Old River (QCCC), the North Bay Aqueduct export (QNBAQ), and State Water Project exports (Banks Pumping Plant or Clifton Court Intake, QSWP).	South Delta	Dayflow: Total Delta Exports and Diversions/Transfers (QEXPORTS).
EXPIN	The Export/Inflow Ratio is the combined State and Federal Exports divided by the total Delta inflow (QTOT). EXPIN = (QCVP+QSWP-BBID)/QTOT (8)	Delta	Dayflow: Export/Inflow Ratio (EXPIN)

CD	The Dayflow parameter net channel depletion (QCD) is an estimate of the quantity of water removed from Delta channels to meet consumptive use (QGCD)	Delta	Dayflow: Net Channel Depletion (QCD)
CVP	Dayflow parameter for Central Valley Project pumping at Tracy (QCVP)	Delta	

2016

2017 **Table C.2 Environmental variables used in length and growth analysis of Fall Chinook**

Covariate Name	Description	Location	Data Origin
Keswick discharge	Average monthly water discharge (cfs) at Keswick Dam	Keswick Dam	USGS 11370500 SACRAMENTO R A KESWICK CA
Battle discharge	Average monthly water discharge (cfs) on Battle Creek	Cottonwood, Battle Creek	USGS 11376550 BATTLE C BL COLEMAN FISH HATCHERY NR COTTONWOOD CA
Battle height	Peak guage height for the water year	Cottonwood, Battle Creek	USGS 11376550 BATTLE C BL COLEMAN FISH HATCHERY NR COTTONWOOD CA
Feather discharge	Average monthly water discharge (cfs) on the Feather River	Oronville, Feather River	USGS 11407000 FEATHER R A OROVILLE CA
Feather temp	Feather River average maximum temperature from USGS gage with (daily) interploations from Sacramento, CA air temperature (1992+)	Oronville, Feather River	USGS 11407000 FEATHER R A OROVILLE CA
American temp	American River average maximum temperature from USGS gage with (daily) interploations from Sacramento, CA air temperature (~1978-1998)	Fair Oaks, American River	USGS 11446500 AMERICAN R A FAIR OAKS CA
Yolo flow	Peak (maximum) streamflow into YOLO Bypass at Woodland, CA	Into Yolo at Woodland, CA	USGS 11453000 YOLO BYPASS NR WOODLAND

			CA
Bass	Index of Striped Bass abundance as number of striped bass kept. This is NOT effort standardized, but effort data is not available <1980	Delta	Marty Gingris personal comm.
GEO	The amount of water reaching the Mokelumne River system from the Sacramento River via the Delta Cross Channel and Georgiana Slough	Delta: DCC and Georgiana Slough	Dayflow: Delta Cross Channel and Georgiana Slough Flow Estimate (QXGEO)
EXP	Accounts for all water diverted from the Delta by the Federal and State governments to meet water agreements and contracts. These include Central Valley Project pumping at Tracy (QCVP), the Contra Costa Water District Diversions at Middle River (new for WY 2010; data begin on 01AUG2010), Rock Slough, and Old River (QCCC), the North Bay Aqueduct export (QNBAQ), and State Water Project exports (Banks Pumping Plant or Clifton Court Intake, QSWP).	South Delta	Dayflow: Total Delta Exports and Diversions/Transfers (QEXPORTS).
EXPIN	The Export/Inflow Ratio is the combined State and Federal Exports divided by the total Delta inflow (QTOT). EXPIN = (QCVP+QSWP-BBID)/QTOT (8)	Delta	Dayflow: Export/Inflow Ratio (EXPIN)
CD	The Dayflow parameter net channel depletion (QCD) is an estimate of the quantity of water removed from Delta channels to meet consumptive use (QGCD)	Delta	Dayflow: Net Channel Depletion (QCD)
CVP	Dayflow parameter for Central Valley Project pumping at Tracy (QCVP)	Delta	Dayflow: Central Valley Project Pumping (QCVP)
SWP	Dayflow parameter for State Water Project exports (Banks Pumping	Delta	Dayflow: State Water Project Pumping

	Plant or Clifton Court Intake, QSWP)		(QSWP)

Length and Growth analysis

We examined environmental factors affecting length at recapture at Chipps Island of fish with known and unknown release lengths. Where length at release was known, we examined growth rates. We associated each size and growth record with environmental factors experienced by each race of salmon each year the sizes were recorded. We compared fall and spring length at capture at Chipps Island from two separate surveys. The CWT table provided an estimate of growth for fall and spring hatchery releases. The mid-water trawls did not distinguish between wild and hatchery fish, so those analyses pertain to the race as a whole, without distinction about release locations or wild/hatchery distinctions. We also obtained sizes from DJFMP seines in Region 1 (upstream from the Delta) and compared those sizes with Chipps Island size information. Since seine samples do not distinguish between populations, growth obtained from subtracting upstream seine sizes from Chipps Island trawl sizes provide estimates of aggregate Fall and Spring run sizes, but cannot distinguish between release locations or between wild and hatchery releases.

SEINE/TRAWL - growth by race from mid-Sacramento to Chipps Island.

We queried the DJFMP seine database to obtain estimates of growth for Spring and Fall runs. Region 1 of the DJFMP beach seine runs from Colusa State Park to Elkhorn. We averaged lengths of Spring and Fall seine lengths for each year for fish collected between January and June, and compared those to Chipps Island midwater trawl sizes. The trawl survey assigned fish to Fall and Spring runs based on size ranges and records indicated that all collections occurred in May and June. We calculated the growth for each race of fish each year as the difference between the average trawl length and the average seine length. We refer to these growth estimates as the SEINE/TRAWL dataset.

We examined growth patterns in relation to environmental variables listed in Tables C.1 and C.2. We performed stepwise linear regressions of growth in relation to each variable, adding variables according to best p-value, and stopping when no further significant variables were found.

CWT –growth and length by hatchery source.

When hatchery fish are released, the average size of a sample of the release batch is used as the release length of record for fish in the batch. When recaptures occur at Chipps Island, a record for each fish recaptured can be compared to a release length record on the basis of CWT codes. To get reasonable sample sizes for recaptures, we were forced to aggregate hatchery releases such that release locations were ignored. We aggregated all release locations within the Sacramento drainage for each hatchery source. Since a release batch contains a range of lengths, it is possible for the smallest recaptured fish to be smaller than the average released fish. The growth record for each year was calculated as the average of all the recapture lengths minus the average release length. The average of release length was calculated as the weighted release length, weighted by the number released at each location at each time of release. We refer to the length and growth estimates from this method as the CWT dataset.

We tested for statistical relationships between size at recapture and environmental variables for Spring and Fall hatchery releases from Coleman National Fish Hatchery (CNFH) and Feather Fish Hatchery (FFH). We examined growth and length patterns in relation to environmental variables listed in Tables C.1 and C.2. We performed stepwise linear regressions of growth and length in relation to each variable, adding variables according to best p-value, and stopping when no further significant variables were found.

TRAWL – length by race at Chipps Island.

We selected records that were not limited to CWT tagged fish (the TRAWL dataset in this analysis) from Chipps Island, and assembled all records of Spring and Fall chinook to look at the size. By not being limited to CWT matches, the sample size was much larger than for the CWT matched database, but for the TRAWL dataset, the origin of fish could not be determined. The race of the fish was assigned by a length/timing criteria established by the DJFMP (the "Race Table" found at www.fws.gov/stockton/jfmp). Using these records we looked for temporal trends, comparisons between Spring and Fall runs, and relationships between size at capture and environmental factors. Annual average size records for Spring and Fall Chinook do not distinguish between hatchery and wild, and there is no growth estimate because the size at release is not known, and there is no way to distinguish between Butte, Mill, and Deer creeks. The TRAWL dataset provides an aggregate estimate of length at Chipps Island by race alone.

We examined growth patterns in relation to environmental variables listed in Tables C.1 and C.2. We performed stepwise linear regressions of length in relation to each variable, adding variables according to best p-value, and stopping when no further significant variables were found. We treat length as a surrogate for growth on the assumption that some initial length can be treated as a constant across and all variability can be thought of as occurring after that initial length.

RST – Lengths in tributaries

Deer, Mill, and Butte creek rotary screw trap records were queried to obtain estimates of outmigrating juvenile sizes. We took the average size of all samples obtained from the traps between January and June of each migration year. We attempted to match CWT releases from Butte Creek each year to recoveries within the Sacramento basin to obtain growth estimates at various sample locations, but found that recoveries were too few to obtain good estimates of growth. Butte Creek CWT release records with Chipps Island recapture events began in 1996, but recaptures amounted to fewer than 10 fish per year at Chipps Island. It was not possible to relate RST lengths to downstream lengths at Chipps Island for a growth estimate. We therefore limited our examination of RST data to showing temporal trends of sizes of Deer, Mill and Butte creeks.

RESULTS

SEINE/TRAWL - growth by race from mid-Sacramento to Chipps Island.

The average growth of Spring and Fall Chinook are shown in Figure C.1 along with the time elapsed between Seine surveys and mid-water trawls. The temporal trend in growth is shown in Figure C.2. Fall Chinook appear to be slightly larger and on average seen in seine surveys about half of a month later. Predominantly, Fall Chinook appear to grow slightly

more between Seine and mid-water trawl surveys, which is noteworthy, since they do so in less time as seen in the average month seined calculation.

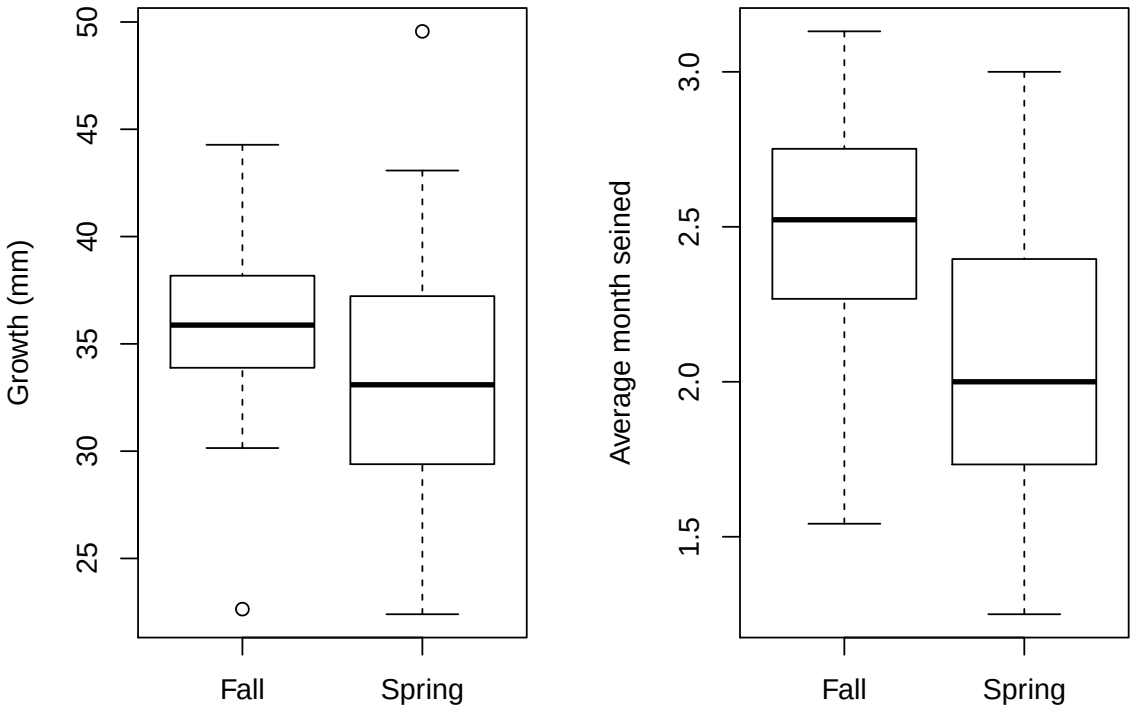

Figure C.1 Growth between release and sampling at Chipps Island (left panel) and month at which Region 1 seine was sampled (right panel).

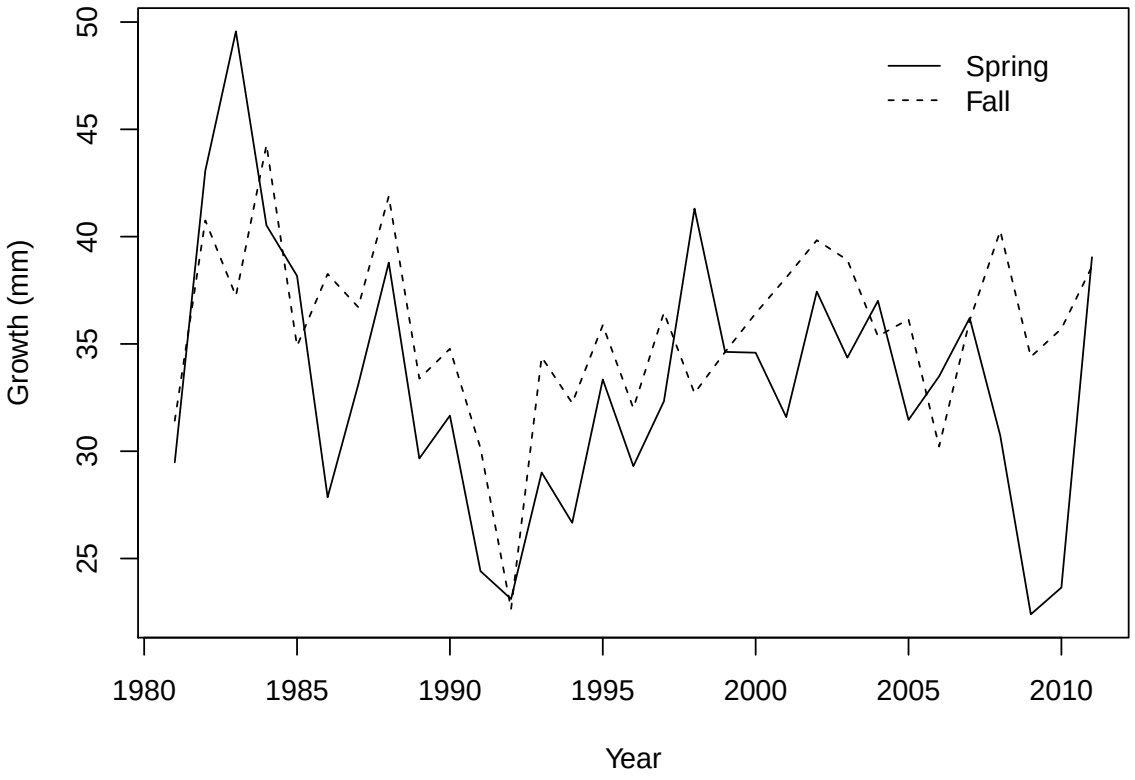

Figure C.2 Temporal trends in Spring and Fall Chinook growth evaluated from beach seine and mid-water trawl surveys.

Table C.3 shows the results of stepwise linear regressions. The regression results show that there are significant effects of Bass, Central Valley Project exports, race (spring or fall run) , and the export to inflow ratio (EXPIN). The bass index shows a positive effect on growth. Central Valley Project exports also show a positive effect, but the export to inflow ratio shows a negative effect. The adjusted R-squared value for the fit was 0.4068. The diagnostic plot of the fit is shown in Figure C.3.

Table C.3 Regression results of growth in SEINE/TRAWL data in relation to environmental variables. Intercept in parentheses.

Coefficients:	Estimate	Std. Error	t value	Pr(>|t|)	Signif
(int-Fall)	38.3357	0.9227	41.546	<2.00E-16	***
Bass	5.4229	1.3838	3.919	0.000241	***
CVP	3.8959	0.7293	5.342	1.67E-06	***
Spring	-3.5728	1.0712	-3.335	0.001503	**
EXPIN	-1.3115	0.6071	-2.16	0.034961	*

*** p<0.001, **p<0.01, *p<0.05, . p<0.1

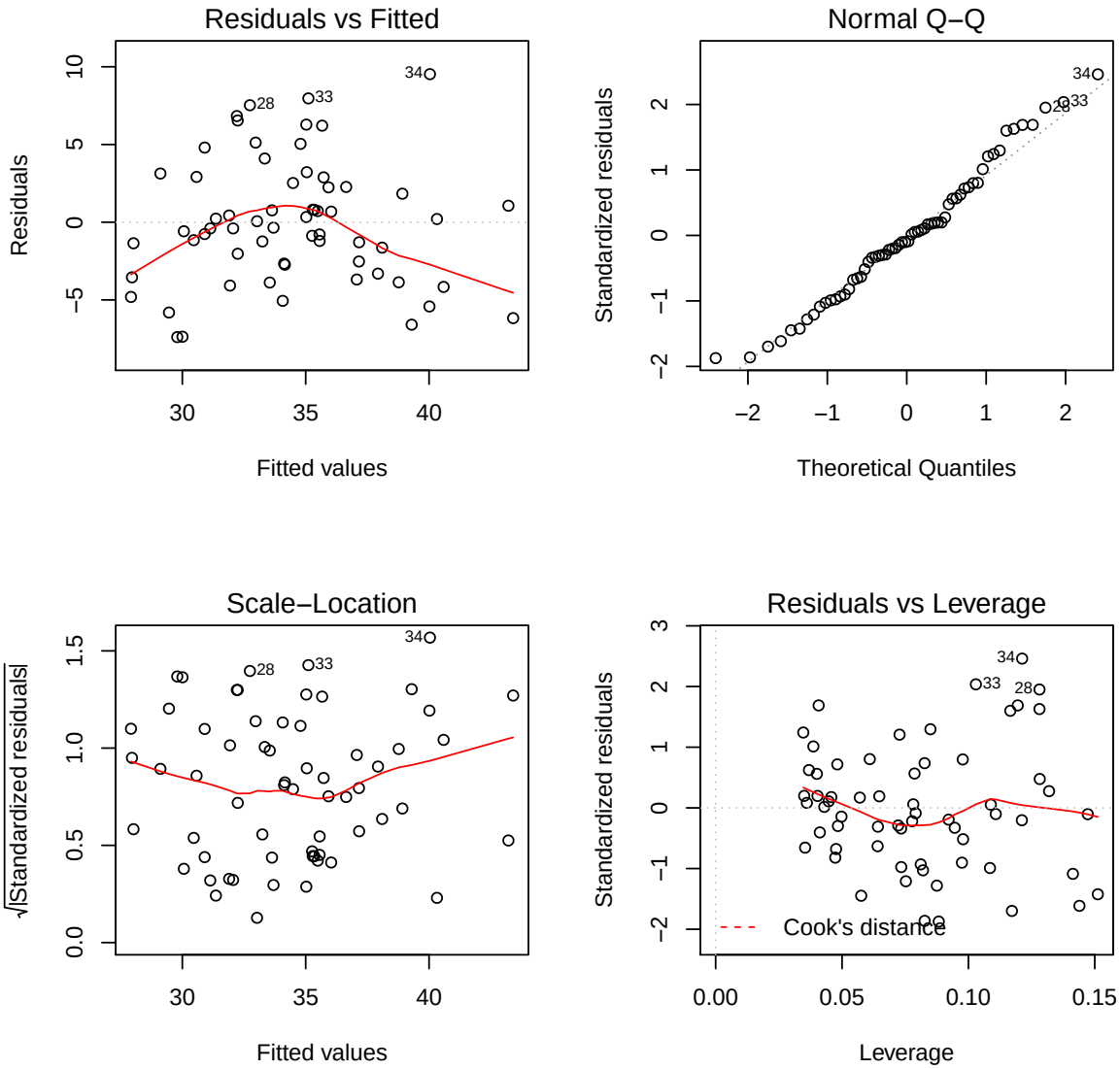

Figure C.3 Diagnostic plot of best fitting model of seine-trawl growth of Spring and Fall chinook.

CWT –growth and length by hatchery source.

Feather Fish Hatchery (FFH) spring Chinook and Coleman National Fish Hatchery (CNFH) fall Chinook growth and lengths at Chipps Island are shown in Figure C.4. We see that there is considerable variability in growth, and that Spring run fish appear to have grown faster than Fall run until the early 1990's, but are now growing less than Fall run (see Figure C.4 upper panel). Table C.4 shows the results of stepwise regressions of length against all Spring and Fall run covariates. The export to inflow ratio was the only significant predictor of catch length in the Chipps Island trawl, with EXPIN having a positive effect. The adjusted R-squared for the best fitting model shown was 0.3414. Diagnostic plots of the best fit are shown in Figure C.5, where we can see that the residuals are normal. Regressions show a

hatchery effect, finding that FFH fish arrive at Chipps Island 3.5 mm larger than CNFH fish, but FFH fish included Spring run, which were larger. Despite growth of Spring run recoveries appearing to decline from 1985, the lengths of Spring run fish at Chipps Island appears to be relatively constant. We found no significant relationships between growth and environmental variables.

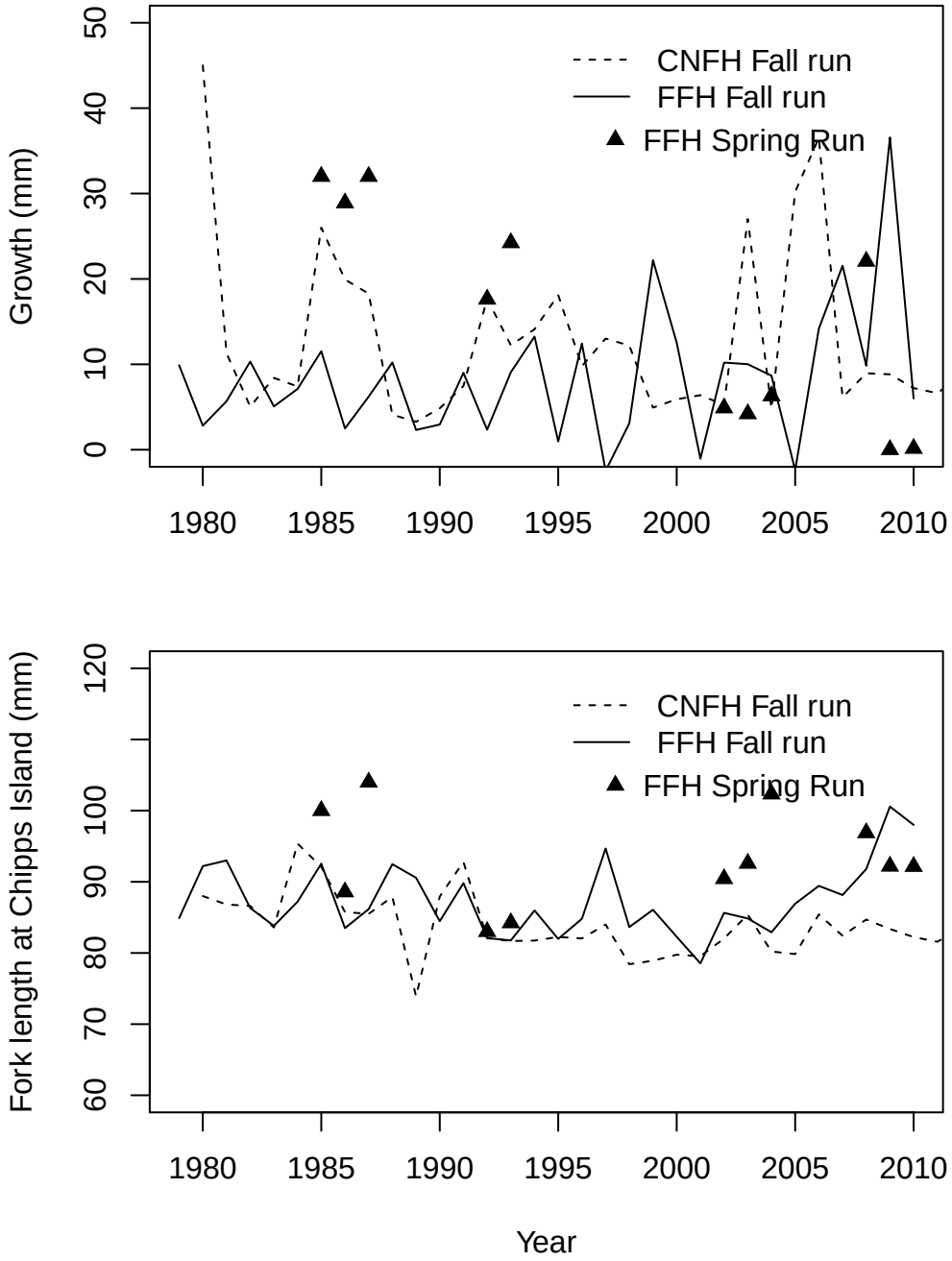

Figure C.4 Growth of CNFH and FFH Fall runs, and FFH Spring run (upper panel) and length at Chipps Island (lower panel).

Table C.4 Regression results of relationship between CWT length at Chipps Island and environmental variables. Intercept in parentheses for Fall CNFH.

Coefficients:	Estimate	Std. Error	t value	Pr(>|t|)	Signif
(Intercept)	83.8357	0.8361	100.27	<2.00E-16	***
Race Spring	5.6019	1.6816	3.331	0.00137	**
EXPIN	1.7117	0.5764	2.969	0.00405	**
Source FFH	3.4654	1.1919	2.907	0.00484	**

*** p<0.001, **p<0.01, *p<0.05, . p<0.1

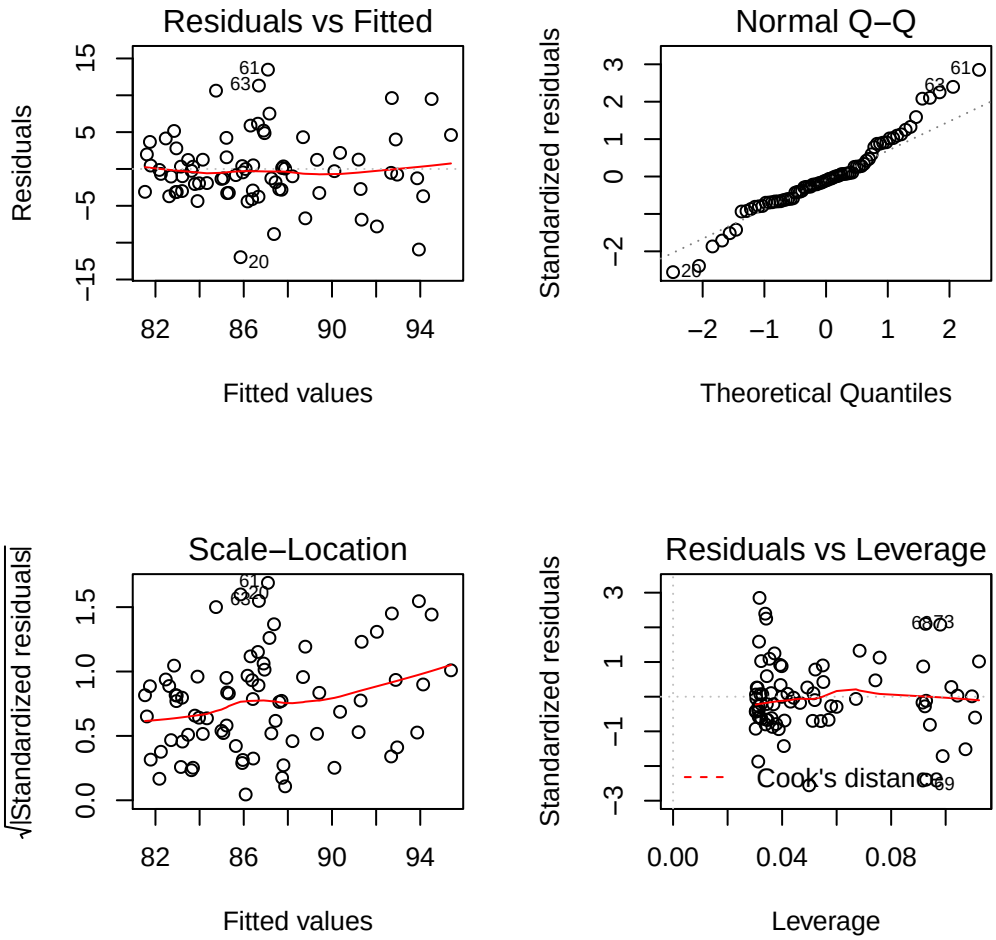

Figure C.5 Diagnostic plots of best fit of length at recapture at Chipps Island to environmental variables.

TRAWL – length by race at Chipps Island.

Unlike the CWT lengths from hatchery specific releases, the aggregated relative Spring and Fall lengths remain consistent from the 1980's until present. Spring run appear to be consistently larger that Fall run (see Figure C.6). Regression results are shown in Table C.5 and indicate that Yolo flow, the Central Valley Project exports, the export to inflow ratio, water passing via the Delta Cross Channel, and the bass index are all significant predictors of size. The Adjusted R-squared of the best fit shown is 0.785. The diagnostic plots of the best

fit is shown in Figure C.7. The TRAWL dataset had the largest samples, and despite being aggregated wild and hatchery fish, and despite not identifying source drainages, the regression results yield the highest R-squared. The diagnostics show normality in residuals as well as the majority of residuals concentrated on predicted theoretical quantiles.

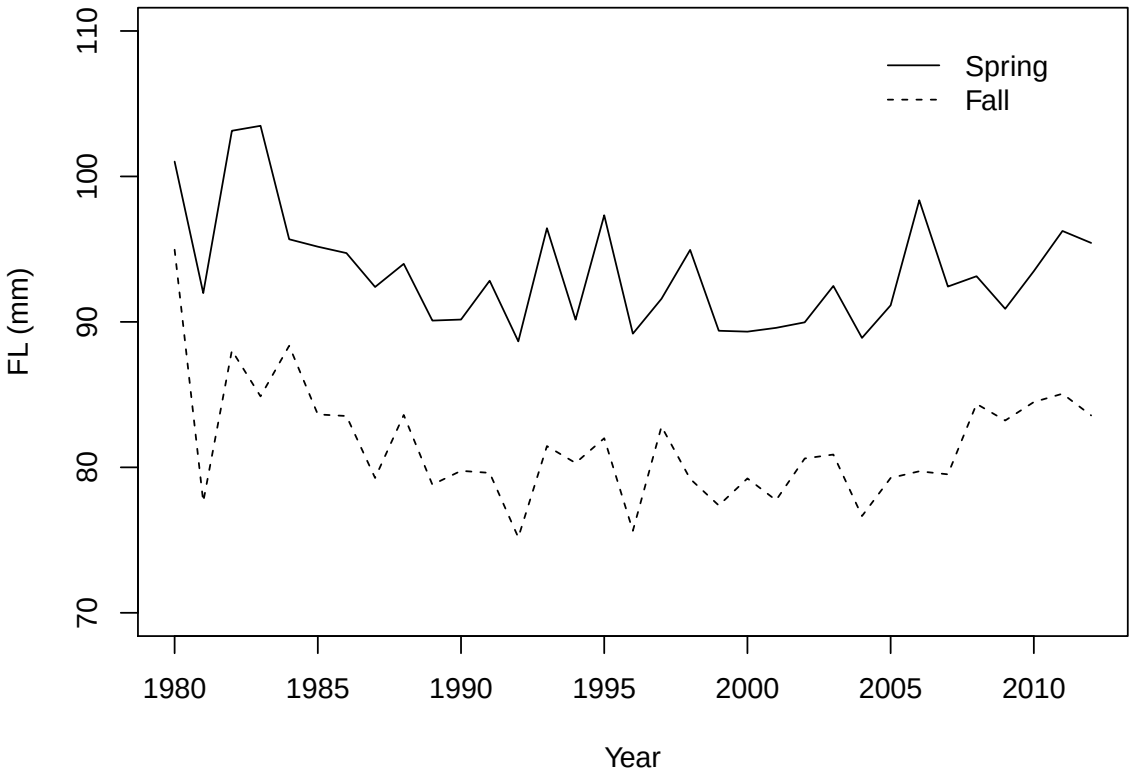

Figure C.6 Lengths of Spring and Fall aggregates at Chipps Island in TRAWL data.

Table C.5 Regression results of best fit of trawl lengths to environmental variables.

Coefficients:	Estimate	Std. Error	t value	Pr(>|t|)	Signif
(Intercept)	80.9897	0.7322	110.604	<2.00E-16	***
race Spring	11.4344	0.8359	13.678	<2.00E-16	***
Yolo flow	0.99	0.5468	1.811	0.075288	.
CVP	2.6729	0.7082	3.774	0.000375	***
EXPIN	-2.5741	0.7566	-3.402	0.001206	**
GEO	-1.4716	0.6551	-2.246	0.028449	*
BASS	-1.8643	1.0438	-1.786	0.079228	.

*** p<0.001, **p<0.01, *p<0.05, . p<0.1

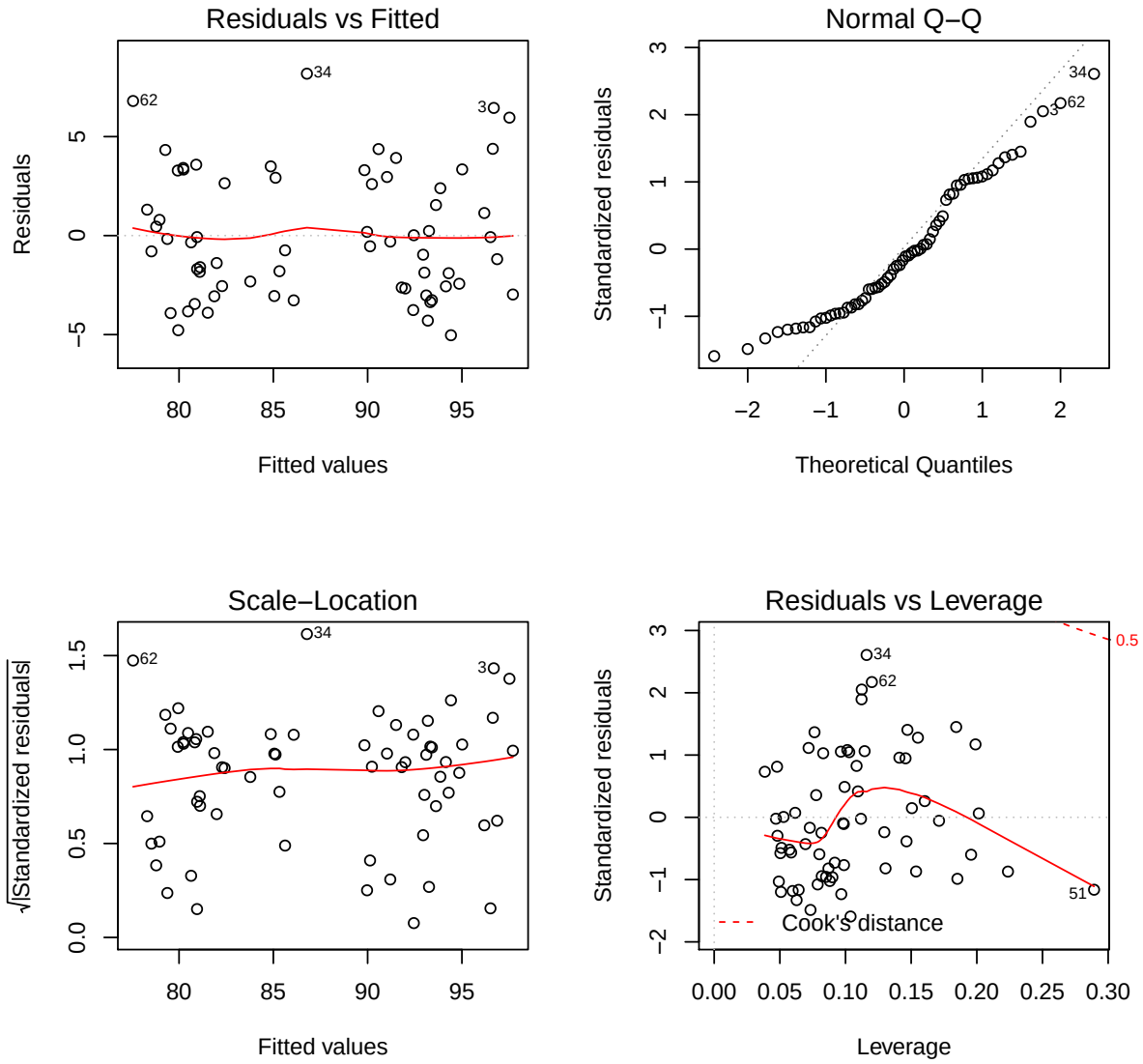

Figure C.7 Diagnostic plot of best fitting model of relationship between length at Chipps Island mid-water trawl and environmental variables.

RST – Lengths in tributaries

Mill, Deer, and Butte creek Spring run average fish sizes from rotary screw trap operations are shown in Figure C.8. We see that Mill, Deer and Butte creeks are on average about 45-55 mm in length between January and June when records were aggregated for outmigration estimates. The temporal pattern in sizes is shown in Figure C.9. We see no major trend in size in tributaries between January and June, only that Butte creek fish appear to run a bit smaller.

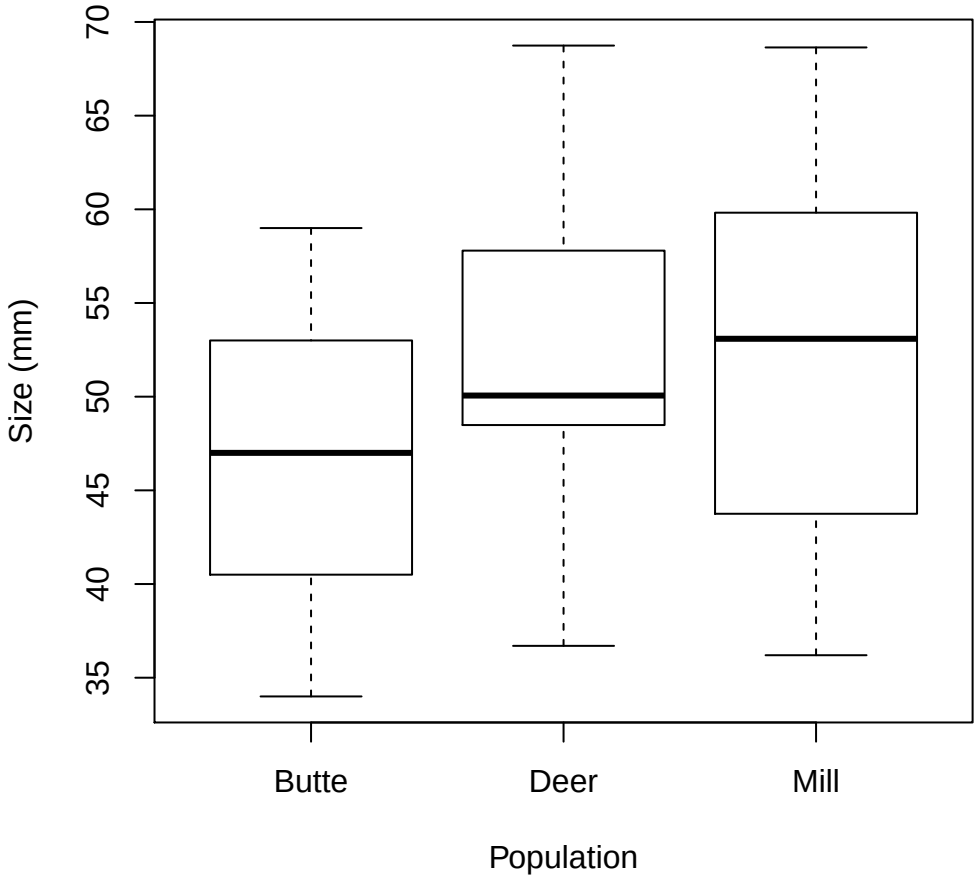

Figure C.8 Average size of juveniles obtained from rotary screw traps operating in Butte, Deer and Mill creeks between January and June.

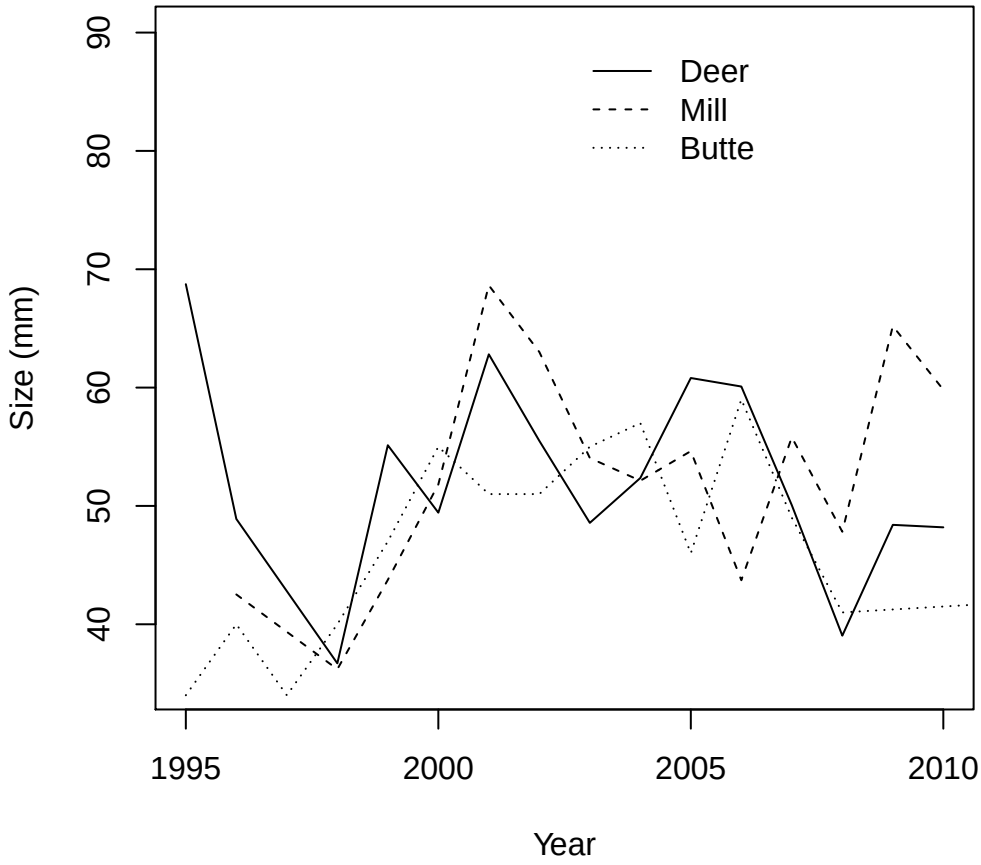

Figure C.9 Temporal trend in juvenile sizes obtained from rotary screw traps operating in Deer, Butte and Mill creeks between January and June.

DISCUSSION

This analysis drew upon varied sources of fish length information in the Sacramento River drainage. The summary of rotary screw trap lengths indicates that Spring run out-migrating Chinook from Deer, Mill and Butte creeks are approximately the same size, and have been stable at approximately 55 mm in recent years. Regression analysis of recoveries from mid-water trawl surveys at Chipps Island indicates that growth of fish from North of the Delta to Chipps Island, as well as the length at recapture in Chipps Island trawls varied in relation to environmental variables. Regression analyses showed that the length at Chipps Island from the perspective of two different types of length statistics proved to be related to environmental variables regardless of the data source of the length estimates.

We used two different growth metrics. One growth metric came from lengths of CWT recoveries and releases of hatchery fish, and the other came from seine and trawl surveys. The CWT growth was derived from average recovery length at Chipps Island and average release lengths at various release locations and times. The average recovery length is a statistic based on a very small sample size relative to the release length statistic. If you

consider the how many fish are released relative to recaptured, and if you consider that tagged fish are released at various locations and at different times, it is easy to see how biased the growth estimate might be. The SEINE/TRAWL growth estimate made no distinction between hatchery and non-hatchery fish and it represents an estimate of the growth of all Fall or Spring run fish between Region 1 seines and Chipps Island. In comparison to the CWT estimate, it will be more complex in it's stock composition (with hatchery and non-hatchery fish of all origins), but it is much simpler in upstream capture and release size sampling. All stocks were sampled from the same locations for sizing regardless of origin. We found a relationship between SEINE/TRAWL growth and environmental variables, but no relationship between CWT growth and environmental variables. This may be due to the complexity of how the release length was calculated for the CWT growth estimate.

The environmental predictors that best explained growth were the Central Valley Project exports (CVP), the ratio of combined state and federal exports to the total Delta inflow (EXPIN), and the bass index. CVP and EXPIN are both related to flows in complex ways. CVP is related to flow because exports would tend to be less restricted at higher flows, but would have its highest impact when flows are low. We would expect that juvenile salmon growth could be high when CVP is highest under that logic. EXPIN is related to flow by a similar logic, but since EXPIN is a ratio, we would expect the largest fraction of flows to be exported when flows are low (for a given level of exports). We would expect juvenile salmon growth to be lowest when EXPIN is highest at the lowest flows.

Figure C.10 illustrates some the general patterns in environmental covariation. In the upper left panel we see that CVP has the greatest degree of variability at the lowest flows (with Yolo flow being used as a surrogate for average flow at export locations). Across a range of flow values we can see that the lower bound of CVP increases. This is consistent with a general tendency of reducing exports at lower flows. The relative impact of exports at a given flow is seen with EXPIN, which we see (lower left) diminishes at higher flows. We also see that more water reaches downstream to the Mokelumne river when EXPIN is lower (lower right panel). Finally, there is a general pattern of CVP being larger when EXPIN is higher, but recall that the highest EXPIN may coincide with low flows.

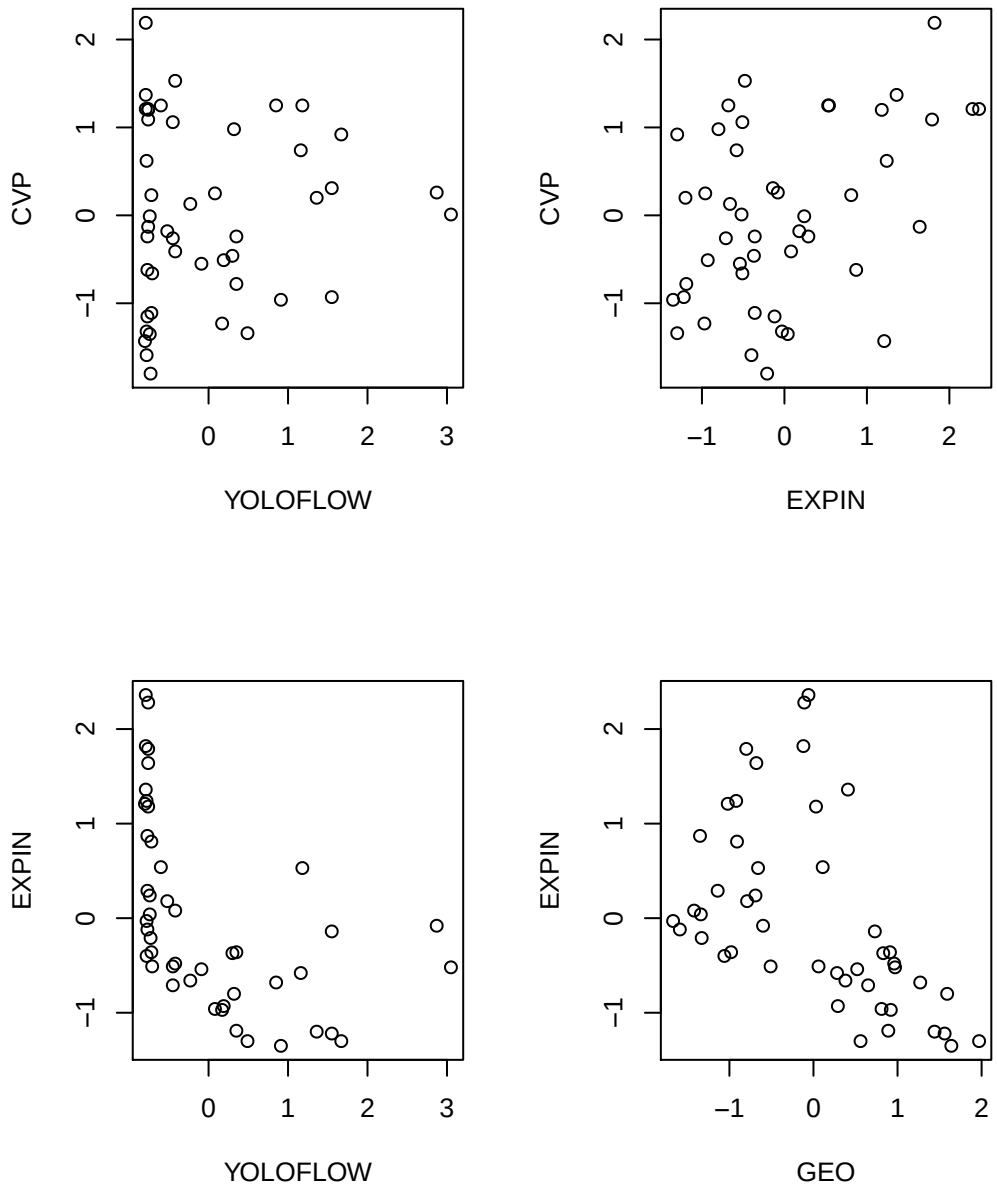

Figure C.10 Covariation between significant environmental predictors.

EXPIN was a significant predictor of length when both CWT and TRAWL datasets were used. It was significant with $p<0.01$ in both cases. EXPIN was also a significant predictor ($p<0.01$) of growth estimates of Fall and Spring aggregates obtained from the SEINE/TRAWL dataset. The CWT length regression is in conflict with the SEINE/TRAWL growth regression and the TRAWL length regression though. The CWT result predicts a positive effect of EXPIN, versus a negative effect for the other two regression analyses. A possible reason for this would be that the CWT dataset was exclusively measuring hatchery fish (although hatchery fish would also have been present in the other two analyses). If EXPIN has a positive effect on hatchery fish length at Chipps Island as shown in the CWT length regression, and a negative effect on the aggregate of both hatchery and non-hatchery fish seen in the TRAWL length and SEINE/TRAWL growth analysis, it might suggest that that the negative effect on non-hatchery growth is even stronger than seen in the TRAWL

surveys. It could also be a size related issue. If hatchery fish are smaller and more vulnerable to entrainment, removal of the smaller fish from the outmigrating cohort would make it appear as if they grew on average, when in fact it was just the smaller ones that did not make it into the downstream survey sample.

The relationship between flows and exports, and resulting growth and survival are complex. We found that growth and length are negatively related to EXPIN, but positively related to CVP. A possible mechanism, is that there is a threshold flow/export relationship where in smaller fish become more vulnerable to entrainment. Such a mechanism would predict that more larger fish than smaller fish make it downstream to be sampled at Chipps Island, which has the effect of making the growth appear larger on the basis of the average recovery size. This would appear to be favorable growth conditions despite the fact that all individuals did not grow better on those conditions. If a relatively high CVP export year were where to coincide with an average flow year, and if more small fish were entrained, it would appear that fish where larger at Chipps Island.

Results also indicated that Spring run were longer at Chipps Island, despite the fact that the SEINE/TRAWL regression showed that Spring run growth was less than Fall run. Total Central Valley Projects (combined state and federal) exports showed positively effect on growth in the SEINE/TRAWL regression and length in the TRAWL analysis. Since there was a negative effect from the export to inflow ratio, it may be suggest that total flows have a positive effect, and that there may be a relationship between exports and flows that is dictated by water extraction policies.

It is interesting that regression results show that bass has a positive effect on the growth estimates evaluated from the SEINE/TRAWL, yet has a negative effect on lengths estimated from the TRAWL data. Since the bass index is not standardized to effort, it can't imply a direct predation rate change on a size class of Chinook juveniles, but depending on the relationship between the index and the size of the bass caught, it might imply a shift in the size of Chinook vulnerable to bass predation at a given abundance of bass. It could be that smaller fish are more vulnerable and predation biases the growth estimate by removing smaller fish.

Our examination of length/growth sensitivity to environmental variation points to a few results. First, EXPIN is a statistically significant predictor of size and growth, with a negative effect on both. Our samples conflate the story a bit, but if you consider that the only positive effect was seen in the length of hatchery fish, and if you consider that the CWT dataset had race and hatchery factors, the positive effect of EXPIN in the regression result of the CWT data should not detract from the regression results found in both the SEINE/TRAWL and TRAWL dataset. It should be noted however, that the highest regression coefficient value for an environmental effect in any of our regressions was about 5, meaning that about 5 mm per standard deviation was the maximum variability in size predicted by variability in an environmental effect. This implies that at the extreme of 2 standard deviations, only 10 mm of net difference in size at Chipps Island would be predicted. Still, two standard deviations explains about 95% of the variation in environmental factors, and 10 mm explains 10-15% of the variability in length at Chipps Island (assuming 85 mm length at Chipps Island). Since the same environmental variables explain significant variation in rearing survival, it is feasible that length may be an instrumental in the mechanism of rearing survival.

REFERENCES

Brandes, P.L. and J.S. McLain. 2001. Juvenile Chinook salmon abundance, distribution, and survival in the Sacramento-San Joaquin Estuary. Pages 39 – 138 *in* R.L. Brown, editor. Contributions to the Biology of Central Valley Salmonids, Volume 2, Fish Bulletin 179. California Department of Fish and Game, Sacramento, California.

California Department Of Fish And Game. 1998. Butte Creek Spring-Run Chinook Salmon, *Oncorhynchus Tshawytscha*, Juvenile Outmigration And Life History 1995-1998. Administrative Report No. 99-5.

California Department Of Fish And Game. 2000. Butte And Big Chico Creeks Spring-Run Chinook Salmon, *Oncoryhnchus Tshawytscha* Life History Investigation 1998-2000. Administrative Report No. 2004-2.

California Department Of Fish And Game. 2004. Butte And Big Chico Creeks Spring-Run Chinook Salmon, *Oncoryhnchus Tshawytscha* Life History Investigation 2000-2001. Administrative Report No. 2004-3.

Garman, C.E and T. R. McReynolds. 2008. Spring-Run Chinook Salmon, Oncoryhnchus tshawytscha, Life History Investigation. California Department of Fish and Game. Inland Fisheries Administrative Report No. 2009-1.

U.S. Fish and Wildlife Service – Stockton Fish and Wildlife Office. March 2014. Metadata for the Stockton Fish and Wildlife Office's Delta Juvenile Fish Monitoring Program. http://www.fws.gov/stockton/jfmp/.

Appendix D Modeling the influence of historical factors on population dynamics of salmon: the OBAN model

DRAFT

A.N. Hendrix[1], R. Hilborn[2], W. Kimmerer[3], and B. Lessard[4]

[1]QEDA Consulting, LLC, 4007 Densmore Ave N., Seattle, WA, 98103 noblehendrix@gmail.com

[2]School of Aquatic and Fishery Sciences, University of Washington,1122 Northeast Boat Street, Seattle, WA 98105

[3]Romberg Tiburon Center, San Francisco State University, 3152 Paradise Drive, Tiburon, CA 94920

[4]Columbia River Inter-Tribal Fish Commission, 700 NE Multnomah St Suite 1200, Portland, OR 97232

December 20, 2014

Abstract

We developed a general state-space modeling framework to evaluate the influence of factors on trends in abundance of multiple life-history stages of salmon. The model utilizes Beverton-Holt transitions among life stages, and incorporates factors into the transitions by modeling the dependence of the Beverton-Holt productivity p (survival) and capacity K parameters as functions of driving factors. We estimated model coefficients in a Bayesian framework to provide inference on factors hypothesized to affect the population dynamics by fitting to indices of abundance. We call the modeling framework Oncorhynchus Bayesian Analysis (OBAN), and we applied it to winter run Chinook in the Sacramento River, California, a salmon run listed as endangered in 1994. Using the OBAN framework we were able to place probability statements on the relationships between certain environmental and anthropogenic factors and winter-run population dynamics. We found that temperatures and minimum flow in the spawning reaches and ocean productivity had a high probability of affecting survival (≥ 0.8), whereas water diversions and water routing had lower

probabilities of affecting survival. The OBAN framework provides a means for understanding how historical management of hydrology and harvest coupled with environmental variability shape the trends in abundance, and thus facilitates understanding how future management actions may affect population recovery.

Keywords: state-space, WinBUGS, Bayesian, winter-run, California, water management

Introduction

Recovery of endangered animals requires an analysis of the factors responsible for affecting the population dynamics historically and modifying those factors to facilitate recovery of the population. This is particularly true of salmon populations that have seen decreases in their abundances through the majority of their range, but particularly in the southerly portions of their distribution (NMFS 2014). Understanding what factors have lead to the decline in abundances is an important step toward developing future management actions. Incorporation of uncertainty is important when evaluating these factors to be able to identify the level of confidence that one has in the relationship between historical factors and changes in population abundance. An additional complication arises when abundance measurements are made with relatively poor accuracy. Furthermore, natural variability in the population dynamics (i.e., spawner recruitment relationships) may obfiscate the signal between causative factors and the response of the population to such factors. To address these needs, we developed a state-space modeling framework that is capable of reflecting uncertainty in the factors affecting salmon population dynamics.

The population dynamics uses stages to structure the chronology of factors affecting different portions of the life cycle with density dependence among stages described by Beverton-Holt transitions (Moussalli and Hilborn 1986, Scheuerell et al. 2006, Greene and Beechie 2004). The dynamics incorporate process noise to reflect natural variability in the dynamics of the population and an observation process that describes a state-space modeling framework (Newman et al. 2014). Although the parameters of such models can be estimated using maximum likelihood methods (Maunder et al. 2011) we estimate the model parameters in a Bayesian framework to allow prior knowledge and the observation process to inform the parameter estimates (i.e., using posterior distributions to integrate information from these two sources). Fitting such non-linear state-space models in a Bayesian context is becoming relatively commonplace (King et al. 2010, Newman and Lindley 2006) and this is an extension of those methods.

The development of this modeling framework arises from a practical problem related to a population that

may have a moderate probability of extinction (Lindley et al. 2007, Botsford and Brittnacher 1998). The Sacramento River winter-run Chinook (*Oncorhynchus tshawytscha*) currently listed as endangered under the Federal and California Endangered Species Acts, and it has seen a decline in escapement since the 1970's. Like many salmon populations in decline, a list of factors that could potentially affect winter-run (and other salmon transiting the Sacramento River and the San Francisco Delta) have been compiled. Some of these factors include: 1) thermal mortality of eggs and alevin in the spawning reaches; 2) flow related survival after emergence; 3) rearing in off-channel areas such as the Yolo bypass (Sommer et al. 2005); 4) entrapment into the interior delta due to positioning of channel flow gates (Perry et al. 2010); 5) alterations in the outmigration flow vectors due to exportation of water from the system (Newman and Brandes 2010; Newman 2003); 6) predation from piscivorous fishes such as striped bass (*Morone saxatilis*) (Newman and Lindley 2006). Salmon exiting the Bay-Delta ecosystem enter the Gulf of the Farallones and transition to a near-shore environment with annual variability in productivity tied to the strength and location of upwelling (Wells et al. 2007). Once winter-run attain an age of 3 years (2-ocean), they are vulnerable to the west coast salmon fishery that primarily targets fall-run Chinook from the Klamath River, OR and Sacramento Rivers but also catches winter-run (O'Farrell 2012); however, timing and area closures to minimize fishery impacts on winter-run have been in place since the late 1990's (O'Farrell 2012). Yet, the ability to quantitatively evaluate the importance of all of these factors for explaining trends in winter-run escapament has not occurred.

The objectives of our work is to provide a general overview of the Onchorynchus Bayesian Analysis (OBAN) modeling framework and to provide an analyiss of the winter-run Chinook in the Sacramento River as an example of how the framework was utilized.

Methods

Population Dynamics Model

The OBAN modelling framework provides a quantitative tool to evaluate historical patterns in salmon abundance as a function of hypothesized explanatory factors. Specifically, the model: 1) estimates model coefficients by fitting predictions of the population dynamics model to observed indices of abundance; 2) evaluates factors that may explain dynamic vital rates; 3) accounts for mortality during all phases of the salmon life history; and 4) incorporates uncertainty in the estimation of model coefficients by fitting in a Bayesian framework.

The first step to the modeling framework is to define the life-history stages. The OBAN model structure

can define life-history stages based on management objectives, such as important locations of anthropogenic or environmental driving factors by the locations where indices of abundance are observed. The number of life-stages is application specific, but it has to incorporate at least two stages for freshwater (egg and juvenile stages), and an ocean stage for each age of returning adult (e.g., a stage for each of the age $2, ..., L$ ages of escaping adults). The OBAN model uses temporally implicit stage durations. Each freshwater stage may be defined such that it reflects the duration that the salmon are within that stage, thus stages do not need to be the same duration. As a consequence, inference on the population vital rates for that stage are predicated on its duration.

The OBAN framework begins with eggs as the first stage and defines the egg abundance as a function of the escapment.

$$N_{1,t} = E_t \times f_t \tag{D.1}$$

where $N_{1,t}$ is the first stage (egg) abundance, E_t is the escapement, and f_t is the fecundity at time t. If only females are being modeled, then the fecundity reflects estimates of eggs per female. Alternatively, if escapement is not sex-specific then fecundity can be defined in terms of fecundity per adult.

The OBAN framework uses Beverton-Holt transitions to calculate the density-dependent transition in abundance among freshwater life stages $(1, ..., M)$ after the egg stage.

$$N_{i,t+1} = N_{i,t} \times \frac{p_{i,t}}{1 + \frac{p_{i,t} N_{i,t}}{K_{i,t}}} \tag{D.2}$$

where $p_{i,t}$ is the productivity parameter, $K_{i,t}$ is the capacity parameter of the Beverton Holt transition and $K_{i,t}$ is the capacity parameter for stage $i = 2, ..., Q$ in year t. Because the production of eggs is captured in equation (1), productivities are equivalent to survival rates in the absence of density dependence and are confined to the range $(0, 1)$. If density dependence is not expected to occur between two stages, the $K_{i,t}$ parameter can be set to a large value to effectively remove the density-dependent portion of the equation.

The productivity parameter ($p_{i,t}$) and capacity parameter ($K_{i,t}$) in a given life stage i from brood year t can be modeled as 1) a constant value; 2) as a constant value with annual variation via random effects; or 3) as a dynamic rate with dependence on a set of time-varying covariates ($X_{j,t}$ for factor j in year t). By using the final formulation, the influence of anthropogenic and environmental factors on specific life history stages can be evaluated. The productivity parameter can be influenced by independent factors acting simultaneously on the life history stage to drive demographic rates, for example environmental variables that represent

water conditions such as temperature or flow, biotic factors such as predator abundance, food abundance, or anthropogenic factors such as diking, water diversions, and harvest.

The dynamic productivities are modeled as a function of various factors by using a logit transformation, which ensures that the productivities remain between 0 and 1.

$$\text{logit}(p_{i,t}) = \sum_{j=1}^{F} \beta_j X_{j,t} \tag{D.3}$$

where β_j is the coefficient associated with factor $X_{j,t}$.

Likewise, there may be processes occuring that affect annual stage-specific capacities, such as the amount of available spawning area or the amount of flooded off-channel rearing habitat. To model the dynamic capacities, a log transformation is used, which causes the capacities to remain between 0 and ∞, which is the appropriate parameter space for capacity.

$$\log(K_{i,t}) = \sum_{j=1}^{F} \gamma_j X_{j,t} \tag{D.4}$$

where γ_j is the coefficient associated with factor $X_{j,t}$.

After Chinook enter the ocean, they mature and can return to spawn after a single summer or after overwintering in the ocean for multiple years (Healey 1991). When Chinook enter the ocean, we shift the notation to O_{age} to reflect the fact that some Chinook will remain in the ocean, whiles others will mature and migrate back to freshwater after escaping the fishery. The transition from juvenile rearing to ocean stages occurs via the following transition equation

$$O_{2,t} = N_{M,t} \times \frac{p_{M,t}}{1 + \frac{p_{M,t} O_{i,t}}{K_{M,t}}} \tag{D.5}$$

Maturations of ocean stages for ages $2, ..., L$ are calculated using the following equation:

$$M_{t+age} = O_{age,t} \phi_{age} z_{age} \tag{D.6}$$

where M_{age} is the maturation of the adults at a specific age returning to freshwater according to the conditional maturation rate ϕ_{age}. The number of fish remaining in the ocean $O_{age,t}$ is a function of those that remain and survive to the following year. Because harvest is one of the major sources of mortality in the ocean stages, the above formulation assumes that harvest occurs before maturation; however, this order could be altered to reflect the specific dynamics of the stock of Chinook being modeled.

$$O_{age+1,t} = (1 - h_{age,t})(1 - \phi_{age})O_{age,t} \times \frac{p_{age,t}}{1 + \frac{p_{i,t}O_{age,t}}{K_{age,t}}} \tag{D.7}$$

In the final stage, all Chinook of age L return, thus $M_{t+L} = O_{L,t}$. Survival and capacities can be modelled in the ocean stages just as in the freshwater stages to reflect the effects of localized nearshore productivity. Furthermore the conditional maturation rates may also be modeled as a function of factors using logistic regression. For example, due to differential size at ocean entry or size at release in the case of modeling a hatchery population.

$$\text{logit}(\phi_{age,t}) = \sum_{j=1}^{F} \delta_j X_{j,t} \tag{D.8}$$

where δ_j is the coefficient associated with factor $X_{j,t}$.

Finally, the escapement in calendar year y is the sum of the mature fish returning from the ocean at ages $2, ..., L$ from brood years $y - 2, ..., y - L$.

$$E_y = \sum_{age=2}^{L} M_{age,t} \tag{D.9}$$

Process noise can be added to the stage-specific survivals and capacities by allowing them to vary as a random effect. For example, extra variability could be incorporated through a residual error term in either equation (1) or equation (2) to add variability in the production (fecundity) relationship or in the stage transitions, respectively. To implement process noise, stage-specific random effects, e.g., $Z_{i,t}\ N(0, \sigma^2_{i,p})$ can be added to the equation to express annual variation, where $\sigma^2_{i,p}$ reflects the variance due to process noise in stage i. The amount of process noise may require some additional structure (e.g., through prior specification), otherwise, all the observed data may ostensibly be fitted exactly by allowing the variance in the process noise to be sufficiently large.

Finally, the timing of the influence of factors has to be matched with the timing of the life stages such that the factors are affecting the appropriate cohort. The time subscript t refers to the brood year, thus the covariates, which are typically provided by calendar year y, are lagged appropriately for the population under study.

Bayesian Estimation

Estimation of the model parameters occurs by comparing model predictions to observed data across multiple competing "states of nature" or parameter values. This is achieved through Bayesian estimation of the likelihood of observing the data times the prior probability of the model parameter values (Gelman et al. 2004). The general framework described above is used to compute predicted abundances that are then compared with observed abundances obtained through some sampling method. As a result, a sampling model is defined for each observation. The stage abundances are related to the observed indices of abundance through a sampling model $g()$. The framework is relatively flexible in that any type of sampling data can be incorporated by specifying an appropriate sampling model. Multiple types of abundance indices, $I_{i,k,y}$ for stage i of index type k in year y, can be included in the modeling framework by defining the observation process $g()$ as a function of the sampling model and observation error σ_k^2. For example, the observation process $g()$ could be defined as a lognormal for abundances or biomass, Poisson or negative binomial for counts, or Binomial for capture-recapture studies. Note that if the observation process is modeled with lognormal errors, the variance can be defined in terms of the coefficient of variation (CV = mean/standard deviation) as $\sigma_k^2 = \log(CV_k^2 + 1)$.

$$I_{i,k,t} \sim g(N_{i,t}, \sigma_k^2) \tag{D.10}$$

Priors

Prior probability distributions are required for all model coefficients that are estimated within the modeling framework. For example the coefficients of the logistic regression to define stage-specific survival rates (β_j's) and coefficients of the log-linear model (γ_j 's) to define stage-specific capacities will require prior probability distributions; normal distributions can be used to define the prior probabilities for both of these coefficients due to the transformations used in equations (3) and (4). Care should be taken in specifying the priors for the β coefficients given their inclusion into a logit() transformation, however. King et al. (2010) suggest that N(0,2.5) priors may be used in the coefficients of logistic regression to ensure that excessive mass is not placed in the values near 0 and 1 (as might be the case with a more diffuse normal prior). The conditional maturation rates ϕ_{age} are required to be in the interval $(0, 1)$; therefore, Beta distributions can be used as priors for these coefficients. Finally, the variance of the measurement error on the observation process (σ_k^2) and the variance of any process noise ($\sigma_{i,p}^2$ for stage i) will also require a prior and can be specified as either

inverse gamma on the variance or alternatively as a uniform prior on the standard deviation of the variance (Gelman et al. 2006).

Implementation of Bayesian Estimation

The posterior distributions of the model parameters can be estimated by drawing samples from the full conditional distributions of each parameter given values of all other parameters through a Metropolis within Gibbs Markov Chain Monte Carlo (MCMC) approach (Gelman et al. 2004, Gilks and Spiegelhalter 1996). If conjugate priors are used, then the Gibbs sampler can be employed; however, if posterior distributions for the parameters can not be updated using the Gibbs sampler (Roberts and Polson 1994), they can instead updated by using distribution-free adaptive rejection Metropolis steps (Gilks and Spiegelhalter 1996, Spiegelhalter et al. 2003) which is the approach adopted in WinBUGS (Spiegelhalter et al. 2003).

To evaluate if the posterior draws were arising from a stationary target distribution, multiple chains were run from dispersed initial values for each model and the scale reduction factor (SRF, Gelman et al. 2004) was computed for all monitored quantities (model coefficients and abundance estimates). The diagnostics were implemented using the R2WinBUGS package (Sturtz et al. 2005) in R (R Core Team 2013). Monitored parameters in all models had SRF values that indicated samples were being drawn from the target distribution (i.e. SRF ≈ 1) by 75,000 samples (Gelman and Rubin 1992). The initial 50% of the samples were used to reach the stationary target distribution and were discarded with the subsequent samples thinned to produce approximately 1,000 draws from the stationary target distributions. The 1,000 draws were used to compute the posterior mean and symmetric 95% probability intervals or credible intervals (95% CrI).

Application of Model to Winter Run Chinook

We defined 7 life-history stages in the winter-run OBAN model including 6 freshwater and marine transition stages and 3 annual ocean stages: 1) eggs, 2) fry 3) juveniles in the Delta (delta), 4) juveniles in the Gulf of the Farallones (gulf) 5) age 2 in the ocean, 6) age 3 in the ocean, and 7) age 4 in the ocean. The escapement was composed of mature individuals that returned at age 2, 3, and 4 (Table D.1).

Fecundity was assumed to vary annually, and the annual values were sampled from probability distribution, i.e., $f_t \sim logN(\mu_f, \sigma_p^2)$. This formulation allowed process noise to be incorporated into the population dynamics, but empirical information on fecundity restricted the range of process noise in the model. Multiple environmental and anthropogenic factors were incorporated into the winter-run model at different stages in the life-history based on hypotheses about factors affecting (Table D.2). The mean fecundity is calculated

by assuming that each adult spawner produces 2,450 eggs (Williams 2006, Winship et al. 2014).

Winter Run Abundance Indices

Estimates of winter-run escapement in the Central Valley have been conducted since 1967, and we used an escapement abundance index from 1967 to 2008. Different methods were used to estimate escapement over this period, which may affect the precision of the spawner escapement estimates (Williams 2006, Botsford and Brittnacher 1998). Prior to 1987, all returning spawners passed via a counting ladder at Red Bluff Diversion Dam (RBDD, Figure D.1). From 1987 onward the gates of the diversion dam have been opened to enhance upstream survival of winter-run Chinook salmon, but also likely improved access to areas above RBDD. The current operation of RBDD makes counts of winter-run Chinook salmon after closing the gates on May 15. On average, 15% of the winter run passed RBDD by May 15, but the specific percentage in a given year was as low as 3% or as high as 48% (Snider et al. 2000). Since 2001 the annual escapement estimates have been calculated using a Jolly-Seber estimator derived from the carcass count data (California Department of Fish and Game 2004). Juvenile production indices were calculated from rotary screw trap samples and trap capture probabilities at Red Bluff Diversion Dam for 1995 through 1999 and 2002 through 2008 (Poytress and Carrillo 2011).

Winter Run Factors

Several environmental and anthropogenic factors were used to help describe variability in winter-run juvenile and adult abundance indices (Table D.2). Because the abundance indices occur at RBDD, which coincides with the fry stage, a basal survival rate could be estimated for the egg to fry stages and a second basal rate for the fry to escapement stages. Explanatory factors were incorporated into the survival during the fry stage, delta stage, and gulf stages (Table D.2). We provide a short rationale for the inclusion of each of the factors here.

Water temperatures in the spawning reach above RBDD can sometimes reach stressful levels, thus July through September mean daily water temperature (C) in the Sacramento River at Bend Bridge (TEMP) was used to explain annual variability in egg to fry survival. In addition, low flow can affect survival rates of alevin, so August through November minimum monthly flow in the Sacramento River at Bend Bridge was also used to affect egg to fry survival. In addition, an interaction term of TEMP:FLOW was incorporated into the model to determine if there was some additional mortality associated with either high temperatures or low flow.

In the delta stage, several factors may affect winter-run survival rates. Access to the Yolo bypass, a large floodplain that provides the potential for increased survival and growth of fall-run Chinook (Sommer et al. 2005), may also provide similar benefits for winter-run via bypassing the delta. The Yolo bypass floods when flows on the Sacramento River surpass 56,000 cfs; each day when flows were great enough to enter the Yolo bypass between December and March was a potential opportunity for winter-run to enter the floodplain habitat (YOLO). The Delta Cross Channel is a dual gate structure that conveys water to the interior delta, and late-fall Chinook salmon that enter the interior delta have lower survival rates relative to those that migrate down the Sacramento River (Perry et al. 2010). In the southern delta, the Central Valley Project and State Water Project export water from the delta to supply agricultural and municipal water needs. The levels of exports can vary annually and have been associated with differential survival rates of fall run Chinook (Newman and Brandes 2010, Newman 2003).

Finally, nearshore ocean processes can have important consequences for Chinook salmon (Wells et al. 2007, Woodson et al. 2013), and here we evaluated upwelling in a region south of the entrance to San Francisco Bay (UPW) and the sea surface temperature in the Gulf of the Farallones (FARA).

The ocean stages were modeled as a function of maturation rates and age-3 impact rates. Information for the maturation rates were taken from an analysis of 1998, 1999, and 2000 coded wire tag (CWT) data (Grover et al. 2004) and more recent analyses of maturation rates (O'Farrell et al. 2012). Age-3 impact rates for winter-run were calculated for 1978 - 2011 from a combination of estimated impact rates from CWT returns (1998 - 2008) and from a hindcast of impact rates given spatial allocation of fishing effort (O'Farrell, M., NMFS unpublished data). Until 1987, there was little regulation of the Central Valley Chinook salmon shery and estimates of the mortality rate on winter-run Chinook salmon in the ocean shery were approximately 0.7 of the mortality rate experienced by fall-run Chinook salmon.

Most winter-run Chinook salmon return to spawn as 3-year-olds; however, the winter-run age-4 oceannstages are more likely to be captured in the commercial fishery because of their larger size. Grover et al. (2004) found that the harvest-related mortality of age-4 winter-run Chinook salmon was 2.5 to 3.7 times the rate of age-3. The age-4 impact rate in a calendar year y was assumed to be double the instantaneous rate of age-3 ($h_{4,y} = \exp(\log(h_{3,y}/2))$).

Results

Observed winter-run escapement was on the order of several tens of thousands in the late 1960's and early 1970's and declined to levels in the low thousands during the 1980's with a low abundance estimate of 194 in 1994. Since the mid-1990's the population has recovered to some degree with escapements in the mid 2000's on the order of several thousands. The winter-run OBAN model captured this declining trend and recovery in escapement (Figure D.2). In particular, the model was able to capture the decline in the late 1970's (along with the spike in escapement in 1980), the continued decline through the mid-1990s, and the subsequent increase through early 2000. The three different sampling methods had median estimated CV's ranging from 0.68 for the early period, 1.34 for the middle period, and 0.97 for the later period. As a result, the model was more sensitive to those sampling methods with higher precision (lower CV). In particular, the model fits to the intermediate period (in which counts were expanded assuming 15% passed RBDD by May 15) indicated that the escapement in 1990, 1991, and 1994 was underestimated relative to model predictions (Figure D.2). In contrast, the winter-OBAN model predictions of escapements during the early period (1967 - 1987) and the later period (2001-2008) fit the annual variability in escapement estimates more closely. The winter-OBAN model also fit well to patterns in the juvenile abundance index at RBDD from 1995 to 2007. The median estimated CV on the juvenile index data was 1.2, indicating that the model had intermediate sensitivity to the juvenile indices relative to escapement. The winter-run model predictions of juveniles at RBDD captured the relatively low production of fry during the late 1990's, subsequent increase in early 2000's due to higher escapements, and the declline in the index in 2007 (Figure D.3).

Annual patterns in stage-specific survivals

To predict escapement and juvenile index values, stage-specific survivals were estimated as a function of the environmental and anthropogenic factors. The estimated survival from egg to fry at RBDD averaged 0.24 95%CrI(0.11, 0.48) (Table D.3); however, survival from the 1970's to mid-1990's was highly variable. There were two years in the late 1970's where median survival was predicted to be approximately zero and periods in the early 1980's and early 1990's when survival in the alevin stage was also low (Figure D.4). Since the mid-1990's the survival rates for alevin have been more stable relative to the prior periods. Survival through the delta stage, which spans fry at RBDD to the nearshore ocean, was 0.0097 (95%CrI: 0.0041, 0.022) (Table D.3). Within the delta, annual variability was less pronounced with median survival ranging from a high of 0.017 in 1969 to a low of 0.0063 in 2004. Median delta survivals were relatively stable at approximately 0.009 through the 1980's and 1990's with slightly lower survivals during 2001 to 2004 of approximately

0.006 (Figure D.4). Average survival in the gulf stage was assumed to be 0.5 and variability in survival among years was reflective of ocean productivity. For winter-run Chinook the mid 1980's and mid 1990's were periods of poor survival, whereas 1998 and 2000 - 2001 were years of relatively good survival. Finally, patterns in age-3 survival rates (which were a deterministic function of harvest rates and annual survival rate of 0.8) indicated relatively low survival rates for brood years through the mid-1990's, with improving ocean survival for brood years after 1995 (Figure D.4).

Although the magnitude of the effect from each factor cannot be evaluated directly via the magnitude of the coefficient estimate (due to dependence on the stage-specific intercept), the sign of the coefficients associated with factors provide an indication of the effect of the factor: positive values increase survival relative to the average and negative values decrease survival. Because the winter-run OBAN model was fit in a Bayesian framework, the coefficients are described by posterior distributions and the probability that the coefficent value was positive was calculated (Table D.3). In the egg to fry stage, temperatures in the spawning reaches (TEMP) had a consistent negative effect on survival, whereas minimum flows (FLMIN) had a consistent positive effect on survival (Table D.3). A positive TEMP:FLMIN interaction term of flow and temperature would exacerbate the negative effect of high temperatures and low minimum flows, and the interaction term had a 0.73 probability of being positive. In the delta stage, access to the Yolo bypass (YOLO) and DCC gate position open (DCC) had a positive effect on survival, whereas export levels (EXPT) were negative. Finally, in the gulf stage, high tempeartures in the Farallone Islands (FARA) had a negative effect on winter-run survival, whereas upwelling south of the entrance to San Francisco Bay (UPW) had a positive effect on survival (Table D.3). Several additional parameters were given informative priors to structure the winter-run OBAN model, although if the data were informative on the coefficients, this would be reflected in the posterior. The posteriors on the conditional maturation rates largely reflected the informative priors. as did the CV on the process error (Table D.3).

The magnitude of the effect for each of the factors can not be discerned directly from the magnitude of the coefficient estimate (e.g., in Table D.3), because the coefficients associated with the covariates are dependent upon the intercept terms. To understand how the various factors affect the overall survival of winter-run Chinook, we increased each of the covariates one at a time by 1 standard deviation (SD). The survival rates under the one-at-a-time increases were compared to a baseline case, which was the survival rate with all factors at their mean 1967 to 2008 level. The survival rates began at the egg stage and ended at the end of age 2, prior to harvest affecting survival. To facilitate comparison, we calculated the percent change relative to the baseline survival (i.e., $(alt_k - base)/base \times 100\%$), where alt_k describes a model with

factor k increased by 1 SD. Minimum flow had the largest effect per unit SD on winter-run survival with a median increase of 128% (Figure D.5). Temperature also had a strong effect with a negative median effect of -96.7% per unit SD. The other notable factors were exports which had a negative effect of - 12.4% per unit SD, Yolo with a median positive effect of 11.3% and upwelling with a positive effect of 42.3% per unit SD (Figure D.5). The standard deviations are not the same on a percentage basis among factors, however. For example 1 SD of TEMP is equal to 6.8% of the mean, whereas 1 SD of EXPT is equal to 25.6% of the mean. Calculations of the effects of each factor on a percent basis indicated that temperature provides the largest effect with an 11.9% decrease in survival per percent increase in temperature. Minimum flows in the spawning reach provided a median 5.73% change, temperature in the Farallones provided a median -1.55%, and upwelling provided a median 1.78% change, whereas all other factors provided a less than 1% change in survival for a 1% increase in the factor (EXPT -0.48%, YOLO 0.10%, and DCC 0.16%).

Correlation among coefficients was generally low with the exception of the two intercept terms β_{alevin} and β_{delta} (Pearson correlation coefficient on posterior samples = - 0.685). Despite juvenile data being present for the latter portion of the time series, some negative correlation among these two coefficients was expected due to the model structure. This correlation did not inhibit the MCMC algorithm from converging, however. All scale reduction factors on monitored parameters were approximately 1, which indicated that the 3 chains had converged to a stable distribution.

Discussion

The winter-OBAN framework provided a means to evaluate the importance of several anthropogenic and environmental factors hypothesized to affect winter-run Chinook in the Central Valley. The model results support the importance of the environmental conditions in the natal spawning and rearing area and early ocean conditions with important but more subtle effects of delta survival. Our results are comparable with previous models of winter-run Chinook, providing some justification of the overall model structure and its inference. Our estimate of delta survival can be compared with Winship et al. (2014), who estimated the fry to end of age 2 survival rate for 1996 - 2008 of 0.4%. In comparison, our delta survival rate was 0.9% times the average age 2 value of 0.5 equals a 0.45% estimate for our model from fry to the end of age 2.

Median egg to fry survivals were slightly lower than estimated by Winship et al. (2014), in which the median egg to fry survival was 0.30. Furthermore, they found little variability in annual egg to fry survival. Similar fry data were used for both models; however, the winter-run OBAN model was able to use the

1995-2008 survival relationships to improve inference on factors affecting egg to fry survival in the 1970's to mid-1990's, prior to the analysis of Winship et al. (2014). We too found low variability among years in egg to fry survival from 1996 to 2008, but in contrast we found that there was high variability in survival prior to 1995 due to temperature and flow effects, and it played an important role in the decline of winter-run Chinook during the late 1970's and 1980's.

The factors leading to the decline in winter-run abundance during the 1970's can be explained by several periods of poor egg to fry survival tied to low flows and high water temperatures in the spawning reaches. While survival through the delta did not vary dramatically, survival at early ocean entry also had several periods with generally poor survival. Concurrent with this period of episodic recruitment failure and variable ocean conditions, impact rates of age-3 winter-run averaged 0.38 from 1969 to 1997. The recovery of winter run beginning in the late 1990's and early 2000 can be attributed to several managment actions and good ocean productivity from 2001 - 2003. The installation of a temperature control device in 1991 has generally reduced the variability in temperature with subsequent reduction in variability of egg to fry survival since 1993 (Figure D.4). Concurrent with the installation of the temperature control device, harvest rate management reduced the impact rates on winter-run (1998-2009 average of 0.153) (O'Farrell et al. 2012). In addition, survival through the delta was generally better during the 1996 to 1998 period due to lower than average exports and greater than average access to Yolo bypass.

Model Critique

Although the OBAN modeling framework can incorporate density dependence in the model structure, the winter-run implementation here did not include it based on previous work fitting density dependence to winter-run abundance indices. Estimation of the density dependence requires a signal in the data, namely the reduction in survival as a function of abundance. Previous efforts to include density dependence in models of winter-run population dynamics have had mixed results. Newman and Lindley (2006) included density dependence in the egg to fry transition and found little support for density dependence in a model without process noise, but they found strong evidence when process noise was included as a random effect in each stage under a state-space formulation. The information in the data to support the density dependence came from accounting for autocorrelation in the juvenile abundance state variables as well as measurement errors. Winship et al. (2014) found little support for density dependence in the egg to fry stage using a state-space model that estimated process noise, but fixed measurement error based on estimates of CV from sampling design. Based on the similarity of our model design to Winship et al. (2014), we did not include

capacity in the model structure. We return to the topic of density dependence below.

We also did not include hatchery output explicitly in the winter-run OBAN implementation. We did, however, incorporate a process noise component to the egg production stage, which was able to vary among years. Hatchery supplementation should be reflected in deviations of recruitment variability, if it was in fact improving the productivity of the population. Hatchery supplementation was initiated in 1991 with some releases in 1994 and 1995; however, production began in ernest in 2000 with between 20 to 57 natural origin females removed from the spawning population for hatchery brood stock (Winship et al. 2014). A more direct approach would be to include a dummy factor in the egg production equation that identified years of hatchery production. The hatchery term could be restricted to have a positive value, reflecting a hypothesized expected benefit of hatchery supplementation, or allowed to be positive or negative reflecting the potential for negative hatchery effects on production of natural origin juveniles.

Recovery

Recovery of winter-run is likely to occur through management of factors under human control while being aware of the influence of uncontrollable environmental conditions (e.g., upwelling). Winter-run appear to be particularly sensitive to temperatures and flows in the spawning reaches. Estimates of the temperature during 1977 indicated that it was 4 standard deviations above the mean (17.6 C) during the July to September period. Mortality in the egg to fry stage was similar in 1976, though, when the temperature was only 1.2 standard deviations (14.6 C) above the mean. The installation of a temperature control device at Shasta Dam provides the ability to decouple water temperatures from flow out of the dam, and manages tempeatures by mixing cold hypolimnetic water with warmer surface water. While this provides a method for controlling temperatures, the operations of the control device may be complicated by the multi-year climate cycles that affect the reservoir storage and thus the amount of cold water available. Still, the winter-run OBAN model results suggest that small deviations in temperature can have substantial impacts on survival from the egg to fry stage, and managing thermal mortality can have important consequences for the population dynamics.

Management of factors in the delta appear to also affect winter-run, but to a lesser degree than the temperature and flow effects during egg to fry survival. Within the delta, increasing access to Yolo bypass and reducing exports can have a positive effect on survival. Water flows into the Yolo bypass over an approximately 1.5 mile weir when flows on the Sacramento River exceed 56,000 cfs at Verona. Winter-run juveniles rear above the weir location and their downstream movement is triggered by flow cues (del Rosario et al. 2013). Access to the Yolo bypass occurs when these flow pulses are also substantial enough to overtop

the weir. Given the general lack of off-channel rearing area for salmonids in the Central Valley, improving access to Yolo bypass has been identified as an important management action for recovery of Central Valley salmonids, and winter-run in particular (NMFS 2014).

For the model with a density dependent effect in Newman and Lindley (2006), a Beverton-Holt model was used and the estimated capacity was on the order of 11.5 million fry. Using these values of capacity for fry, estimated fry to age-2 survival of 0.45% and ocean age 2 and age 3 survival rates of 0.5, and 0.8 respectively would suggest a capacity of approximately 20,500 winter-run in the absence of harvest. This capacity level was exceeded every year from 1967 to 1977; thus it may not be an appropriate capacity estimate for that period, but could potentially reflect more recent conditions as the Newman et al. (2006) model focused on 1992 to 2003. More importantly, the existence of a carrying capacity at this level may have important implications for modeling the expected responses to recovery of winter-run. Both the Newman and Lindley (2006) and Winship et al. (2014) models included density dependence in the egg to fry stage, presumably because spawner and juvenile data were available. Yet density dependence could more likely be in the spawning stage given that winter-run are currently spawning below Keswick dam, rather than in their natal tributaries surrounding Mt. Shasta (Yoshiyama et al. 2001). For evaluating the potential for reconnecting winter-run populations to their natal spawning reaches, such an analysis could provide information on potential population sizes under expanded habitat.

The state-space modeling framework has proven to be an important component to ecological modeling due to its ability to reflect uncertainties in the biological processes via process noise and in the observation process via measurement error. In most applications, the process noise is ascribed to random effects (e.g. Newman and Lindley 2006, Winship et al. 2014), but some of the variation in process noise may be explained by realtionships to anthropogenic and environmental factors. Thus, the OBAN framework attempts to move inference toward evaluating hypotheses by formally laying out a framework by which stage-specific variability can be ascribed to explanatory factors rather than to random effects. This linkage can be particularly powerful if some of the factors affecting the population dynamics can be managed for salmonid recovery.

Acknowledgements

We thank the School of Aquatic and Fisheries Sciences at the University of Washington for providing feedback through their Quantitative Seminar series, Eva Jennings for providing help with data management, and Curry Cunningham for thoughtful discussions on state-space modeling and Chinook population dynamics. Support

427 for this project was received under Grant Agreement 2039 from the Delta Stewardship Council.

References

Botsford, L. W. and Brittnacher, J. G. 1998. Viability of Sacramento River winter-run Chinook salmon. *Conservation Biology* **12**(1): 65–79

California Department of Fish and Game. 2004. Sacramento River winter-run Chinook salmon: 2002-2003 biennial report. Tech. rep., California Department of Fish and Game, Native Anadromous Fish and Watershed Branch

del Rosario, R. B., Redler, Y. J., Newman, K., Brandes, P. L., Sommer, T., Reece, K. and Vincik, R. 2013. Migration patterns of juvenile winter-run-sized Chinook salmon (Oncorhynchus tshawytscha) through the SacramentoSan Joaquin Delta. *San Francisco Estuary and Watershed Science* **11**(1). URL `http://www.escholarship.org/uc/item/36d88128`

Gelman, A., Carlin, J., Stern, H. S. and Rubin, D. B. 2004. Bayesian Data Analysis. CRC Press

Gelman, A. and Rubin, D. B. 1992. Inference from iterative simulation using multiple sequences. *Statistical science* 457–472

Gelman, A. et al. 2006. Prior distributions for variance parameters in hierarchical models (comment on article by Browne and Draper). *Bayesian analysis* **1**(3): 515–534

Gilks, W. and Spiegelhalter, D. 1996. Markov chain Monte Carlo in practice. Chapman & Hall/CRC

Greene, C. M. and Beechie, T. J. 2004. Consequences of potential density-dependent mechanisms on recovery of ocean-type Chinook salmon (Oncorhynchus tshawytscha). *Canadian Journal of Fisheries and Aquatic Sciences* **61**(4): 590–602

Grover, A., Lowe, A., Ward, P., Smith, J., Mohr, M., Viele, D. and Tracy, C. 2004. Recommendations for developing fishery management plan conservation objectives for Sacramento River winter Chinook and Sacramento River spring Chinook. Tech. Rep. Progress Report, Sacramento River Winter and Spring Chinook (SRWSC) Interagency Workgroup

Healey, M. 1991. Life history of Chinook salmon (Oncorhynchus tshawytscha). In C. Groot and L. Margolis, eds., Pacific Salmon Life Histories, 311–393. University of British Columbia Press, Vancouver, B.C., Canada

King, R., Morgan, B., Gimenez, O. and Brooks, S. 2010. Bayesian analysis for population ecology. CRC Press

Lindley, S. T., Schick, R. S., Mora, E., Adams, P., Anderson, J., Greene, S., Hanson, C., May, B., McEwan, D., MacFarlane, R. B., Swanson, C. and Williams, J. 2007. Framework for Assessing Viability of Threatened and Endangered Chinook Salmon and Steelhead in the Sacramento-San Joaquin Basin. *San Francisco Estuary and Watershed Science* **5**(1): Article 4

Maunder, M. N., Deriso, R. B. and Waters, C. 2011. A state–space multistage life cycle model to evaluate population impacts in the presence of density dependence: illustrated with application to delta smelt (Hyposmesus transpacificus). *Canadian Journal of Fisheries and Aquatic Sciences* **68**(7): 1285–1306

Moussalli, E. and Hilborn, R. 1986. Optimal stock size and harvest rate in multistage life history models. *Canadian Journal of Fisheries and Aquatic Sciences* **43**(1): 135–141

Newman, K. 2003. Modelling paired release-recovery data in the presence of survival and capture heterogeneity with application to marked juvenile salmon. *Statistical Modelling* **3**(3): 157–177

Newman, K., Buckland, S., Morgan, B. J., King, R., Borchers, D., Cole, D. J., Besbeas, P., Gimenez, O. and Thomas, L. 2014. Modelling Population Dynamics. Springer

Newman, K. B. and Brandes, P. L. 2010. Hierarchical Modeling of Juvenile Chinook Salmon Survival as a Function of Sacramento-San Joaquin Delta Water Exports. *North American Journal of Fisheries Management* **30**(1): 157–169

NMFS. 2014. Recovery Plan for the Evolutionarily Significant Units of Sacramento River Winter-run Chinook Salmon and Central Valley Spring-run Chinook Salmon and the Distinct Population Segment of California Central Valley Steelhead. Tech. rep., National Marine Fisheries Service

O'Farrell, M. R., Mohr, M. S., Grover, A. M. and Satterthwaite, W. H. 2012. Sacramento River winter Chinook cohort reconstruction: analysis of ocean fishery impacts. URL `http://swfsc.noaa.gov/publications/TM/SWFSC/NOAA-TM-NMFS-SWFSC-491.pdf`

Perry, R. W., Skalski, J. R., Brandes, P. L., Sandstrom, P. T., Klimley, A. P., Ammann, A. and MacFarlane, B. 2010. Estimating survival and migration route probabilities of juvenile Chinook salmon in the Sacramento-San Joaquin River Delta. *North American Journal of Fisheries Man-*

agement **30**(1): 142–156. doi:Doi 10.1577/M08-200.1. URL <Go to ISI>://WOS:000277113900013; http://www.tandfonline.com/doi/full/10.1577/M08-200.1

Poytress, W. R. and Carrillo, F. D. 2011. Brood-year 2008 and 2009 winter Chinook juvenile production indices with comparisons to juvenile production estimates derived from adult escapement. Tech. Rep. Draft Annual Report 2008 and 2009, U.S. Fish and Wildlife Service

R Core Team. 2013. R: A Language and Environment for Statistical Computing. R Foundation for Statistical Computing, Vienna, Austria. URL http://www.R-project.org/

Roberts, G. and Polson, N. G. 1994. On the geometric convergence of the Gibbs sampler. *J. Roy. Stat. Soc. B* **56**: 377–384

Scheuerell, M. D., Hilborn, R., Ruckelshaus, M. H., Bartz, K. K., Lagueux, K. M., Haas, A. D. and Rawson, K. 2006. The Shiraz model: a tool for incorporating anthropogenic effects and fish-habitat relationships in conservation planning. *Canadian Journal of Fisheries and Aquatic Sciences* **63**(7): 1596–1607

Snider, B., Reavis, B. and Hill, S. 2000. 1999 Upper Sacramento River winter-run Chinook salmon escapement survey, May - August 1999. Tech. Rep. Technical Report No. 00-1, California Department of Fish and Game, Stream Evaluation Program

Sommer, T. R., Harrell, W. C. and Nobriga, M. L. 2005. Habitat use and stranding risk of juvenile Chinook salmon on a seasonal floodplain. *North American Journal of Fisheries Management* **25**(4): 1493–1504

Spiegelhalter, D., Thomas, A., Best, N. and Lunn, D. 2003. WinBUGS version 1.4 user manual. Tech. rep., MRC Biostatistics Unit, Cambridge, UK

Sturtz, S., Ligges, U. and Gelman, A. 2005. R2WinBUGS: A Package for Running WinBUGS from R. *Journal of Statistical Software* **12**(3): 1–16. URL http://www.jstatsoft.org

Wells, B. K., Grimes, C. B. and Waldvogel, J. B. 2007. Quantifying the effects of wind, upwelling, curl, sea surface temperature and sea level height on growth and maturation of a California Chinook salmon (Oncorhynchus tshawytscha) population. *Fisheries Oceanography* **16**(4): 363–382. doi:DOI 10.1111/j.1365-2419.2007.00437.x. URL <Go to ISI>://WOS:000247440500005; http://onlinelibrary.wiley.com/doi/10.1111/j.1365-2419.2007.00437.x/full

Williams, J. G. 2006. Central Valley Salmon: A Perspective on Chinook and Steelhead in the Central Valley of California. *San Francisco Estuary and Watershed Science* **4**(3): Article 2

Winship, A. J., OFarrell, M. R. and Mohr, M. S. 2014. Fishery and Hatchery Effects on an Endangered Salmon Population with Low Productivity. *Transactions of the American Fisheries Society* **143**(4): 957–971. doi:10.1080/00028487.2014.892532. URL http://www.tandfonline.com/doi/abs/10.1080/00028487.2014.892532

Woodson, L. E., Wells, B. K., Weber, P. K., MacFarlane, R. B., Whitman, G. E. and Johnson, R. C. 2013. Size, growth and origin-dependent mortality of juvenile Chinook salmon Oncorhynchus tshawytscha during early ocean residence. *Marine Ecology Progress Series* **487**: 163–175. doi:10.3354/meps10353

Yoshiyama, R., Gerstung, E., Fisher, F. and Moyle, P. 2001. Historical and present distribution of Chinook salmon in the Central Valley drainage of California. In R. Brown, ed., Contributions to the Biology of Central Valley Salmonids. Fish Bulletin 179(1), 71–176. California Department of Fish and Game, Sacramento, California

Table D.1: Model parameters, state variables, and observable indices of abundance for winter-run OBAN model.

Symbol	Value	Description
Indices		
i	egg, alelvin, fry, delta, bay, gulf	freshwater stages
j		covariate index
k		gear type for observation process
t	1967, .., 2004	brood year
y	1967, .., 2008	calendar year
age	2, 3, 4	ocean age
State Variables		
$N_{i,t}$		abundance of freshwater stage
$O_{age,t}$		abundance of ocean stage
$M_{age,t}$		abundance of mature fish
Parameters		
$\beta_{i,j}$		coefficient relating factor j to survival in stage i
$\gamma_{i,j}$		coefficient relating factor j to capacity in stage i
$\delta_{age,j}$		coefficient relating factor j to maturation at age
ϕ_{age}	(0,1)	conditional maturation in age age
$CV_{E,k}$		coefficient of variation for escapement observation process k
CV_J		coefficient of variation for juvenile observation process k
CV_p		coefficient of variation of process noise
f_t	2450	fecundity per spawner
$h_{age,t}$		impact rate due to harvest
$p_{i,t}$	$(0,1)$	productivity in stage i and brood year t
$K_{i,t}$	$(0,\infty)$	capacity in stage i and brood year t
z_2	0.5	age 2 average natural survival rate
z_3	0.8	age 3 average natural survival rate
z_4	0.8	age 4 average natural survival rate
Observables		
$I_{y,E}$		Escapement 1967 - 2008
$I_{y,J}$		Juvenile abundance at Red Bluff Diversion Dam 1995 - 1999, 2002-2007

Figure D.1. Map of the Central Valley (black lines), Sacramento River, San Francisco Estuary, and ocean habitats used by winter-run Chinook.

Figure D.2. Model fit to observed winter-run escapement data (squares) from three collection methods: 1) Red Bluff Diversion Dam (RBDD) counts, 2) expansion of RBDD counts assuming 15% passage by May 15, and 3) carcass mark-recapture. Verticle lines indicate 1 standard deviation. Heavy line is the mean winter-run OBAN prediction, whereas thin lines are the 95% credible interval on model predictions of the

Table D.2: Covariates used in the winter-run OBAN model.

Covariate	Mean	Standard Deviation	Stage	Description
TEMP	13.4	0.9	alevin	Jul - Sept mean temperature at Bend Bridge (C)[1]
FLMIN	6605	1477	alevin	Aug - Nov minimum of monthly average flow at Bend Bridge (cfs)[2]
YOLO	22.9	24.7	delta	Dec - Mar number of days where flow is greater than 56,000 on the Sacramento River at Verona[3]
DCC	0.46	0.42	delta	Dec - Mar proportion of time when Delta Cross Channel gates are open[4]
EXPT	1250154	320854	delta	Dec - Jun total exports (cfs)[3]
UPW	210.5	49.8	gulf	Apr-Jun upwelling index[5]
FARA	11.8	0.9	gulf	Feb - Apr mean temperature in the Farallon Islands (C)[6]

[1] Temperature regresssions for 1967 - 1970; modeled temperature data 1970-2005; gage data 2005-2008 CDEC-BND
[2] CDEC-BND station or USGS 11377100 station
[3] Dayflow (http://www.water.ca.gov/dayflow/output/Output.cfm)
[4] US Bureau of Reclamation (http://www.usbr.gov/mp/cvo/vungvari/Ccgates.pdf)
[5]Pacific Fisheries Environmental Laboratory (http://las.pfeg.noaa.gov/LAS/docs/upwell.nc.html)
[6]University of California San Diego (http://shorestation.ucsd.edu/active/index_active.html#farallonstation)

Table D.3: Prior and posterior distributions in the winter-OBAN model.

Parameter	Prior	Mean	Median	95%CrI	Pr > 0
β_{alevin}	N(0, 2.5)	-1.17	-1.21	(-2.09, -0.09)	0.21
β_{delta}	N(0, 2.5)	-4.63	-4.64	(-5.48, -3.79)	0.00
β_{TEMP}	N(0, 2.5)	-2.00	-1.99	(-3.66, -0.35)	0.004
β_{FLMIN}	N(0, 2.5)	1.48	1.42	(0.42, 2.86)	1.00
$\beta_{TEMP:FLMIN}$	N(0, 2.5)	0.52	0.53	(-0.91, 2.06)	0.73
β_{YOLO}	N(0, 2.5)	0.13	0.11	(-0.54, 0.84)	0.65
β_{DCC}	N(0, 2.5)	0.15	0.14	(-0.37, 0.78)	0.70
β_{EXPT}	N(0, 2.5)	-0.13	-0.13	(-0.95, 0.66)	0.39
β_{UPW}	N(0, 2.5)	0.94	0.90	(-0.71, 2.83)	0.83
β_{FARA}	N(0, 2.5)	-0.24	-0.23	(-1.53, 0.91)	0.35
CV_{E1}	U(0,CV_{E3})	0.71	0.68	(0.46,1.12)	NA
CV_{E2}	U(CV_{E3}, 2)	1.36	1.34	(0.80, 1.96)	NA
CV_{E3}	U(0,2)	1.03	0.97	(0.62, 1.79)	NA
CV_J	U(0,2)	1.20	1.20	(0.42, 1.93)	NA
CV_p	[1]B(2,6)	0.26	0.25	(0.02, 0.59)	NA
ϕ_2	[2]B(1,10)	0.038	0.030	(0.004, 0.128)	NA
ϕ_3	[3]B(10,1)	0.907	0.928	(0.700, 0.997)	NA

[1] Informative prior with a mean of 0.25, 95% interval (0.036, 0.58)
[2] Informative prior with mean of 0.091, 95% interval (0.0025, 0.31)
[3] Informative prior with mean of 0.91, 95% interval (0.69, 0.99)

state variable of escapement.

Figure D.3. Model fit to observed winter-run juvenile abundance index (squares) at Red Bluff Diversion Dam from 1996 to 2008. Verticle lines indicate 1 standard deviation. Heavy line is the mean winter-run OBAN prediction, whereas thin lines are the 95% credible interval on model predictions of the state variable of fry abundance.

Figure D.4. Predicted survival in the egg to fry (alevin) stage above Red Bluff Diversion Dam (A), in the delta (B), in the gulf (C), and as age 3 in the ocean (D). For A - C the dark line represents the median model prediction, whereas thin lines are the 95% credible interval on model predictions. For D the dark line represents the assumed survival rate of age-3 due to natural mortality and harvest.

Figure D.5. Analysis of factors affecting winter-run survival to the end of age 2. Factors were increased by 1 standard deviation and the percent change in survival to the end of age 2 relative to a baseline (all factors at their 1967 2008 mean levels) was calculated for each factor. Please see Table D.2 for a description of each factor.


Red Bluff
diversion dam
Yolo
bypass
Delta
cross channel
Chipps
Island

Figure D.1:

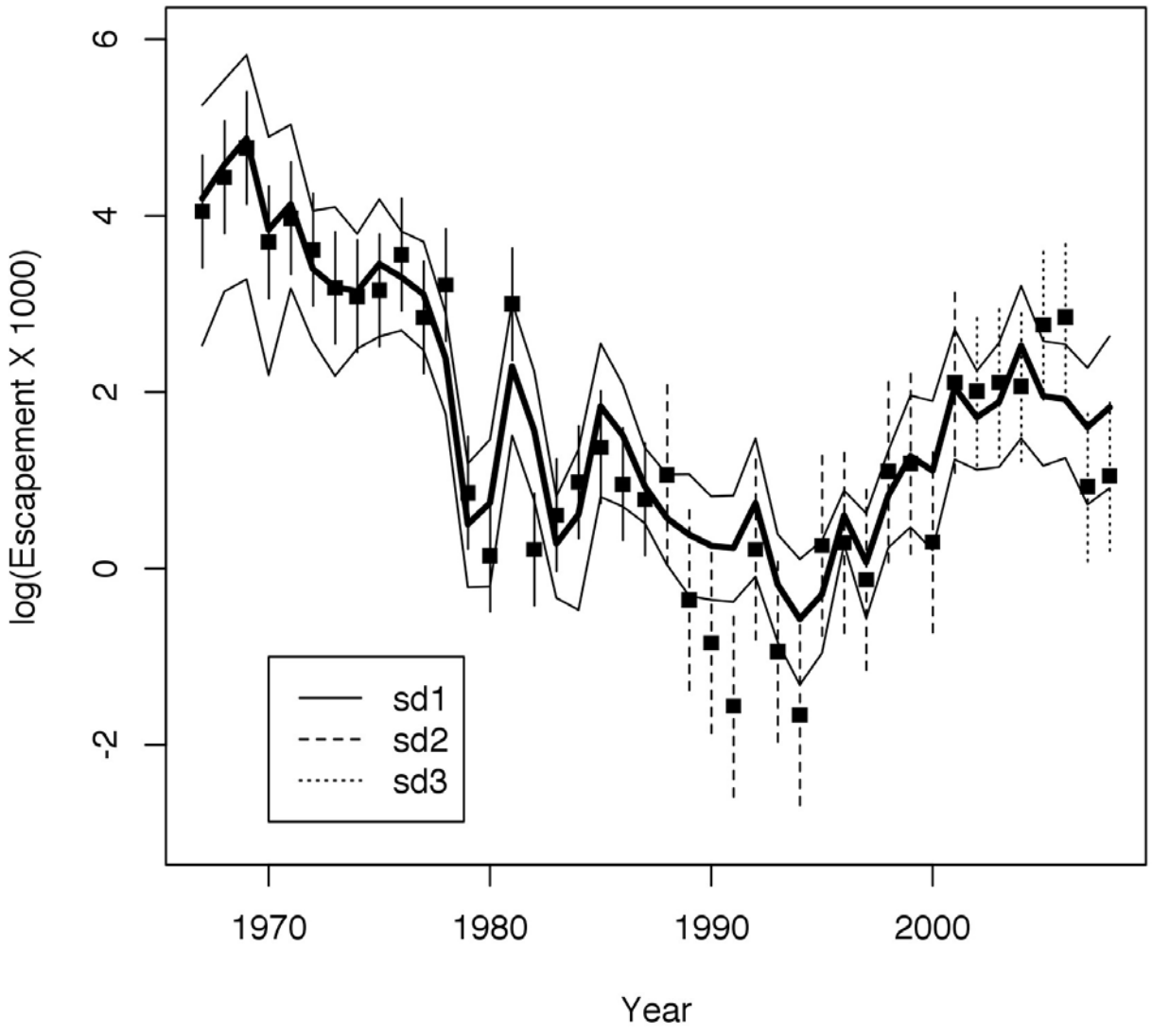
log(Escapement X 1000)
6
4
2
0
-2
1970
1980
1990
2000
Year
sd1
sd2
sd3

Figure D.2:

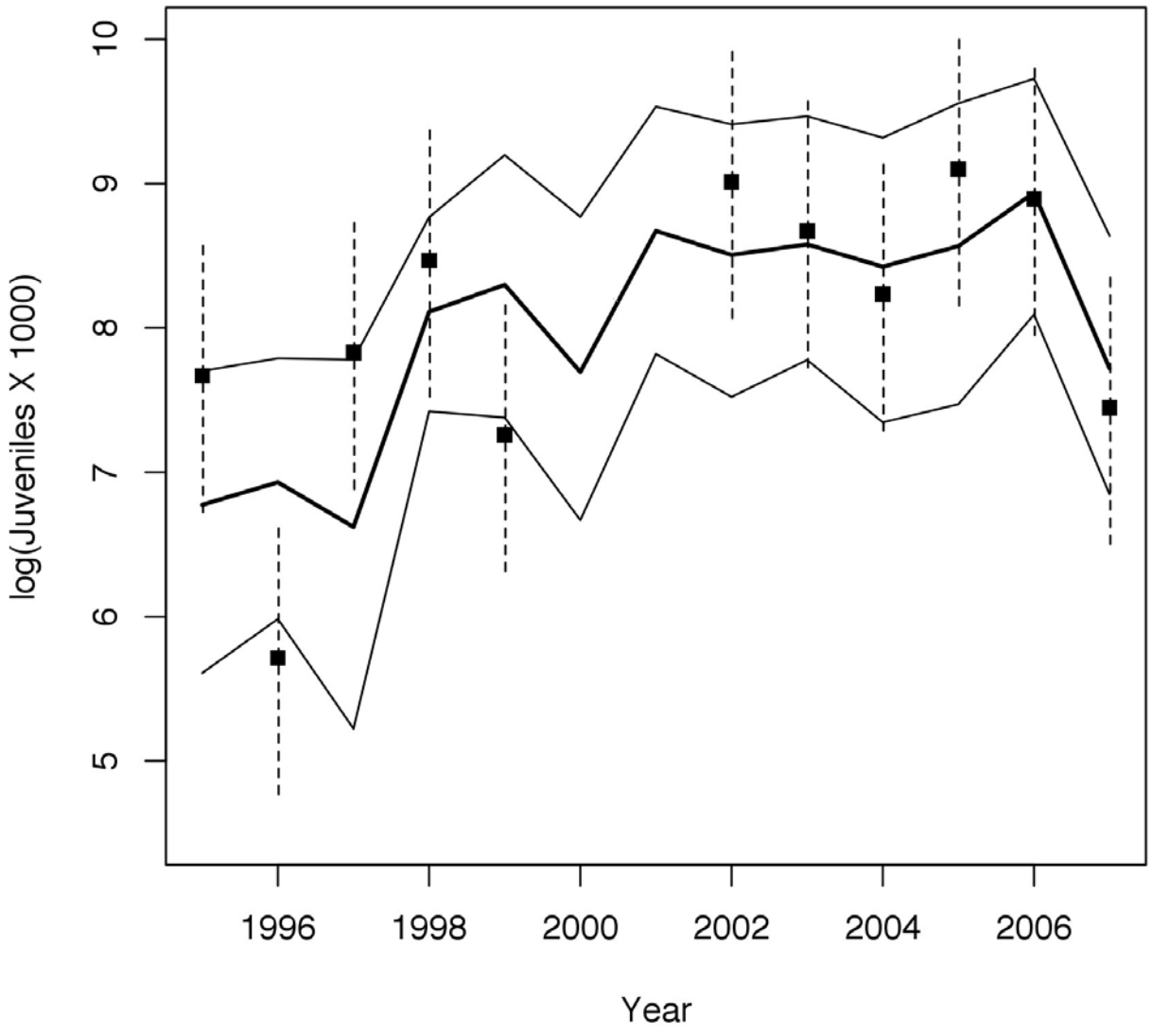
log(Juveniles X 1000)
5
6
7
8
9
10
1996
1998
2000
2002
2004
2006
Year

Figure D.3:

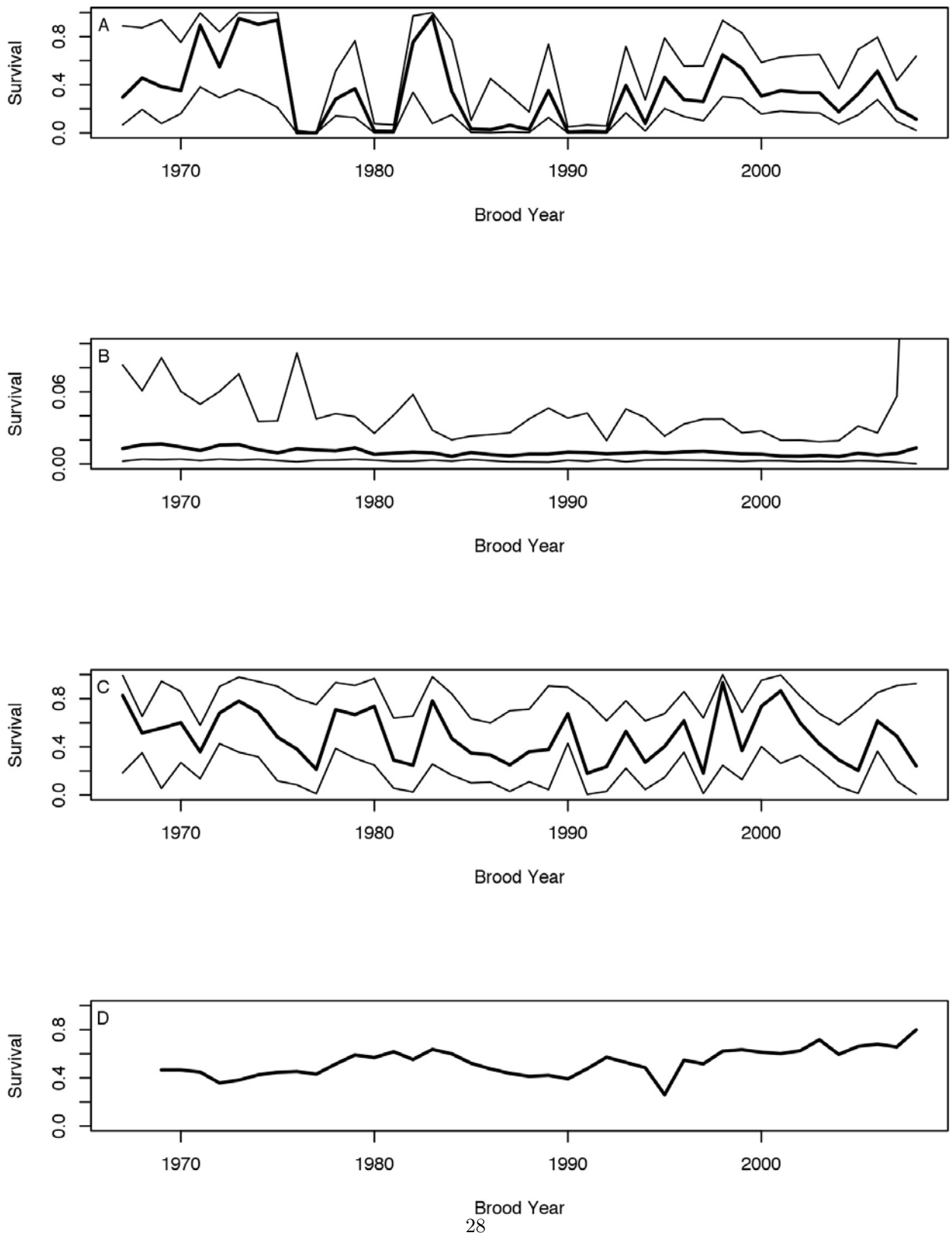
A
Survival
0.0
0.4
0.8
1970
1980
1990
2000
Brood Year
B
Survival
0.00
0.06
1970
1980
1990
2000
Brood Year
C
Survival
0.0
0.4
0.8
1970
1980
1990
2000
Brood Year
D
Survival
0.0
0.4
0.8
1970
1980
1990
2000
Brood Year

Figure D.4:

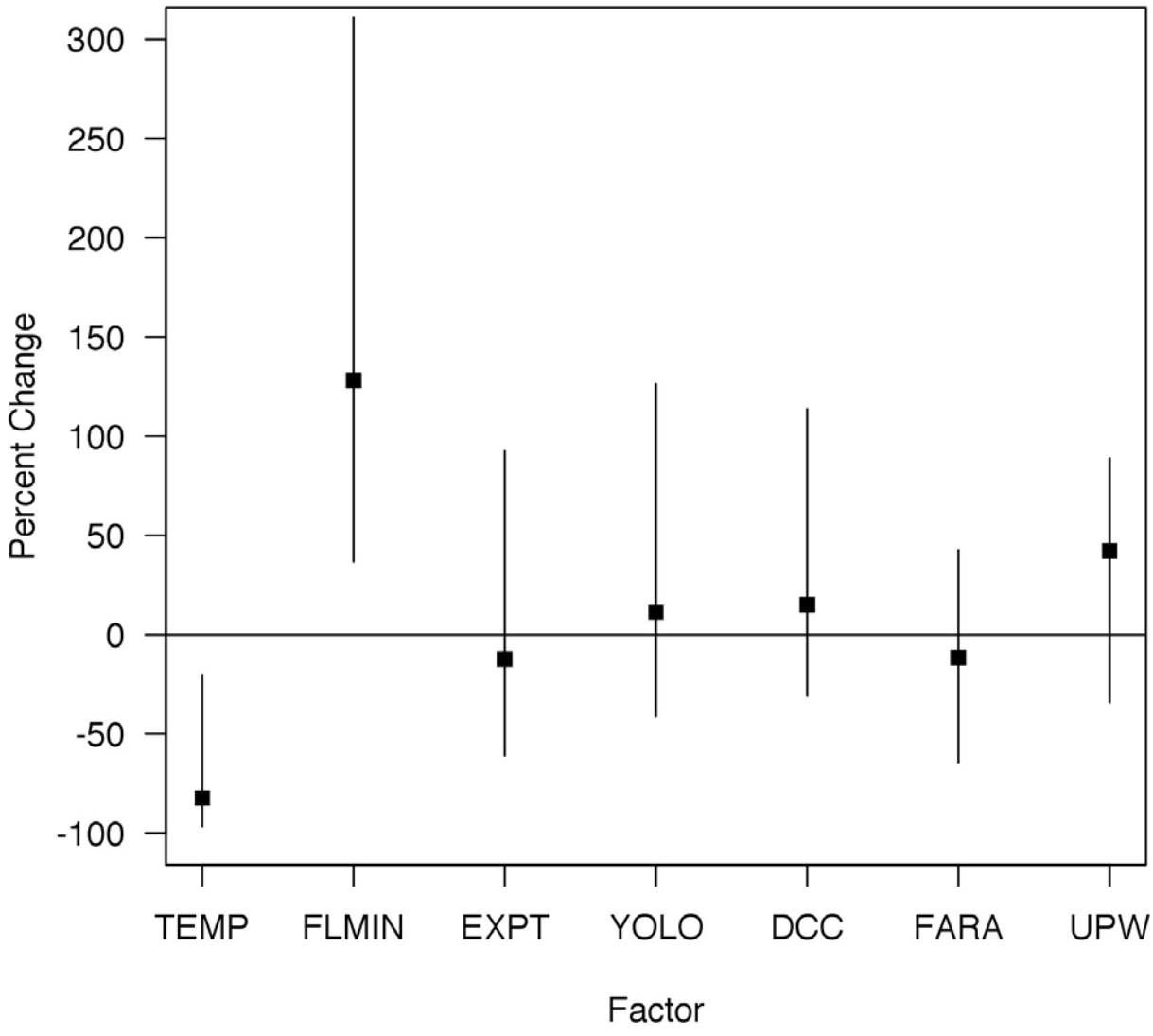
300
250
200
150
100
50
0
-50
-100
Percent Change
TEMP
FLMIN
EXPT
YOLO
DCC
FARA
UPW
Factor

Figure D.5: